INTEGRATING SPATIAL HETEROGENEITY INTO SUSTAINABILITY ASSESSMENTS OF BIOFUELS FROM WASTEWATER ALGAE

By

Marie-Odile Payne Fortier

Submitted to the graduate degree program in the Department of Civil, Environmental and Architectural Engineering and the Graduate Faculty of the University of Kansas in partial fulfillment of the requirements for the degree of Doctor of Philosophy.

_____

Chairperson Dr. Belinda S.M. Sturm

_____

Dr. Nathaniel Brunsell

_____

Dr. Edward Peltier

_____

Dr. Susan M. Stagg-Williams

_____

Dr. C. Bryan Young

Date Defended: July 7th, 2015

The Dissertation Committee for Marie-Odile Payne Fortier

certifies that this is the approved version of the following dissertation:

INTEGRATING SPATIAL HETEROGENEITY INTO SUSTAINABILITY ASSESSMENTS OF BIOFUELS FROM WASTEWATER ALGAE

_____

Chairperson Dr. Belinda S.M. Sturm

Date approved: July 7th, 2015

Abstract

Microalgae are a promising biofuel feedstock whose potential to replace petroleum fuels has improved with the application of hydrothermal liquefaction (HTL) and the use of municipal wastewater. It was hypothesized that the sustainability of biofuels from wastewater algae is sensitive to geographic factors. The availability of land and wastewater near WWTPs in urban and rural areas, the life cycle greenhouse gas emissions of producing algal biofuel through HTL sited at a WWTP and at a refinery, and the life cycle climate change impacts of changing potentially available land near WWTPs to algal ponds were investigated. GIS and life cycle assessment (LCA) methods were developed, and literature data and primary data collected from algae cultivation in wastewater effluent and conversion to biocrude were used in these analyses.

The results of the geographic analysis showed trade-offs in water and land availability for algae cultivation at rural and urban WWTPs. The LCA of algal bio-jet fuel using geographic input data showed that siting HTL at a WWTP so that only biocrude is transported from the plant instead of minimally dewatered algae resulted in lower life cycle greenhouse gas emissions. To further incorporate spatial heterogeneity into assessing the life cycle climate change impacts of algal biofuels, methods were developed to integrate direct land use change (LUC) impacts, transportation distances, and an algal growth model into Python models for a baseline LCA, sensitivity analysis, and Monte Carlo analysis of algal renewable gasoline. This methodology was applied to the Level II ecoregions of the continental United States using data collected from GIS datasets. The results show that LUC impacts can have similar magnitudes as foreground process impacts, and that these impacts can differ significantly even between two ecoregions that have nearly identical algal productivities. The inclusion of LUC impacts increases the uncertainty range in Monte Carlo results. Additionally, the higher foreground process impacts arising from the lower annual algal productivity of colder ecoregions were offset by the cooling

albedo change impacts of the empty ponds during the months when production is halted. The geographically sensitive analyses that comprise this dissertation show the necessity for incorporating spatial heterogeneity in sustainability assessments of biofuels from wastewater algae.

Acknowledgements

I would like to thank my advisor, Dr. Belinda S.M. Sturm, with whom I had an excellent graduate education with many opportunities that helped me advance my career. I would also like to thank my coauthors on two papers that became part of my dissertation, Drs. Griffin W. Roberts and Susan M. Stagg-Williams, who developed the research branch on hydrothermal liquefaction of algae at the University of Kansas. I am grateful to Xanthippe Wedel of the University of Kansas Institute for Policy & Social Research for helping me obtain the information to geocode wastewater treatment plants systematically in ArcGIS, and Kevin Dobbs of the Kansas Biological Survey and Dr. C. Bryan Young at the University of Kansas for their assistance in developing my GIS-based analysis. In addition to Drs. Sturm, Young, and Stagg-Williams, I thank my other dissertation committee members, Drs. Nathaniel Brunsell and Edward “Ted” Peltier.

I am also grateful for all of the students who contributed to algae research in the laboratory and field, including Emily Cook, Elizabeth “Tess” Murray, Cody Siroka, Cale Mages, Quentin Cole, Luigi Basalo, Triton Wolfe, Malcolm Squire, and Katie Legenski. Additionally, I would like to thank Lindsey Witthaus and the Kansas Department of Health and Environment for providing monthly effluent data for Kansas wastewater treatment plants. I thank the Lawrence Wastewater Treatment Plant for allowing me to visit regularly to maintain and sample from the algal pond reactors and also for hosting this pilot-scale system.

I would like to thank my funding sources for my research and for associated algal biofuel research at the University of Kansas: C-CHANGE IGERT program at the University of Kansas (NSF #0801522), the NASA EPSCOR Grant NNX07AO27A, the NSF EPSCOR Grant EPS-0903806 with matching support from the State of Kansas through Kansas Technology Enterprise Corporation, the Department of Energy Grant DE-EE0000408, and the University of Kansas

Transportation Research Institute Grant DT0S59-06-G-00047 (funded by the U.S. Department of Transportation Research and Innovative Technology Administration). I am particularly grateful for the IGERT program at the University of Kansas, which equipped me with the tools to perform interdisciplinary research on climate change impacts, and to the program director, Dr. Joane Nagel. Thank you to the Department of Civil, Environmental and Architectural Engineering at the University of Kansas for my graduate teaching assistant assignments as well.

Finally, I am thankful for my family, from my husband Dr. Steven W. Payne to my mother Marie-Josée Fortier and my siblings Eugénie Fortier and Louis-Christophe Fortier, for their support as I undertook a doctorate degree and their understanding for long periods of time without being able to see each other. Thank you to my friends, especially those in academia and in animal rescue and advocacy, for their encouragement too.

Table of Contents

List of Figures

List of Tables

Nomenclature

ACP	Aqueous coproduct
ASDC	NASA Atmospheric Science and Data Center (ASDC)
BNR	Biological nutrient removal
CCLUB	Carbon Calculator for Land Use Change from Biofuels Production
CWNS	Clean Watersheds Needs Survey
DOE	Department of Energy
EISA 2007	Energy Independence and Security Act of 2007
EPA	United States Environmental Protection Agency
GIS	Geographic information system
GJ	Gigajoule
GREET	Greenhouse Gases, Regulated Emissions, and Energy Use in Transportation
HTL	Hydrothermal liquefaction
KU	University of Kansas
LCA	Life cycle assessment
LC-GHG	Life cycle greenhouse gas
LUC	Land use change
MODIS	MODerate-resolution Imaging Spectroradiometer
NACP	North American Carbon Program
NASA	National Aeronautics and Space Administration
NED	National Elevation Dataset
NLCD	National Land Cover Dataset
NPP	Net primary production
NRCS	Natural Resources Conservation Service

NREL	National Renewable Energy Laboratory
NSF	National Science Foundation
ORNL	Oak Ridge National Laboratory
OSU	Oregon State University
PAD-US	National Gap Analysis Program Protected Areas Data
PRISM	Parameter-elevation Relationships on Independent Slopes Model
RE	Radial extent
TRACI	Tool for Reduction & Assessment of Chemical and Other Environmental Impacts
TN	Total nitrogen
TP	Total phosphorus
TSS	Total suspended solids
USDA	United States Department of Agriculture
USGS	United States Geological Survey
UV	Ultraviolet
WWTP	Wastewater treatment plant

1 Introduction

1.1 Historical Motivation for Algal Biofuel Research

The substitution of petroleum-based fuels with algal biofuels has the potential to (1) contribute to national energy security, which is the resilient access to an ample supply of affordable energy products, and (2) act as a climate change mitigation strategy, substituting fossil greenhouse gas-emitting conventional fuels.

Energy security has been defined as the "absence of, protection from, or adaptability to threats that are caused by or have an impact on the energy supply chain."[1] Energy security definitions range from the assurance of appropriate and reliable energy supplies at reasonable prices[2] to the prevention of the "loss of welfare that may occur as the result of a change in price or availability of energy."[3] Energy security is a priority for the United States government and a significant component to national security.[4] Domestically-produced renewable sources of fuels could contribute towards energy security in the United States.

Climate change concerns are another driver for algal biofuel research. Petroleum-based liquid fuels release fossil carbon dioxide to the atmosphere when combusted, thus they contribute to increasing atmospheric greenhouse gas concentrations and climate change. Biofuels are created from biological feedstocks, like algae or crops. The carbon in biomass has been more recently fixed from the atmosphere through photosynthesis, so the carbon dioxide emitted when these biofuels are combusted for energy does not contribute directly to climate change. This carbon is cycling between the photosynthetic biofuel feedstocks, the fuel, and the atmosphere. The use of biofuels displaces the use of petroleum fuels, thus preventing an equivalent amount of fuel from a fossil source from being combusted, and its fossil carbon from being released as carbon dioxide to the atmosphere. Thus, research into biofuels can be driven by climate change

concerns. The production and use of biofuels is viewed as a climate change mitigation strategy, or an anthropogenic action towards enhancing the sinks or reducing the sources of greenhouse gases, thereby aiming to decrease the rate of climate change.[5]

Although energy security was the primary motive for algal biofuel research from 1978 to 1996, concerns over climate change and energy security became interconnected in driving algal biofuel research in the 2000s. When algal biofuel research began in the 1970s, energy security was the primary motive for research and development.[6] The oil embargo of the early 1970s and the subsequent rise in oil prices led the Department of Energy (DOE) to establish a federal laboratory which investigated, among other sources of alternative energy, the potential for algal biodiesel production through the Aquatic Species Program.[7] The program ran from 1978 to 1996, when it ended due to budget cuts and the perception that the cost of algal biofuels could not compete with the cost of petroleum fuels.[7] A decade later, when climate change and energy security issues were discovered to be associated with corn biofuel production, a renewed interest in algal biofuel research resulted, as those issues were not as severe for algal feedstocks.

Although the Energy Policy Act of 2005 and the subsequent Energy Independence and Security Act of 2007 are motivated by energy security goals, they include provisions to increase the production of renewable energy that has lower impacts on climate change. The Energy Independence and Security Act of 2007 calls for the majority of the biofuel production goal to consist of "advanced biofuels," which are defined as biofuels with 50% less life cycle greenhouse gas emissions compared to their petroleum fuel counterparts.[8] National laboratories under the Department of Energy began researching algal biofuels with motivations that ranged from climate change concerns to energy security concerns. At the same time, as numerous life cycle assessments were published to determine the climate change impacts of potential pathways of algal biofuel production, resource demand and techno-economic analyses were performed to

determine whether large-scale production in the United States would be feasible. Life cycle assessments frequently mention elements of energy security such as depleting petroleum resources and growing national energy consumption among their motivations for research.

A National Research Council report published in 2012 notes sustainability concerns for algal biofuel development, which span from an energy security focus to a climate change focus. Increasingly, energy security and climate change are becoming interconnected as motives for continued algal biofuel research as they both contribute to the overall sustainability of algal biofuel production at a national scale.

1.1.1 The Aquatic Species Program (1978-1996)

Under the Aquatic Species Program, algal biofuel research was conducted for energy security purposes following a sharp increase in crude oil prices and availability. In 1973, members of the Organization of the Petroleum Exporting Countries (OPEC) placed an embargo on oil exports to the United States and other nations, allowing world oil prices to triple.[9] To sustain these high oil prices, OPEC members severely reduced their oil production until 1986, when they abandoned this approach in order to regain their market share.[9] In the middle of this period of high crude oil prices, the United States government undertook further research into possible alternative fuels, including algal biofuel, as a way to provide a more secure and diverse energy portfolio for the nation.[10]

The Office of Fuels Development within the United States Department of Energy (DOE) created the Aquatic Species Program in 1978 to investigate microalgae as an energy source.[7] This program laid the scientific foundation for harvesting algal lipids and transforming them into fuel.[10] The Aquatic Species Program produced research on algal species and cultivation systems,

and the program developed pilot testing facilities that demonstrated the technological feasibility and highlighted future directions in algal biofuel research.[6]

The program was relatively inexpensive to fund at a total cost of $25 million, or less than $100 million when adjusted for inflation, from 1978 to 1996, which was 5.5% of the DOE's total budget for biofuels during that time.[6, 10] However, in 1996, the DOE faced budget cuts and chose to eliminate funding for algal biofuel research.[6] The price of crude oil had decreased to a stable, lower price for a decade before the Aquatic Species Program was unfunded.[11] It was perceived that algal biofuels would never be cost-competitive with petroleum-based fuels at the time of the DOE funding decision.[7] In 1996, the DOE chose to focus primarily on ethanol research in the short term.[10]

The researchers involved in the Aquatic Species Program produced a closeout report, which summarized the research performed over the sixteen years of the program. This report provided background information on algal biology, algae production systems, and resource availability for those who pursued new research a decade after the program ended.[6] The closeout report notes explicitly that "energy security is the number one driving force" behind biofuels research at the DOE. Thus, from 1978 to 1996, algal biofuel research was primarily motivated by energy security concerns as it was conducted almost entirely under or in conjunction with the DOE.

1.1.2 Lapse Period (1996-2005)

After the Aquatic Species Program ended, relatively little research in algal biofuels was published for approximately a decade. The applied research on algae took a different turn towards bioremediation and biological nutrient removal from waste streams. Scientists studied the use of macroalgae in treating dairy wastewaters and anaerobically digested dairy manure,[12, 13]

municipal wastewater,[14, 15] industrial waste wastewaters,[16, 17] and flue gas from coal power plants,[18] among other applications. The study of the waste treatment applications of microalgae during this time paved the way for the incorporation of waste sources of nutrients and water in making algal biofuel production more sustainable. This research also continued as a parallel to algal biofuel research past 2005.

1.1.3 Renewed Interest in Algal Biofuels

The renewed interest in algal biofuels in the mid-to-late 2000s occurred as several environmental and energy security-related disadvantages were discovered about corn biofuels, and as the Energy Independence and Security Act of 2007 promoted large-scale biofuel production with a goal primarily for biofuels to produce less greenhouse gas emissions on a life cycle basis.

Analyses published from 2004 to 2009 have shown that corn ethanol and corn biodiesel may not be suitable replacements for their petroleum-based counterparts from an energy security perspective and from a climate change perspective. One analysis suggested that there is not enough available land to produce substantial amounts of corn-based biofuels. In 2007, a review paper by Yusuf Chisti showed that the land area needed to produce 50% of the United States transportation fuel needs through corn biodiesel would be 846% of existing cropland.[19] Meeting just 5% of the demand would then require an unavailable percentage (84.6%) of the nation's cropland, thus corn biofuel has a low feasibility of replacing fossil fuels at a large scale. Furthermore, a 2004 paper showed that more fossil energy is consumed in the production of corn ethanol than the ethanol's embodied energy.[20] Additionally, when the greenhouse gas emissions associated with indirect land use change are considered, the greenhouse gas emissions over the life cycle of corn ethanol increase to nearly twice those of petroleum-based gasoline.[21] From

both an environmental sustainability and energy security perspective, these were unfavorable findings for corn ethanol.

Other unintended negative environmental impacts of corn biofuels also became known during this time, including nitrate releases to natural waters from agriculture intensification and greenhouse gas emissions from fertilizer supplementation. Corn production requires the addition of nitrogen-rich fertilizers. Increased fertilizer application rates, especially on maize crops, is one of three factors[a] that has historically influenced the doubling of nitrate transport to the Gulf of Mexico by the Mississippi River since 1960.[22] An analysis determined that the increased corn cultivation that would allow for the production of 15 to 36 billion gallons of corn-based biofuels would increase the discharges of dissolved inorganic nitrogen to the Atchafalaya and Mississippi Rivers by 10 to 34%, which contributes to deteriorating water quality and the formation of the seasonal hypoxic zone in the Gulf of Mexico.[22, 23] The nitrogenous fertilizers applied for corn cultivation also release nitrous oxide (N_2O), a greenhouse gas that has a 100-year average global warming potential that is 296 times that of carbon dioxide on a mass basis.[24] Nitrous oxide is released primarily through direct emissions from fertilized soil, indirect emissions from nitrogen in agricultural runoff, and emissions after biological and chemical transformations as nitrogen moves through agricultural systems.[24] These N_2O emissions can be equal to or greater than the greenhouse gas emissions avoided by displacing fossil fuels with biofuels, depending on the nitrogen fertilizer uptake efficiency of the corn and the fertilizer amounts utilized.[24] In contrast, a 2011 study determined through laboratory experiments that any direct N_2O emissions from open ponds growing microalgae are negligible.[25]

Furthermore, the diversion of harvested corn to fuel production instead of food markets raises practical and ethical issues, because the arable and productive land is needed to feed

[a] The other two factors are increased soybean production and increased runoff in the Mississippi Basin.

people, especially in times of worldwide food shortages.[26] In 2007, a United Nations official claimed that the conversion of food crops into fuel was a "a crime against humanity."[10] The consumptive water use of corn biofuel production also presents a predicament in the face of drought and major aquifer depletion.[27] Analyses differ in their calculations of the volume of water consumed per gallon of corn biofuel produced or per mile driven on corn biofuel, but most conclude that the amount of water consumed in corn biofuel production is greater than that consumed in petroleum gasoline production.[27, 28] Moreover, as bioethanol production extended into areas that require more irrigation, the consumptive water use to produce these biofuels increased 246% from 2005 to 2008, while actual bioethanol production only increased 133% during that period.[29] These findings indicate that in attempt to provide for energy security with corn biofuels, food security and water security can be compromised, and by extension, long-term energy security might not be achieved with corn biofuels.

As these environmental and energy security problems associated with the use of corn feedstocks for biofuels were published, the amount of research conducted and published on algal biofuels concurrently increased. There was a need for another renewable source of biofuels with greater energy security potential and lower life cycle climate change impacts as the price of crude oil increased again.[11] In 2007, Yusuf Chisti published a description of the potential for algal biodiesel.[19] The publication noted several advantages of algal feedstocks for biofuels: microalgae can be produced in areas where the climate or land is unsuitable for crops; it can grow rapidly, often doubling in biomass in 24 hours; it can be produced using waste sources of water and nutrients, thus alleviating the demand on freshwater and fertilizer supplies; and production of 50% of the United States biodiesel demand would require 2.5% of existing cropland instead of 846% for corn biodiesel.[19] Interest in algal biofuel research resurged around

the time of this publication, and over 4800 studies have cited this paper to note the benefits of algae as a biofuel feedstock.

1.1.4 Climate Change and Energy Security as Sustainability Concerns

The passing of the Energy Independence and Security Act of 2007 (EISA 2007), which updated the Energy Policy Act of 2005, reflects the convergence of climate change concerns and energy security concerns as drivers for algal biofuel research. In spite of the energy security focus of the EISA 2007, its Renewable Fuel Standard calls for the majority of the biofuel production goal to consist of "advanced biofuels," which are defined as biofuels with 50% less life cycle greenhouse gas emissions compared to their petroleum fuel counterparts.[8] The following excerpt from the Statement of Need for the Renewable Fuel Standard illustrates this point (emphasis mine):

> "The United States' dependence on imported petroleum to meet its growing demand for transportation fuel exacts a cost on the nation in terms of *energy security*. In addition, petroleum-based fuel exacts a cost on the nation with respect to *environmental quality*. The Renewable Fuel Standard (RFS) program *increases national energy security* by creating a market for renewable fuel as a substitute for petroleum-based fuel. By incorporating incentives for investing in research and development of renewable fuels, the RFS program also seeks to accelerate the nation's progress toward *energy independence*. In addition, the RFS program helps *to reduce the country's greenhouse gas emissions*, thereby reducing the nation's contribution to *global climate change* and its potential effects on the U.S. economy, security, and public health."[30]

The United States Department of Energy (DOE) had played a major role in algal biofuel research prior to 1996, and it regained this status in the resurgence of algal biofuel research in the mid-2000s. The DOE led a workshop in 2008 to develop the National Algal Biofuels Technology Roadmap, which discusses the challenges in the development of a national-scale algal biofuels industry and aims to guide future algal biofuel research efforts.[7] The Roadmap notes both energy security concerns (dependence on foreign oil, diminishing petroleum supplies, rising global energy demand) and environmental concerns (climate change) as motivations for algal biofuel research.[7]

The DOE also participates in algal biofuel research through its national laboratories, including the Sandia National Laboratories, the Pacific Northwest National Laboratory (PNNL), the National Renewable Energy Laboratory (NREL), Los Alamos National Laboratory, and Argonne National Laboratory. The official missions of the Los Alamos National Laboratory and Sandia National Laboratories focus significantly on national security and directly include energy security.[31, 32] The missions of Argonne National Laboratory and PNNL note both energy security and environmental concerns, while the mission of NREL only explicitly states a sustainability and environmental focus.[33-35] Together, these national laboratories represent the range of concerns noted in the DOE's own mission statement: "to ensure America's security and prosperity by addressing its energy, environmental and nuclear challenges through transformative science and technology solutions."[36]

In the late 2000s, researchers at universities and laboratories began to perform life cycle assessments for algal biofuel production. Life cycle assessment is a technique that determines the environmental impacts of a product or process through its life cycle by first compiling an inventory of material and energy inputs and their environmental releases, and then evaluating the potential environmental impacts of these inputs and outputs of the system.[37] A common

environmental impact category for biofuel life cycle assessments is climate change impact, which is typically determined from the net releases of greenhouse gases scaled to carbon dioxide equivalents per unit of biofuel analyzed.[38] A major effort from the Argonne National Laboratory has been to develop and publish an open-source platform for life cycle assessments of biofuels called the Greenhouse Gases, Regulated Emissions, and Energy Use in Transportation (GREET) Model, and this model was expanded to also include algal biofuel production.[39] Thus, this national laboratory became involved in algal biofuel research from the perspective of a climate change concern.

During the resurgence of interest in algal biofuels, one algal biofuel life cycle assessment was published in 2005, followed by one other assessment in 2009, five in 2010, nine in 2011, and increasing numbers in recent years, indicating that [39-54] climate change concerns are becoming increasingly important as drivers for algal biofuel research. However, in addition to concerns about greenhouse gas emissions and climate change, some of these life cycle assessment publications note "petroleum shortages,"[43] "fossil fuel depletion,"[49, 50] and "energy independence"[55] as motivation for their research into the sustainability of algal biofuels. One study has made it clear that "international concerns of fossil fuel depletion, energy security and CO_2 emissions are the main drivers" for algal biofuel research.[50]

At the same time as numerous life cycle assessments were published to determine the climate change impacts of potential pathways of algal biofuel production, geographic resource demand and techno-economic analyses were performed, though in lesser numbers, to determine whether large-scale production in the United States would be feasible.[56-77] These analyses aim to determine the availability and identify the location of resources for large-scale production of algal biofuel, to investigate potential competition between this new demand for resources and

their current allocation to other sectors, and to estimate the price of algal biofuels under different production scenarios. Therefore, these analyses are heavily focused on energy security.

In 2012, the National Academies and National Research Council published a report on the "Sustainable Development of Algal Biofuels in the United States" which ties both energy security and climate change concerns as part of the sustainability of algal biofuels. Several sustainability concerns of high, medium, and low importance are listed as areas where further research and development must occur.[78] The report lists energy security concerns (quantity of water required for algal cultivation; availability of appropriate land area for cultivation), climate change concerns (life cycle greenhouse gas emissions of algal biofuels; effects from land use change), and mixed energy security and climate change concerns (energy return on investment; potential local climate impacts; supply of key nutrients for algal cultivation and their fossil inputs for production; waste products from processing algae to fuels) among concerns of high and medium importance for the sustainability of algal biofuels.[78]

1.2 Objectives for the Presented Sustainability Assessment for Algal Biofuels

The potential sustainability of algal biofuels can be enhanced through the substitution of freshwater and commercial fertilizers with nutrients embodied in municipal wastewater and through the use of hydrothermal liquefaction in lieu of conventional lipid extraction methods. However, the environmental impacts of producing biofuels from wastewater algae in the United States will vary by geographic region as resource availability, transportation distances between facilities, environmental conditions for algal cultivation, and direct land use change impacts differ spatially. A new frontier in sustainability assessments of biofuels is the integration of geographic variables that provide more meaningful results to guide implementation decisions.[79] The work performed for this dissertation aims to incorporate aspects of spatial heterogeneity that

have previously not been examined by other sustainability assessments for algal biofuel production in the scientific literature.

The four chapters presented in this dissertation were performed in order to determine geographically specific environmental aspects of producing biofuels from wastewater algae. Chapter 2 analyzes the potential availability of wastewater and land within set distances from municipal wastewater treatment plants and whether the limiting resource differs between urban, near-urban, and rural locations using Kansas as a case study. The hypothesis for Chapter II is that there is a tradeoff in availability of water and land resources collocated with wastewater treatment plants in rural versus urban areas. Chapter 3 compares the life cycle greenhouse gas emissions of bio-jet fuel produced through hydrothermal liquefaction of wastewater algae to those of conventional jet fuel and compares the impacts of transportation distances and of siting hydrothermal liquefaction at wastewater treatment plants versus at petroleum refineries. It is hypothesized that the life cycle greenhouse gas emissions of algal bio-jet fuel produced through this method are lower than those of conventional jet fuel. Chapter 4 establishes a framework for integrating geographic variables that affect algal growth and direct land use change impacts into a life cycle assessment of algal biofuels, with a hypothesis that direct land use change impacts are as significant as foreground process impacts, and that they vary by region even if climatic conditions are similar. Chapter 5 uses this methodology to compare the life cycle climate change impacts of renewable gasoline from wastewater algae by the Level II ecoregion in which the algal feedstock is cultivated. It is hypothesized that the life cycle climate change impacts of algal renewable gasoline differs significantly by ecoregion and that patterns between characteristics of the ecoregions and the impacts can be determined from this analysis.

2 A Geographic Analysis of the Feasibility of Collocating Algal Biomass Production with Wastewater Treatment Plants

This chapter is a peer-reviewed journal article in *Environmental Science & Technology* shown in its entirety with the Supporting Information in Appendix A.

Reproduced with permission from:Fortier, M.-O. P., & Sturm, B. S. M. (2012). Geographic Analysis of the Feasibility of Collocating Algal Biomass Production with Wastewater Treatment Plants. *Environmental Science & Technology*, *46*(20), 11426-11434. doi: 10.1021/es302127f

2.1 Abstract

Resource demand analyses indicate that algal biodiesel production would require unsustainable amounts of freshwater and fertilizer supplies. Alternatively, municipal wastewater effluent can be used, but this restricts production of algae to areas near wastewater treatment plants (WWTPs), and to date, there has been no geospatial analysis of the feasibility of collocating large algal ponds with WWTPs. The goals of this analysis were to determine the available areas by land cover type within radial extents (REs) up to 1.5 miles from WWTPs; to determine the limiting factor for algal production using wastewater; and to investigate the potential algal biomass production at urban, near-urban, and rural WWTPs in Kansas. Over 50% and 87% of the land around urban and rural WWTPs, respectively, was found to be potentially available for algal production. The analysis highlights a tradeoff between urban WWTPs, which are generally land-limited but have excess wastewater effluent, and rural WWTPs, which are generally water-limited but have 96% of the total available land. Overall, commercial-scale algae production collocated with WWTPs is feasible; 50% of the Kansas liquid fuel demand could be met with implementation of ponds within 1 mile of all WWTPs and supplementation of water and nutrients when these are limited.

2.2 Introduction

The substitution of petroleum-derived fuels with renewable, affordable, and low carbon-emitting fuels is necessary to reduce continued detrimental human impact to the environment and support future economic growth. Biofuels derived from agricultural crops are increasingly being produced, but meeting even a portion of the United States' transportation fuel needs would require an unsustainably large percentage of existing cultivation areas.[19] Unlike other biofuel

feedstocks (i.e., corn and soy), algae do not compete with existing food commodities, can grow on marginal lands not suitable for conventional agriculture, and may not require large volumes of fresh water. Several different water and nutrient sources have been tested for algal production, including fresh or saline aquifers and sea water supplemented with fertilizers; municipal wastewaters;[80, 81] and some agricultural or industrial wastewaters.[82, 83]

Recently performed geographic and resource demand analyses for algal biofuel feedstock production highlight the critical need for alternative water and nutrient supplies to realize sustainable production of algal biofuels. Pate et al.'s analysis of resource demands for algal production from freshwater and fertilizer-supplied algal reactors estimated that production of 50 billion gallons per year of biofuel in the Midwest would require diversion of 97% of irrigation water and 221% of nitrogen fertilizers for algal cultivation efforts every year.[62] Wigmosta et al. determined that if production was limited to areas with the lowest potential evaporative water loss, meeting the Energy Independence and Security Act of 2007 renewable fuel target for "advanced biofuels" of 21 billion gallons[84] would require an amount of water equal to 25% of the irrigation water consumed in agriculture.[65] These sizeable estimated freshwater demands would create competition between water for food and water for biofuels, which could worsen current water shortages. The water footprint of other biofuels, in particular corn-based ethanol, has been discussed as one of the major environmental limitations of biofuel production.[27]

A promising solution to reduce the freshwater and fertilizer demand of algal biomass production is to utilize municipal wastewater effluent, which contains nitrogen, phosphorus, and other necessary nutrients. Indeed, wastewater treatment plants (WWTPs) are under increasing pressures to remove nitrogen and phosphorus from their effluent discharges, particularly in the Midwest and the Gulf of Mexico watershed.[85] Therefore, algal production at WWTPs has the potential to produce a biofuel commodity while performing biological nutrient removal (BNR).

Despite the many benefits of using wastewater for algal biomass production, it is unknown whether there is sufficient land or wastewater available for large-scale fuel production. The use of wastewater restricts algal production to areas near WWTPs. In turn, the availability of wastewater effluent or land within short distances from WWTPs may limit potential production. Although previous geographic or resource demand analyses have been performed on algal biodiesel feedstock production, to the authors' knowledge, none have focused on collocation with wastewater treatment plants or analyzed algal production potential within urban areas. Table 2.1 outlines the differences in analytical approach between this study and four geographic and resource demand analyses of algal biofuel feedstock production.

The goals of this analysis were to determine the available areas by land cover types within known distances from WWTPs, to determine the limiting factor for production of algal biodiesel using wastewater effluent, and to investigate the feasibility of producing algae for biodiesel in rural, near-urban, and urban areas. The study was performed for the state of Kansas as a representative state with rural and urban environments, a range of WWTP sizes, and a climatic gradient that results in a large span of net evaporation rates. Kansas was also chosen as a representative state for this study due to the availability of primary data on microalgae grown in wastewater effluent in open pond reactors.[80, 86] The average algal productivity and lipid content determined from these pilot-scale studies in Lawrence, KS, provide realistic baseline values for algal biodiesel production potential in the region. The use of a representative state allows for detailed geospatial analysis of WWTP locations and the development of a methodology that could be expanded to a larger geographic area in future work.

2.3 Methods

2.3.1 Study Area and Algal Productivity Assumptions

Wastewater treatment plants in Kansas with at least 50% existing municipal flow and a National Pollution Discharge Elimination System (NPDES) permit were selected from the 2008 Clean Watersheds Needs Survey.[87] The El Dorado WWTP, despite meeting these criteria, was excluded from the analysis because its surrounding land has been converted to constructed wetlands for wastewater treatment, and its effluent and land are thus considered unavailable. The remaining 387 WWTPs meeting the criteria were classified as urban, near-urban, or rural based on their proximity to urbanized areas and urban clusters as defined by the UA/UC Census 2000 Boundary shapefile.[88] Near-urban WWTPs were designated as WWTPs outside of urban areas but within 2 miles of an urban boundary.

Potential production was evaluated for a baseline algal production (BAP) scenario and a high algal production (HAP) scenario. The baseline algal production scenario is based on the results of a pilot study for algal production in wastewater effluent in Lawrence, Kansas.[89] The BAP scenario involves an algal areal productivity of 12 g m^{-2} d^{-1} and a lipid content of 10% based on dry weight. The high algal production scenario is based on an algal productivity of 25 g m^{-2} d^{-1} and a lipid content of 30%. The HAP parameters have been modeled in algal biodiesel production life cycle assessments,[42, 44, 45, 49, 50, 53] and though they have not been observed at the Lawrence WWTP, they may be possible with supplementation of CO_2, which is not currently performed in the pilot study. The BAP scenario parameters contribute to the most conservative algal biodiesel yields per unit area for Kansas among published geographic and resource demand analyses (Table 2.1). The HAP scenario depicts a higher algal biodiesel yield per unit area for the state than the Wigmosta et al.[65] and the Quinn et al.[90] analyses, but a lower yield than assumed by Pate et al.[62] For both scenarios, a 214-day annual production schedule was chosen

for the potential production calculations to represent the tested growing season for the Lawrence WWTP pilot study, from April 1 through October 31.

Table 2.2: Comparison of the design of this study to the approaches of other geographic and resource demand analyses of algal biofuel feedstock production in the United States.

	Murphy & Allen (2011)	**Pate, Klise & Wu (2011)**	**Quinn et al. (2011)**	**Wigmosta et al. (2011)**	**This study**
Goal	To determine the state-specific and US weighed mean amount of energy required for algal cultivation and the potential energy output per unit area of available land	To assess the land, CO_2, nitrogen, phosphorus, and water demands of producing 10, 20, 50, and 100 billion gallons per year of algal biofuel feedstock in four multi-state scenario regions	To assess the national potential lipid production from microalgae grown in industrial-scale photobioreactors on available land	To determine where algal production can occur, the amount of land and water required, and the amount of energy that could be produced nationally	To determine the land cover types of available areas within known distances from Kansas WWTPs and to assess the potential biodiesel production from collocation of WWTPs and algal production
Definition of available land	Rural and nonfederal land, excluding prime pasture and rangeland, forests, and cropland	Land categorized as pasture in each scenario region	Land that is categorized as shrubland, scrubland, grasslands, barren or herbaceous and that with no greater than a 2% slope	Land that can hold a 490 ha facility and that is not sloped greater than 1% or categorized as protected or environmentally sensitive areas, open water, urban areas, cultivated cropland, orchards, or airports	Land that is not sloped greater than 5%, occupied by WWTP infrastructure, water bodies, or of urban residential, urban commercial, or urban industrial land cover types
Percent of available area occupied by new infrastructure	37.5%	0%	0%	18.4%	15.0%
Water source	Saline water from aquifers	Freshwater	Freshwater	Freshwater	Municipal wastewater effluent
Nutrient source	Not defined	Ammonia and phosphate rock-derived fertilizer	Not defined	Not defined	Municipal wastewater effluent
Algal biofuel production potential for Kansas (barrels/acre-yr)[a]	-	97.6[b]	40.7[c]	15.1[d]	HAP scenario: 75.9[e] BAP scenario: 12.1[e]
Growing season	365 days/year	365 days/year	Based on temperature; production ends when the production system freezes	Determined spatially and based on a water temperature of at least 10 degrees Celsius	214 days/year

a. Values are reported either as algal lipid productivity or algal biofuel production potential with a conversion efficiency of 100% from algal lipids to biofuels.
b. Based on the Midwest scenario region with an assumed algae oil productivity of 4100 gal/acre-yr.
c. Based on an average current realizable algal lipid productivity potential of 16 m^3/ha-yr determined from Figure 4 of Quinn et al. (2011).
d. Based on the average biofuel production rate achievable with current technology of 4750 L/ha-yr determined from Figure 3 of Wigmosta et al. (2011) and removing the 80% conversion efficiency.
e. Calculated from the algal productivity and lipid content values using a 918 kg/m^3 algal oil density and an efficiency of 100%.

The total amount of oil that could be produced annually under each productivity scenario was calculated based on the land or wastewater available near Kansas municipal WWTPs in order to determine the limiting factor of production and to assess the potential of either resource in producing algal biodiesel. A 75% overall processing efficiency was assumed for the conversion of algal lipids to biodiesel. A lipid density of 918 kg m^{-3} was assumed.[91] The percentage of the Kansas annual liquid fuel consumption of 62.44 million barrels that would be met by algal biodiesel production was evaluated.[92] This amount includes other fuel types in addition to diesel, such as jet fuel and gasoline, and thus it provides a more conservative evaluation of the potential biofuel production from algae grown at Kansas WWTPs.

2.3.2 Potential production under wastewater limitation

The potential algal biofuel production under wastewater limitation was determined using wastewater effluent concentrations of nitrogen and phosphorus reported by municipal Kansas WWTPs from 2000 to 2011 to the Kansas Department of Health and Environment.[93] The monthly average total nitrogen (TN) and total phosphorus (TP) concentrations in units of mg L^{-1} over this decade were determined for each reporting WWTP. Average monthly nutrient concentrations for urban, near-urban, and rural WWTPs were calculated and the molar N:P ratio was determined for these groups of WWTPs for each month of the growing season (April-October). The molar N:P ratio was used to determine whether the WWTPs were overall nitrogen-limited (N:P <16) or phosphorus-limited (N:P >16) each month using the Redfield expression for an algal cell, $C_{106}H_{263}O_{110}N_{16}P_1$.[94]

The approximate percentages of nitrogen and phosphorus by weight in an algal cell can be determined using the stoichiometric ratio provided by experimental results or the Redfield expression, $C_{106}H_{263}O_{110}N_{16}P_1$.[94] From weekly measurements during the pilot experiment, the particulate N:P molar ratio averaged 6.4 ± 5.9, with a minimum of 0.7 and a maximum of 30.0; these results have been previously published.[80] Although this experimental data was available, the Redfield ratio was used for our calculations since that provided more conservative estimates of algal biomass production and were consistent with the Pate et al. approach.[62] Accordingly, 15.9 mg of dry algal biomass are assumed to be produced from the uptake of 1 mg of nitrogen from wastewater effluent, and 115 mg of dry algal biomass are assumed from the uptake of 1 mg of phosphorus. For an N:P ratio lower than 16, the algal biofuel production calculations were based on the nitrogen concentration. Conversely, for an N:P ratio higher than 16, these calculations were based on the phosphorus concentration instead.

The potential algal biodiesel production was calculated by growing season month under the BAP and HAP scenarios using the calculated average nitrogen or phosphorus concentration, the nutrient to algal biomass stoichiometric ratio obtained from the Redfield expression, and the cumulative wastewater flow for urban (148.8 MGD), near-urban (62.33 MGD), or rural (21.64 MGD) Kansas WWTPs (see Supporting Information). The potential annual algal biodiesel production under wastewater limitation for each scenario was determined by the sum of the barrels produced monthly over the growing season for all three WWTP types. To provide some sensitivity analysis for the variability in nutrient concentrations, additional combinations of maximum nutrient concentrations (average value plus one standard deviation) and minimum nutrient concentrations (average value minus one standard deviation) were also analyzed.

2.3.3 Potential production under land limitation

The 387 Kansas municipal WWTPs were geocoded in ArcGIS 9.3.1 using the location data from their National Pollutant Discharge Elimination System (NPDES) permits. Their point locations were checked and adjusted to the actual locations if initially incorrect using 2008 National Agriculture Imagery Program (NAIP) aerial imagery for Kansas.[95] Land area was assumed to be unavailable for algal production if currently occupied by WWTP infrastructure, water bodies, specific land cover types (urban residential, urban commercial, or urban industrial land cover types), or if sloped greater than 5%. The Department of Energy notes that land sloped beyond 5% would be prohibitively expensive to level in order to install algal ponds.[96] Areas with slopes greater than 5% were located within 25 m grids using ArcGIS Spatial Analyst and USGS National Elevation Dataset digital elevation models. The existing WWTP infrastructure was digitized using 2008 NAIP aerial imagery for Kansas.[95] Water bodies and areas of unavailable land cover types were defined using the 2005 Kansas Land Cover Patterns (KLCP)

Level I map from the Kansas Applied Remote Sensing Program.[97] The following land cover types were deemed potentially available land if not covered by WWTP infrastructure or sloped greater than 5%: urban openland, urban woodland, cropland, woodland, grassland, Conservation Reserve Program (CRP) land, and other land (Figure 2.1). Buffers were created within 0.25, 0.50, 0.75, 1.0, and 1.5 miles from the WWTPs to delineate radial extents (REs) of algal production implementation (Figure 2.1). The KLCP map and the combined unavailable area were clipped to the buffers to determine the available land area at each distance and its current land cover types. The area that would be occupied by algal ponds was calculated from the available land assuming that 15% of the available land would be used for new infrastructure such as pump stations, roads, walkways, and piping. The area required for downstream processing of harvested algae was not considered in this analysis. The potential algal biodiesel production at each RE was determined using the available area for the BAP and HAP scenarios.

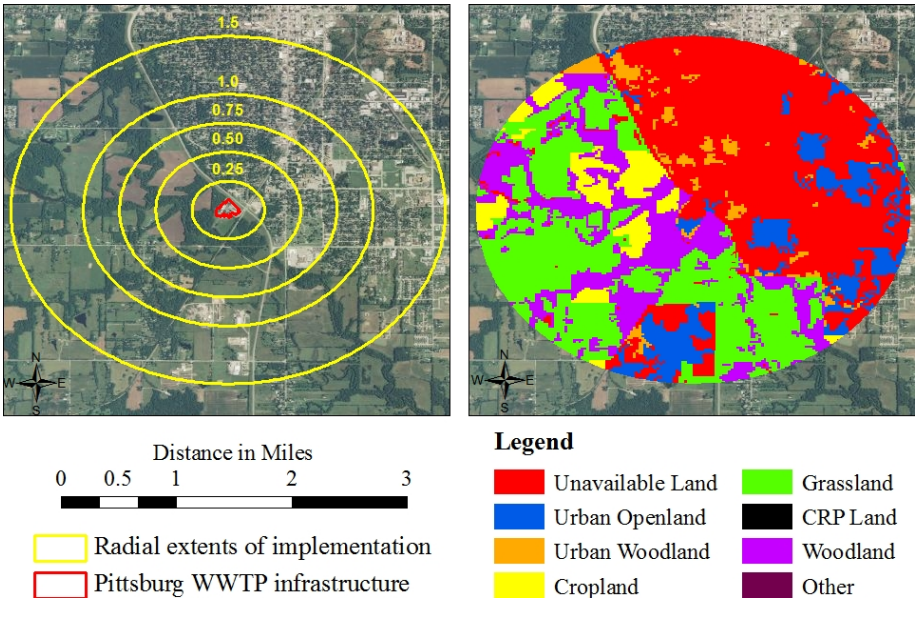

Figure 2.2: Example of land availability analysis results in ArcGIS. Left: Radial extents in miles around the Pittsburg WWTP in Kansas, which is delineated with a red outline. Right: Available land by land cover type and unavailable land within 1.5 miles from the Pittsburg WWTP.

2.3.4 Evaporative demand as a water availability constraint

Each WWTP was matched to the potential net evaporation rate in inches per year for its township and range as calculated by the Kansas Department of Agriculture.[98] The potential net evaporation rate was calculated as the annual average evaporation, derived from pan evaporation data, minus the annual precipitation.[98] One limitation of this method is the lack of differentiation for monthly fluctuations in evaporation. The net evaporation rate and the available land at each RE were used to determine the annual volume of water that is expected to evaporate from algal ponds. This evaporative demand was compared to the effluent wastewater flow rate at each WWTP to determine whether an individual plant is water-limited or land-limited. If the calculated volume evaporated at a WWTP annually was found to exceed the annual wastewater discharge, the WWTP was classified as water-limited.

2.4 Results and discussion

2.4.1 Statistics on Kansas municipal wastewater treatment plants

There are 387 WWTPs in Kansas that have at least 50% municipal wastewater flow and an NPDES permit. There are 26 WWTPs (6.7%) in urban areas, 63 (16.3%) in near-urban areas, and 298 (77.0%) in rural areas (see Supporting Information). Their total existing flows range from 0.006 MGD to 40.6 MGD. The range of net evaporation rates experienced by Kansas WWTPs is 1 to 51 in yr^{-1}.[98] As the RE of algal pond implementation was increased, specific WWTPs were removed from the analysis when the radius reached beyond the boundary of the state and the corresponding land cover layer. Fourteen WWTPs were excluded at the largest RE, 1.5 miles. Additionally, as the RE was increased, the available area at certain WWTPs became merged with the available area at nearby WWTPs. A list of excluded WWTPs and merged WWTP complexes can be found in the Supporting Information.

Although TN and TP data was not uniformly available for every year or month, all 26 urban WWTPs contributed nutrient concentration data over the months of April through October. Additionally, fifty of the 63 near-urban WWTPs contributed nutrient data, as well as 57 of the 298 rural WWTPs. The lack of data for each individual WWTP further supports the use of average monthly nitrogen and phosphorus concentrations for WWTPs grouped by their proximity to urban areas. The average monthly TN and TP for urban, near-urban, and rural WWTPs over the growing season is shown in the Supporting Information.

2.4.2 Land availability for algal pond implementation surrounding WWTPs

Available land area for algal production was defined as land sloped less than 5% that is not occupied by existing WWTP infrastructure, water bodies, or specific land cover types (urban residential, urban commercial, or urban industrial), at radial extents from 0.25 to 1.5 miles. Of the 26 urban WWTPs analyzed, 7.29 to 81.8% of the land within a 0.25 mile RE is potentially available for installation of algal ponds and associated infrastructure. On average, 50.9% of the land within 0.25 mile of urban WWTPs is potentially available land for algal production and new infrastructure (see Supporting Information). This mean proportion of available land stays relatively constant as the RE is increased to one mile from the center of urban WWTPs, and it increases to over 54% at an RE of 1.5 miles. For the 63 near-urban WWTPs, 25.1 to 98.6% of the land within 0.25 miles is available to implement algal production. At this RE, an average of 75% of the land is potentially available. At the four larger REs analyzed, this proportion of available land increases to 79%. For the 298 rural WWTPs, 41.0 to 100% of the land at an RE of 0.25 miles is potentially available for algal production systems. An average of 87% of the land within 0.25 to 1.0 miles from rural WWTPs is potentially available. This average increases to 89.5% at an RE of 1.5 miles.

Figure 2.2 presents the percent of available land for each of six land cover types (urban openland, cropland, grassland, woodland, CRP land and other) for urban, near-urban, and rural WWTPs. Since the distribution of land cover types did not vary significantly with the RE surrounding near-urban or rural WWTPs, the average distribution for all REs is presented for those WWTP types in Figure 2.2. For urban plants, urban openland is the prominent land cover type at all REs of algal pond implementation, followed by cropland and grassland. Urban openland is mainly open grassland, sometimes with the sparse presence of trees, within an urban setting.[97] The available land around near-urban and rural WWTPs is categorized primarily as cropland and grassland. Different land types will have different social and economic acceptability, which may make certain classes (urban openland and woodland) less likely to be converted to algal ponds. Land classes have been ordered from bottom-up in Figure 2.2 and 2.3 according to perceived social and economic acceptability. This is discussed below under "Implications for siting commercial production."

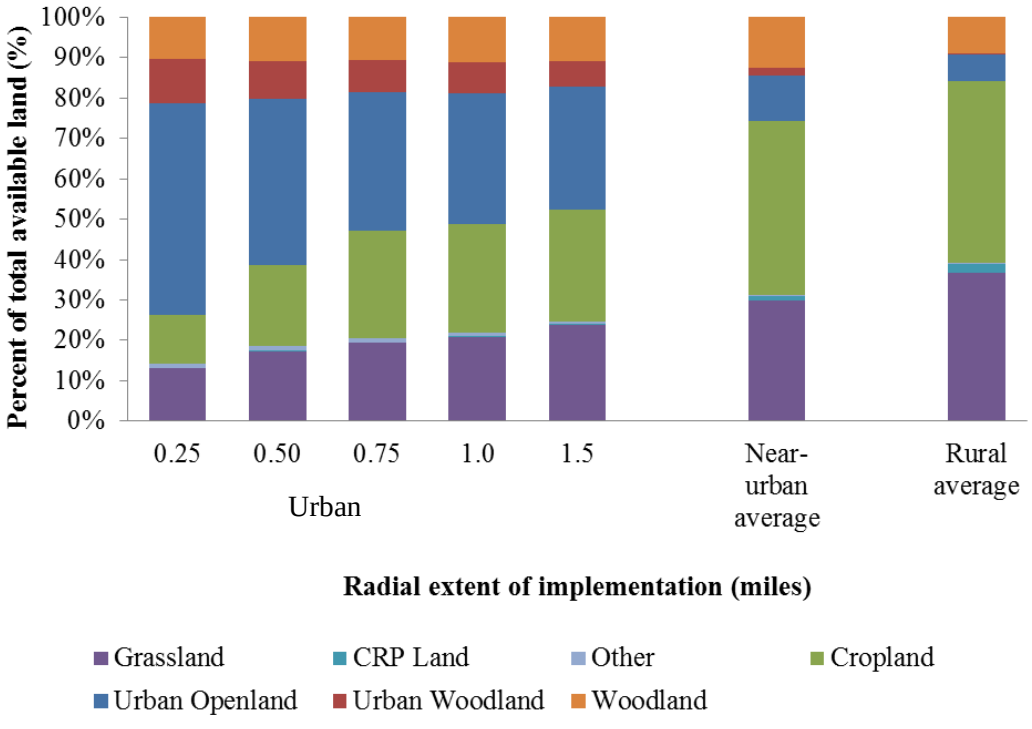

Figure 2.2: Distribution of land cover types for available land around Kansas WWTPs. For urban WWTPs, the distribution is reported as a function of the radial extent (RE) of implementation. For near-urban and rural WWTPs, the average distribution of land cover types for all REs of implementation is reported.

Within one mile from all Kansas WWTPs, a total of over 630,000 acres are potentially available for algal ponds. When the RE is increased to 1.5 miles, over 1.43 million acres are identified as available land (Figure 2.3). The rural WWTPs contribute 81% of this total land, while the near-urban WWTPs contribute 15%, and the urban municipal WWTPs in Kansas account for 4% of land that is potentially available for installation of algal ponds. These proportions do not change significantly by RE analyzed.

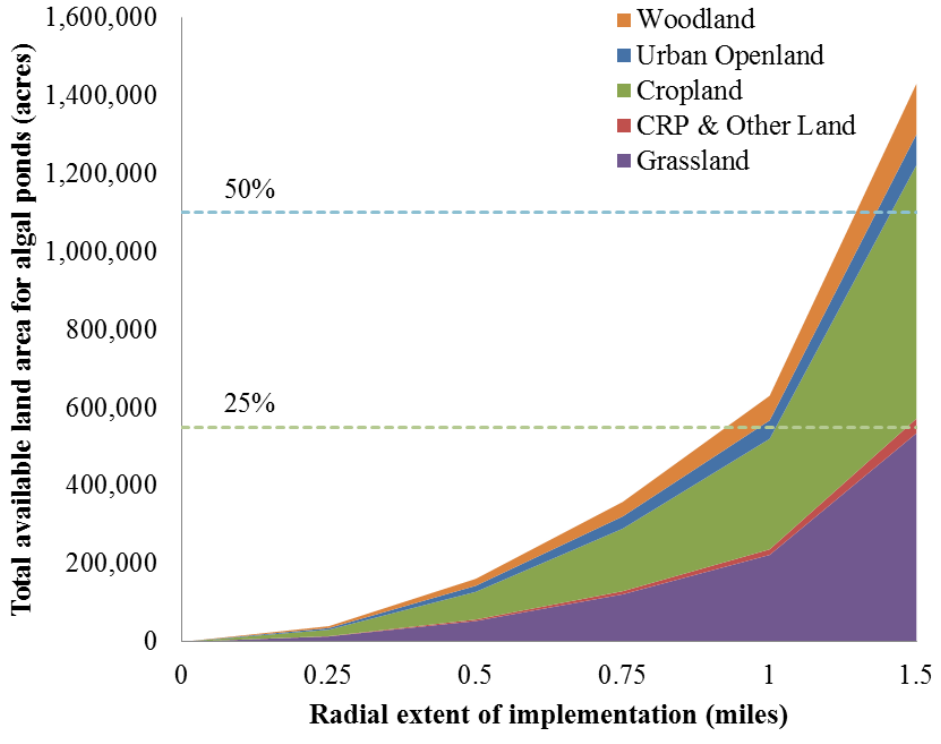

Figure 2.3: Available land area for algal pond installation near all Kansas WWTPs for varying radial extents of implementation. Dotted lines represent the area required to produce 25% to 50% of the Kansas annual fuel consumption, assuming that sufficient water and nutrients are provided and that the HAP scenario applies.

The distribution of available land among land cover types by radius from WWTPs is shown in Figure 2.3 relative to the area needed to meet 25% and 50% of the Kansas annual fuel consumption of 62.44 million barrels.[92] This area was calculated assuming the HAP scenario conditions, a lipid to fuel conversion efficiency of 75%, a lipid density of 918 kg m^{-3}, a proportion of available land used for algal production of 0.85, and sufficient water and nutrient supplies (see Supporting Information). If all available land within 0.75 miles of Kansas WWTPs were used to produce algae for biodiesel under these conditions, 16.3% of the Kansas fuel

demand could be met. Algal biodiesel production matches 28.6% of the Kansas fuel demand when the available land within one mile of WWTPs is used. At an RE of 1.5 miles, 65% of the fuel demand for the state could be fulfilled through algal biofuels.

2.4.3 Determination of the limiting production factor (land or wastewater)

In order to determine the limiting factor for algae production at Kansas municipal WWTPs, the amount of algal biodiesel that could be produced annually was calculated based on the land or wastewater resources from all 387 Kansas municipal WWTPs combined. The results of these calculations are shown in Table 2.2. Under the HAP scenario, 11.8 times more algal biodiesel can be produced annually on the available land at an RE of 0.25 miles (1.14 million barrels) than can be obtained from the wastewater resources, assuming maximum nutrient concentrations (97,000 barrels). Thus, wastewater resources are more limiting to algal production than nearby available land when the resources of all Kansas municipal WWTPs are combined. However, the limiting factor varies by WWTP and by RE of algal implementation when the evaporative water demand is introduced as a constraint. Figure 2.4 shows the percentage of WWTPs that were determined to be land-limited instead of water-limited at each RE for the three classifications of WWTPs; the percentage is calculated for all available land types and for grassland only, which may be perceived as the most available land. The majority of rural WWTPs are water-limited at all REs, meaning that these WWTPs have more land available than they have wastewater discharge to cover that land and meet the evaporative demand of the shallow algal pond systems. At 0.75 miles from rural WWTPs, only two plants are land-limited. The number of rural WWTPs that are land-limited decreased to one and zero at distances of 1.0 and 1.5 miles from the plants, respectively. Because there is more available land

than can be sustained by wastewater effluent at most rural WWTPs, using all or most of the available land would require a supplemental source of water and nutrients.

Table 2.2: Limiting factor analysis results for production at all 387 Kansas municipal WWTPs, in which the associated land and wastewater resources were investigated for their algal production potential. a) The minimum TN and TP concentrations represent one standard deviation below the average values, while the maximum TN and TP concentrations are one standard deviation above the average values.

	Potential algal biodiesel production (thousand barrels/year)		**Percent of Kansas liquid fuel demand met (%)**	
	BAP	*HAP*	*BAP*	*HAP*
Land-limited production				
RE = 0.25 miles	183	1.14×10^3	0.29	1.83
RE = 0.50 miles	733	4.58×10^3	1.17	7.30
RE = 0.75 miles	1.63×10^3	1.02×10^4	2.61	16.3
RE = 1.00 miles	2.86×10^3	1.79×10^4	4.58	28.6
RE = 1.50 miles	6.49×10^3	4.06×10^4	10.4	65.0
Wastewater-limited production				
Average TN and TP	20.5	61.5	0.0328	0.0985
Minimum TN and TP[a]	8.28	24.8	0.0133	0.0398
Maximum TN and TP	32.3	96.9	0.0518	0.1553
Maximum TN and minimum TP	19.0	57.0	0.0304	0.0913
Minimum TN and maximum TP	8.59	25.8	0.0138	0.0413

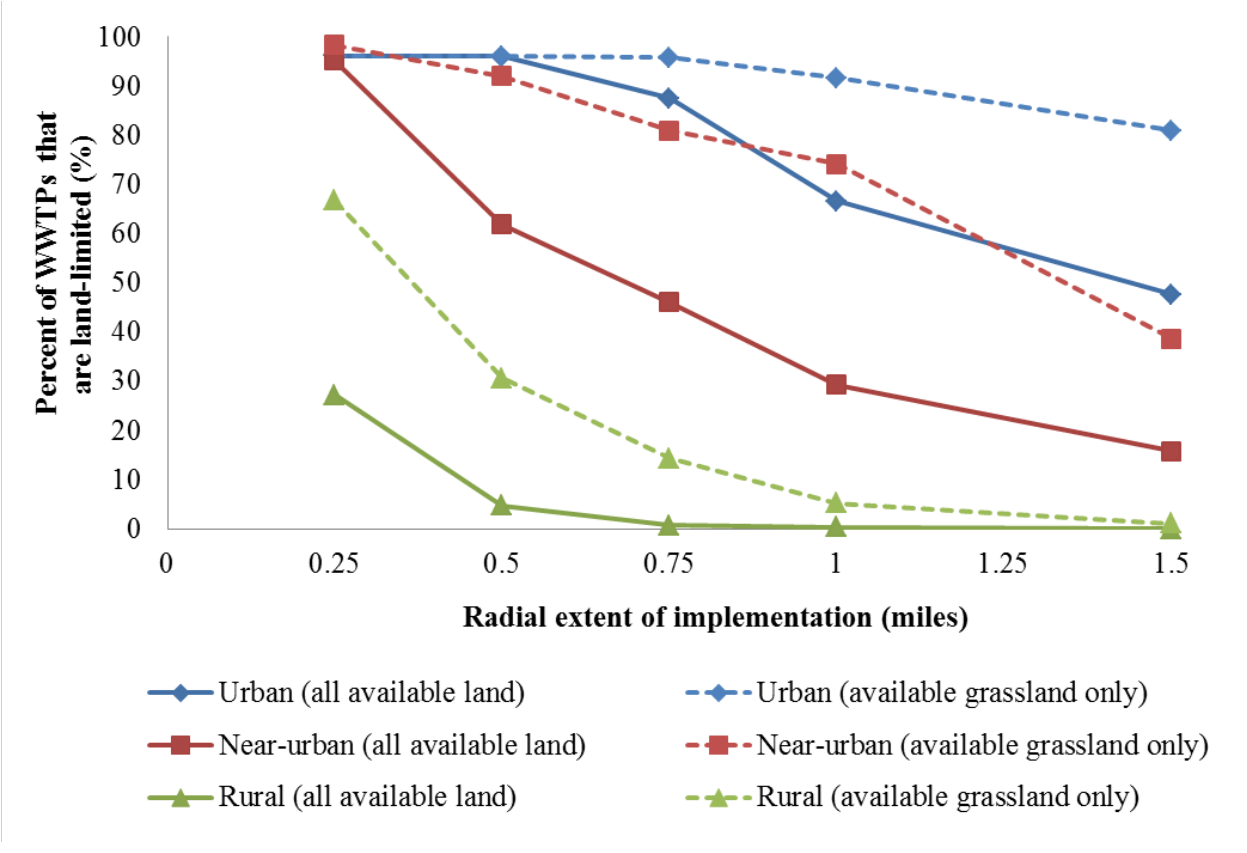

Figure 2.4: Percent of Kansas WWTPs that are limited by available land area when land and wastewater restrictions are compared at individual WWTP and evaporative demand is included.

In contrast, at distances less than 0.75 miles from near-urban and urban WWTPs, the majority of WWTPs are land-limited. At the largest RE analyzed (1.5 miles), 47.6% of urban WWTPs are land-limited, and nine WWTPs would need to divert less than 15% of their wastewater effluent to meet the evaporative demand. To fully utilize the water volume and nutrient potential embodied in the unused wastewater effluent, algal ponds could be installed on available land beyond 1.5 miles from the WWTP, or the effluent could be routed to nearby water-limited near-urban or rural WWTPs, where 96% of the potentially available land for algal production around Kansas municipal WWTPs is located. This excess wastewater effluent would

not be sufficient to fully utilize the land area available near these WWTPs, however, and other supplemental sources of water and nutrients should be considered to extend production beyond the resources directly available at most rural and near-urban municipal WWTPs.

2.4.4 Nutrient and water supplementation possibilities for rural WWTPs

Because wastewater was found to be the limiting factor for most rural WWTPs in Kansas, supplemental sources of nutrients and water would be necessary to fully utilize the substantial land potential for algae production at these WWTPs. There are many possible sources for these, including agricultural wastewaters. Previous studies have shown that algae can grow in diluted wastewater (often after anaerobic digestion or secondary treatment) from dairies,[13, 81] slaughterhouses,[99] breweries,[100] distilleries,[101] aquaculture facilities,[102, 103] and concentrated animal feeding operations (CAFOs).[104, 105] The amounts of nitrogen and phosphorus available through dairy and slaughterhouse wastewaters are calculated in the Supporting Information. Algae has also been cultivated in the supernatant from anaerobic digestion of poultry litter.[83] Other sources of non-fresh water and nutrients include collected runoff from farms and stormwater runoff from fertilizer production facilities. Finally, nutrients could be recycled from the processes of converting algal biomass into biodiesel, methane gas via anaerobic digestion,[106] or biocrude via hydrothermal liquefaction.[107, 108] Hydrothermal liquefaction produces an aqueous wastewater that is nutrient-rich and can be diluted and used for algal biomass production.[108-110]

In addition to these possible supplies of concentrated nutrients in wastewaters, a supplemental source of water would be necessary to meet the land potential for algal growth at rural wastewater treatment plants in Kansas. Ideally, this added water should not be freshwater that could be used for agriculture or drinking water. Two promising sources of additional water

are saline aquifer water[63] and industrial wastewaters, provided that the industrial effluent does not contain high concentrations of chemicals that may be toxic to algae or that this effluent is sufficiently diluted with municipal wastewater to prevent possible inhibitory effects to algal growth. Algae has been cultivated in wastewater from a carpet mill,[82] an oil refinery,[16] and a sugar mill.[17]

2.4.5 Implications for siting commercial production

Urban WWTPs have certain advantages over near-urban or rural WWTPs in Kansas for collocation of algal production and wastewater treatment. Urban WWTPs in Kansas process significantly larger wastewater flows than near-urban or rural WWTPs ($p<0.05$). The majority of urban WWTPs have sufficient wastewater flow to meet the land potential within an RE of one mile, while most rural WWTPs in Kansas would be unable to use the available land within 0.25 mile. Some urban WWTPs have flow rates that can meet the evaporative water demand of algae production on available land beyond a distance of 1.5 miles from the plant. These results suggest that implementing commercial-scale algae production for biodiesel in urban settings would be feasible due to the quantities of both wastewater and land. However, limiting algal production to urban areas would underutilize the total amount of land on which algal ponds could be installed near WWTPs in Kansas by 96%. Other nutrient and water sources (i.e., animal agriculture waste) are likely to be located in rural areas, thus allowing for increased use of the available land for algal production beyond the limitations imposed by municipal wastewater availability and the rate of evaporation.

This analysis also highlights the different land cover types that would need to be converted for commercial algal biomass production. One limitation to collocating algal production with urban WWTPs is that urban openland may include areas that would be difficult

or unfeasible to convert, such as cemeteries, zoos, urban parks, and golf courses, which have ecological, economic, and social significance.[97] The cost of undeveloped land in urban areas is typically higher than rural land as well. The average value of cropland in Kansas in 2011 was $1300 per acre,[111] while the average price of undeveloped land in Johnson County, a mostly urban county which includes Kansas City, KS, was over $43,000 per acre in 2010.[112] Although cropland is relatively inexpensive, the use of cropland would involve converting arable land from food production to fuel production, which is a controversial issue for the sustainability of the corn ethanol industry that algal biofuel producers aim to avoid. It is also unknown whether clearing areas of specific land cover types such as woodland would lead to higher overall greenhouse gas emissions from the loss of carbon-sequestering vegetation than could be avoided through the substitution of algal biofuels for conventional fuels.

Grassland may be the most promising land cover type for conversion to algal ponds, but limiting algal production to current grassland areas would reduce available land areas by 76.1% to 86.8% for urban WWTPs depending on the RE, or by an average of 70.3% for near-urban WWTP and 63.4% for rural WWTPs. Potential algal production at water-limited WWTPs, which could not use all available land with their wastewater resources alone, might not be heavily impacted by limiting available land to grassland. However, urban WWTPs which tend to be land-limited would either be less likely to install algal ponds due to the additional obstacles in obtaining nearby land, or they would need to consider land beyond a radial extent of 1.5 miles to produce large amounts of algae as biofuel feedstock.

Other considerations for collocation would further restrict which WWTPs are likely to implement algal production. The proximity of a plant to an appropriate biorefinery or to a waste source of CO_2 gas, which would enhance algal growth, could influence a WWTP operator's decision to install algal ponds. The presence of nearby agricultural operations that produce

nutrient-rich wastewaters would be a significant factor in implementing algal production at water-limited WWTPs. Additionally, the downstream functions of a WWTP's effluent should be considered. Wastewater discharges could be significant contributions to the local hydrologic cycle, or they could be needed for re-use or for the satisfaction of downstream water rights.

If solutions to these impediments to future algal production at municipal WWTPs can be found, there is potential in co-locating algal production with wastewater treatment. If sufficient supplemental quantities of waste nutrients and water can be provided at every Kansas municipal WWTP that is water-limited at an RE of 1.0 mile, then 17.9 million barrels of algal biodiesel could be produced annually under HAP conditions on all potentially available land, and nearly 29% of Kansas' liquid fuel demand could be met by these renewable fuels without diverting freshwater and fertilizer from the agricultural sector. In the analysis by Pate et al.,[62] meeting approximately 33% of the nation's diesel demand through algal production using traditional resources in the nineteen lower-tier state region would require 12.1 trillion gallons of freshwater (39% of irrigation water used in the region), 31 million metric tons of nitrogen (221% of fertilizer N consumed in the region), and 4.2 million metric tons of phosphorus annually (102% of fertilizer P consumed in the region). Whereas generating substantial amounts of biodiesel from algal feedstocks is found to be unsustainable using these resources, the collocation of algal production with wastewater treatment plants using the resources available at WWTPs supplemented with nutrient-rich waste streams might be a viable system for large-scale algal biodiesel production.

3 Life Cycle Assessment of Bio-Jet Fuel from Hydrothermal Liquefaction of Microalgae

This chapter is the entirety of the following peer-reviewed journal article published in *Applied Energy*, with the Supplemental Information as Appendix B.

Fortier, M.-O. P., Roberts, G. W., Stagg-Williams, S. M., & Sturm, B. S. M. (2014). Life cycle assessment of bio-jet fuel from hydrothermal liquefaction of microalgae. *Applied Energy, 122*, 73-82. doi: http://dx.doi.org/10.1016/j.apenergy.2014.01.077

3.1 Abstract

Bio-jet fuel is increasingly being produced from feedstocks such as algae and tested in flight. As the industry adopts bio-jet fuels from various feedstocks and conversion processes, life cycle assessment (LCA) is necessary to determine whether these renewable fuels result in lower life cycle greenhouse gas (LC-GHG) emissions than conventional jet fuel. An LCA was performed for a functional unit of 1 GJ of bio-jet fuel produced through thermochemical conversion (hydrothermal liquefaction (HTL)) of microalgae cultivated in wastewater effluent. Two pathways were analyzed to compare the impacts of siting HTL at a wastewater treatment plant (WWTP) to those of siting HTL at a refinery. Base cases for each pathway were developed in part using primary data from algae production in wastewater effluent and HTL experiments of this algae at the University of Kansas. The LC-GHG emissions of these cases were compared to those of conventional jet fuel, and a sensitivity analysis and Monte Carlo analyses were performed. When algal conversion using HTL was modeled at a refinery versus at the WWTP site, the transportation steps of biomass and waste nutrients were major contributors to the LC-GHG emissions of algal bio-jet fuel. The LC-GHG emissions were lower for the algal bio-jet fuel pathway that performs HTL at a WWTP (35.2 kg CO_{2eq}/GJ for the base case) than for the pathway for HTL at a refinery (86.5 kg CO_{2eq}/GJ for the base case). The LCA results were particularly sensitive to the extent of heat integration, the source of the heat for HTL, and the solids content of dewatered algae. The GHG emissions of algal bio-jet fuel can be reduced by 76% compared to conventional jet fuel with feasible improvements in those sensitive parameters and siting HTL at a WWTP. Therefore, it is critical that transportation logistics, heat integration of biomass conversion processes, and nutrient supply chains be considered as investment and production of bio-jet fuels increase.

3.2 Introduction

Bio-jet fuel is increasingly being used in attempts to reduce the environmental impacts of aviation and to ensure energy security in the industry. The International Air Transport Association aspires to use 6% biofuel blends in aircraft by 2020,[113] which corresponds to 1.31 billion gallons of bio-jet fuel needed annually to meet the United States' demand of 21.85 billion gallons of liquid fuels in 2011.[114] Several test flights have already been performed on blends of conventional jet fuel and bio-jet fuel from algae, camelina, and other plant-based feedstocks on commercial airlines and military aircraft.[115] In July 2011, the ASTM standard D7566 for aviation fuel containing synthesized hydrocarbons, including those from biological sources, was published.[116] This revised standard provides quality control guidelines for the growing commercial use of bio-jet fuel.

Microalgae has been investigated as a feedstock for biofuels due to its fast growth, its relatively high lipid content, and its ability to be harvested continuously and to be cultivated on non-arable land.[19] Bio-jet fuel derived from algae has been produced by companies such as Solazyme and tested in flight.[115] Continental Airlines conducted a commercial flight between Houston and Chicago on a 40% blend of algal bio-jet fuel, and the United States Navy demonstrated a 50% blend of algal bio-jet fuel in a military helicopter.[115]

At these early stages in the production of algal bio-jet fuel, a life cycle assessment (LCA) is necessary to ensure that bio-jet fuel produced from algal feedstocks does not result in higher life-cycle greenhouse gas (LC-GHG) emissions than conventional jet fuel. Life cycle assessment can also determine which processes contribute the most to the climate change impacts of algal bio-jet fuel production and use, thus identifying the processes that require further research and development to improve the sustainability of these fuels.

This “cradle-to-wake” LCA proceeds from the cultivation of microalgae in municipal wastewater effluent to thermochemical conversion using hydrothermal liquefaction, upgrading to bio-jet fuel, and combustion in a jet engine. The majority of the data for the life cycle of algal bio-jet fuel upstream of upgrading processes was obtained from our pilot-scale algae cultivation experiments in wastewater effluent and subsequent lab-scale hydrothermal liquefaction reactions of the collected and dewatered algae.[89, 117, 118] Additionally, this LCA is unique among bio-jet fuel and algal biofuel LCAs due to the use of municipal wastewater effluent supplemented with recycled nutrients from hydrothermal liquefaction as the growth medium and the use of hydrothermal liquefaction in lieu of traditional algal lipid extraction methods.

Municipal wastewater effluent can be utilized as a growth medium for algae because it contains nitrogen and phosphorus among other necessary nutrients, which would otherwise be discharged to a receiving water body. Several published LCAs discuss that lower LC-GHG emissions could potentially be achieved by using wastewater to grow algae instead of freshwater supplemented with commercial fertilizers,[41, 42, 46, 48, 119] and a few LCAs have analyzed cases which use wastewater in algae cultivation either as a main growth media or as a supplement.[43, 45, 55, 119] However, the potential algal biomass production at municipal wastewater treatment plants (WWTPs) is typically limited by the nutrient quantities available when a conventional lipid extraction process is used in the conversion of algae to biofuels.[69] Additionally, wastewater-fed cultures of microalgae have relatively lower lipid contents than under controlled nitrogen-limited growth conditions,[19, 89, 120] which limits the amount of fuel that can be produced through upgrading extracted algal lipids.

Hydrothermal liquefaction (HTL) is a technology that has the potential to overcome the limitations for commercial-scale algal biofuel production imposed by the nutrient quantities available in wastewater effluent and the low lipid content typically observed in wastewater-

grown microalgae. Hydrothermal liquefaction uses subcritical water to convert biomass to a carbon-rich biocrude.[121, 122] The entire algal biomass can be processed through HTL because other cellular components beyond lipids are converted into biocrude.[121-124] The biocrude yields from HTL are 5 to 30% higher than the initial algal lipid content,[123, 125-133] and thus HTL is particularly appropriate for low-lipid microalgae. Hydrothermal liquefaction also generates an aqueous co-product (ACP), which contains elements (C, N, P) embodied in the original algal biomass.[110, 134] The ACP could potentially be supplemented to algal pond reactors to recycle these nutrients into additional algal biomass.[107, 110, 134] The combination of nutrient recycling and HTL could greatly increase the biofuel yields possible from cultivating algae in wastewater effluent, avoiding the need for freshwater and fertilizers.

An algal biofuel production process that includes HTL may also be more sustainable than one that employs conventional lipid extraction. Unlike lipid extraction, HTL can be performed on biomass with low solids content (5-30% solids). This reduces the need for complete dewatering and drying, which are energy-intensive processes that can account for up to 69% of the energy needed for an algae-to-biofuel pathway.[45] Previously published life cycle assessments have determined that dewatering processes and/or fertilizer production are among the most energy-intensive steps in algal biofuel production.[41-43, 45-47, 51, 119, 135-139] Additionally, because HTL uses the entire algal biomass, less biomass must be converted to useful co-products or discarded as waste. The proposed system addresses several of the sustainability concerns identified by the United States National Research Council's "Sustainable Development of Algal Biofuels Report,"[78, 118] including the sources of water and nutrients and the fate of waste products from processing algae to fuels. However, the LC-GHG emissions of producing algal biofuels using HTL as a conversion process and utilizing waste sources of water and nutrients for algal growth need to be fully assessed for commercial-scale applications. For example, the

greenhouse gas emissions from transporting larger volumes of water along with algal biomass may lead to prominent climate change impacts in the life cycle of algal bio-jet fuel, and thus transportation steps are included in this LCA.

The goals of this life cycle assessment are:

- To utilize primary data collected from algae production and hydrothermal liquefaction experiments at the University of Kansas to build a life cycle inventory for algal bio-jet fuel production,
- To compare the LC-GHG emissions of algal bio-jet fuel produced through hydrothermal liquefaction pathways to those of conventional jet fuel,
- To identify the processes that are associated with the highest greenhouse gas emissions in the production of bio-jet fuel from algal feedstocks, and
- To perform a sensitivity analysis and Monte Carlo analyses for this algal bio-jet fuel LCA based on feasible ranges of input parameters.

3.3 Methods

3.3.1 Algal bio-jet fuel LCA

This LCA was performed well-to-wake using SimaPro 7.3.3 software. The functional unit was 1 gigajoule (GJ) of fuel produced, which was converted to mass and volume units using an average energy density and specific energy for synthetic paraffinic kerosene.[140] Labor, construction, and infrastructure impacts were not included within the system boundary. The system boundary also did not include the benefit of biological nutrient removal imparted by algal cultivation in municipal wastewater in order to conservatively compare the LC-GHG emissions of algal bio-jet fuel to conventional jet fuel without incorporating impacts related to wastewater treatment. When available, our experimental data at the University of Kansas was utilized as life

cycle inventory inputs. At the University of Kansas, microalgae is cultivated in four 2500-gallon open pond reactors fed with municipal wastewater effluent, collected in gravity sedimentation tanks, dewatered with an Evodos type 10 pilot centrifuge (Evodos B.V., Breda, The Netherlands), and processed in lab-scale batch HTL reactions.[89, 118]

The life cycle impact assessment method was the Environmental Protection Agency's Tool for the Reduction and Assessment of Chemical and Other Environmental Impacts 2.0 (EPA TRACI 2.0), which utilizes the Intergovernmental Panel on Climate Change (IPCC) global warming potentials to calculate the potency of greenhouse gases such as CH_4 relative to CO_2.[141] These climate change impacts were combined as CO_2 equivalents (CO_{2eq}).

The LC-GHG emissions of algal bio-jet fuel produced through HTL were analyzed and compared to those of conventional jet fuel. The LC-GHG emissions of conventional jet fuel have been determined by Skone & Gerdes (2008) to be 88.1 kg CO_{2eq}/GJ for well-to-wake processes: raw material acquisition, raw material transport, liquid fuel production, product transport and refueling, and aircraft operation.[142] Two algal bio-jet fuel production pathways were analyzed in which HTL occurs at a petroleum refinery or at a WWTP (Figure 3.1). These two pathways will be referred to as the Refinery HTL pathway and the WWTP HTL pathway, respectively.

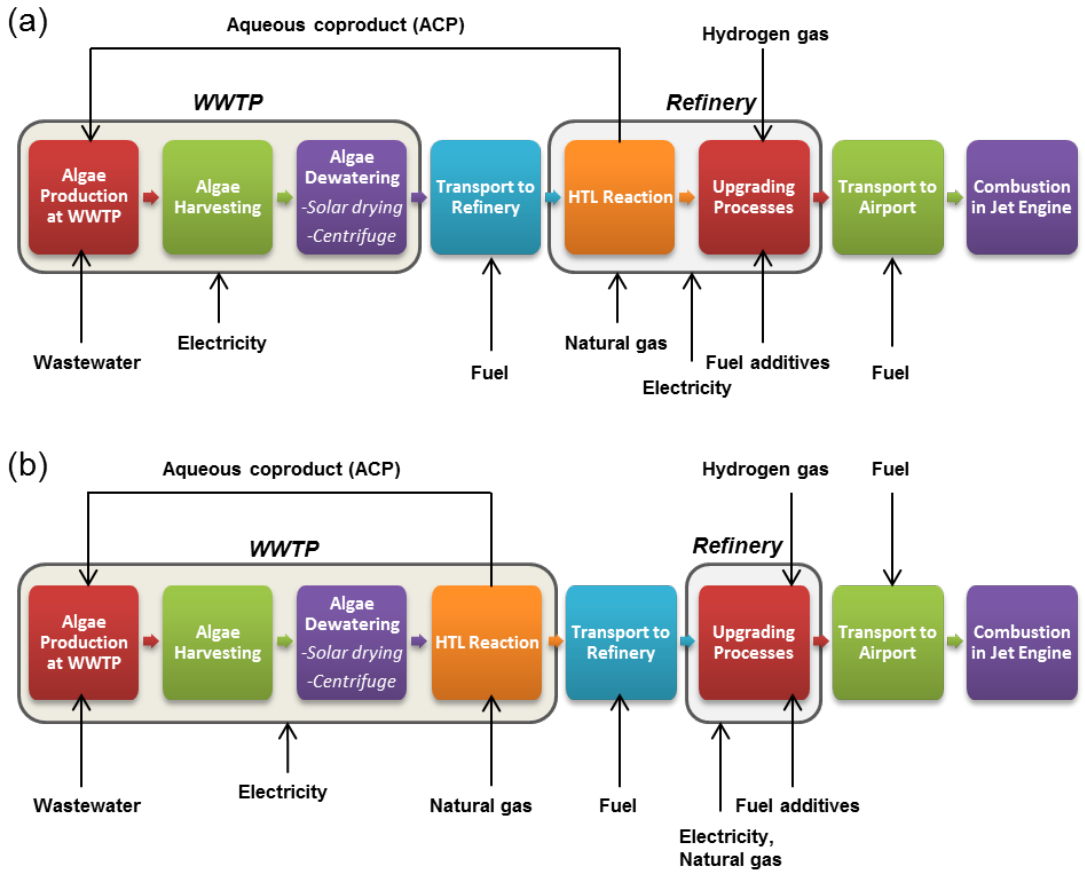

Figure 3.1: The life cycle foreground process chains for the (a) Refinery HTL and the (b) WWTP HTL algal bio-jet fuel production pathways with selected major inputs shown.

The Refinery HTL pathway begins with the cultivation of microalgae in municipal wastewater and recycled aqueous coproduct (ACP) from HTL. The microalgae is then harvested in gravity sedimentation tanks and dewatered either through solar drying to 5.7% solids or centrifugation to 10% solids. This degree of dewatering has been used in HTL studies[108, 118, 123, 125, 126, 129, 132, 133, 143] and is easily achievable with existing technology. The dewatered algae is transported by truck from the WWTP to a refinery. Hydrothermal liquefaction is performed, and the products (ACP, biocrude, and biochar) are separated by a disc bowl centrifuge. The biochar contains a fraction of the original carbon from algal biomass, which is modeled as sequestered

carbon. The ACP is transported back to the WWTP while the biocrude is upgraded through traditional refinery processes with more extensive hydrotreatment to remove heteroatoms (Table 3.1). The algal bio-jet fuel is then transported to an airport and combusted in a jet engine.

Table 3.1: Comparison of algal biocrude to petroleum crude

	Algal biocrude[118]	**Petroleum crude**[125, 126, 142, 144]
Sulfur content (wt %)	~0.5	1.42
Oxygen content (wt %)	5.5	0.1 – 1.5
Nitrogen content (wt %)	4.4	0.1 – 2.0
Carbon content (wt %)	78.7	83-87

The WWTP HTL pathway involves HTL at the site of algal cultivation (Figure 3.1). Thus, only the produced biocrude is subsequently transported to a refinery, and there is no transportation step to return the ACP to the WWTP. The design of each process modeled in this LCA for the two algal bio-jet fuel pathways is described in the Supporting Information.

The base cases for each pathway were modeled using the nominal parameter values shown in Table 3.2. The range of possible values for these parameters are bound by the minimum and maximum values listed. The nominal parameter values and their ranges are achievable as reported from the literature or from primary data from experiments performed at the University of Kansas. The specific sources for the parameter values are shown in Table 3.2. A sensitivity analysis was performed, and then optimized cases of the two pathways were designed. Monte Carlo analyses of the base and optimized cases were also performed, using the range of inputs shown in Tables 3.2 and 3.3.

Table 3.2: Algae production, hydrothermal liquefaction, and upgrading parameters modeled in the algal bio-jet fuel LCA. The nominal values were used for the base case. KU = University of Kansas.

Parameter	Units	Minimum value	Nominal value	Maximum value	Sources for nominal value	Sources for the range of values
Algae production parameters						
Lipid content	% dw	7	14	30	[118]	N/A
Settling efficiency	-	0.48	0.90	0.99	KU unpublished data	KU unpublished data
Distance to refinery	km	50.0	167	286	Calculated in ArcGIS [87, 145]	Calculated in ArcGIS [87, 145]
Percent of ash in microalgae	%	6.0	29	50	[118]	[108, 109, 118, 123, 125, 126, 129-133, 143, 146, 147]
Carbon content of biochar	%	5.0	20	30	[118]	N/A
Solids content of dewatered algae	%	5.0	5.7	30	[118]	[108, 109, 118, 123, 125, 126, 129-133, 143, 146-150]
Wastewater P concentration	mg/L	3.5	5.5	7.5	KU unpublished data	KU unpublished data
Wastewater N concentration	mg/L	23.1	30.4	37.7	KU unpublished data	KU unpublished data
Algae nutrient uptake fraction	-	0.614	0.900	0.989	[89]	[89]
Molar N:P composition of algae	-	6.0	6.0	27	[117]	[94, 117, 151]
Hydrothermal liquefaction and upgrading parameters						
Temperature for HTL reaction	°C	250	300	350	[108, 109, 125, 126, 129, 130, 132, 133, 147, 148, 152, 153]	[108, 109, 118, 123, 125, 126, 129-133, 143, 146-150, 152]
Percent of HTL heat recycled	%	0	80	90	N/A	N/A
Distance to airport	km	43.5	177	312	Calculated in ArcGIS [87, 154]	Calculated in ArcGIS [87, 154]

Parameter (continued)	Units	Minimum value	Nominal value	Maximum value	Sources for nominal value	Sources for the range of values
Uncertainty in biocrude yield	-	0.75	1.0	1.25	N/A	N/A
Fraction of ACP recycled	-	0	0.05	0.10	N/A	N/A
ACP nitrogen concentration	mg/L	1600	2000	2400	KU unpublished data	KU unpublished data
ACP phosphorus concentration	mg/L	3.0	15	30	KU unpublished data	KU unpublished data
Percent of heat from fossil versus biogenic methane	%	0	85	100	N/A	N/A
Additional hydrogen provided	g H_2/ kg feed	23.5	31.7	39.9	Calculated using Table 3.1 and [155]	Calculated using Table 3.1 and [155]
LC-GHG emissions from H_2 production	kg CO_{2eq} / kg H_2	0.161	7.77	11.8	SimaPro 7.3: Industry data	Table 3.5
Refining fuel yield	%	75	90	98	N/A	N/A

Table 3.3: Parameters altered for the optimized cases

Parameter	Units	Minimum values	Nominal values	Maximum values
Solids content of dewatered algae	%	10	15	30
Temperature for HTL reaction	°C	250	300	300
Percent of HTL heat recycled	%	75	85	90
Percent of heat from fossil versus biogenic methane	%	25	50	75
Additional hydrogen provided	g H_2/ kg feed	23.5	27.6	31.7
Life cycle greenhouse gas emissions from H_2 production	kg CO_{2eq}/ kg H_2	0.161	1.28	2.40

3.3.2 Sensitivity analysis

A sensitivity analysis of the algal bio-jet fuel LCA was performed by varying one input parameter to its minimum or maximum value while keeping all other parameters at their nominal values. The difference between the LC-GHG emissions when the parameter is set to its minimum and to its maximum value was calculated. The results of this LCA are most sensitive to the parameters with the largest relative differences in LC-GHG emissions.

3.3.3 Optimized cases

An optimized case of each pathway was analyzed after the sensitivity analysis revealed the input parameters of the LCA which had the largest relative impacts on the overall LC-GHG emissions of algal bio-jet fuel. Their minimum, nominal, and maximum values were changed to values (listed in Table 3.3) within their original feasible ranges (Table 3.2) to determine their combined impacts on the LC-GHG emissions of algal bio-jet fuel when optimized. Algal dewatering was modeled with centrifugation for these optimized cases.

3.3.4 Monte Carlo analysis

A Monte Carlo analysis was performed for both the base case (with centrifugation as the algae dewatering method for a more conservative analysis) and optimized case of each pathway using 10,000 runs in SimaPro in order to determine the probability distribution of the LC-GHG emissions of the modeled algal bio-jet fuel production system encompassing the uncertainty in parameter values. Uniform distributions between minimum and maximum parameter values were modeled in these Monte Carlo analyses.

3.4 Results and Discussion

3.4.1 Algal bio-jet fuel LCA base cases

The LCA results for the base cases are presented first. In each case, HTL is either performed at the WWTP or the refinery (referred to as WWTP HTL or Refinery HTL), and dewatering is either performed with solar drying to 5.7% solids or centrifugation to 10% solids. The Refinery HTL base case with solar drying to 5.7% solids resulted in 49.7% higher LC-GHG emissions for algal bio-jet fuel (131.9 kg CO_{eq}/GJ) compared to conventional jet fuel (88.1 kg CO_{eq}/GJ). The Refinery HTL base case with centrifugation to 10% solids resulted in a 1.83% decrease in LC-GHG emissions at 86.5 kg CO_{eq}/GJ (Figure 3.2). Both of the WWTP HTL base cases resulted in lower LC-GHG emissions than conventional jet fuel at 39.3 kg CO_{eq}/GJ for the solar drying to 5.7% solids case and 35.2 kg CO_{eq}/GJ for the centrifugation to 10% solids case (Figure 3.2), which correspond to a 55.4% and 60.1% reduction in LC-GHG emissions compared to conventional jet fuel, respectively.

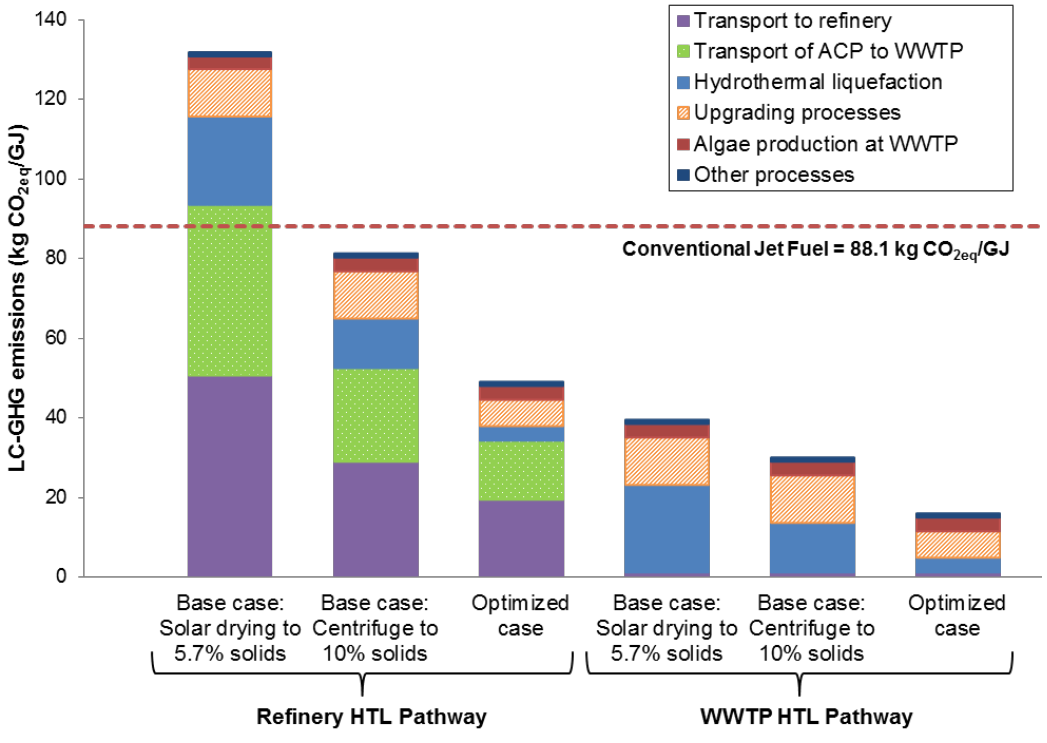

Figure 3.2: Algal bio-jet fuel LCA results for each case analyzed compared against the life cycle climate change impacts of conventional jet fuel. The "Other processes" category includes three processes that were combined due to their comparatively small LC-GHG emissions: algae harvesting; transport to an airport; and combustion in a jet engine.

In the Refinery HTL base cases, transport of dewatered algae to the refinery, transport of ACP to the WWTP, and HTL were the processes that contributed the most to the LC-GHG emissions of algal bio-jet fuel (Table 3.4). In the WWTP HTL base cases, HTL and upgrading processes together contributed the majority of the algal bio-jet fuel LC-GHG emissions (Table 3.4). Algae dewatering accounted for 15.3% of the LC-GHG emissions when algal biomass was centrifuged to 10% solids, but this further dewatering extent reduced the LC-GHG emissions of the WWTP HTL pathway by 10.5% in spite of the added electricity required for dewatering.

Table 3.4: Percent contribution of each process step to the LC-GHG emissions of algal bio-jet fuel

Algal bio-jet fuel life cycle process step	Refinery HTL Pathway			WWTP HTL Pathway		
	Base case: Solar drying to 5.7% solids	Base case: Centrifuge to 10% solids	Optimized case	Base case: Solar drying to 5.7% solids	Base case: Centrifuge to 10% solids	Optimized case
Algae production at WWTP	2.58%	3.94%	6.28%	8.68%	9.69%	16.1%
Algae harvesting	0.185%	0.282%	0.449%	0.621%	0.694%	1.15%
Algae dewatering	N/A	6.23%	9.92%	N/A	15.3%	25.4%
Transport to refinery	38.3%	33.3%	35.4%	2.12%	2.37%	3.93%
Hydrothermal liquefaction	16.7%	14.6%	7.14%	56.2%	35.8%	18.3%
Transport of ACP to WWTP	32.5%	27.0%	27.1%	N/A	N/A	N/A
Upgrading processes	9.01%	13.7%	12.2%	30.3%	33.8%	31.2%
Transport to airport	0.606%	0.925%	1.47%	2.04%	2.28%	3.78%
Combustion in a jet engine	0.0118%	0.0180%	0.0287%	0.0397%	0.0443%	0.0736%

3.4.2 Sensitivity analysis

Ranges of feasible parameter values were used to encompass different possibilities in the algal bio-jet fuel production system at commercial scale. A sensitivity analysis was performed to determine the relative impacts of changes from minimum to maximum parameter values on the overall algal bio-jet fuel LCA results. The sensitivity analysis of the base case parameters indicated that the modeled system was particularly sensitive to the extent of heat integration from HTL (Figure 3.3). Because of the high sensitivity of this parameter and the relatively large contribution of HTL to the overall LC-GHG emissions of algal bio-jet fuel through the WWTP HTL pathway, optimized heat integration is necessary.

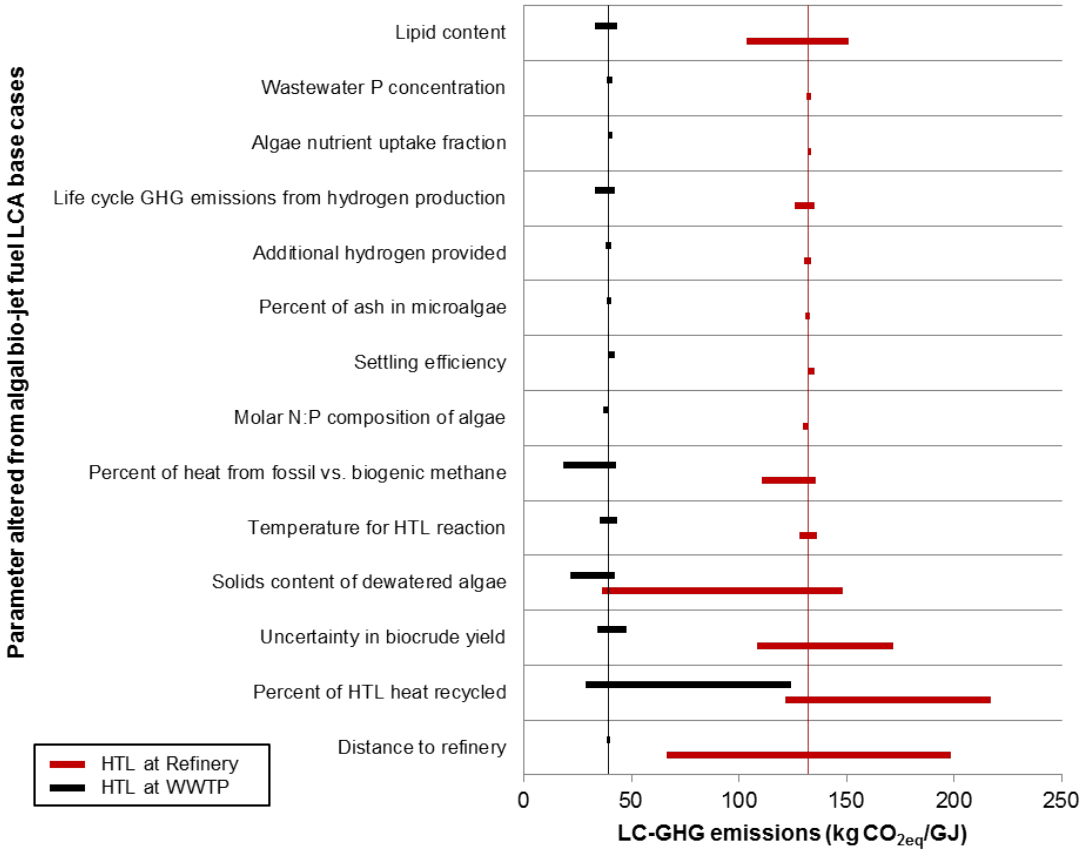

Figure 3.3: Sensitivity analysis for the modeled parameters of algal bio-jet fuel production. The bars span the difference in the algal bio-jet fuel LC-GHG emissions when a parameter is changed from its minimum to its maximum value. The base case LC-GHG emissions for the Refinery HTL and the WWTP HTL pathways are shown as baselines. The parameters that are excluded in this graph resulted in a less than 2 kg CO_{2eq}/GJ difference when the maximum and the minimum parameter values were modeled.

The results of this algal bio-jet fuel LCA were more sensitive to the distance to the refinery, the lipid content of the algae, the solids content of dewatered algae, and the uncertainty in the biocrude yield through the Refinery HTL pathway than through the WWTP HTL pathway. The larger number of sensitive parameters for algal bio-jet fuel production through the Refinery

HTL pathway implies a greater challenge in assuring the sustainability of algal bio-jet fuel when HTL is sited at a refinery instead of at the site of algal biomass production.

The Refinery HTL results were sensitive to both the algal lipid content and the biocrude yield. This is a concern for commercial implementation because the relationship between microalgal macromolecular and elemental composition and the HTL biocrude yield has not yet been carefully investigated. Additionally, the microalgal composition would be dynamic over time due to the nature of wastewater effluent and due to variable environmental conditions during algae cultivation.

The Refinery HTL pathway was more sensitive to the distance to the refinery than the WWTP HTL pathway because a larger mass must be transported when algal biomass of 5-30% solids content is moved instead of simply the biocrude produced from HTL of this biomass. Thus, this pathway would lead to relatively high GHG emissions when algae of a low solids content and a low conversion rate to biocrude is transported across a long distance to undergo HTL at a refinery. This limits the WWTP locations that would allow for algal bio-jet fuel to have lower LC-GHG emissions than conventional jet fuel.

The lower sensitivity of the WWTP HTL pathway to the dewatered algae solids content suggests that there is more flexibility in drying methods and extents when HTL occurs at the site of algal biomass production. In areas where the weather is favorable for solar drying and where there is sufficient land area available, solar drying could be used for algae dewatering, thus avoiding the capital cost of a centrifuge or other drying equipment. Solar drying also minimizes electricity consumption compared to other dewatering methods, so it has been modeled in other algal biofuel LCAs.[40, 45, 119, 156, 157] Although this method has not been demonstrated at commercial scale for harvested microalgae to the authors' knowledge, it has been implemented

successfully for municipal wastewater sludge in numerous facilities (Parkson Corporation, Fort Lauderdale, FL).

There was minimal difference in the LC-GHG emissions of algal bio-jet fuel when the percent of ash in the algae or the carbon fraction in the biochar were changed from minimum to maximum values. The carbon sequestration potential of the biochar collected from HTL did not have a substantial impact on the overall LCA. There may be more beneficial uses of this biochar, such as a soil amendment or catalyst supports, that deserve investigation in future work because the biochar can account for 45% of the dry weight of wastewater algae biomass.[118]

The algal bio-jet fuel LCA model was also robust to the extent of ACP recycling and the N and P concentrations of ACP. However, this may not be the case when the system boundary is expanded to include the environmental impacts of treating this industrial wastewater stream through conventional methods. It is most likely that the ACP would be treated on-site in the Refinery HTL pathway if there was no nutrient recycling in the system, which would lead to reduced LC-GHG emissions from transportation but increased emissions from industrial wastewater treatment. As there is no available information on an industrial wastewater treatment process at this time, this was not modeled.

Wastewater nutrient composition varies by season, temperature, and locality. The Monte Carlo analysis for this LCA studied the sensitivity of wastewater N and P concentrations, and the resulting LC-GHG emissions were robust to these fluctuations. Thus, although the wastewater N and P concentrations influence the total production capacity of a WWTP, they have a minimal impact on the LC-GHG emissions of algal bio-jet fuel normalized to the functional unit.

3.4.3 Algal bio-jet fuel LCA optimized cases

The optimized cases were designed by narrowing the ranges of six sensitive parameters that were associated with higher LC-GHG emissions for the modeled algal bio-jet fuel system. These parameters were the solids content of dewatered algae, the temperature for the HTL reaction, the percent of HTL heat recycled, the percent of heat from fossil versus biogenic methane, the additional hydrogen provided in upgrading, and the LC-GHG emissions from hydrogen gas production (Table 3.3). The LC-GHG emissions from hydrogen gas production in the optimized cases represent hydrogen gas production from methods that do not include steam reforming of natural gas or coal gasification, because of the high LC-GHG emissions associated with these in Table 3.5. The input ranges, although smaller are still within the applicable ranges of currently available technology.

Table 3.5: Life cycle greenhouse gas emissions for hydrogen gas by method of production, excluding infrastructure materials, construction, and facility dismantling

Production process	**Hydrogen source material**	**Life cycle greenhouse gas emissions (kg CO_{2eq}/kg H_2)**	**Source**
Steam reforming	Natural gas	11.8	Spath & Mann (2001) [158]
Gasification	Coal	10.9	Cetinkaya et al. (2012) [159]
Steam reforming	Natural gas	8.92	Cetinkaya et al. (2012) [159]
Steam reforming	Natural gas	7.77	SimaPro 7.3: Industry data
Gasification-electric power	Biomass	2.40	Koroneos et al. (2008) [160]
Thermochemical Cu-Cl cycle	Water	2.16	Cetinkaya et al. (2012) [159]
Cracking	Fossil fuels	1.69	SimaPro 7.3: Industry data
Thermochemical Cu-Cl cycle	Water	0.737	Ozbilen et al. (2011) [161]
Wind-powered electrolysis	Water	0.213	Cetinkaya et al. (2012) [159]
Solar-powered electrolysis	Water	0.161	Cetinkaya et al. (2012) [159]

The Refinery HTL optimized case resulted in 38.4% lower LC-GHG emissions for algal bio-jet fuel (54.2 kg CO_{eq}/GJ) compared to conventional jet fuel (Figure 3.2). In the Refinery

HTL optimized case, transport of dewatered algae to the refinery and transport of ACP to the WWTP were the processes that contributed the most to the LC-GHG emissions of algal bio-jet fuel, followed by upgrading processes and algae dewatering (Table 3.4). Unlike the base cases, the LC-GHG emissions associated with HTL contributed less to the overall LCA results for the optimized case due to greater heat integration, an increase in heat from biogenic methane sources relative to fossil sources, and a decrease in the mass of water that requires heating through increasing the solid content.

The WWTP HTL optimized case resulted in a 76.0% decrease in LC-GHG emissions at 21.2 kg CO_{eq}/GJ (Figure 3.2). In this optimized case, the processes that contributed the most to the LC-GHG emissions of algal bio-jet fuel were (from highest to lowest) the upgrading processes, algae dewatering, HTL, and algae production at the WWTP (Table 3.4). Together, these processes contributed 91.1% of the algal bio-jet fuel LC-GHG emissions. As in the Refinery HTL optimized case, the relative contribution of LC-GHG emissions from HTL was reduced in this optimized case through reducing the amount of fossil methane required for the reaction.

3.4.4 Monte Carlo analyses

Monte Carlo analysis yields statistical data for possible LCA results from random combinations of parameter values within their specified ranges. Monte Carlo simulations have been performed to provide uncertainty analyses in other algal biofuel LCA studies.[43, 55, 135] The average LC-GHG emissions for the Refinery HTL base case Monte Carlo analysis were 63.6 ± 37.1 kg CO_{2eq}/GJ (n = 10,000). The average LC-GHG emissions for the WWTP HTL base case were 29.3 ± 15.7 kg CO_{2eq}/GJ (n = 10,000) (Figure 3.4). The cumulative probability that algal bio-jet fuel produced through the Refinery HTL pathway would have higher LC-GHG emissions

than conventional jet fuel was determined to be 0.181, while the probability is 0.011 when HTL is performed at the WWTP.

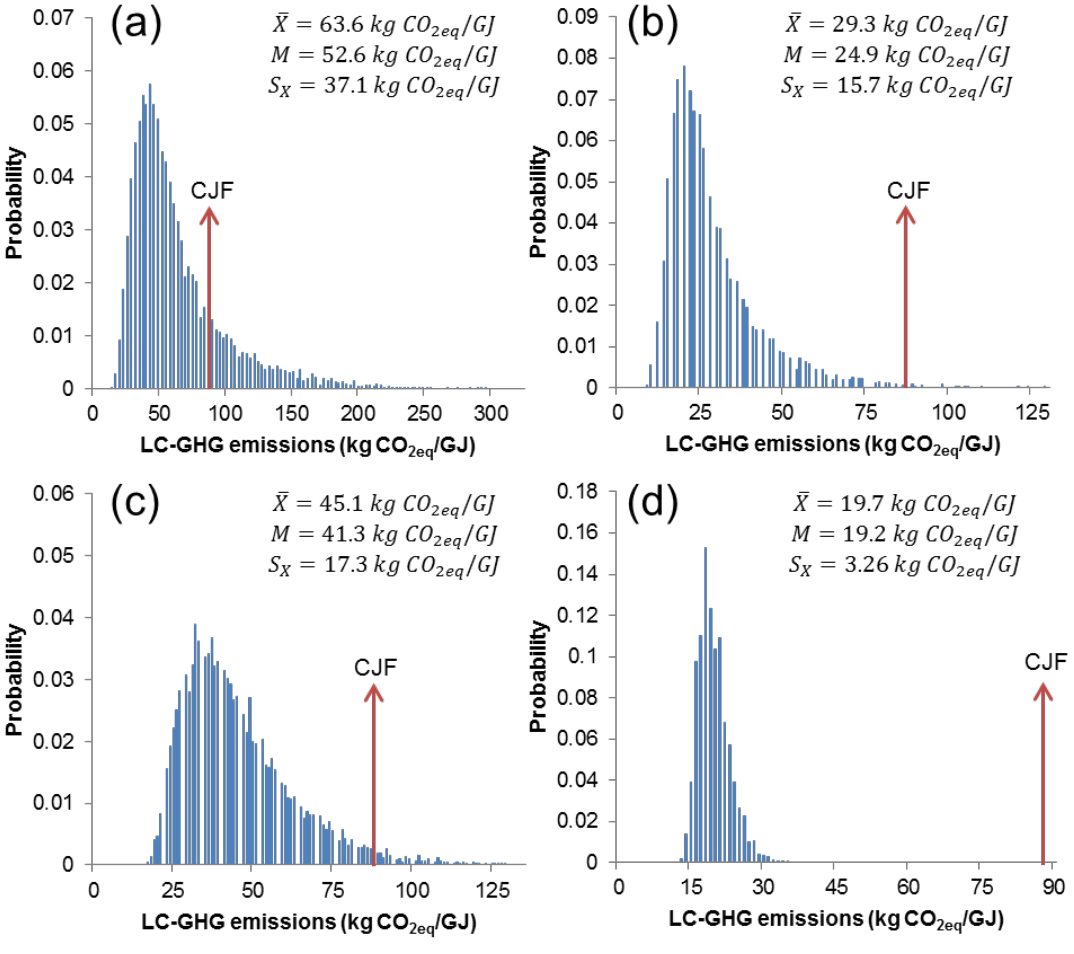

Figure 3.4: Monte Carlo analyses of algal bio-jet fuel LCA results for (a) the Refinery HTL base case, (b) the WWTP HTL base case, (c) the Refinery HTL optimized case, and (d) the WWTP HTL optimized case. CJF = conventional jet fuel, $\overline{X}$ = mean, M = median, and S_X = standard deviation.

The average LC-GHG emissions for the Refinery HTL optimized case were 45.1 ± 17.3 kg CO_{2eq}/GJ (n = 10,000) (Figure 3.4). The cumulative probability that these emissions would

exceed those of conventional jet fuel was calculated to be 0.025. The average LC-GHG emissions for the WWTP HTL optimized case were 19.7 ± 3.26 kg CO_{2eq}/GJ (n = 10,000) (Figure 3.4). All of the Monte Carlo runs for this optimized case resulted in at least a 60% reduction in LC-GHG emissions for algal bio-jet fuel compared to conventional jet fuel.

All of the average LC-GHG emissions from the Monte Carlo analyses were lower than the results of their corresponding base or optimized case. As emphasized in past LCAs of algal biofuels,[119, 135, 162-164] results depicting the range of possible environmental impacts are more informative than single values due to the uncertainties involved in the design of algal biofuel production systems. The results of the Monte Carlo analyses for these four cases suggest that, for this algal bio-jet fuel production system to have lower life cycle climate change impacts than conventional jet fuel, it should reflect the optimized cases more closely than the base cases, and HTL ideally should occur at the WWTP or at a refinery that is a relatively short distance away from the WWTP supplying algal biomass.

3.4.5 Limitations of this LCA study

The system boundary excluded traditional industrial wastewater treatment of ACP when not recycled to the ponds, land use change impacts, the environmental benefits from using algae as a biological nutrient removal (BNR) method, transportation of the biochar to a secondary facility or a landfill, and coproduct allocation for potential uses of the biochar. In particular, expanding the system boundary to account for the avoided LC-GHG emissions associated with traditional BNR systems through algae cultivation as a biofuel feedstock would lead to LCA results that are more favorable for algal bio-jet fuel. Traditional BNR at US WWTPs requires between 600 and 2600 kWh per million gallons treated. For the functional unit of 1 GJ of algal bio-jet fuel, between 421 and 1825 kg CO_{2eq} would be avoided by substituting algal cultivation

for this system. However, because BNR is only applied at less than 2% of municipal WWTPs in the United States,[118] and because many small WWTPs consist solely of a lagoon and would most likely not implement traditional BNR systems in the near future, these avoided LC-GHG emissions were not included in determining the life cycle climate change impacts of algal bio-jet fuel.

In addition, although this LCA utilizes primary data as much as possible, the majority of this data originates from pilot-scale and lab-scale experiments. Future technological developments and differences in parameters at scale could alter the results of this study.

3.4.6 Comparison to other bio-jet fuel LCA studies

The results of this LCA were assessed against other bio-jet fuel LCA results (Table 3.6). It is difficult to compare between algal biofuel LCA results from different studies due to the differences in technical assumptions, types of data used, methods of data aggregation, and the life cycle processes modeled and included within the system boundaries [135, 137, 165, 166]. This LCA is the first for bio-jet fuel from HTL of algae, whereas other algal bio-jet fuel LCAs modeled lipid extraction to obtain fuel precursors.[157, 164, 165]

Table 3.6: Comparison to other bio-jet fuel LCA results

Jet fuel feedstock	Case	LC-GHG emissions (kg CO_{2eq}/GJ)	Source
Petroleum	-	88.1	Skone & Gerdes (2008) [142]
Petroleum	No imports	80.7	Stratton et al. (2010) [157]
Petroleum	Average	87.5	Stratton et al. (2010) [157]
Camelina	-	22.4	Shonnard et al. (2010) [167]
Jatropha curcas	Low land use change	13	Bailis & Baka (2010) [168]
Jatropha curcas	High land use change	141	Bailis & Baka (2010) [168]
Microalgae	Low	14.1	Stratton et al. (2010) [157]
Microalgae	Baseline	50.7	Stratton et al. (2010) [157]
Microalgae	High	193	Stratton et al. (2010) [157]
Microalgae	Low	53.8	Handler et al. (2012) [165]
Microalgae	Average	128	Handler et al. (2012) [165]
Microalgae	High	476	Handler et al. (2012) [165]
Microalgae	Refinery HTL base case, solar drying to 5.7% solids	131.9	This study
Microalgae	Refinery HTL base case, centrifuge to 10% solids	86.5	This study
Microalgae	WWTP HTL base case, solar drying to 5.7% solids	39.3	This study
Microalgae	WWTP HTL base case, centrifuge to 10% solids	35.2	This study
Microalgae	Refinery HTL optimized case	54.2	This study
Microalgae	WWTP HTL optimized case	21.2	This study

Although this LCA is unique for bio-jet fuel from HTL of algae, Frank et al. (2012), Sills et al. (2013), and Liu et al. (2013) determined the LC-GHG emissions for renewable diesel and gasoline from HTL of algae.[135, 139, 162] Unlike this study, none of these LCAs for algal biofuels from HTL of algae included wastewater effluent as a source of water and nutrients for algal cultivation.[135, 139, 162] The Frank et al. (2012) LCA also differed in its modeled algal biofuel production system through the use of catalytic hydrothermal gasification (CHG) of the residuals from HTL for heat and power generation, and return of ammonia produced in CHG to supplement algae cultivation instead of diluting the ACP into the growth medium.[162] The Liu et al. (2013) modeled ACP recycling directly into algal cultivation like this LCA, but differed in its dewatering methods in addition to its modeled source of water and nutrients.[139] The Sills et al.

(2013) LCA modeled dewatering by belt filter press and animal feed and anaerobic digestion-derived methane as potential coproducts.[135] In addition, the transportation distances were not GIS-based in the Frank et al. (2012) LCA for renewable diesel from HTL of algae unlike in this LCA for bio-jet fuel.[39, 162] In most algal biofuel LCAs published to date, a transportation distance is assumed for algal biomass or biofuel,[42, 43, 45, 46] or, as in the Sills et al. (2013) and the Liu et al. (2013) LCAs, the model is constructed without these transportation steps with the assumption that transportation steps have negligible impact on LC-GHG emissions of algal biofuel, or that all processes from algal cultivation through fuel production are collocated.[41, 139, 169] The results of the Liu et al. (2013) and Frank et al. (2012) LCAs show the sensitivity of the parameters associated with HTL heat, but unlike in this LCA, a significant portion of the climate change impacts in all three of these LCAs of biofuel from HTL of microalgae were associated with fertilizer production for nutrients.[135, 139, 162] The results of other bio-jet fuel LCAs highlight the importance of land use change impacts (Table 3.6); bio-jet fuel produced from *Jatropha curcas* is associated with LC-GHG emissions ranging from 13 to 141 kg CO_{2eq}/GJ depending on the previous land use of the area converted for cultivation.[168] In future work, the land use change impacts can similarly be incorporated into an LCA of algal bio-jet fuel.

3.4.7 Implications for commercial-scale applications

Past LCAs have shown the importance of siting algal cultivation near sources of pond inputs,[56, 119] and the results of this LCA highlight the comparable need to locate downstream processing of algal biomass near algal cultivation sites to reduce LC-GHG emissions from transportation. The results of this LCA indicate that the transportation of dewatered algal biomass from a WWTP to a refinery can be a major contributor to the LC-GHG emissions of algal bio-jet fuel when HTL is performed at a refinery. The distance between a WWTP and the

receiving refinery can make the difference between algal bio-jet fuel producing more or less LC-GHG emissions than conventional jet fuel. This could be an important consideration in choosing WWTPs as algae cultivation sites or in siting new biorefineries. It is possible that this climate change impact from transportation could be also reduced by changing the mode of transportation or by decreasing the mass that must be transported to a refinery. To reduce the transported mass, the algae could be dewatered further and rehydrated for HTL, or the HTL reaction and subsequent phase separation by cyclone could be performed at a WWTP, the latter of which was investigated in this study.

It may be more feasible to operate smaller HTL reactors at numerous WWTPs than larger reactors at the less numerous existing petroleum refineries due to the lower capital investments required per reactor. Furthermore, there is potentially greater access to biogenic methane for heat generation at municipal WWTPs that have anaerobic digesters than at petroleum refineries, which would further decrease the LC-GHG emissions associated with producing algal bio-jet fuel. This system also has the added benefit of keeping existing wastewater effluent flows to their current water bodies instead of displacing large volumes of water that may serve a hydrologic or ecological function in their region. However, there would need to be more trained personnel to operate multiple reactors at different facilities. This system is more likely to be implemented at regional clusters of urban WWTPs which have large flows that could produce substantial algal biomass, where expertise could be shared regionally.

3.5 Conclusions

In general, LC-GHG emissions are lower for an algal bio-jet fuel pathway that performs HTL at a wastewater treatment plant than at the refinery. Additionally, bio-jet fuel produced from wastewater algae processed through HTL at a WWTP can have a lower contribution to

climate change than conventional jet fuel. The base case for the WWTP HTL pathway utilizing centrifugation shows a 55.4% reduction in LC-GHG emissions compared to conventional jet fuel. When optimized, a 76.0% reduction in LC-GHG emissions is realized for this production pathway.

The transportation steps between the WWTP and the refinery in the Refinery HTL pathway can contribute greatly to the LC-GHG emissions of algal bio-jet fuel due to the mass of water that must be transported along with algal biomass relative to the mass of biocrude produced. The LCA results are sensitive to the extent of heat recycling and the source of methane used to provide heat for HTL reactions. At commercial scale, it would be important to manage the energy expended in hydrothermal liquefaction to prevent the production of a bio-jet fuel that has higher LC-GHG emissions than conventional jet fuel.

4 Land use change impacts from change in albedo and carbon flux and loss of original biomass in algal biofuel feedstocks production

4.1 Abstract

Geographic factors including land use change (LUC) impacts could significantly affect the sustainability of algal biofuels. Life cycle assessments (LCAs) of algal biofuels must evolve in their methodology in order to more accurately reflect the spatial and temporal heterogeneity of environmental impacts, which includes impacts arising from direct LUC. LCA methods were developed to integrate climate change impacts of direct LUC associated with cultivation of microalgae in open ponds and the effects of temporal and geographic variables on algal growth. The climate change impacts of LUC include the impacts of changing the surface albedo of an area, changing the carbon flux on the land, and removing the original biomass from the transformed land. Two LCA cases were analyzed for algal biofuel feedstocks production in climatically similar regions: the Everglades ecoregion and the Tamaulipas-Texas Semi-Arid Plain ecoregion. The relative contributions of foreground fuel production processes and LUC to the life cycle climate change impacts of renewable gasoline from microalgae produced on potentially available land near municipal wastewater treatment plants were compared. Site-specific GIS data was collected to model algal production on potentially available land for the two case studies. The LUC impacts contributed significantly to the life cycle climate change impacts and also differed between the two regions. The baseline life cycle climate change impacts of algal renewable gasoline production with LUC impacts in the Everglades are 33.8% higher than those of conventional gasoline, while production in the Tamaulipas-Texas Semi-Arid Plain leads to 8.97% lower life cycle climate change impacts. The inclusion of LUC impacts increased the mean result and the range of the Monte Carlo simulations for both ecoregions. This

methodology is important to assess the geographically specific sustainability of algal biofuels on a life cycle basis and can guide future siting decisions for algal biofuel feedstock production.

4.2 Introduction

Life cycle assessments (LCAs) enable scientists to compare the environmental impacts of biofuels to those of petroleum fuels and to identify production aspects that can be optimized to lower environmental impacts. An LCA for biofuels can produce more complete and location-specific results with the inclusion of spatially explicit data,[170, 171] such as climatic variables that affect feedstock production and land use change (LUC) impacts.[21, 172, 173] However, the methodology for integrating geographic factors into LCAs must be developed, including LUC impacts and the impacts of varying algal productivities based on local climate.

LUC impacts have been shown to play a significant role in the results of LCAs of crop-derived biofuels.[174, 175] Notably, Searchinger et al. demonstrated in 2008 that the production of corn ethanol and switchgrass-derived biofuels creates substantially greater life cycle greenhouse gas (LC-GHG) emissions than the production of conventional gasoline when indirect LUC impacts are considered.[21] Indirect LUC impacts arise from displacement of cropland into new cultivation areas when cropland is allocated to biofuel production. Unlike in most crop-based biofuel feedstock production systems, where food production on cropland is displaced, indirect LUC impacts may be minimized or avoided for algal biofuel feedstock production, which does not require arable land. Nonetheless, direct LUC impacts are still incurred; these include changes incurred during the initial transformation of a land area and during its occupation by the system investigated.[176, 177] Three major direct LUC impacts that can be included into an algal biofuel LCA model are:

1. Removal of the original carbon stored in vegetation on the land during implementation of algal cultivation
2. Change in the surface albedo of an area
3. Change in the fluxes of greenhouse gases during algal production compared to the original carbon cycling on the occupied land

Although some LCAs of biofuels produced from algae have incorporated the calculated land area required for production of the functional unit as a separate impact category,[41, 43, 47, 49] none have examined the geographically-specific life cycle climate change impacts from direct LUC impacts.

A prominent study of the direct LUC impacts of crop-based biofuels by Fargione et al. (2008) determined the "carbon debt" incurred by converting existing land cover types to soy, palm, and corn cropland for biodiesel and ethanol production.[175] The land cover types that were considered for conversion to biofuel feedstock cultivation in this analysis were Amazonian rainforest, Brazilian woody cerrado, grassy cerrado, southeast Asian rainforest and peatland, US central grassland, US abandoned cropland, and US marginal cropland.[175] The Fargione et al. study considered the annual net primary productivity of the original land cover in its calculations of "carbon debt" as well.[175] This approach has been used in multiple biofuel LCAs.[157, 178] The Stratton et al. (2010) report assessed direct LUC impacts for multiple bio-jet fuel feedstocks (albeit not algae) primarily by using the data published by Fargione et al. (2008).[157, 175] The LUC impacts determined in the Stratton et al. report were subsequently incorporated into other LCAs, including the Caiazzo et al. (2014) study which added albedo change impacts to LCA studies of numerous crop-based biofuels.[119, 179]

The approach used by Fargione et al. for direct LUC impacts can be improved upon with geographic datasets that have become available since its publication. When geographic datasets

are available, they are preferable to single values pulled from multiple literature sources for their ability to be adapt biofuel LCAs to various geographic contexts. For example, the above-ground biomass carbon values used by Fargione et al. for the Amazonian rainforest was averaged from two studies,[180, 181] one of which lists the measured above-ground biomass from 44 sites collected from 36 studies with varying methodologies published between 1957 and 1997.[180] Through this questionably systematic method, the temporal and geographic sensitivity of these values is diminished and the source of the data and the data collection methodology are occasionally unclear. More recently, published biofuel LCAs, including LCAs that do not incorporate LUC impacts, have also begun to include more geographically specific data,[170, 171, 173] such as GIS datasets for existing biomass on land and land cover types, and satellite data measured uniformly on a known temporal basis and with known precision and methodology over large geographic areas. Other LUC studies have developed methods that do not rely on the Fargione et al. data in order to include spatial heterogeneity. Elliott et al. (2014) presented a spatial modeling methodology to determine the LC-GHG emissions of specific crop-based biofuels arising from LUC that uses some similar datasets to those used in this analysis.[173] Many of these methods stem from the Argonne Carbon Calculator for Land Use Change from Biofuels Production (CCLUB), which is designed to determine the LC-GHG emissions from LUC impacts of producing ethanol from switchgrass, corn, miscanthus, and corn stover.[182] However, the impacts of albedo change and change in carbon flux were not included in this model.

The LUC impacts of algae require an adapted approach from the methodology for LUC impacts of crop-based biofuels. Microalgae has a different harvesting schedule and can potentially be continuously harvested throughout a growing season, whereas most crops are harvested once per growing season. In addition to a difference in harvesting frequency, the surface of cultivation areas is different between crop-based and algal biofuel feedstocks, which

subsequently affects their relative albedo change impacts. The surface of plant biomass defines the surface albedo of crops, while a water medium with suspended matter defines the surface albedo of open algal ponds. Microalgae may need non-fresh water and nutrient sources to lower the environmental impacts of production,[41-43, 45, 46, 48, 55, 119, 169, 183] which would require collocation with municipal wastewater treatment plants (WWTPs) or water and resource recovery facilities (WRRFs) and implementation on the available land around these plants. The direct LUC impacts of algal biofuel feedstocks production will depend on the original conditions on the land adjacent to municipal WWTPs. The greenhouse gas emissions associated with changing an area of land to algal ponds depends on the prior land cover, which can be determined for each site. Additionally, it is possible that the conversion of the same land cover type to algal ponds in different geographic regions would lead to different LUC impacts, due to differences in algal productivity and thus carbon fixation. A spatially explicit biofuel LCA would appropriately account for regional differences in factors that affect feedstock growth.[171]

The objectives of this study are to develop a geographically specific algal biofuel LCA model that includes direct LUC impacts and to investigate the extent to which these LUC impacts contribute to the overall life cycle climate change impacts of renewable gasoline produced from wastewater algae. Two regional case studies were chosen due to their similarities in climate for algae production and differences in land conditions (Table 4.1). The areas represent two EPA-designated Level II ecoregions: the Everglades and the Tamaulipas-Texas Semi-Arid Plain (Tamaulipas). With these two regions, the impact of direct LUC due to land conditions can be compared while controlling for algal productivity, which is dependent on temperature, solar radiation, and nutrient concentrations in wastewater.

Table 4.1: Comparison of existing land characteristics near wastewater treatment plants in the Everglades and the Tamaulipas-Texas Semi-Arid Plain ecoregions

Characteristics	**Everglades**	**Tamaulipas-Texas Semi-Arid Plain**
Average monthly temperature range (°C)	18.81 – 28.37	12.60 – 30.14
Average monthly solar radiation range (kWh m^{-2} day^{-1})	3.959 – 5.994	3.974 – 6.089
Average above-ground biomass (kg m^{-2})	2.646	0.353
Average annual net primary productivity (kg m^{-2} $year^{-1}$)	3.191	0.425
Average monthly albedo range	0.1339 – 0.1467	0.1512 – 0.1633

4.3 Methods

An LCA model was developed in Python code for the determination of the life cycle climate change impacts of renewable gasoline produced through hydrothermal liquefaction (HTL) of microalgae cultivated in wastewater effluent (Figure 4.1). Python codes were also developed and used for sensitivity analyses and Monte Carlo analyses. The LCA model determines the life cycle climate change impacts of 1 GJ of algal renewable gasoline based on 102 variable input parameters with minimum, baseline, and maximum values. The parameters in Table 4.2 were the same for both case studies and are not geographically specific. The sources of these values are described in their respective Methods sections below.

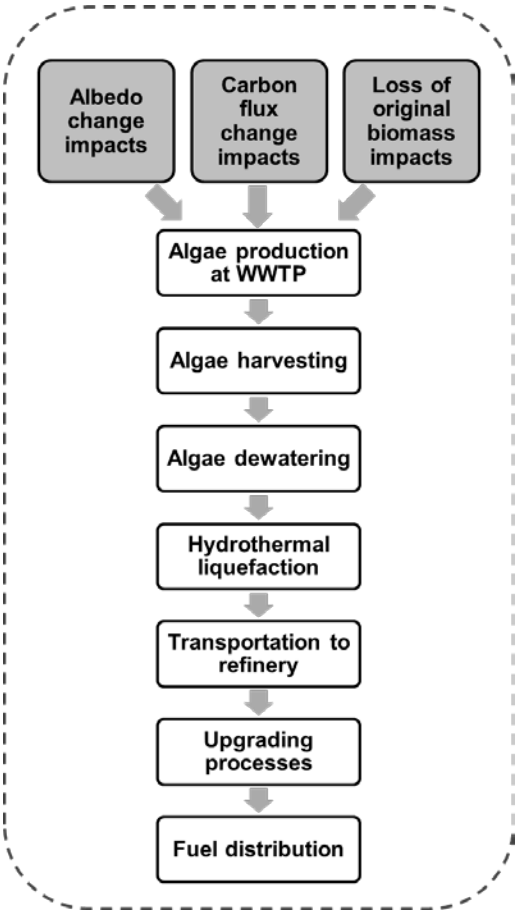

Figure 4.1: Processes included in the life cycle assessment of algal renewable gasoline, in which foreground production processes are shown in white boxes and direct land use change impacts are shown in gray boxes. The dotted line illustrates the system boundary; raw materials entering and leaving the system boundary are not shown in this figure.

Table 4.2: LCA model input parameter values that are constant for both geographic regions

Input parameter	Minimum value	Baseline value	Maximum value	Units
Additional hydrogen provided	23.5	31.7	39.9	g H_2 kg^{-1} feed
Algae nutrient uptake fraction	0.614	0.900	0.989	-
Algal lipid content	7.0	14	30	%
Carbon content of algae	0.45	0.50	0.55	-
Carbon content of original biomass on land	0.45	0.50	0.55	-
Distance from WWTP to ponds	0	500	1250	m
Elevation difference from WWTP to ponds	0.0	2.5	10	m
Energy density of natural gas	36.0	36.6	37.3	MJ m^{-3}
Facility lifetime	20	30	40	years
Final albedo calibration factor	0.416	0.477	0.696	-
Fuel yield from refining processes	0.94	0.96	0.98	-
Hydraulic residence time (HRT) of ponds	5.0	7.5	10	days
Life cycle greenhouse gas (LC-GHG) emissions from H2 production	0.161	7.77	11.8	kg CO_{2eq} kg^{-1} H_2
Molar N:P composition of algae	6.0	6.0	27	-
N concentration of aqueous coproduct (ACP)	1600	2000	2400	mg L^{-1}
P concentration of aqueous coproduct (ACP)	3.0	15	30	mg L^{-1}
Fraction of ash in microalgae	0.060	0.29	0.50	-
Fraction of heat from fossil vs. biogenic methane	0.15	0.85	1.0	-
Fraction of HTL heat recycled	0.75	0.85	0.90	-
Pond depth	0.2	0.4	0.6	m
Settling efficiency	0.75	0.90	0.99	-
Solids content of dewatered algae	0.05	0.1	0.3	-
Surface albedo of empty ponds	0.2	0.5	0.8	-
Temperature for HTL reaction	250	300	350	°C
Uncertainty in biocrude yield	0.750	1.00	1.25	-
Volumetric fraction of pond water from ACP	0	0.05	0.1	-
Wastewater N concentration (January)	0.55	13.73	29.27	mg L^{-1}
Wastewater N concentration (February)	1.61	13.28	30.70	mg L^{-1}
Wastewater N concentration (March)	0.60	12.55	29.33	mg L^{-1}
Wastewater N concentration (April)	0.53	11.88	29.21	mg L^{-1}
Wastewater N concentration (May)	1.45	11.61	27.66	mg L^{-1}
Wastewater N concentration (June)	1.54	11.07	26.08	mg L^{-1}
Wastewater N concentration (July)	1.51	11.67	25.89	mg L^{-1}
Wastewater N concentration (August)	1.25	12.15	27.20	mg L^{-1}
Wastewater N concentration (September)	2.13	12.61	27.92	mg L^{-1}
Wastewater N concentration (October)	1.61	13.37	29.74	mg L^{-1}
Wastewater N concentration (November)	0.75	12.94	30.38	mg L^{-1}
Wastewater N concentration (December)	0.34	14.22	35.26	mg L^{-1}
Wastewater P concentration (January)	0.73	3.82	13.30	mg L^{-1}

Wastewater P concentration (February)	0.36	3.52	11.07	mg L^{-1}
Input parameter (continued)	**Minimum value**	**Baseline value**	**Maximum value**	**Units**
Wastewater P concentration (March)	0.48	3.56	11.40	mg L^{-1}
Wastewater P concentration (April)	0.84	3.59	11.10	mg L^{-1}
Wastewater P concentration (May)	0.73	3.70	11.34	mg L^{-1}
Wastewater P concentration (June)	0.76	3.58	10.89	mg L^{-1}
Wastewater P concentration (July)	1.07	3.80	10.54	mg L^{-1}
Wastewater P concentration (August)	0.77	4.09	11.91	mg L^{-1}
Wastewater P concentration (September)	0.50	4.03	11.65	mg L^{-1}
Wastewater P concentration (October)	0.41	3.87	12.21	mg L^{-1}
Wastewater P concentration (November)	0.34	4.38	17.12	mg L^{-1}
Wastewater P concentration (December)	0.23	4.03	15.03	mg L^{-1}

Geographic data was collected for potentially available land within a 5-km radius of municipal wastewater treatment plants (WWTPs) in two Level II ecoregions: the Everglades and the Tamaulipas-Texas Semi-Arid Plain (Tamaulipas). The determination of potentially available land is described in the methods of Chapter 5. The Everglades ecoregion is at the southern tip of the state of Florida, and the Tamaulipas ecoregion is located in southwest Texas (Figure 4.2). These regions have similar average temperatures and solar radiation, but they differ in their current net primary productivity (NPP), albedo, and above-ground biomass (Table 4.1). The comparison of these two regions controls for differences in factors that influence algal growth, so the effects of factors that contribute to LUC impacts, such as the existing NPP, albedo, and above-ground biomass on the land, can be analyzed in two similar geographic regions where algae can be cultivated throughout the year. The geographically sensitive parameter values that were determined and used as inputs in the LCA model for the Everglades and the Tamaulipas ecoregions are shown in Tables 4.3 and 4.4, respectively. Their sources are described in the methods below.

Figure 4.2: Close-up view of the Everglades (shaded orange) and the Tamaulipas (shaded yellow) ecoregions in the southern United States.

Table 4.3: Everglades-specific LCA model input parameters

Input parameter	**Minimum value**	**Baseline value**	**Maximum value**	**Units**
Temperature (January)	17.14	18.81	19.94	°C
Temperature (February)	18.51	19.91	20.90	°C
Temperature (March)	20.19	21.27	22.00	°C
Temperature (April)	22.21	23.15	23.82	°C
Temperature (May)	25.04	25.56	26.06	°C
Temperature (June)	27.03	27.46	27.71	°C
Temperature (July)	27.83	28.23	28.61	°C
Temperature (August)	27.97	28.37	28.59	°C
Temperature (September)	27.24	27.79	28.00	°C
Temperature (October)	24.72	25.83	26.35	°C
Temperature (November)	21.41	22.76	23.65	°C
Temperature (December)	18.39	20.08	21.15	°C
Solar radiation (January)	4.743	5.203	5.839	kWh m^{-2} day^{-1}
Solar radiation (February)	4.914	5.315	6.102	kWh m^{-2} day^{-1}
Solar radiation (March)	4.948	5.577	6.421	kWh m^{-2} day^{-1}
Solar radiation (April)	5.499	5.994	6.730	kWh m^{-2} day^{-1}
Solar radiation (May)	5.026	5.422	5.951	kWh m^{-2} day^{-1}
Solar radiation (June)	3.924	4.280	4.814	kWh m^{-2} day^{-1}

Input parameter (continued)	Minimum value	Baseline value	Maximum value	Units
Solar radiation (July)	3.871	4.457	5.148	kWh m^{-2} day^{-1}
Solar radiation (August)	3.913	4.322	4.987	kWh m^{-2} day^{-1}
Solar radiation (September)	3.624	3.959	4.504	kWh m^{-2} day^{-1}
Solar radiation (October)	3.956	4.486	5.082	kWh m^{-2} day^{-1}
Solar radiation (November)	4.008	4.663	5.304	kWh m^{-2} day^{-1}
Solar radiation (December)	3.816	4.328	4.995	kWh m^{-2} day^{-1}
Atmospheric transmittance, Kt (January)	0.430	0.540	0.600	-
Atmospheric transmittance, Kt (February)	0.500	0.553	0.620	-
Atmospheric transmittance, Kt (March)	0.480	0.556	0.630	-
Atmospheric transmittance, Kt (April)	0.500	0.571	0.650	-
Atmospheric transmittance, Kt (May)	0.490	0.551	0.590	-
Atmospheric transmittance, Kt (June)	0.380	0.477	0.570	-
Atmospheric transmittance, Kt (July)	0.430	0.485	0.560	-
Atmospheric transmittance, Kt (August)	0.430	0.486	0.520	-
Atmospheric transmittance, Kt (September)	0.410	0.483	0.530	-
Atmospheric transmittance, Kt (October)	0.470	0.531	0.590	-
Atmospheric transmittance, Kt (November)	0.440	0.540	0.590	-
Atmospheric transmittance, Kt (December)	0.470	0.540	0.590	-
Albedo of original land conditions (January)	0.1398	0.1421	0.1446	-
Albedo of original land conditions (February)	0.1374	0.1409	0.1444	-
Albedo of original land conditions (March)	0.1401	0.1427	0.1468	-
Albedo of original land conditions (April)	0.1414	0.1438	0.1498	-
Albedo of original land conditions (May)	0.1444	0.1467	0.1503	-
Albedo of original land conditions (June)	0.1330	0.1387	0.1442	-
Albedo of original land conditions (July)	0.1346	0.1388	0.1444	-
Albedo of original land conditions (August)	0.1260	0.1339	0.1384	-
Albedo of original land conditions (September)	0.1298	0.1357	0.1402	-
Albedo of original land conditions (October)	0.1349	0.1389	0.1409	-
Albedo of original land conditions (November)	0.1393	0.1409	0.1431	-
Albedo of original land conditions (December)	0.1385	0.1420	0.1445	-
Original net primary productivity (NPP)	0.00108	0.00874	0.01795	kg C m^{-2} day^{-1}
Latitude	25.853	26.237	26.742	°
Amount of original biomass on land	0.000	2.646	9.667	kg m^{-2}
Distance to refinery	597	656	692	km

Table 4.4: Tamaulipas-Texas Semi-Arid Plain-specific LCA model input parameters

Input parameter	Minimum value	Baseline value	Maximum value	Units
Temperature (January)	10.93	12.60	15.39	°C
Temperature (February)	12.95	14.75	17.56	°C
Temperature (March)	16.64	18.53	20.92	°C
Temperature (April)	20.53	22.45	24.63	°C
Temperature (May)	24.76	26.35	27.93	°C
Temperature (June)	27.69	29.01	30.53	°C
Temperature (July)	28.79	29.86	30.92	°C
Temperature (August)	29.06	30.14	31.30	°C
Temperature (September)	26.21	27.38	28.55	°C
Temperature (October)	21.63	23.03	24.76	°C
Temperature (November)	16.15	17.73	20.24	°C
Temperature (December)	11.27	13.00	15.97	°C
Solar radiation (January)	3.335	4.034	4.687	$kWh\ m^{-2}\ day^{-1}$
Solar radiation (February)	3.726	4.424	5.234	$kWh\ m^{-2}\ day^{-1}$
Solar radiation (March)	3.768	4.394	5.209	$kWh\ m^{-2}\ day^{-1}$
Solar radiation (April)	4.110	4.714	5.172	$kWh\ m^{-2}\ day^{-1}$
Solar radiation (May)	4.502	5.073	5.603	$kWh\ m^{-2}\ day^{-1}$
Solar radiation (June)	5.359	5.989	6.663	$kWh\ m^{-2}\ day^{-1}$
Solar radiation (July)	5.499	6.089	6.705	$kWh\ m^{-2}\ day^{-1}$
Solar radiation (August)	5.333	6.083	6.671	$kWh\ m^{-2}\ day^{-1}$
Solar radiation (September)	4.577	5.292	5.745	$kWh\ m^{-2}\ day^{-1}$
Solar radiation (October)	4.519	4.800	5.545	$kWh\ m^{-2}\ day^{-1}$
Solar radiation (November)	3.816	4.292	4.759	$kWh\ m^{-2}\ day^{-1}$
Solar radiation (December)	3.391	3.974	4.882	$kWh\ m^{-2}\ day^{-1}$
Atmospheric transmittance, Kt (January)	0.400	0.493	0.630	-
Atmospheric transmittance, Kt (February)	0.340	0.498	0.620	-
Atmospheric transmittance, Kt (March)	0.410	0.530	0.660	-
Atmospheric transmittance, Kt (April)	0.410	0.530	0.660	-
Atmospheric transmittance, Kt (May)	0.470	0.529	0.610	-
Atmospheric transmittance, Kt (June)	0.500	0.567	0.660	-
Atmospheric transmittance, Kt (July)	0.520	0.599	0.670	-

Input parameter (continued)	Minimum value	Baseline value	Maximum value	Units
Atmospheric transmittance, Kt (August)	0.490	0.580	0.630	-
Atmospheric transmittance, Kt (September)	0.470	0.556	0.640	-
Atmospheric transmittance, Kt (October)	0.390	0.532	0.620	-
Atmospheric transmittance, Kt (November)	0.410	0.520	0.640	-
Atmospheric transmittance, Kt (December)	0.360	0.501	0.610	-
Albedo of original land conditions (January)	0.1464	0.1525	0.1585	-
Albedo of original land conditions (February)	0.1460	0.1513	0.1563	-
Albedo of original land conditions (March)	0.1486	0.1512	0.1537	-
Albedo of original land conditions (April)	0.1477	0.1520	0.1561	-
Albedo of original land conditions (May)	0.1442	0.1515	0.1590	-
Albedo of original land conditions (June)	0.1469	0.1576	0.1643	-
Albedo of original land conditions (July)	0.1447	0.1573	0.1674	-
Albedo of original land conditions (August)	0.1470	0.1601	0.1739	-
Albedo of original land conditions (September)	0.1441	0.1566	0.1728	-
Albedo of original land conditions (October)	0.1521	0.1578	0.1699	-
Albedo of original land conditions (November)	0.1585	0.1633	0.1708	-
Albedo of original land conditions (December)	0.1510	0.1597	0.1675	-
Original net primary productivity (NPP)	0.000322	0.001163	0.004563	kg C m^{-2} day^{-1}
Latitude	26.214	28.363	29.344	°
Amount of original biomass on land	0.000	0.353	2.330	kg m^{-2}
Distance to refinery	11.8	125	239	km

A baseline LCA was performed using the average parameter values for each of the two ecoregions. A sensitivity analysis was performed for each ecoregion by changing one parameter at a time to its minimum or maximum value, while keeping all other parameters at their baseline values. Sensitivity analysis elucidates the effect of one parameter on the total algal renewable gasoline life cycle climate change impacts. The uncertainty analyses consisted of 100,000 Monte Carlo iterations using the range of minimum to maximum input parameters assuming a uniform distribution for each parameter; the analysis was performed with and without LUC impact processes in each ecoregion. The LC-GHG emissions of algal green gasoline were compared between ecoregions, and they were compared to the LC-GHG emissions of petroleum-derived conventional gasoline. The Skone & Gerdes (2008) LCA reports that the total well-to-wheels life

cycle greenhouse gas emissions of conventional gasoline are 96.3 kg CO_{2eq}/MMBtu LHV fuel consumed, which is equivalent to approximately 91.3 kg CO_{2eq}/GJ fuel.[142]

4.3.1 Adaptation of past LCA model to renewable gasoline

The LCA model is largely based on a previously published LCA by Fortier et al. (2014) (and included as Chapter 3 of this dissertation) for bio-jet fuel produced through HTL of wastewater microalgae at a WWTP, with transportation of the biocrude to a petroleum refinery for upgrading to a finished fuel.[183] It was altered by (a) incorporating direct LUC impacts and a geographically sensitive algal growth model, (b) changing the wastewater effluent nutrient concentrations for seasonal plant performance on nutrient removal, (c) including the impacts of pumping water a horizontal distance from a WWTP to algal ponds, (d) removing the step in which carbon is sequestered in biochar to reflect the purification of the biochar to the higher-value product of hydroxyapatite,[184] and (e) adjusting the model from production of bio-jet fuel to production of renewable gasoline. Finally, the baseline LCA model, the Monte Carlo analyses, and the sensitivity analyses were coded in Python programming language and performed in Python.

To adapt the previous work to an algal renewable gasoline framework, the following processes were removed from the LCA model: aromatic hydrocarbon additives required for ASTM jet fuel standards, carbon sequestration in biochar, and combustion emissions from jet engines. Gasoline does not require the aromatic hydrocarbon additives required for jet fuel. The biochar produced in HTL of wastewater microalgae is substituted hydroxyapatite,[184] and the carbon contained in this class of compounds is not sequestered due to the different ways in which the compound could be upgraded or purified. In order to examine the impacts purely from a conservative biofuel-production perspective, no impacts are allocated to the production of these

higher-value solids, or to the biological nutrient removal imparted on the original wastewater stream. It is assumed that carbon fixed by algae will be returned to the atmosphere during HTL and combustion of the produced fuel. Due to these emissions consisting of biogenic carbon dioxide, no process step was included for combustion of the fuel in assessing the life cycle climate change impacts of algal renewable gasoline.

The foreground process step for transportation of the produced fuel was altered from the Fortier et al. (2014) LCA in order to match the approach of distributing gasoline in the Skone & Gerdes (2008) LCA report on petroleum products. The foreground process step for transportation of the biocrude to a petroleum refinery was updated with distances specific to the WWTPs in the Everglades and the Tamaulipas ecoregions, and their nearest petroleum refineries.

The LCA equations from the Fortier et al. (2014) LCA for bio-jet fuel were adjusted, in order to scale all impacts to the new functional unit of 1 GJ renewable gasoline. The fuel energy density was changed to 34.62 MJ kg^{-1} for renewable gasoline, and the volumetric density was changed to 0.7480 kg L^{-1}, based on data from the Argonne National Laboratory GREET model.[185] The climate change impacts of the refining step and the fuel distribution step of the algal renewable gasoline life cycle were based on the same foreground process steps in the Skone & Gerdes (2008) assessment converted to units of kg CO_{2eq}/GJ fuel.

Due to the sparse availability of WWTP-specific data and the lack of uniformity in nutrient concentration reporting at the national level, wastewater effluent concentrations of total nitrogen and total phosphorus were obtained from a record of monthly Kansas WWTP data collected from 2000 to 2011 by the Kansas Department of Health and Environment.[93] This consistent, long-term record serves as an appropriate proxy because it includes both rural and urban WWTPs and provides temporal variability in effluent nutrient concentrations experienced by a municipal WWTP in the center of the continental United States that performs nitrification

but does not perform biological nutrient removal. The dataset was averaged by WWTP for each month over the time series, and the average total nitrogen and total phosphorus concentrations by month were used as the baseline parameter values in the LCA model. The ranges of concentrations were defined from the minimum monthly concentrations to the average plus two standard deviations for the maximum monthly concentrations.

To determine certain aspects of direct LUC impacts, including the impacts of the loss of original biomass scaled to the functional unit of algal renewable gasoline a lifetime for the use of the cultivation site was needed. A facility lifetime of 30 years was chosen as the baseline value. Facility lifetimes of 20 years and 30 years have been chosen for past LCAs and techno-economic analyses of algal biofuel feedstocks production.[61, 67, 138, 170]

4.3.2 Algal growth model

An algae growth model was adapted to determine the potential dry matter microalgae concentration in open ponds for a month-long period based on whether the nitrogen concentration, phosphorus concentration, light availability, or temperature limits algal growth given the input conditions. The potential algal concentrations based on these factors were calculated for each month, and the lowest calculated monthly algal concentration was used in the LCA model. An algal concentration of 0 mg/L was modeled if the input monthly ambient temperature is less than 10°C, which does not occur for the two ecoregions in this study. It is assumed that algal cultivation is halted during months of cold temperatures, and the ponds are emptied. The calculations for potential algal concentration based on nitrogen and phosphorus concentrations were derived from the stoichiometric and nutrient availability equations outlined in the Supporting Information of Fortier et al. (2014).[183]

The potential algal concentration based on light availability was calculated using the equations and the variables defining the current technology case in Wigmosta et al. (2011).[65] The Wigmosta et al. (2011) algal growth model was developed for open ponds and yields an aerial algal productivity.[65] The model was adapted with a pond depth as a parameter in the LCA model, so that shallow ponds are more concentrated than deeper ponds under identical conditions due to identical aerial productivity with all other parameters held constant. This allowed for light attenuation with depth.

The protein and carbohydrate contents were assumed to be equal in the light-limited algal production model adapted from Wigmosta et al. to determine the energy content per unit of biomass, E_a.[65] The light saturation constant I_s was calculated to be approximately 0.8038 kWh m^{-2} day^{-1} by converting the value of 150 μmol m^{-2} s^{-1} using the calculated energy of a photon over the spectrum of photosynthetically active radiation (PAR). The calculation for the energy of a photon over the PAR spectrum (400 nm to 700 nm) is demonstrated in Equation 1 where *h* is Planck's constant, *c* is the speed of light, and λ is the wavelength.

$$E_{photon,PAR} = \frac{1}{300 \times 10^{-9}\, m} \int_{400\, nm}^{700\, nm} \frac{hc}{\lambda} d\lambda \qquad \text{(Equation 1)}$$

The light saturation constant I_s and the incident solar radiation I_e were used to determine the light utilization efficiency ε_s (Equation 2).[65, 186] Subsequently, the photoconversion efficiency ε_a was calculated as in Wigmosta et al.,[65] and the monthly algal productivity $P_{mass,i}$ was calculated in units of kg m^{-2} s^{-1} as shown in Equation 3 using a fraction of PAR-spectrum radiation available (C_{PAR}) of 0.46.

$$\varepsilon_s = \frac{I_s}{I_e} * \left(1 + \ln \frac{I_e}{I_s}\right) \qquad \text{(Equation 2)}$$

$$P_{mass,i} = \frac{0.90 C_{PAR} \varepsilon_a I_e}{E_a} * \frac{1\ day}{24\ hr} * \frac{1000\ W}{1\ kW} * \frac{1\ MJ/s}{10^6\ W} \quad \text{(Equation 3)}$$

Finally, the concentration of algae with light as the limiting factor for growth was calculated using Equation 4. The hydraulic residence time of the ponds is in units of days (HRT), the algal productivity ($P_{mass,i}$), and the depth of the ponds in meters (D).

$$C_{alg,light} = HRT * P_{mass,i} * \frac{1}{D} * \frac{86{,}400\ s}{1\ day} * \frac{10^6\ mg}{1\ kg} * \frac{1\ m^3}{1000\ L} \quad \text{(Equation 4)}$$

4.3.3 Loss of original biomass impacts

When land is cleared, plowed, and converted to algal ponds, the carbon stored in the original vegetation on that land is lost. It is assumed that the vegetation would be incinerated or would decompose naturally after removal, which would release approximately all of the original biomass carbon to the atmosphere. The net loss of carbon from transforming the land to algal ponds was determined by calculating the existing aboveground biomass on potentially available land using the version 2 North American Carbon Program (NACP) Aboveground Biomass and Carbon Baseline Data in ArcGIS.[187] The average biomass content value on the potentially available land in each region was set as the baseline value for the amount of original biomass on the land. The maximum value was the average plus two standard deviations for each region. The minimum value was the measured minimum on the potentially available land areas within each of the two regions. The carbon fraction of the biomass on the land, assumed to range from 0.45 to 0.55 with a baseline value of 0.50 (Table 4.2), was multiplied by the amount of biomass to obtain the original mass of biomass carbon sequestered on the land (kg C m^{-2}).

To determine the mass of carbon sequestered after implementation of algal ponds, the average annual algal concentration in the ponds was multiplied by the pond depth and the carbon fraction of algal biomass to yield units of kg C m^{-2}. The standing mass of algal carbon was subtracted from the original mass of biomass carbon on the land and converted to kg CO_2 m^{-2}. This loss of original biomass carbon on the land as CO_{2eq} was scaled to the functional unit by multiplying by the area-time occupied by the functional unit (described in the following sentences) and dividing by the lifetime of the facility. The area-time occupied by the functional unit is calculated by dividing the dry mass of algae needed to produce the functional unit of 1 GJ of fuel by the algal areal productivity. The units of this variable are m^2 yr GJ^{-1}. This allows for flexibility in time and space to produce the functional unit and to assign LUC impacts. This functional unit scaling methodology was also used by Muñoz et al. (2010) for determining the life cycle climate change impacts, including albedo change impacts, of tomatoes produced in greenhouses.[188]

4.3.4 Carbon flux change impacts

Land use dictates the transfer of carbon dioxide and other greenhouse gases like methane and nitrous oxide between the air and vegetation, soil, or water, thus affecting the climatic impact of a system that occupies an area of land.[189] The net amount of CO_{2eq} fixed over time in a given area is changed when land is converted to algal pond from its prior land cover. The original fluxes in carbon can be determined from the net primary productivity (NPP) of an area.[175] Other LUC analyses have estimated carbon fluxes from net primary production or net ecosystem production values.[190-192] In this analysis, one-sixth of the original NPP was modeled as carbon that would have remained fixed for decades on the land based on the average proportion of global NPP contributing to the global net ecosystem production (NEP), which

corresponds to medium-term carbon storage, noted by the Intergovernmental Panel on Climate Change (IPCC).[193] This value of one-sixth of the original NPP (kg C m^{-2} yr^{-1}) was converted from carbon to CO_{2eq} and subsequently scaled to the functional unit by multiplying it by the area-time occupied by the functional unit (m^2 yr GJ^{-1}) to obtain a carbon flux change impact (kg CO_{2eq}/GJ fuel) in the LCA model.

In this study, the NPP of the available land prior to implementation of algal cultivation was determined by averaging the three most recently available years (2008, 2009, and 2010) of the MODIS Gross/Net Primary Production product (MOD17).[194] For sensitivity and uncertainty analysis, the range of NPP values modeled for each ecoregion was bounded by the minimum NPP and a maximum value chosen as the average NPP plus two standard deviations. Since the land cover types designated as potentially available land (defined in Chapter 5 as shrubland, grassland, barren land, developed open land, and pasture) do not typically receive fertilizer, the original fluxes of N_2O were assumed to be negligible.

The portion of the algal NPP that would have remained fixed for decades was modeled as zero because the carbon fixed on the land occupied by ponds will be released to the atmosphere as the algal renewable gasoline is combusted. There is no incremental increase in carbon stored on the land during algal cultivation, in comparison to the one-sixth of the original NPP on the land that is assumed to be fixed for decades. Methane emissions from algal ponds are expected to be negligible because anaerobic activity is minimized when ponds are well-mixed. Direct nitrous oxide (N_2O) emissions from well-mixed open algal ponds subjected to diurnal light-dark cycling have been shown to be nearly negligible through bench-scale experiments.[25]

4.3.5 Albedo change impacts

Climatic impacts can also arise from land use change when the albedo of an area is modified.[189] The albedo of a surface is a measure of its reflectivity.[195, 196] It can be calculated as the ratio of reflected solar radiation to the solar radiation incident upon a surface, or as the average reflectance of a surface over the spectrum of solar radiation. A change in albedo induces a radiative forcing by affecting the shortwave radiation budget.[197] Because radiative forcings can be expressed as CO_{2eq},[188, 198, 199] there have been efforts to translate albedo changes over a known area into greenhouse gas emission equivalents. Several papers have developed methods to express albedo changes as changes in CO_{2eq} emissions,[188, 195, 196, 198, 200, 201] and some of these studies focused on the integration of albedo changes into LCAs,[188, 195, 200] although no previously published work incorporates albedo change impacts into an algal biofuel LCA.

Albedo change has been shown to contribute to the life cycle climate change impacts of various systems, including pavement[202] and crop-derived biofuels,[179] and to have a significant effect in forest expansion[201, 203] and forest rotation decisions.[204] Indeed, the climate change impacts of albedo change have been shown to have the same magnitude as other LUC impacts.[179, 205] Albedo change effects may increase or decrease the effectiveness of a climate change mitigation technology depending on the albedo difference between the original and converted land area. A study by Caiazzo et al. (2014) showed that the LC-GHG emissions of biofuels produced from soybeans cultivated on land that was previously rainforest were decreased by 28% when the cooling effects of the resulting albedo change were included in their LCA models.[179] The results of this study showed an opposite effect for biofuels produced from salicornia on converted desert land, where the large decrease in albedo caused a nearly fourfold increase in the LC-GHG emissions of these fuels.[179] The Caiazzo et al. study and a study by Cherubini et al. (2012) are the only published crop-derived biofuel LCAs that have included

albedo change effects among LUC impacts, and both demonstrate the significance of these effects to biofuel LCA results.[179, 192] However, the albedo change impacts associated with algal biofuels have not yet been assessed in the literature or addressed as future areas of research for the sustainability of algal biofuels.[78]

The magnitude and direction of albedo change impacts on the life cycle climate change impacts of algal biofuels depends on the original surface albedo at a given location, which can be determined through geographic analysis, and on the modeled albedo of algal ponds. The albedo of a water surface depends on the solar zenith angle, which is dependent on time (time of day and day of the year) and space (latitude).[206, 207] The latitude affects the incoming radiation from the sun at the top of the atmosphere.[204] Additionally, the albedo depends on the atmospheric transmittance.[206]

To determine the monthly average original albedo of potentially available land around the WWTPs in each ecoregion, five consecutive years of raster data from the MODerate-resolution Imaging Spectroradiometer (MODIS) Albedo product MCD43A3 were used.[208] The MCD43A3 product was used in the Caiazzo et al. (2014) study on the impacts of albedo change on biofuel LCAs,[179] and it is a validated dataset with low uncertainty.[195] The albedo values used from this MODIS Albedo product were the black-sky shortwave broadband albedo values, which span both the near-infrared and visible spectra. The overlapping time step values of the MCD43A3 raster tiles that were clipped and mosaicked on potentially available land areas were converted to monthly average values for each of the five years of albedo data. The monthly minimum, average, and maximum albedo values of each ecoregion for the years 2008 through 2012 comprised the original albedo parameter baseline values and ranges.

The final albedo of the areas occupied by algal ponds was modeled monthly with location-specific variables. An empirically determined equation for the surface albedo of lakes

and ponds developed by Dvoracek & Hannabas (1990) was used with a calibration factor to model the final albedo of the algal ponds in the Everglades and the Tamaulipas ecoregions on a monthly basis (Equation 5).[209, 210] The equation models green water and 2.5-cm high ripples,[209, 210] and it responds to the latitude- and time-dependent solar elevation angle β. The solar elevation angle β was averaged over the course of a day by integrating the cosine of the hour angle ω from $-\pi/2$ to $\pi/2$ and dividing by $1/\pi$. This calculation yielded an average daily cos(ω) value of $2/\pi$, which was used in Equation 6 with the latitude φ and the declination angle δ to determine the solar elevation angle for the final albedo equation.[211]

$$\alpha_f = k * 0.22^{(0.7 \sin\beta + 1)} \quad \text{(Equation 5)}$$

$$\sin\beta = \cos\varphi \cos\delta \cos\omega + \sin\varphi \sin\delta \quad \text{(Equation 6)}$$

Equation 5 was calibrated with a factor *k* based on satellite data for the albedo values for two sites that each have characteristics that are representative of the algal raceways ponds modeled in this study: the Cyanotech spirulina raceways in Kona, Hawaii and the City of Logan municipal wastewater treatment plant lagoons in Logan, Utah. The Cyanotech raceway ponds produce spirulina, a prokaryotic algal species, throughout the year. The City of Logan WWTP lagoons in Utah cover an area approximately nine times that of the Cyanotech raceways in Hawaii, but with seasonal freezing temperatures, only the months from April to November could be reliably used for calibration of the calculated albedo of ponds that are actively producing algae. The algal raceway ponds at Cyanotech and the City of Logan WWTP lagoons were delineated in ArcMap using aerial imagery, and the albedo values for the year 2014 were obtained and averaged by month over the water surface area at each site using the MCD43A3 dataset. The monthly albedo expected for algal ponds at each site was calculated using Equation

5 and the latitudes of each site, without a calibration factor initially. To calibrate Equation 5 to the average Cyanotech algae raceway albedo by month, the equation was modified with the constant *k*, where *k* = 0.477 (Figure 4.3). The minimum and maximum values for *k* were found to be 0.416 and 0.552 respectively for the Cyanotech raceways. To calibrate Equation 5 to the monthly City of Logan WWTP lagoons albedo values, the minimum, average, and maximum *k* values were found to be 0.628, 0.657, and 0.696, respectively. Thus, a baseline value of 0.477 and a range of 0.416 to 0.696 were modeled for the final albedo calibration factor in the LCA model.

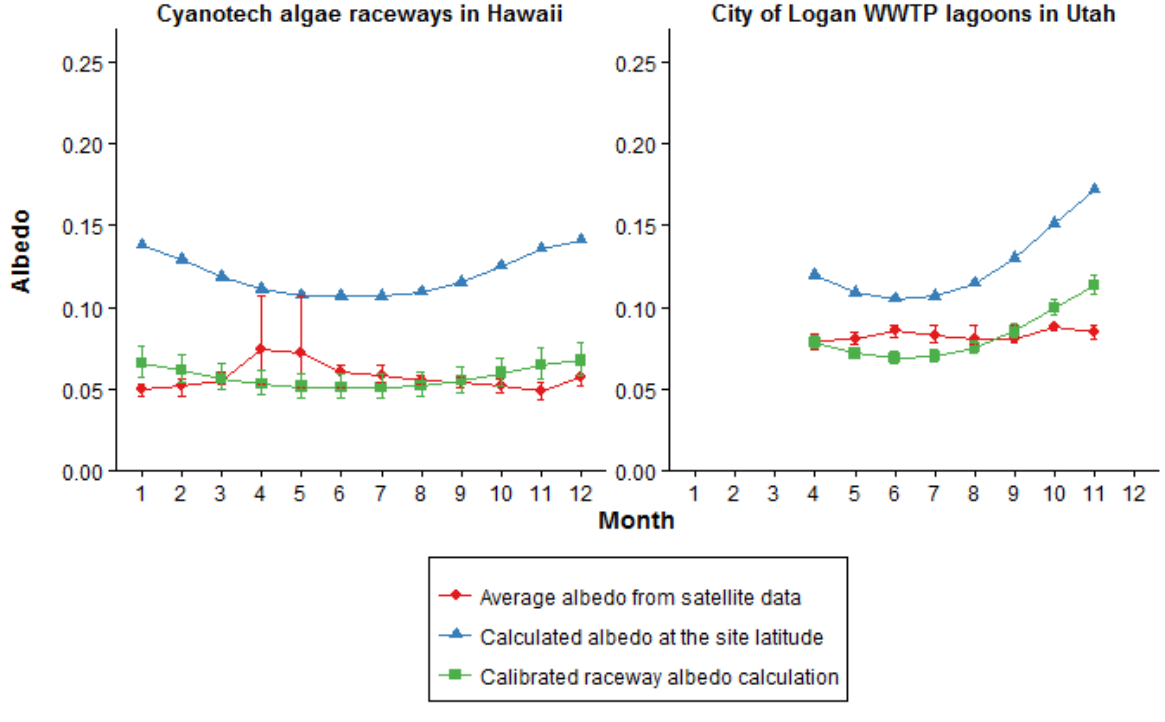

Figure 4.3: Calibration of albedo equation to satellite data at two sites. Error bars represent the minimum and maximum albedo values either measured from satellite data during that month or from using the minimum and maximum calibration factors.

To convert the change from the original to the final albedo to a life cycle climate change impact, methods from Betts (2000), Bright et al. (2012), and Cherubini et al. (2012) were used.[192, 195, 198] These methods were adapted by Caiazzo et al. (2014) for biofuel life cycle assessment,[179] and this study made further changes to accommodate for the case of algal biofuels. This approach has also been used in other analyses of albedo change impacts.[204, 212] The albedo change impacts of algae production were aggregated by month and subsequently averaged to an annual impact. First, for each Julian day in a given month (*day*), the solar declination angle ∂ and the sunset hour angle ω were averaged at the average latitude φ for a region.

$$\partial_{day} = 23.45 \sin\left(360 * \frac{284+day}{365}\right) \quad \text{(Equation 7)}$$

$$\omega_{day} = \cos^{-1}[-\tan\varphi * \tan(\partial_{day})] \quad \text{(Equation 8)}$$

The final albedo was also calculated daily using the calibrated Equation 5 and the daily solar elevation angle determined through Equation 6. The daily local radiative flux at the top of the atmosphere, R_{TOA}, was then calculated using Equation 9, in which R_{sc} is the solar constant (1362 W m^{-2}),[179] α_f is the final daily albedo for the algal ponds, and α_o is the albedo of the original land. These daily R_{TOA} values were subsequently averaged by month.

$$R_{TOA,day} = \frac{R_{sc}}{\pi} * \left(1 + 0.033 \cos\frac{360*day}{365}\right) * \left(\cos\varphi \cos\delta_{day} \sin\omega_{day} + \frac{\pi\omega_{day}}{180} \sin\varphi \sin\delta_{day}\right) * (\alpha_f - \alpha_o)$$

(Equation 9)

The global radiative forcing for a month $\Delta RF_{global,month}$ was calculated using Equation 10 using the atmospheric transmittance for that site and month K_T, the total surface area of Earth A_{earth} (5.10072 x 10^{14} m^2),[179] the albedo decay function $\gamma_\alpha(t)$, and the transmittance factor T_a. The albedo decay function $\gamma_\alpha(t)$, was set as one unity for continuous algal cultivation over the time step, because the growth dynamics of continuous microalgal harvesting lead to a steady state algal concentration on the area of interest, which differs from crop growth dynamics. The global annual average value, 0.854, was used for the transmittance factor T_a across sites as performed in other studies.[179, 188, 192] This transmittance factor is the percent of the radiation that is reflected from a surface that subsequently reaches the top of the atmosphere.[204] The monthly and site-specific values for K_T were obtained from the 22-year insolation clearness index values at the average latitude of each ecoregion from the NASA Langley Research Center Atmospheric Science Data Center Surface meteorological and Solar Energy (SSE) web portal.[213]

$$\Delta RF_{global,month} = -R_{TOA,month} K_T T_a y_\alpha(t) / A_{earth} \quad \text{(Equation 10)}$$

Equation 11 was used to calculate the monthly equivalent tonnes of carbon lost per square meter ΔC_T using the following factors: the carbon dioxide concentration in the atmosphere in ppm C_0, the radiative efficiency of carbon dioxide RF_{CO2}, the mass of the atmosphere M_{atm} (5.113 x 10^{15} tons),[179] the molecular weight of dry air M_{air} (28.97 g mol^{-1}),[179] the molecular weight of carbon dioxide M_{CO2}, and the airborne fraction AF of carbon dioxide on a time horizon of 100 years (0.5240).[179] Finally, the life cycle climate change impacts arising from albedo change during a given month were calculated by multiplying $\Delta C_{T,month}$ by the area-time occupied by the functional unit, dividing by the facility lifetime, and converting to units of kg CO_{2eq}/GJ fuel.

$$\Delta C_{T,month} = \frac{C_0 \Delta RF_{global,month} M_{atm} M_{CO2}}{M_{air} RF_{CO2} AF * 10^6} \quad \text{(Equation 11)}$$

4.4 Results and discussion

4.4.1 Results and discussion of the two case studies

The baseline foreground production process life cycle climate change impacts are 55.96 kg CO_{2eq}/GJ fuel for algal renewable gasoline produced in the Everglades and 52.29 kg CO_{2eq}/GJ fuel for algal renewable gasoline produced in the Tamaulipas ecoregion (Table 4.5). At a pond depth of 0.4 m and an HRT of 7.5 days in the Everglades, the algal growth model predicted an average algal pond concentration of 274 mg/L, or an algal dry matter areal productivity of 14.6 g m^{-2} day^{-1}. The algal growth model predicted a similar average annual algal pond concentration of 277 mg/L in the Tamaulipas. Although both regions have similar algal production and harvesting impacts due to similar climates through the year, the WWTPs in the Everglades ecoregion are farther away from petroleum refineries compared to the WWTPs in the Tamaulipas ecoregion, and thus production of algal renewable gasoline in the Everglades leads to higher impacts from transportation of biocrude to a refinery for upgrading (Figure 4.4). For both ecoregions, the total life cycle climate change impacts without the inclusion of LUC are lower than the life cycle climate change impacts of conventional gasoline.

Table 4.5: Baseline LCA results for foreground production processes and land use change of renewable algal gasoline production in two ecoregions

Life cycle greenhouse gas emissions (kg CO_{2eq}/GJ fuel)	**Everglades**	**Tamaulipas-Texas Semiarid Plain**
Total from foreground processes	55.96	52.29
Total from land use change	66.20	30.82
Original biomass loss impact	3.33	0.31
Carbon flux change impact	41.93	5.51
Albedo change impact	20.94	25.00
Life cycle total	122.16	83.11

The inclusion of LUC impacts from loss of original biomass, albedo change, and carbon flux change increases the baseline life cycle climate change impacts in both ecoregions. The magnitude of these impacts differs between the two geographic locations (Table 4.5), resulting in higher life cycle climate change impacts than conventional gasoline in the Everglades but lower impacts than conventional gasoline in the Tamaulipas despite having similar total foreground process life cycle climate change impacts. The Everglades has higher impacts from original biomass lost and carbon flux change than the Tamaulipas, and the Tamaulipas has a higher albedo change impact. The original NPP on potentially available land in the Everglades is 7.5 times higher than that of the Tamaulipas, leading to larger carbon flux change impacts.

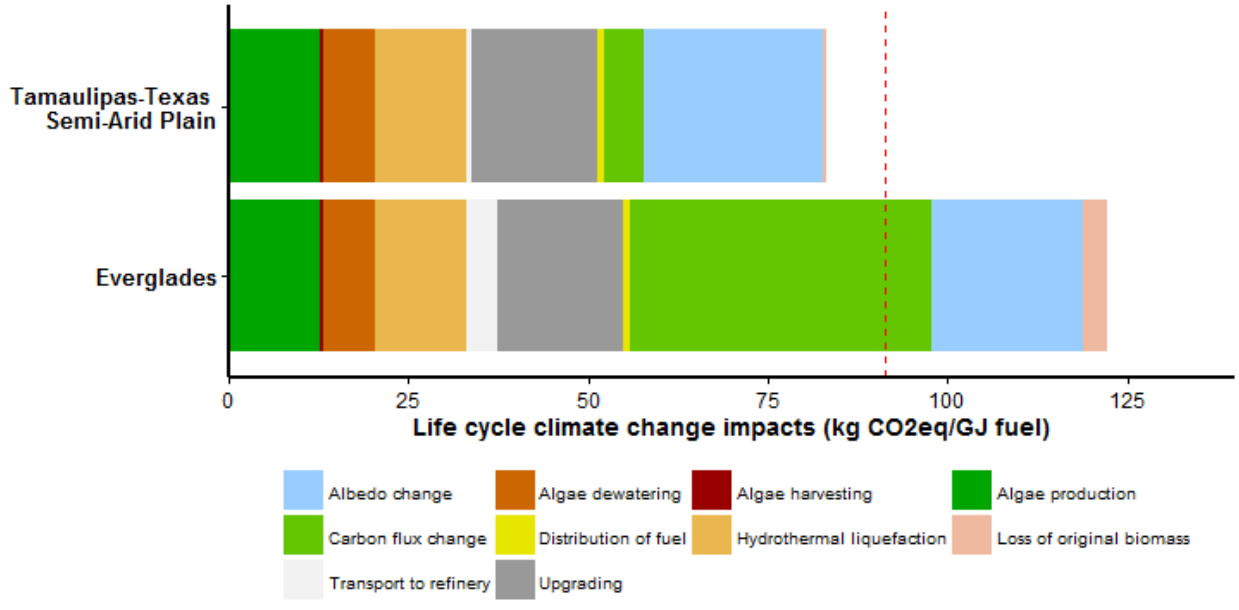

Figure 4.4: Baseline results for algal renewable gasoline production in the Everglades and in the Tamaulipas-Texas Semi-Arid Plain. The red dashed line represents the life cycle greenhouse gas emissions of conventional gasoline.

The albedo change results in the two case studies are influenced by urban albedo values more than the cases shown in Caiazzo et al. for crop-based biofuels[179] because the land is near WWTPs, which are in turn close to population centers. The albedos of urban areas range between 0.10 and 0.20 in general.[214, 215] Areas that have sandy surfaces, which more closely describes parts of the Tamaulipas compared to the Everglades, tend to have higher albedo. For example, dry white sand has an albedo of approximately 0.35.[214] Consequently, the LUC impacts arising from albedo change are higher in the Tamaulipas than in the Everglades.

The Monte Carlo results for the LCA model were very similar when only the foreground processes were modeled (Figure 4.5). The majority of the 100,000 simulations for algal renewable gasoline in the Everglades (99.15%) and the Tamaulipas (99.44%) resulted in lower life cycle climate change impacts than conventional gasoline. The inclusion of direct LUC

impacts broadened the ranges of Monte Carlo results and increased the means, medians, and standard deviations of the results in each region (Figure 4.5). The mean and standard deviation increased from 52.7 ± 12.3 kg CO_{2eq}/GJ fuel to 122.9 ± 36.7 kg CO_{2eq}/GJ fuel in the Everglades and from 49.1 ± 12.2 kg CO_{2eq}/GJ fuel to 85.8 ± 20.7 kg CO_{2eq}/GJ fuel in the Tamaulipas. The range of the Monte Carlo results increased 315% with the inclusion of LUC impacts in the Everglades case and 109% in the Tamaulipas case. These increases in the ranges and the standard deviations of the Monte Carlo results indicate increased uncertainty in the LCA results. Instead of over 99% of the Monte Carlo simulation results being lower than the life cycle climate change impact of conventional gasoline, only 19.64% and 65.78% of the Monte Carlo results met the criteria for the Everglades and the Tamaulipas LCA cases, respectively, when LUC impacts were included.

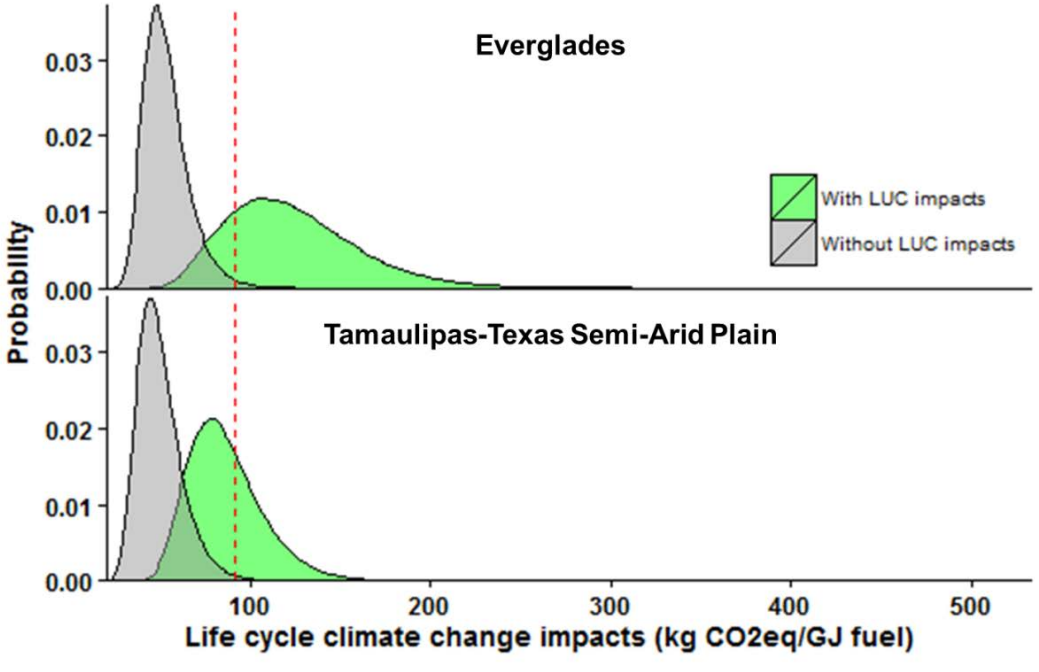

Figure 4.5: Results of 100,000 Monte Carlo simulations for Everglades (top) and Tamaulipas-Texas Semi-Arid Plain (bottom), with and without the inclusion of land use change (LUC) impacts. The red dashed line represents the LC-GHG emissions of conventional gasoline.

The sensitivity analysis results show that LUC parameters such as the net primary productivity (NPP) of the original land conditions, the final albedo calibration factor, and the amount of original biomass on the land are among the parameters to which the LCA results for the two regions are the most sensitive (Figure 4.6). The pond depth is also a sensitive parameter due to its impact on algal growth and concentration. The sensitivity of the individual LUC parameters differs between the two regions due to the geographically measured parameter ranges. The Everglades is more sensitive to differences in the original NPP and the amount of original biomass lost than the Tamaulipas. The sensitivity results show that the life cycle climate change impacts of algal renewable gasoline can be lower than those of conventional gasoline when algal cultivation is implemented on potentially available land with the lowest observed original NPP in the Everglades.

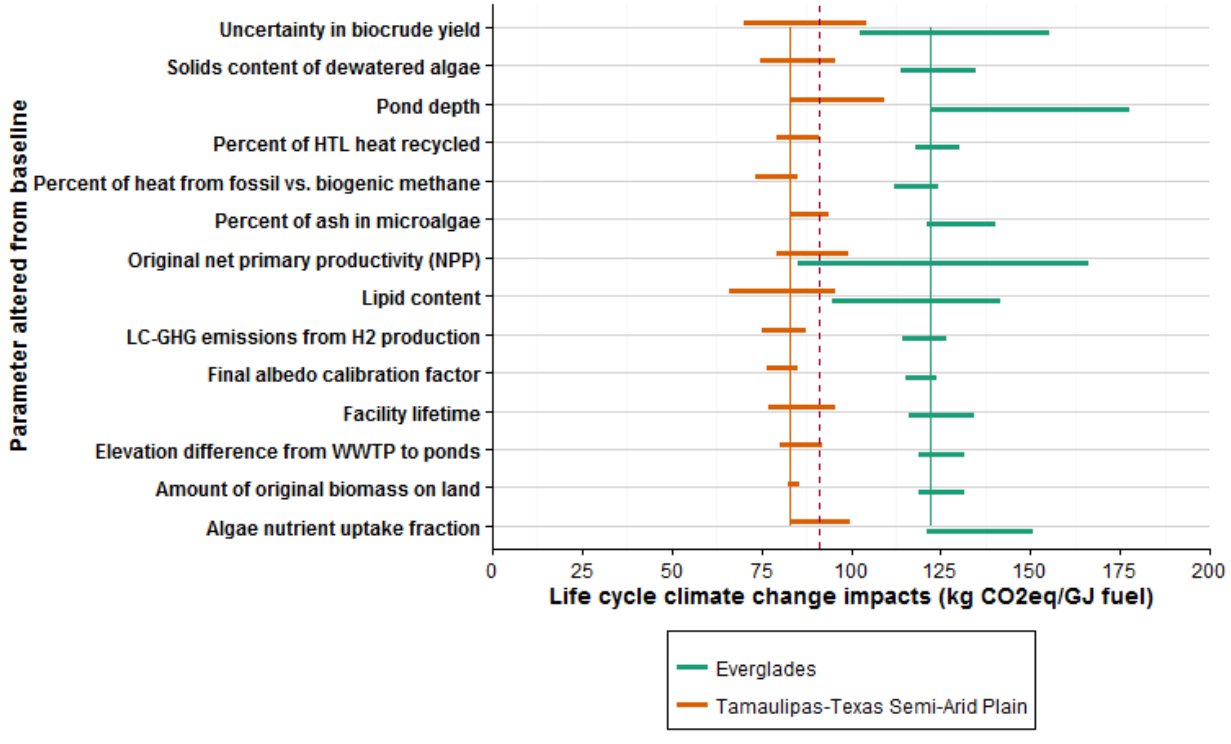

Figure 4.6: Sensitivity analysis results for algal renewable gasoline production in the Everglades and in the Tamaulipas-Texas Semi-Arid Plain. The parameters shown are those to which the results for either ecoregion were the most sensitive. The red dashed line represents the life cycle greenhouse gas emissions of conventional gasoline.

4.4.2 Algal cultivation management for minimization of LUC impacts

The impacts of original biomass loss, although smaller than other LUC impacts, can be mitigated by converting the original biomass removed from the land into an energy product, such as converting woody shrubs to pellets for incineration or to cellulosic biofuels. Grasses could be anaerobically digested for methane production, and dry biomass could be incinerated for heat. This may allow for forested land to be considered as potentially available land as well, because

the original biomass could be harvested for bioenergy prior to installing algal ponds, thus lowering the associated LUC impact of original biomass loss.

The change in carbon flux between the original land and algal production is among the largest contributors to the life cycle climate change impacts of algal biofuel, and the NPP of the original land is a sensitive parameter to the LCA model. Therefore, areas with lower NPP rates should be identified for algal biofuel feedstocks production. The original NPP could be measured with existing geographic datasets, but ideally, more precise measurements would be obtained directly at potential sites. Substantial climate change impacts can occur if algal cultivation is implemented on land with a relatively high NPP, such as the land near WWTPs in the Everglades ecoregion.

There is potential for the albedo change impacts to be reduced or to become negative based on the configuration and management of algal cultivation. The albedo change impacts would be negative if the final albedo is higher than the initial albedo of the land, because more shortwave radiation and less longwave radiation would be emitted from the surface than under the original conditions on the land, thus decreasing the current radiative forcing associated with the fate of incident sunlight on the area. The final albedo could be higher if greenhouses are utilized to grow algae; the surface albedo of typical plastic greenhouses is approximately 0.40.[216] However, the life cycle climate change impacts of greenhouse infrastructure and maintenance could lower the net climate change mitigation effect of cultivating algal biofuel feedstocks in greenhouses. Another possible method of increasing the albedo of algal ponds would be to induce more turbulent mixing of the ponds. Turbulent mixing could create whitecaps on the water surface, which would increase the albedo of algal ponds.[217] However, the energy required to maintain turbulent mixing would contribute to the life cycle climate change impacts of the produced fuel and decrease the magnitude of this benefit. The bottom surface of the algal ponds

should also have a reflective nature, such as a light or white color, so that the overall albedo of the surface of the shallow water column is higher. A high surface albedo for empty ponds would also lead to lower albedo change impacts for algal biofuels produced in colder regions where the growing season is limited to certain months, compared to the Everglades and the Tamaulipas ecoregions where cultivation can be continuous throughout the year.

4.4.3 Limitations of the model and future work

Although the presented model advances the imperative integration of geographic and temporal factors in an LCA of algal biofuels, it contains limitations that must be addressed in future work. The temporal and spatial resolutions of the available geographic data products limit the applicability of their use to compare individual sites instead of larger geographic areas, although the LUC impact framework presented in this study would still be applicable. The NACP dataset for the amount of original biomass has a resolution of 30 m, while the MCD43A3 albedo rasters have a resolution of 500 m and the MOD17 rasters for the original NPP have a resolution of 1000 m. Due to a level of spatial heterogeneity being lost at the larger resolutions, finer-scale measurements should be taken at prospective algal cultivation sites to more accurately determine the potential LUC impacts of production. In particular, the NPP values are derived from satellite remote sensing data at coarse resolution, which may deviate from measurements taken directly at a site. Furthermore, the temporal resolution of the datasets for NPP values and original biomass on the land is an annual value for a given location. This limits the ability to investigate sub-annual temporal changes associated with carbon flux and albedo changes, which should vary throughout the year. The NACP data for the original biomass on the land is also only available for the year 2000, whereas annual NPP data up to the year 2010 is available from MOD17 and the albedo data is updated every eight days up to present day.

In addition to improving measurements that define the original conditions of land, one aspect of the transformed land must be further investigated for improvement of the LUC impact model: the albedo of algal ponds. The albedo of algal ponds depends on the depth of the water body,[207, 218] concentration of algae and other particulates and the type of other suspended matter,[207, 218-221] surface roughness,[206] and the albedo of the bottom surface.[207, 218] To more precisely measure the magnitude of the climate change impact from albedo change, the albedo of these shallow, concentrated algal ponds should be monitored throughout the year to calibrate a model that not only accounts for latitude and time of year, but also for additional parameters such as the measured algal concentration, surface roughness of the water, depth of the ponds, and surface albedo of the bottom of the ponds.

Although the LUC impacts associated with the loss of above-ground biomass were included, losses of soil carbon were not incorporated into this LCA model. A fraction of soil carbon would be degraded as algal ponds are installed and the soils are sealed under the impervious surfaces of pond structures and liners,[222, 223] but these impacts have not yet been extensively quantified. The decomposition of organic matter in the soils after algal pond installation could be added to the model in the future. The life cycle production and LUC impacts of infrastructure associated with algal biofuel feedstocks production, including walkways and pumping equipment, were also not included in this LCA model and could be incorporated in future studies.

With the baseline lipid content of 14% and an assumed oil density of 880 kg m^{-3},[224] the average lipid production rate for algal cultivation in the Everglades is approximately 8.49 m^3 ha^{-1} yr^{-1}. Quinn et al. (2012) determined an average algal lipid production rate between 20 and 22 m^3 ha^{-1} yr^{-1} for photobioreactor systems modeled in the Everglades area.[64] Photobioreactors are expected to yield higher areal productivities of algae compared to open ponds.[19, 78] The use of

photobioreactors was not analyzed in this study, and a comparison of the LUC impacts of open ponds and those of photobioreactors could be facilitated with changes in the algal growth model and the albedo change equations to reflect the differences between the two configurations for cultivating microalgae.

The LCA results for algal renewable gasoline produced in the Everglades and the Tamaulipas were compared against a single value for the life cycle climate change impacts of conventional gasoline. The comparison could be improved by determining the geographically sensitive life cycle climate change impacts of conventional gasoline and including emerging research on the LUC impacts of new oil production in North America.[225]

4.5 Conclusions

Although the two case study regions were very similar in climate, algal productivities, and life cycle climate change impacts of foreground fuel production processes, the inclusion of the climate change impacts arising from land use change resulted in large differences between the two ecoregions. Algal renewable gasoline produced in the Everglades would have a 33.8% greater baseline life cycle climate change impact than petroleum gasoline. Algal renewable gasoline produced in the Tamaulipas would have an 8.97% lower baseline impact than petroleum.

The change in carbon fixation and the initial loss of existing biomass on the land that is converted to algal ponds increase the life cycle climate change impacts of algal biofuels. The change in albedo from the original land conditions to continuous algal cultivation throughout the year further contributes to the climate change impacts of renewable gasoline from algae. To further refine the albedo change impacts of algal biofuels, the albedo of actual algal ponds should

be measured and monitored over time and under different conditions to develop a predictive model.

Additionally, the inclusion of land use change impacts increases the uncertainty of the Monte Carlo analysis results. Parameters which directly affect land use change impacts were among the most sensitive parameters in the algal biofuel LCA model. These results both support the importance of including land use change impacts in algal biofuel LCAs and the need to refine the precision of geographic data to determine the life cycle climate change impacts of algal biofuels at a selected site.

The magnitude of the impacts from these direct land use change aspects depends on the original and final conditions on the land and is thus geographically specific. For LCAs to most accurately reflect the life cycle climate change impacts of algal biofuels, they must be performed based on a geographic location of interest and include the impacts arising from direct land use change.

5 Geographic differences in the life cycle climate change impacts of green gasoline from wastewater algae

5.1 Abstract

As the industry adopts the use of algal biofuels, life cycle assessment (LCA) is crucial to determine whether fuels produced from algal feedstocks have lower life cycle climate change impacts than petroleum-derived fuels. Furthermore, the location-dependent environmental impacts of implementing algal cultivation such as direct land use change impacts must be considered for siting decisions. An LCA for a functional unit of 1 GJ of renewable gasoline produced through hydrothermal liquefaction of microalgae grown in wastewater effluent was performed for each Level II ecoregion in the continental United States. To determine geographically specific parameter values in ArcGIS, potentially available land for algae cultivation was defined as areas with a maximum 2% slope and categorized as barren land, developed open space, grassland, shrubland, or pasture land within a 5-km radius from the center of municipal wastewater treatment plants within each ecoregion. An algal growth model was coupled to the LCA model to incorporate geographic differences in algal productivity. The life cycle climate change impacts arising from land use change were also included in this analysis. The climate change impacts of land use change include the impacts of removing original carbon stored on the land; changing the carbon flux between the atmosphere, vegetation, and soils; and changing the surface albedo of an area. The ecoregions with algae growing seasons of 5 to 7 months differed from those with growing seasons of 9 to 12 months in their baseline LCA, sensitivity analysis, and Monte Carlo analysis results. The results suggest that the geographic regions that are typically noted as most favorable for algae cultivation are possibly less sustainable than regions that cannot produce algae throughout the year. Land use change impacts caused notable differences in net life cycle climate change impacts of algal renewable gasoline

between ecoregions. For sustainable implementation of algal biofuel feedstocks production, areas with lower albedo than warm deserts and lower existing net primary productivities and amounts of biomass on potentially available land than southern Florida should be utilized.

5.2 Introduction

The substitution of petroleum-based fuels with more sustainable renewable fuels is necessary to reduce detrimental human impacts on the environment, to support future economic growth, and to increase energy security in the United States. Government policy is promoting the adoption of biofuels through the Energy Independence and Security Act of 2007 (EISA 2007), which sets a target annual production of 36 billion gallons of renewable fuels by 2022, including 21 billion gallons which must be "advanced biofuel," or fuels that generate 50% less life cycle greenhouse gas (LC-GHG) emissions than their petroleum-derived counterparts.[8] Microalgae is a promising feedstock for renewable fuels at this national scale. Unlike corn, microalgae can be harvested continuously throughout the year and can be cultivated on non-arable land.[19] The biomass growth rate and the oil yield obtained per unit of cultivation area are greater for microalgae than for crop biofuel feedstocks like corn and soybean.[19]

Municipal wastewater effluent can be utilized as a growth medium for algae because it contains nitrogen and phosphorus, which would otherwise be discharged to a receiving water body. Several published life cycle assessments (LCAs) discuss that lower LC-GHG emissions could be achieved by using wastewater to grow algae instead of freshwater supplemented with commercial fertilizers.[41, 42, 46, 48, 119] Furthermore, several LCAs have analyzed cases in which wastewater is used either as a main growth medium or as a supplement for algal cultivation, and the results of these studies confirm the environmental benefits of using wastewater in lieu of freshwater with added fertilizers.[43, 45, 55, 119, 169, 183]

Collocation with wastewater treatment plants (WWTPs) would be necessary for sustainable algal production in municipal wastewater. However, the available land within a short distance from WWTPs was found to be more limiting than wastewater availability for urban WWTPs, which have high flows that could be used for algal cultivation.[69] To maximize the utility of resources necessary for algal cultivation and to mitigate such observed tradeoffs in resource availability,[69, 75] hydrothermal liquefaction (HTL) could be used to process wastewater algae into a fuel precursor instead of lipid extraction. Hydrothermal liquefaction is a high-pressure, high-temperature process which uses subcritical water as the chemical driving force to produce a carbon-rich biocrude from biomass, with yields typically 5 to 30% higher than the original lipid content.[118, 123, 125-133] A geographic analysis by Venteris et al. (2014) showed that HTL can reduce the land requirements for algal biofuel production by at least 50% compared to lipid extraction.[73] Hydrothermal liquefaction also has the potential to reduce the need for nutrients and water compared to lipid extraction for the same amount of algal biofuel produced.[73]

Geographic analyses can help identify the land availability around WWTPs and compare potential algal productivities between sites. Very few geographic analyses have been performed for collocation of algal biofuel production and wastewater treatment.[69, 76] Additionally, previously published geographic analyses identify areas that are most favorable for algal biomass production based on climatic variables and resource availability, but they do not compare the life cycle environmental impacts of production between regions within their area of study.[62, 64, 65, 69-76] Conversely, most previously published LCAs of algal biofuels do not compare differences in location-specific factors which influence algal productivity, transportation distances, and land use change impacts. Although the incorporation of spatial heterogeneity has been listed as one of the grand challenges in applying LCA to biofuels,[79] very few spatially explicit LCAs have been performed for biofuels.[170, 171]

The differences in net life cycle climate change impacts of algal biofuels by geographic location including the direct land use change (LUC) impacts from removing the original biomass on the land, changing the carbon flux through algal cultivation, and changing the albedo of an area are currently unknown. This study uses the methods of Chapter 4 of this dissertation to determine differences in LCA results by the Level II ecoregion in the continental United States in which algal cultivation would be implemented, to investigate geographic patterns in the life cycle climate change impacts of renewable gasoline produced through HTL of wastewater algae, and to discuss the implications for siting sustainable algal biofuel feedstocks production.

5.3 Methods

5.3.1 LCA methods

The Python-based LCA model for renewable gasoline produced from HTL of wastewater microalgae described in Chapter 4 was used to perform this study. The LCA model consists of foreground production process impacts and direct land use change (LUC) impacts. The foreground process steps were algal cultivation in municipal wastewater effluent supplemented with the recycled aqueous coproduct from HTL, algae harvesting by gravity sedimentation, algae dewatering by centrifuge, HTL to produce a biocrude, transportation of the biocrude from the WWTP to the nearest petroleum refinery, upgrading to renewable gasoline, and distribution for use in vehicles. The LUC impacts included the climate change impacts from the loss of original biomass, the change in carbon flux or net primary productivity, and the change in albedo on the land that would be transformed and occupied for algal cultivation. All impacts were scaled to the functional unit of 1 GJ of algal renewable gasoline. The LCA model was coupled to a monthly algal growth model coded in Python and described in Chapter 4. For the months without algal production, the albedo of the empty algal raceways was modeled with a baseline value of 0.5 and

a range from 0.2 to 0.8, assuming that the raceways are painted white and accounting for the material becoming worn and discolored (and thus less reflective) through use. This range also accounted for possible snow accumulation in the raceways during the cold months during which algae cultivation is halted, when average monthly temperatures fall below 10°C.

Baseline cases, Monte Carlo analyses of 100,000 simulations both with and without the inclusion of LUC impacts in the LCA model, and sensitivity analyses were performed using the geographically specific parameter values determined for each EPA-designated Level II ecoregion (n=20) in the continental United States (Figure 5.1). The Level II ecoregions were chosen because they are more diverse than the 10 Level I ecoregions and could reveal trends more clearly than an analysis among the 85 Level III ecoregions in the continental United States.

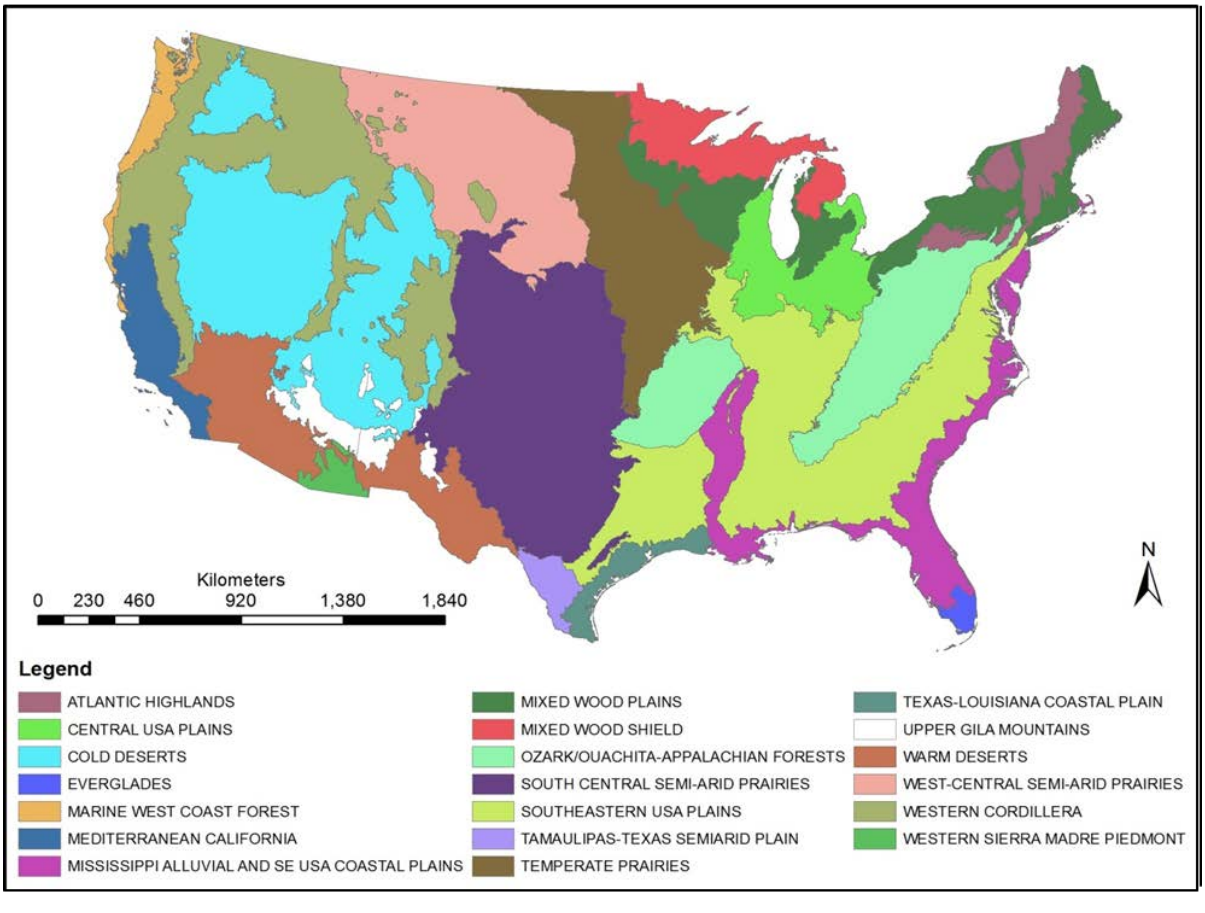

Figure 5.1: Level II ecoregions of the continental United States.

5.3.2 Determination of potentially available land

The potentially available land within a 5-km radius of the municipal WWTPs in each ecoregion was chosen to represent the range of conditions for algal cultivation collocated with wastewater treatment by ecoregion. Geographic analyses of algal biofuel feedstocks production have investigated potential cultivation sites between 400 ha and 4000 ha in size.[65, 70] Economic studies on algal biofuels have recommended that algal cultivation facilities should be at least 400 ha.[39, 61, 67, 226] If all the land around a given WWTP was available, a 400-ha facility would require a radius of 1.13 km, and a radius of 3.57 km would provide 4000 ha. Because only a fraction of the land near WWTPs is typically available,[69] a 5-km radius was determined to be appropriate for this study.

The WWTPs included in this analysis were identified as wastewater treatment plants with National Pollutant Discharge Elimination System (NPDES) permit numbers in the 2008 EPA Clean Watersheds Needs Survey (CWNS).[87] They were geocoded in ArcGIS using the latitude and longitude data entered for their NPDES permits. The plants with less than 50% of total existing flows from municipal wastewater as reported in the CWNS were excluded. A 5-km buffer was created around all of the 12,302 remaining WWTPs in order to define the average conditions on potentially available land within 5 km of the WWTP locations, which were then aggregated by Level II ecoregion.

Protected areas were identified in ArcGIS using the US Geological Survey's Protected Areas Database of the United States (PAD-US) and excluded from potentially available land.[227] Additionally, the National Elevation Dataset 30-m rasters were used to exclude all areas with slopes greater than 2%. Finally, the USGS 2011 National Land Cover Dataset was used to include only the remaining land areas that were designated as the following five land cover types: developed open space, barren land (rock/sand/clay), shrub/scrub, grassland/herbaceous,

and pasture/hay.[228] Similarly, the Quinn et al. (2013) geographic analysis considered only barren, shrub/scrub, and grassland/herbaceous lands; pasture and forest land were also included for a sensitivity case.[70] The Pate et al. (2011) resource demand analysis considered only pasture land as potentially available land.[62] Most of the five chosen land cover types in this study would cause minimal indirect land use change from shifting economically productive activities to other land areas. Additionally, high-quality agricultural land is not expected to be available for algal cultivation because of its relatively higher capital costs and because it could lead to food versus fuel issues, especially if agricultural production is not subsequently shifted to other areas.[78]

Temperature and solar radiation data needed to model potential algal growth on a monthly basis was collected on the potentially available land areas in each ecoregion. The Area Solar Radiation tool in ArcMap 10 was used with the defined slopes to calculate monthly solar radiation on potentially available land areas. This data was supplemented with clear sky direct normal insolation data from the National Renewable Energy Laboratory.[229] The average temperature was aggregated by WWTP from 30-year climate normals from the Parameter-elevation Relationships on Independent Slopes Model (PRISM).[230] The monthly minimum, average, and maximum temperatures were determined at the ecoregion level from the WWTP-level data points.

The minimum, average, and maximum distances from WWTPs in an ecoregion to the nearest petroleum refinery were also calculated in ArcGIS to define a geographically specific LCA input parameter for the transportation of biocrude produced at a WWTP to a refinery for upgrading to renewable gasoline.[145]

The tables in Appendix C show the parameters that were varied by ecoregion. In all, 51 input parameters were varied geographically. The parameters that do not change geographically are shown in Table 4.2 of Chapter 4. Furthermore, the following input parameters were varied

monthly: the wastewater effluent nitrogen concentration, the wastewater effluent phosphorus concentration, the original albedo, the atmospheric transmittance, the temperature, and the solar radiation on potentially available land near municipal WWTPs.

5.4 Results and discussion

5.4.1 Ecoregion-specific LCA results and discussion

The average geographically specific characteristics of the potentially available land within 5 km of each ecoregion are shown in Table 5.1 and outlined in greater detail in the Appendix C.

Table 5.1: Average original characteristics of the potentially available land within 5 km of municipal wastewater treatment plants in each numbered Level II ecoregion in the continental United States. NPP = net primary productivity and WWTPs = wastewater treatment plants.

Ecoregion number	Level II ecoregion name	Number of WWTPs	Average distance to nearest refinery (km)	Average monthly temperature range (°C)	Average monthly solar radiation range (kWh m^{-2} day^{-1})	Average monthly albedo range	Average above-ground biomass (kg m^{-2})	Average annual NPP (kg m^{-2} yr^{-1})
1	Atlantic Highlands	246	249	-6.27 – 20.33	2.379 – 4.562	0.1225 – 0.2973	2.909	1.029
2	Central USA Plains	1199	114	-4.13 – 22.91	2.151 – 5.157	0.1523 – 0.3900	0.714	1.000
3	Cold Deserts	239	249	-1.87 – 22.12	2.992 – 8.511	0.1617 – 0.4355	0.089	0.746
4	Everglades	12	656	18.81 – 28.37	3.959 – 5.994	0.1339 – 0.1467	2.646	3.191
5	Marine West Coast Forest	224	180	5.32 – 17.72	1.558 – 5.953	0.1278 – 0.1485	0.951	1.211
6	Mediterranean California	168	74.2	10.19 – 22.04	3.513 – 8.079	0.1443 – 0.1660	0.395	1.501
7	Mississippi Alluvial & Southeast USA	837	133	6.40 – 26.94	3.527 – 5.099	0.1332 – 0.1428	2.826	1.775
8	Mixed Wood Plains	1655	201	-5.57 – 21.58	2.301 – 5.096	0.1436 – 0.4142	1.463	1.020
9	Mixed Wood Shield	176	216	-10.42 – 19.30	2.285 – 5.687	0.1313 – 0.4341	1.364	0.839
10	Ozark/ Ouachita-Appalachian Forests	1670	141	-0.04 – 23.77	3.024 – 4.713	0.1457 – 0.1845	0.527	0.770
11	South Central Semi-Arid Prairies	855	135	2.65 – 26.88	4.140 – 6.722	0.1545 – 0.1980	0.13	0.489
12	Southeastern USA Plains	2584	136	3.53 – 26.08	3.307 – 5.056	0.1408 – 0.1582	1.53	0.950
13	Tamaulipas-Texas Semi-Arid Plain	28	125	12.60 – 30.14	3.974 – 6.089	0.1512 – 0.1633	0.353	0.425
14	Temperate Prairies	1582	256	-5.19 – 23.98	2.751 – 6.049	0.1503 – 0.3944	0.105	0.523
15	Texas-Louisiana Coastal Plain	392	43.1	12.01 – 28.87	3.432 – 5.216	0.1474 – 0.1545	0.534	1.313
16	Upper Gila Mountains	9	239	2.22 – 21.60	6.522 – 9.292	0.1250 – 0.2394	0.896	1.650
17	Warm Deserts	58	253	9.56 – 30.70	6.252 – 9.029	0.2007 – 0.2115	0.04	0.913
18	West-Central Semi-Arid Prairies	137	237	-6.38 – 22.45	2.807 – 7.410	0.1510 – 0.5008	0.044	0.425
19	Western Cordillera	228	256	-2.28 – 18.97	3.040 – 7.972	0.1427 – 0.3872	0.334	0.619
20	Western Sierra Madre Piedmont	3	377	8.09 – 26.60	6.260 – 9.385	0.1504 – 0.1653	0.185	0.100

The algae growth model defined the growing seasons based on the months with an average temperature above 10°C. The ecoregions with longer algae growing seasons are mostly in the southern areas of the continental United States (Figure 5.2). The baseline LCA results show that twelve ecoregions had an algae growing season of 5 to 7 months and eight ecoregions had an algae growing season of 9 to 12 months. No ecoregion had an algae growing season of 8 months. Due to this divide, the LCA results were also compared by these two groups of growing season lengths in addition to the comparison between individual ecoregions.

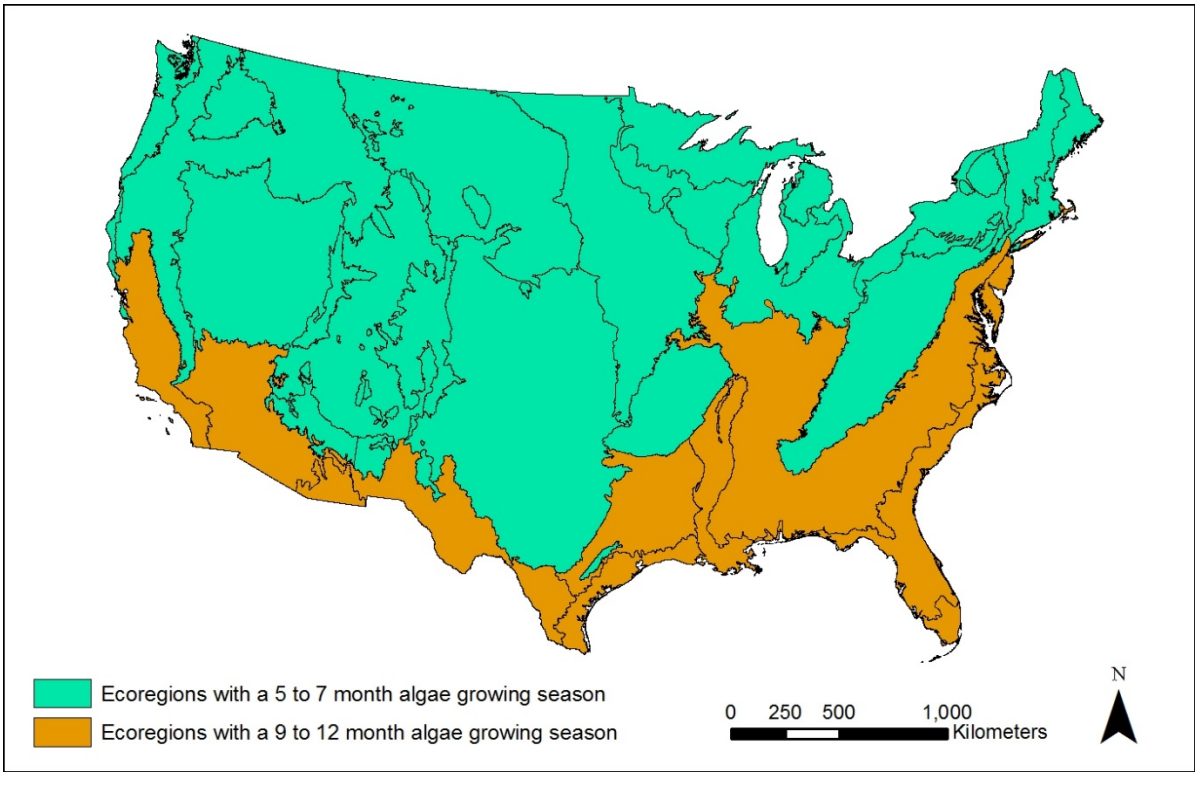

Figure 5.2: Location of ecoregions by the length of their algae growing seasons determined by the algal growth model used in the LCA model.

The baseline LCA results show this division between ecoregions by their algae growing seasons in the climate change impacts from changing the albedo of the original land. This impact is negative and lowers the net life cycle climate change impacts of algal renewable gasoline in most of the ecoregions that could produce algae in outdoor open ponds for only 5 to 7 months annually (Figure 5.3). This is due to the higher albedo of the empty ponds compared to the full ponds, which reverses the albedo change impact during the months when cultivation is halted. The albedo change impacts for the baseline LCA results by ecoregion range from -45.8 kg CO_{2eq}/GJ fuel to 34.9 kg CO_{2eq}/GJ fuel. The ecoregions with the lowest albedo change impacts in ascending order are the Upper Gila Mountains, the Atlantic Highlands, and the Western Cordillera ecoregions. The ecoregions with the albedo change impacts that contribute the most to the life cycle climate change impacts of algal renewable gasoline are the Warm Deserts, Mediterranean California, and the Tamaulipas-Texas Semi-Arid Plain, in descending order. The Warm Deserts ecoregion has the highest original surface albedo among the ecoregions that do not have seasonally large changes in surface albedo due to snow. Converting this high-albedo land to algal ponds that have a relatively low albedo and that can produce for ten months of the year leads to high climate change impacts from changing the albedo of the land.

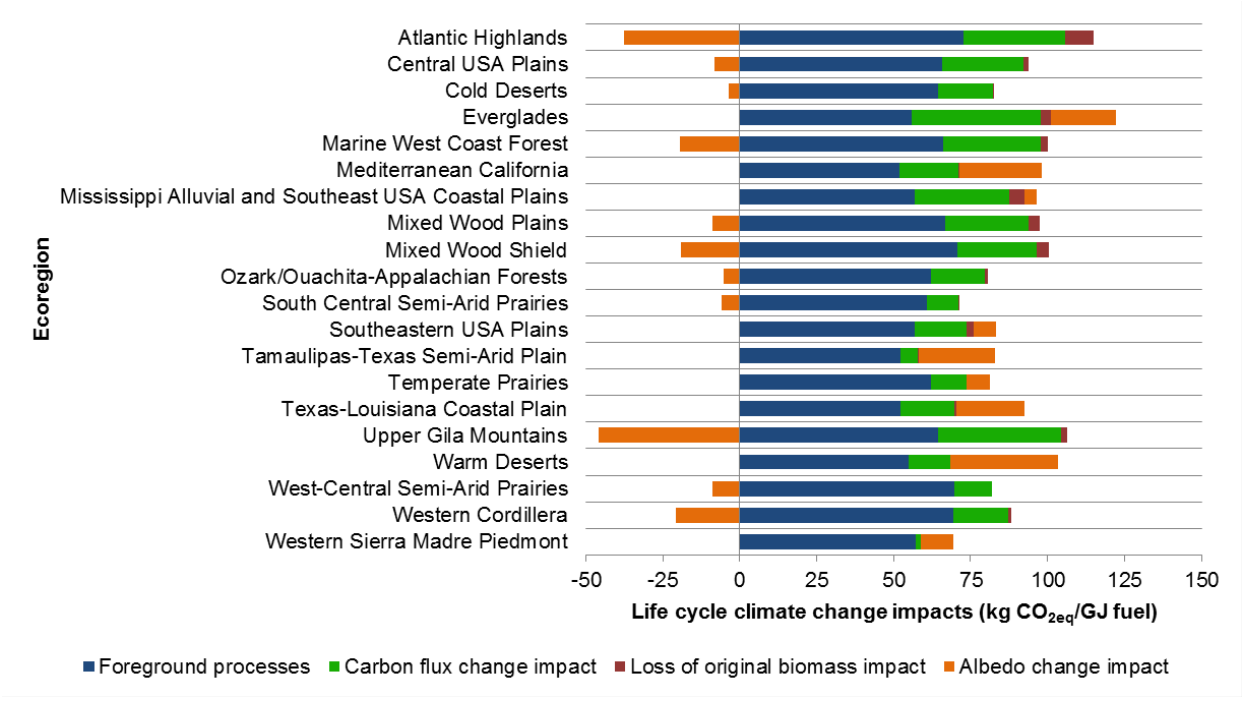

Figure 5.3: Baseline LCA results by ecoregion, showing the contribution of foreground processes and the three direct LUC impacts to the life cycle climate change impacts of renewable gasoline from algae.

The baseline LCA results also show differences in the relative impacts of changing the carbon flux and losing the original biomass on the land transformed to algal ponds (Figure 5.3). For example, the carbon flux change impact for production in the Everglades ecoregion is nearly 26 times that of the Western Sierra Madre Piedmont ecoregion. The ecoregion-specific carbon flux change impacts range from 1.62 kg CO_{2eq}/GJ fuel to 41.9 kg CO_{2eq}/GJ fuel. The ecoregions with the largest carbon flux change impacts in the baseline LCA results in descending order are the Everglades, the Upper Gila Mountains, and the Atlantic Highlands. The ecoregions with the smallest carbon flux change impacts are the Western Sierra Madre Piedmont, the Tamaulipas-Texas Semi-Arid Plain, and the South-Central Semi-Arid Prairies, in ascending order.

The impact from the loss of original biomass on the land is consistently smaller than the carbon flux change impact among the baseline LCA results by ecoregion. It ranges from -0.085 kg CO_{2eq}/GJ fuel to 9.21 kg CO_{2eq}/GJ fuel. Two ecoregions showed negative life cycle climate change impacts from the loss of original biomass, indicating that the average carbon in algae ponds on the occupied land would be higher than the average carbon in the existing biomass on that land. These two ecoregions are the Warm Deserts and the West-Central Semi-Arid Prairies. The Cold Deserts ecoregion shows the third lowest, albeit positive, climate change impact from the loss of original biomass. As expected, these are the three ecoregions with the lowest amount of original biomass per square meter on the potentially available land near WWTPs. The ecoregions with the largest impacts from the loss of original biomass in descending order are the Atlantic Highlands, the Mississippi Alluvial and Southeast USA Coastal Plains, and the Mixed Wood Shield ecoregions.

Compared to most of the LUC impacts, the baseline foreground process impacts show minimal changes between ecoregions from geographic differences in algal productivity and transportation distances between WWTPs and petroleum refineries. The process step for transporting the biocrude from a WWTP to the nearest refinery contributes between 0.31% and 3.58% of the total life cycle climate change impacts of algal renewable gasoline depending on the ecoregion where it is produced. There is greater variability between ecoregions for the algal cultivation and harvesting impacts, which range from 13.1 kg CO_{2eq}/GJ fuel to 32.6 kg CO_{2eq}/GJ fuel between ecoregion-specific LCA baseline cases.

Overall, five of the twenty ecoregions show higher baseline life cycle climate change impacts than conventional gasoline. In order of highest to lowest life cycle climate change impacts, these ecoregions are the Everglades, the Warm Deserts, Mediterranean California, Mississippi Alluvial and Southeast USA Coastal Plains, and the Texas-Louisiana Coastal Plain.

All of these ecoregions have long algae growing seasons of 9 to 12 months and generally favorable climatic conditions for algae cultivation. In fact, these five ecoregions are among the six ecoregions[2] with the lowest total life cycle climate change impacts from foreground processes due primarily to their high algal productivities leading to low algae cultivation and harvesting impacts (Figure 5.3). These regions may have been considered the most sustainable sites for algal biofuel feedstocks production if LUC impacts had not been included among the geographic factors in the LCA model.

Seven ecoregions showed an average Monte Carlo analysis result that is lower than the life cycle climate change impacts of conventional gasoline: the Western Sierra Madre Piedmont, the South Central Semi-Arid Prairies, the West-Central Semi-Arid Prairies, the Temperate Prairies, the Western Cordillera, the Tamaulipas-Texas Semi-Arid Plain, and the Ozark/Ouachita-Appalachian Forests (Figure 5.4). Five of these seven ecoregions have an algal growing season of 5 to 7 months. The negative climate change impact of changing the albedo of the land to the empty pond albedo for approximately half of the year assisted in lowering the net life cycle climate change impacts of these ecoregions that are less productive in algal biomass on average. The span of the ranges of Monte Carlo simulation results for the ecoregions with 9 to 12 month algae growing seasons is between 272 kg CO_{2eq}/GJ fuel for the Western Sierra Madre Piedmont ecoregion and 669 kg CO_{2eq}/GJ fuel for the Southeastern USA Plains. The ranges of Monte Carlo simulation results for the ecoregions with 5 to 7 month algae growing seasons are between 542 kg CO_{2eq}/GJ fuel for the Marine West Coast Forest and 1525 kg CO_{2eq}/GJ fuel for the Western Cordillera ecoregion. Overall, the ecoregions with the shorter algae growing seasons have larger ranges of Monte Carlo analysis results and thus greater variability in possible life cycle climate change impacts for algal renewable gasoline.

[2] The other ecoregion is the Tamaulipas-Texas Semi-Arid Plain.

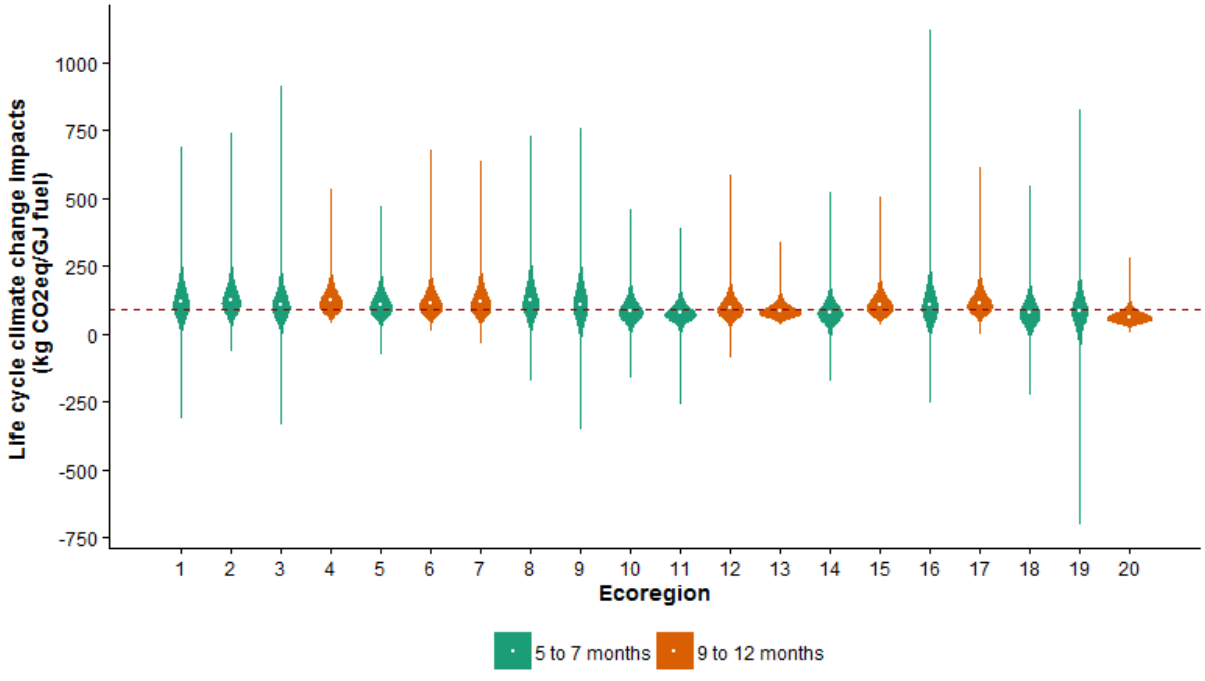

Figure 5.4: Results of 100,000 Monte Carlo simulations for algal green gasoline production in each of the twenty Level II ecoregions in the continental US. The red dashed line represents the life cycle greenhouse gas emissions of conventional gasoline. The white dots represent the means of the simulations.

The ranges of Monte Carlo simulation results were widened by the inclusion of LUC impacts in the LCA model, indicating an increase in the uncertainty of the total life cycle climate change impacts of algal renewable gasoline (Figures 5.4 & 5.5). This is expected as sensitive variable parameters are added to an LCA model. Across all ecoregions, the addition of LUC impacts increased the range of Monte Carlo results by 307% ± 127%. For the eight ecoregions with the longer algae growing seasons, the mean result of the Monte Carlo simulations increased compared to the results of Monte Carlo analyses of the LCA model without LUC impacts by 97.0% ± 39.4%. The mean Monte Carlo results for the twelve LCA cases with the shorter algae

growing seasons increased by a smaller extent of 50.8% ± 27.5% when LUC impacts were added to the LCA model.

None of the twenty ecoregion-level Monte Carlo analyses without LUC impacts resulted in any case in which the life cycle climate change impacts of algal renewable gasoline are below 19.6 kg CO_{2eq}/GJ fuel. However, with the addition of LUC impacts, seventeen ecoregions showed a lower minimum Monte Carlo result, and fourteen ecoregions showed a negative minimum life cycle climate change impact. Two ecoregions with 9-month algae growing seasons had a negative minimum Monte Carlo result, but none of the ecoregions with longer growing seasons showed a negative result, suggesting that the albedo change impact influenced by empty ponds contributes to these cases. Only the Everglades, Tamaulipas-Texas Semi-Arid Plain, and the Texas-Louisiana Coastal Plain had a higher minimum Monte Carlo result with the inclusion of LUC impacts compared to without these impacts in the LCA model. These three ecoregions are among the four ecoregions with a 12-month algae growing season. Despite that cases exist within the LCA model in the other ecoregions where the life cycle climate change impacts of algal renewable gasoline are not only lower than conventional gasoline but are also negative, all ecoregions had a notably higher maximum Monte Carlo result when LUC impacts were included. Thus, there is potential for algal renewable gasoline to contribute to climate change to an even greater magnitude than conventional gasoline.

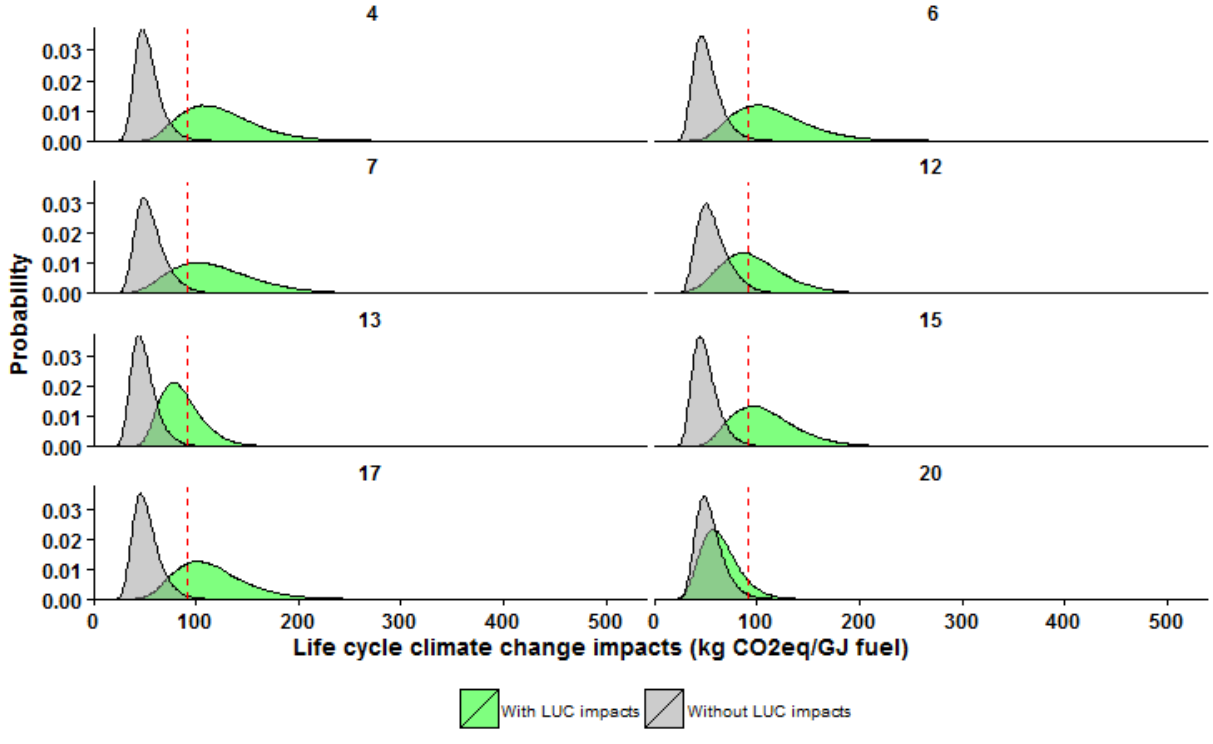

Figure 5.5: Results of 100,000 Monte Carlo simulations for each ecoregion with an algae growing season from 9 to 12 months with and without LUC impacts included in the LCA model. The numbers above the plots denote the ecoregion label.

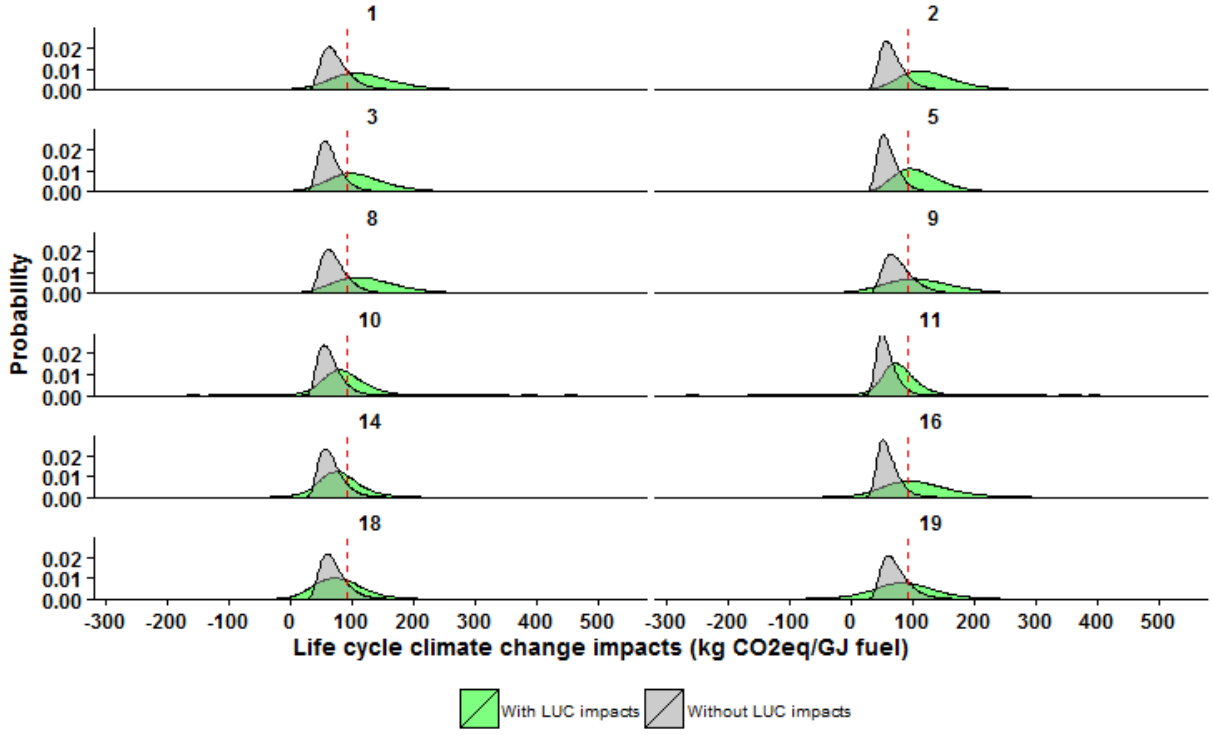

Figure 5.6: Results of 100,000 Monte Carlo simulations for each ecoregion with an algae growing season from 5 to 7 months with and without LUC impacts included in the LCA model. The numbers above the plots denote the ecoregion label.

A one-way ANOVA showed that there is a significant difference in the Monte Carlo simulation results by ecoregion ($p < 0.001$) and between the 5 to 7 month and the 9 to 12 month algae growing season groups ($p < 0.001$). Although the average life cycle climate change impact of the Monte Carlo simulations for both groups of ecoregions is greater than the life cycle climate change impact of conventional gasoline, the impacts vary by ecoregion, and seven ecoregions have an average Monte Carlo result lower than conventional gasoline. Additionally, between 19.6% and 91.5% of the Monte Carlo simulations resulted in lower life cycle climate change impacts than conventional gasoline depending on the ecoregion where the biofuel would be produced (Figure 5.7). The ecoregion with the smallest probability of lower impacts than

conventional gasoline is the Everglades ecoregion, followed by the Central USA Plains and the Warm Deserts ecoregions. The ecoregion with the largest probability of lower impacts than conventional gasoline is the Western Sierra Madre Piedmont, followed by the South Central Semi-Arid Prairies and the Temperate Prairies ecoregions. The choice of an algae cultivation site that narrows the probable life cycle climate change impacts to a range completely below the impacts of conventional gasoline will involve determining the values of key sensitive parameters.

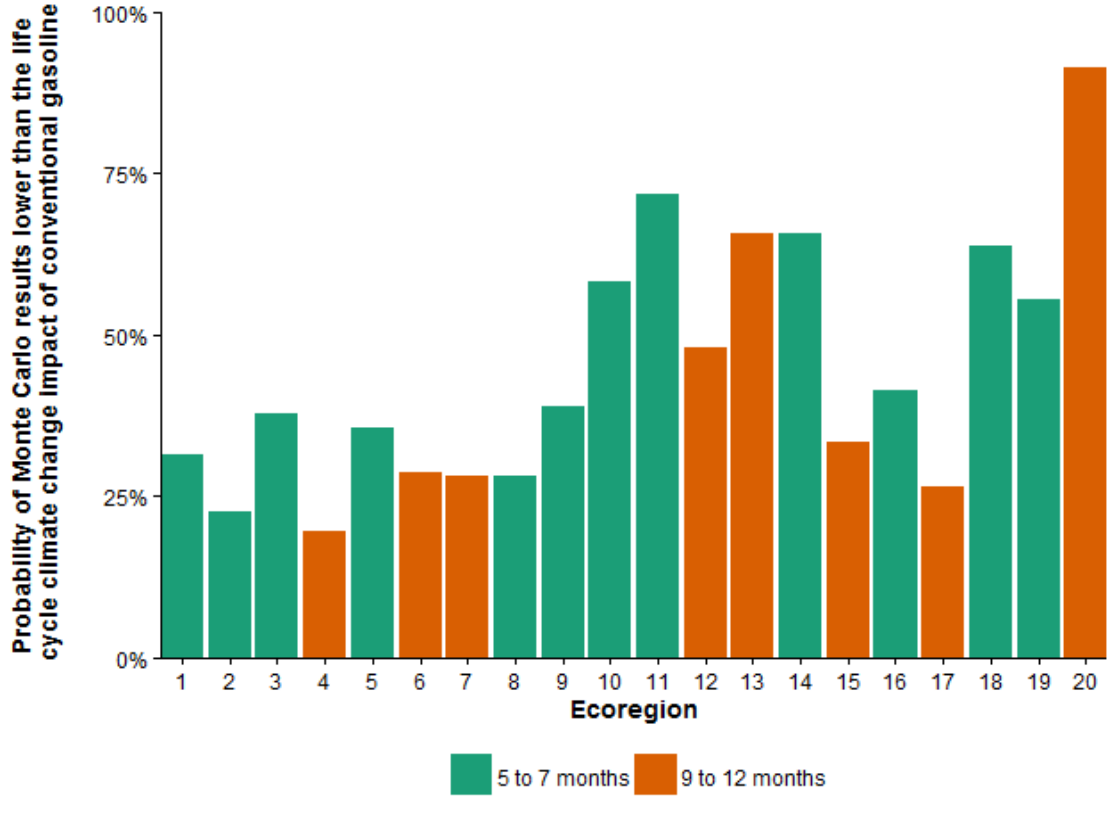

Figure 5.7: Percentage of the 100,000 Monte Carlo simulations that resulted in a lower life cycle climate change impact for algal renewable gasoline than conventional gasoline (91.3 kg CO_{2eq}/GJ fuel).

The sensitivity analysis results highlight differences between the ecoregions with 5 to 7 month algae growing seasons and those with 9 to 12 month algae growing seasons. The parameters shown in Figure 5.8 are all parameters which were among the five to which the baseline LCA results of each ecoregion were the most sensitive. Three parameters that are directly related to LUC impacts are among these eleven key parameters: the original NPP, the amount of original biomass on the land, and the surface albedo of empty ponds. Additionally, the facility lifetime, the pond depth, and the temperature in May (which all affect the LUC impacts) are among these most sensitive parameters. Six of the twelve ecoregions with the shorter growing seasons for algae have minimum temperatures in May that are below 10°C and average temperatures above 10°C in May, thus the LCA model is sensitive to the temperature during that month. The ecoregions with the shorter growing seasons for algae are all most sensitive to the surface albedo of empty ponds, the original net primary productivity, and the uncertainty in the biocrude yield. The ecoregions with the longer growing seasons are generally more sensitive to certain parameters that affect foreground process impacts more directly than LUC impacts. However, in nineteen ecoregions, the most sensitive parameter was either the original NPP or the surface albedo of empty ponds, which both directly affect LUC impacts. While in all of the ecoregions with a 5 to 7 month algae growing season, the second most sensitive parameter was the other parameter related to LUC impacts, in all of the ecoregions with the longer growing seasons, a foreground process-related parameter was the second most sensitive parameter.

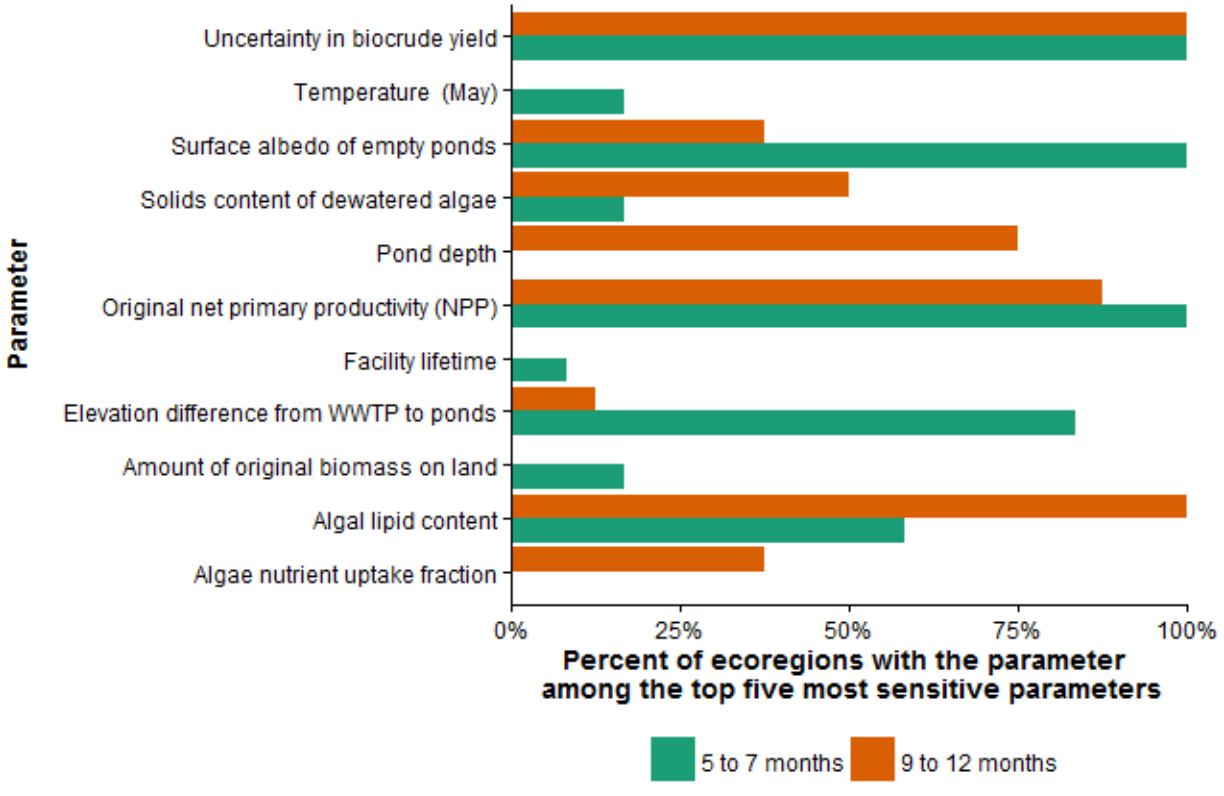

Figure 5.8: Percentage of ecoregions by algae growing season length that have a parameter among the five parameters to which their LCA results are most sensitive.

5.4.2 Comparison to geographic analyses of algal production

Geographic analyses have identified areas that are preferred for algal biofuel feedstocks production in the United States. Orfield et al. (2014) determined that the 14 southern-most states could produce the highest annual algal biomass productivities.[76] Wigmosta et al. (2011) identified the Great Lakes region, southeastern seaboard, and the Gulf coast as areas in the continental U.S. with the least potential consumptive water use per amount of algal oil produced.[65] The Quinn et al. (2013) geographic analysis identified the U.S. southwest, California, southern Texas, and Florida as regions with the highest lipid productivity results from a photobioreactor model.[70] Sperana et al. (2015) identified areas near cities with high populations

in the Gulf of Mexico coastal area, southern Georgia, and Florida as the most viable sites to cultivate algae in the United States.

Although these generally warmer, southern regions have longer growing seasons and favorable climatic conditions for algal growth, the results of this study indicate that they may not be the most sustainable sites for algal cultivation. The Warm Deserts, Mediterranean California, and Tamaulipas-Texas Semi-Arid Plain showed the largest albedo change impacts in the baseline LCA results, while the Everglades had the highest carbon flux change impact and the Mississippi Alluvial and Southeast USA Coastal Plains showed the second highest impacts from loss of original biomass. The Everglades, the Warm Deserts in the southwest, most of California, and the coastal Gulf of Mexico regions and southeastern seaboard (the Mississippi Alluvial and Southeast USA Coastal Plains and the Texas-Louisiana Coastal Plain ecoregions) had the highest net life cycle climate change impacts among the geographically specific LCA baseline cases. The Tamaulipas-Texas Semi-Arid Plain, however, had among the lowest baseline impacts. Furthermore, the inclusion of LUC impacts into the LCA model increased the minimum probable life cycle climate change impacts in the Monte Carlo results for the Everglades, Texas-Louisiana Coastal Plain, and the Tamaulipas-Texas Semi-Arid Plain, creating less possibility for low-impact algal biofuel production in these areas. In all, the Everglades and the Warm Deserts had among the lowest cumulative probabilities of algal renewable gasoline life cycle climate change impacts being lower than those of conventional gasoline through 100,000 Monte Carlo simulations. The results of including LUC impacts into an algal renewable gasoline LCA model suggest that the geographic regions that were previously considered to be the most favorable for algal biofuel feedstocks production are possibly less sustainable than regions that cannot produce algae throughout the year. Additionally, higher albedo regions like the Warm Deserts of the southwest and regions with currently high net primary productivities and large amounts of

biomass on potentially available land like the Everglades ecoregion are among the least sustainable sites for implementing algae cultivation.

5.4.3 Limitations of the ecoregion-level LCA model

These LCA results are specific to algae cultivation collocated with municipal WWTPs on land that is defined to be potentially available by several criteria. In some ecoregions, this land is fragmented into small parcels that would most likely not be used for commercial-scale algal cultivation. The limited availability of land near WWTPs in some regions also led to differences in the amount and spatial heterogeneity of data from GIS datasets with different resolutions.

It should be noted that the results for Ecoregion 20, the Western Sierra Madre Piedmont, do not follow the same trends as other ecoregions with a 9 to 12 month algal growing season. This ecoregion's geographic parameters originate from three WWTPs for which the surrounding potentially available land has a relatively low original NPP and amount of original biomass compared to other ecoregions (Table 5.1). However, the implementation of algal biofuel feedstocks cultivation in wastewater is unlikely in the Western Sierra Madre Piedmont ecoregion due to its available resources of wastewater and land. Approximately 3.40% of the 235.6 km^2 within a 5-km radius of these WWTPs could be defined as potentially available land using the methodology of this study, and the total available wastewater flow is 965 m^3 day^{-1}.

The empty pond albedo was modeled with a range from 0.2 to 0.8 with a baseline value of 0.5. As this parameter was shown to be very sensitive and can vary over the lifetime of the ponds and with different materials used, weather conditions, and general upkeep, the LCA results would be more precise using measured empty algal raceway albedo values. As they are currently modeled, the raceways in the ecoregions that are less productive annually due to short algae growing seasons are mitigated in their climate change impacts by having a lower radiative

forcing when empty during the colder months, but that may not be the case with less reflective raceway materials like black plastics.

Overall, the impacts of albedo change and carbon flux change are as important as foreground process impacts in an algal renewable gasoline LCA. Caiazzo et al. (2014) also determined that direct LUC impacts including the impacts of albedo change are of the same magnitude as foreground process impacts in crop-based biofuel LCAs.[179] However, this study is the first LCA to determine the importance of direct LUC impacts to the sustainability of algal biofuels in a geographically specific context.

5.5 Conclusions

Land use change impacts are variable by ecoregion, and several parameters in the algal renewable gasoline LCA model related to LUC impacts are among the most sensitive parameters. Some regions that were previously considered most favorable for algal cultivation may be less sustainable due to the current conditions on the land, including high albedo in the Warm Deserts ecoregion and high NPP and amounts of original biomass on potentially available land in the Everglades ecoregion. The average life cycle climate change impacts from Monte Carlo simulations of each ecoregion-level LCA case and the baseline results show that overall, LUC impacts increase the net life cycle climate change impacts of algal renewable gasoline.

The higher life cycle climate change impacts for foreground processes associated with lower algal productivity in some ecoregions are balanced with a negative net climate change impact from albedo change, thus lowering the differences in life cycle climate change impacts of algal renewable gasoline produced in colder and warmer ecoregions in the continental United States. The current conditions on the land at each prospective site should be evaluated prior to implementing algal cultivation.

6 Conclusion

The studies presented in this dissertation assessed the geographic sustainability of biofuels produced from wastewater microalgae from the perspectives of resource demands, life cycle climate change impacts, and land use change impacts. Biofuels from wastewater microalgae can be more sustainable than petroleum fuels depending on the geographic factors.

The results show that there is a tradeoff between urban and rural environments in water and land availability for algal cultivation in wastewater effluent. For HTL of wastewater microalgae, the sites of algae cultivation and hydrothermal liquefaction should ideally be collocated to avoid substantial environmental impacts from transporting the wet feedstock. To overcome obstacles in resource availability, transportation, and operations, microalgae cultivation and conversion to biocrude could be implemented in regional clusters of high-flow WWTPs where land, water, infrastructure, and labor could be shared and transportation logistics streamlined.

The results show that even in two regions with similar climatic variables affecting algal growth, the differences in original land conditions can lead to different conclusions on whether algal renewable gasoline has lower life cycle climate change impacts than conventional gasoline. The inclusion of LUC impacts increases the uncertainty of the LCA results, as shown from the Monte Carlo analyses for each ecoregion. To ensure the sustainability of algal biofuel feedstocks, finer scale data on the prospective site should be collected and analyzed in the geographically sensitive LCA model developed for this study.

The significance of geographic factors to the sustainability of algal biofuels, from collocated resource availability, transportation distances, and land use change impacts, suggests that future policy and best management practices regarding algal biofuel production should take note of these aspects which vary regionally.

References

1. Winzer, C., Conceptualizing energy security. *Energy Policy* **2012,** *46*, (0), 36-48.
2. Andrews, C. J., Energy security as a rationale for governmental action. *Technology and Society Magazine, IEEE* **2005,** *24*, (2), 16-25.
3. Bohi, D. R.; Toman, M. A., Energy security: externalities and policies. *Energy Policy* **1993,** *21*, (11), 1093-1109.
4. Bang, G., Energy security and climate change concerns: Triggers for energy policy change in the United States? *Energy Policy* **2010,** *38*, (4), 1645-1653.
5. Klein, R. J. T.; Huq, S.; Denton, F.; Downing, T. E.; Richels, R. G.; Robinson, J. B.; Toth, F. L., Inter-relationships between adaptation and mitigation. In *Climate Change 2007: Impacts, Adaptation and Vulnerability. Contribution of Working Group II to the Fourth Assessment Report of the Intergovernmental Panel on Climate Change*, Parry, M. L.; Canziani, O. F.; Palutikof, J. P.; van der Linden, P. J.; Hanson, C. E., Eds. Cambridge University Press: Cambridge, UK, 2007.
6. Sheehan, J.; Dunahay, T. J.; Benemann, J.; Roessler, P., A look back at the U.S. Department of Energy's Aquatic Species Program: Biodiesel from algae. In Laboratory, N. R. E., Ed. Golden, CO, 1998.
7. US DOE *National Algal Biofuels Technology Roadmap*; College Park, MD, 2010.
8. United States 110th Congress *Energy Independence and Security Act of 2007*; United States, 2007.
9. Greene, D. L., Measuring energy security: Can the United States achieve oil independence? *Energy Policy* **2010,** *38*, (4), 1614-1621.
10. Madrigal, A., *Powering the dream: the history and promise of green technology*. Da Capo Press: Cambridge, MA, 2011.
11. US EIA Short-Term Energy Outlook: Real Prices Viewer. http://www.eia.gov/forecasts/steo/realprices/
12. Kebede-Westhead, E.; Pizarro, C.; Mulbry, W. W.; Wilkie, A. C., Production and nutrient removal by periphyton grown under different loading rates of anaerobically digested flushed dairy manure. *Journal of Phycology* **2003,** *39*, (6), 1275-1282.
13. Wilkie, A. C.; Mulbry, W. W., Recovery of dairy manure nutrients by benthic freshwater algae. *Bioresource Technology* **2002,** *84*, (1), 81-91.
14. Nurdogan, Y.; Oswald, W. J., Enhanced nutrient removal in high-rate ponds. *Water Science and Technology* **1995,** *31*, (12), 33-43.
15. Yun, Y.-S.; Lee, S. B.; Park, J. M.; Lee, C.-I.; Yang, J.-W., Carbon dioxide fixation by algal cultivation using wastewater nutrients. *Journal of Chemical Technology and Biotechnology* **1997,** *69*, 451-455.
16. Joseph, V.; Joseph, A., Algae in the assessment of industrial wastewater holding ponds - A case study of an oil refinery. *Water Air Soil Pollut.* **2001,** *132*, (3-4), 251-261.
17. Valderrama, L. T.; Del Campo, C. M.; Rodriguez, C. M.; de- Bashan, L. E.; Bashan, Y., Treatment of recalcitrant wastewater from ethanol and citric acid production using the microalga Chlorella vulgaris and the macrophyte Lemna minuscula. *Water Res.* **2002,** *36*, (17), 4185-4192.
18. Kadam, K. L., Power plant flue gas as a source of CO2 for microalgae cultivation: Economic impact of different process options. *Energy Conversion and Management* **1997,** *38*, (Supplemental), S505-S510.
19. Chisti, Y., Biodiesel from microalgae. *Biotechnology Advances* **2007,** *25*, (3), 294-306.

20. Patzek, T. W., Thermodynamics of the Corn-Ethanol Biofuel Cycle. *Critical Reviews in Plant Sciences* **2004,** *23*, (6), 519-567.
21. Searchinger, T.; Heimlich, R.; Houghton, R. A.; Dong, F.; Elobeid, A.; Fabiosa, J.; Tokgoz, S.; Hayes, D.; Yu, T.-H., Use of U.S. Croplands for Biofuels Increases Greenhouse Gases Through Emissions from Land-Use Change. *Science* **2008,** *319*, (5867), 1238-1240.
22. Donner, S. D.; Kucharik, C. J.; Foley, J. A., Impact of changing land use practices on nitrate export by the Mississippi River. *Global Biogeochem. Cycles* **2004,** *18*, (1), GB1028.
23. Donner, S. D.; Kucharik, C. J., Corn-based ethanol production compromises goal of reducing nitrogen export by the Mississippi River. *Proceedings of the National Academy of Sciences* **2008,** *105*, (11), 4513-4518.
24. Crutzen, P. J.; Mosier, A. R.; Smith, K. A.; Winiwarter, W., N2O release from agro-biofuel production negates global warming reduction by replacing fossil fuels. *Atmospheric Chemistry and Physics* **2008,** *8*, 389-395.
25. Fagerstone, K. D.; Quinn, J. C.; Bradley, T. H.; De Long, S. K.; Marchese, A. J., Quantitative Measurement of Direct Nitrous Oxide Emissions from Microalgae Cultivation. *Environmental Science & Technology* **2011,** *45*, (21), 9449-9456.
26. Pimentel, D., Ethanol Fuels: Energy Balance, Economics, and Environmental Impacts Are Negative. *Natural Resources Research* **2003,** *12*, (2), 127-134.
27. Dominguez-Faus, R.; Powers, S. E.; Burken, J. G.; Alvarez, P. J., The Water Footprint of Biofuels: A Drink or Drive Issue? *Environmental Science & Technology* **2009,** *43*, (9), 3005-3010.
28. King, C. W.; Webber, M. E., Water Intensity of Transportation. *Environmental Science & Technology* **2008,** *42*, (21), 7866-7872.
29. Chiu, Y.-W.; Walseth, B.; Suh, S., Water Embodied in Bioethanol in the United States. *Environmental Science & Technology* **2009,** *43*, (8), 2688-2692.
30. US EPA *Regulatory Impact Analysis: Renewable Fuel Standard Program*; United States Environmental Protection Agency,: 2007.
31. Los Alamos National Laboratory Mission: Energy Security. http://lanl.gov/mission/energy-security.php
32. Sandia National Laboratories About Sandia. http://www.sandia.gov/about/index.html
33. Argonne National Laboratory About Argonne. http://www.anl.gov/about-argonne
34. Pacific Northwest National Laboratory About PNNL: PNNL Mission, Vision, Values. http://www.pnnl.gov/about/mission.asp
35. National Renewable Energy Laboratory About NREL: Overview. http://www.nrel.gov/about/overview.html
36. US DOE Mission: Department of Energy. http://energy.gov/mission
37. US EPA Life Cycle Assessment (LCA). http://www.epa.gov/nrmrl/std/lca/lca.html
38. Bare, J. C.; Norris, G. A.; Pennington, D. W.; McKone, T., TRACI: The tool for the reduction and assessment of chemical and other environmental impacts. *Journal of Industrial Ecology* **2003,** *6*, (3-4), 49-78.
39. Frank, E. D.; Han, J.; Palou-Rivera, I.; Elgowainy, A.; Wang, M. Q. *Life-Cycle Analysis of Algal Lipid Fuels with the GREET Model*; 2011.
40. Aresta, M.; Dibenedetto, A.; Barberio, G., Utilization of macro-algae for enhanced CO2 fixation and biofuels production: Development of a computing software for an LCA study. *Fuel Processing Technology* **2005,** *86*, (14-15), 1679-1693.
41. Lardon, L.; Helias, A.; Sialve, B.; Steyer, J.-P.; Bernard, O., Life-cycle assessment of biodiesel production from microalgae. *Environmental Science and Technology* **2009,** *43*, (17), 6475-6481.

42. Batan, L.; Quinn, J.; Willson, B.; Bradley, T., Net Energy and Greenhouse Gas Emission Evaluation of Biodiesel Derived from Microalgae. *Environmental Science & Technology* **2010,** *44*, (20), 7975-7980.
43. Clarens, A. F.; Resurreccion, E. P.; White, M. A.; Colosi, L. M., Environmental Life Cycle Comparison of Algae to Other Bioenergy Feedstocks. *Environmental Science & Technology* **2010,** *44*, (5), 1813-1819.
44. Jorquera, O.; Kiperstok, A.; Sales, E. A.; Embirucu, M.; Ghirardi, M. L., Comparative energy life-cycle analyses of microalgal biomass production in open ponds and photobioreactors. *Bioresource Technology* **2010,** *101*, (4), 1406-1413.
45. Sander, K.; Murthy, G. S., Life cycle analysis of algae biodiesel. *International Journal of Life Cycle Assessment* **2010,** *15*, (7), 704-714.
46. Stephenson, A. L.; Kazamia, E.; Dennis, J. S.; Howe, C. J.; Scott, S. A.; Smith, A. G., Life-Cycle Assessment of Potential Algal Biodiesel Production in the United Kingdom: A Comparison of Raceways and Air-Lift Tubular Bioreactors. *Energy & Fuels* **2010,** *24*, 4062-4077.
47. Brentner, L. B.; Eckelman, M. J.; Zimmerman, J. B., Combinatorial life cycle assessment to inform process design of industrial production of algal biodiesel. *Environmental Science & Technology* **2011,** *45*, (16), 7060-7067.
48. Campbell, P. K.; Beer, T.; Batten, D., Life cycle assessment of biodiesel production from microalgae in ponds. *Bioresource Technology* **2011,** *102*, (1), 50-56.
49. Collet, P.; Hélias, A.; Lardon, L.; Ras, M.; Goy, R.-A.; Steyer, J.-P., Life-cycle assessment of microalgae culture coupled to biogas production. *Bioresource Technology* **2011,** *102*, (1), 207-214.
50. Khoo, H. H.; Sharratt, P. N.; Das, P.; Balasubramanian, R. K.; Naraharisetti, P. K.; Shaik, S., Life cycle energy and CO2 analysis of microalgae-to-biodiesel: Preliminary results and comparisons. *Bioresource Technology* **2011,** *102*, (10), 5800-5807.
51. Razon, L. F.; Tan, R. R., Net energy analysis of the production of biodiesel and biogas from the microalgae: Haematococcus pluvialis and Nannochloropsis. *Applied Energy* **2011,** *88*, (10), 3507-3514.
52. Shirvani, T.; Yan, X.; Inderwildi, O. R.; Edwards, P. P.; King, D. A., Life cycle energy and greenhouse gas analysis for algae-derived biodiesel. *Energy & Environmental Science* **2011,** *4*, (10), 3773-3778.
53. Soratana, K.; Landis, A. E., Evaluating industrial symbiosis and algae cultivation from a life cycle perspective. *Bioresource Technology* **2011,** *102*, (13), 6892-6901.
54. Yang, J.; Xu, M.; Zhang, X.; Hu, Q.; Sommerfeld, M.; Chen, Y., Life-cycle analysis on biodiesel production from microalgae: Water footprint and nutrients balance. *Bioresource Technology* **2011,** *102*, 159-165.
55. Clarens, A. F.; Nassau, H.; Resurreccion, E. P.; White, M. A.; Colosi, L. M., Environmental Impacts of Algae-Derived Biodiesel and Bioelectricity for Transportation. *Environmental Science & Technology* **2011,** *45*, (17), 7554-7560.
56. Rickman, M.; Pellegrino, J.; Hock, J.; Shaw, S.; Freeman, B., Life-cycle and techno-economic analysis of utility-connected algae systems. *Algal Research* **2013,** *2*, (1), 59-65.
57. Taylor, B.; Xiao, N.; Sikorski, J.; Yong, M.; Harris, T.; Helme, T.; Smallbone, A.; Bhave, A.; Kraft, M., Techno-economic assessment of carbon-negative algal biodiesel for transport solutions. *Applied Energy* **2013,** *106*, (0), 262-274.
58. Delrue, F.; Li-Beisson, Y.; Setier, P. A.; Sahut, C.; Roubaud, A.; Froment, A. K.; Peltier, G., Comparison of various microalgae liquid biofuel production pathways based on energetic, economic and environmental criteria. *Bioresource Technology* **2013,** *136*, (0), 205-212.

59. Atsonios, K.; Kougioumtzis, M.-A.; D. Panopoulos, K.; Kakaras, E., Alternative thermochemical routes for aviation biofuels via alcohols synthesis: Process modeling, techno-economic assessment and comparison. *Applied Energy* **2015,** *138*, (0), 346-366.
60. Ou, L.; Thilakaratne, R.; Brown, R. C.; Wright, M. M., Techno-economic analysis of transportation fuels from defatted microalgae via hydrothermal liquefaction and hydroprocessing. *Biomass and Bioenergy* **2015,** *72*, (0), 45-54.
61. Davis, R.; Aden, A.; Pienkos, P. T., Techno-economic analysis of autotrophic microalgae for fuel production. *Applied Energy* **2011,** *88*, (10), 3524-3531.
62. Pate, R.; Klise, G.; Wu, B., Resource demand implications for US algae biofuels production scale-up. *Applied Energy* **2011,** *88*, (10), 3377-3388.
63. Murphy, C. F.; Allen, D. T., Energy-Water Nexus for Mass Cultivation of Algae. *Environmental Science & Technology* **2011,** *45*, (13), 5861-5868.
64. Quinn, J.; Catton, K.; Wagner, N.; Bradley, T., Current Large-Scale US Biofuel Potential from Microalgae Cultivated in Photobioreactors. *Bioenergy Research* **2012,** *5*, (1), 49-60.
65. Wigmosta, M. S.; Coleman, A. M.; Skaggs, R. J.; Huesemann, M. H.; Lane, L. J., National microalgae biofuel production potential and resource demand. *Water Resources Research* **2011,** *47*.
66. Venteris, E. R.; Skaggs, R. L.; Coleman, A. M.; Wigmosta, M. S., An assessment of land availability and price in the coterminous United States for conversion to algal biofuel production. *Biomass and Bioenergy*, (0).
67. Lundquist, T.; Woertz, I.; Quinn, N.; Benemann, J. R., A realistic technology and engineering assessment of algae biofuel production. *Energy Biosciences Institute* **2010**, 1.
68. Sun, A.; Davis, R.; Starbuck, M.; Ben-Amotz, A.; Pate, R.; Pienkos, P. T., Comparative cost analysis of algal oil production for biofuels. *Energy* **2011,** *36*, (8), 5169-5179.
69. Fortier, M.-O. P.; Sturm, B. S. M., Geographic Analysis of the Feasibility of Collocating Algal Biomass Production with Wastewater Treatment Plants. *Environmental Science & Technology* **2012,** *46*, (20), 11426-11434.
70. Quinn, J.; Catton, K.; Johnson, S.; Bradley, T., Geographical Assessment of Microalgae Biofuels Potential Incorporating Resource Availability. *Bioenergy Research* **2013,** *6*, (2), 591-600.
71. Venteris, E. R.; Skaggs, R. L.; Coleman, A. M.; Wigmosta, M. S., An assessment of land availability and price in the coterminous United States for conversion to algal biofuel production. *Biomass and Bioenergy* **2012,** *47*, (0), 483-497.
72. Venteris, E. R.; Skaggs, R. L.; Coleman, A. M.; Wigmosta, M. S., A GIS Cost Model to Assess the Availability of Freshwater, Seawater, and Saline Groundwater for Algal Biofuel Production in the United States. *Environmental Science & Technology* **2013,** *47*, (9), 4840-4849.
73. Venteris, E. R.; Skaggs, R. L.; Wigmosta, M. S.; Coleman, A. M., A national-scale comparison of resource and nutrient demands for algae-based biofuel production by lipid extraction and hydrothermal liquefaction. *Biomass and Bioenergy*, (0).
74. Venteris, E. R.; Skaggs, R. L.; Wigmosta, M. S.; Coleman, A. M., Regional algal biofuel production potential in the coterminous United States as affected by resource availability trade-offs. *Algal Research*, (0).
75. Venteris, E. R.; McBride, R. C.; Coleman, A. M.; Skaggs, R. L.; Wigmosta, M. S., Siting algae cultivation facilities for biofuel production in the United States- tradeoffs between growth rate, site constructability, water availability, and infrastructure. *Environmental Science & Technology* **2014**.

76. Orfield, N. D.; Keoleian, G. A.; Love, N. G., A GIS based national assessment of algal bio-oil production potential through flue gas and wastewater co-utilization. *Biomass and Bioenergy*, (0).
77. Amer, L.; Adhikari, B.; Pellegrino, J., Technoeconomic analysis of five microalgae-to-biofuels processes of varying complexity. *Bioresource Technology* **2011,** *102*, (20), 9350-9359.
78. National Research Council, *Sustainable Development of Algal Biofuels*. The National Academies Press: 2012.
79. McKone, T.; Nazaroff, W.; Berck, P.; Auffhammer, M.; Lipman, T.; Torn, M.; Masanet, E.; Lobscheid, A.; Santero, N.; Mishra, U., Grand challenges for life-cycle assessment of biofuels. *Environmental Science & Technology* **2011,** *45*, (5), 1751-1756.
80. Sturm, B. S. M.; Peltier, E.; Smith, V.; deNoyelles, F., Controls of microalgal biomass and lipid production in municipal wastewater-fed bioreactors. *Environmental Progress & Sustainable Energy* **2012,** *31*, (1), 10-16.
81. Woertz, I.; Feffer, A.; Lundquist, T.; Nelson, Y., Algae grown on dairy and municipal wastewater for simultaneous nutrient removal and lipid production for biofuel feedstock. *Journal of Environmental Engineering* **2009,** *135*, (11), 1115-1122.
82. Chinnasamy, S.; Bhatnagar, A.; Hunt, R. W.; Das, K. C., Microalgae cultivation in a wastewater dominated by carpet mill effluents for biofuel applications. *Bioresource Technology* **2010,** *101*, (9), 3097-3105.
83. Singh, M.; Reynolds, D. L.; Das, K. C., Microalgal system for treatment of effluent from poultry litter anaerobic digestion. *Bioresource Technology* **2011,** *102*, (23), 10841-10848.
84. Energy Independence and Security Act of 2007. In United States, 2007.
85. Mitsch, W. J.; Day, J. W.; Gilliam, J. W.; Groffman, P. M.; Hey, D. L.; Randall, G. W.; Wang, N., Reducing Nitrogen Loading to the Gulf of Mexico from the Mississippi River Basin: Strategies to Counter a Persistent Ecological Problem. *BioScience* **2001,** *51*, (5), 373-388.
86. Sturm, B. S. M.; Lamer, S. L. In *Wastewater nutrient removal and algal biomass production - an energy evaluation*, Water Environment Federation Energy and Water, Chicago, IL, 2011; Chicago, IL, 2011.
87. United States Environmental Protection Agency (US EPA), Clean Watersheds Needs Survey 2008 Report to Congress. In US EPA, Office of Water Management: Washington, D.C., 2008.
88. US Census Bureau; Geography Division, UA/UC Census 2000 Boundary Files. In 2002.
89. Sturm, B. S. M.; Lamer, S. L., An energy evaluation of coupling nutrient removal from wastewater with algal biomass production. *Applied Energy* **2011,** *88*, (10), 3499-3506.
90. Quinn, J.; Catton, K.; Wagner, N.; Bradley, T., Current Large-Scale US Biofuel Potential from Microalgae Cultivated in Photobioreactors. *Bioenergy Research*, 1-12.
91. Weyer, K. M.; Bush, D. R.; Darzins, A.; Willson, B. D., Theoretical Maximum Algal Oil Production. *Bioenergy Research* **2010,** *3*, (2), 204-213.
92. United States Energy Information Administration (US EIA) *Kansas Prime Supplier Sales Volumes of Petroleum Products*; Washington, D.C., 2011.
93. Kansas Department of Health and Environment Technical Services Section, Industrial and Municipal Wastewater Discharges. In Kansas Department of Health & Environment, Ed. 2012.
94. Stumm, W.; Morgan, J.; Dreyer, J., *Aquatic Chemistry*. 3rd ed.; Wiley: New York, 1996.
95. United States Department of Agriculture (USDA); Farm Services Agency (FSA) National Agricultural Imagery Program. www.kansasgis.org (April 4, 2011),
96. United States Department of Energy (US DOE) *National Algal Biofuels Technology Roadmap*; College Park, MD, 2010.

97. Kansas Applied Remote Sensing, K. B. S., University of Kansas,, 2005 Kansas Land Cover Patterns, Level I. In Lawrence, KS, 2005.
98. Kansas Department of Agriculture, D. o. W. R., Subbasin Water Resources Management Program, Potential Net Evaporation, in Inches, for Kansas. In Kansas Department of Agriculture, Division of Water Resources, Subbasin Water Resources Management Program: 1996.
99. Siegrist, H.; Hunziker, W.; Hofer, H., Anaerobic digestion of slaughterhouse waste with UF-membrane separation and recycling of permeate CD after free ammonia stripping. *Water Science and Technology* **2005,** *52*, (1-2), 531-536.
100. Raposo, M. F. D.; Oliveira, S. E.; Castro, P. M.; Bandarra, N. M.; Morais, R. M., On the Utilization of Microalgae for Brewery Effluent Treatment and Possible Applications of the Produced Biomass. *J. Inst. Brew.* **2010,** *116*, (3), 285-292.
101. Pant, D.; Adholeya, A., Biological approaches for treatment of distillery wastewater: A review. *Bioresource Technology* **2007,** *98*, (12), 2321-2334.
102. Pagand, P.; Blancheton, J. P.; Lemoalle, J.; Casellas, C., The use of high rate algal ponds for the treatment of marine effluent from a recirculating fish rearing system. *Aquac. Res.* **2000,** *31*, (10), 729-736.
103. Brown, J. J.; Glenn, E. P.; Fitzsimmons, K. M.; Smith, S. E., Halophytes for the treatment of saline aquaculture effluent. *Aquaculture* **1999,** *175*, (3–4), 255-268.
104. Gonzalez, C.; Marciniak, J.; Villaverde, S.; Leon, C.; Garcia, P. A.; Munoz, R., Efficient nutrient removal from swine manure in a tubular biofilm photo-bioreactor using algae-bacteria consortia. *Water Science and Technology* **2008,** *58*, (1), 95-102.
105. An, J. Y.; Sim, S. J.; Lee, J. S.; Kim, B. W., Hydrocarbon production from secondarily treated piggery wastewater by the green alga Botryococcus braunii. *Journal of Applied Phycology* **2003,** *15*, (2-3), 185-191.
106. Sialve, B.; Bernet, N.; Bernard, O., Anaerobic digestion of microalgae as a necessary step to make microalgal biodiesel sustainable. *Biotechnology Advances* **2009,** *27*, (4), 409-416.
107. Zhou, Y.; Schideman, L.; Zhang, Y.; Yu, G.; Wang, Z.; Pham, M., Resolving bottlenecks in current algal wastewater treatment paradigms: a synergistic combination of low-lipid algal wastewater treatment and hydrothermal liquefaction for large-scale biofuel production. In *Energy and Water*, Water Environment Federation: Chicago, Illinois, 2011; pp 347-361.
108. Alba, L. G.; Torri, C.; Samori, C.; van der Spek, J.; Fabbri, D.; Kersten, S. R. A.; Brilman, D. W. F., Hydrothermal Treatment (HIT) of Microalgae: Evaluation of the Process As Conversion Method in an Algae Biorefinery Concept. *Energy & Fuels* **2012,** *26*, (1), 642-657.
109. Yu, G.; Zhang, Y. H.; Schideman, L.; Funk, T.; Wang, Z. C., Distributions of carbon and nitrogen in the products from hydrothermal liquefaction of low-lipid microalgae. *Energy & Environmental Science* **2011,** *4*, (11), 4587-4595.
110. Jena, U.; Vaidyanathan, N.; Chinnasamy, S.; Das, K. C., Evaluation of microalgae cultivation using recovered aqueous co-product from thermochemical liquefaction of algal biomass. *Bioresource Technology* **2011,** *102*, (3), 3380-3387.
111. United States Department of Agriculture (USDA); National Agricultural Statistics Service (NASS); Kansas Field Office *Agricultural Land Values & Cash Rents*; 2011.
112. Kansas Land Brokers LLC Kansas Land Market: Average Per Acre Price Sold. http://kansaslandowner.com/channels/regional_localism/topics/kansas_land_market_-_average_per_acre_price_sold
113. International Air Transport Association (IATA) *A Global Approach to Reducing Aviation Emissions*; Geneva, Switzerland, 2009.
114. United States Energy Information Administration U.S. Product Supplied of Kerosene-Type Jet Fuel http://www.eia.gov/dnav/pet/hist/LeafHandler.ashx?n=PET&s=MKJUPUS1&f=A

115. AllAboutAlgae.com, A. B. O. Algae Fuels: Renewable Aviation Fuel. http://allaboutalgae.com/aviation-fuel/
116. ASTM, ASTM Standard D7566: Specification for Aviation Turbine Fuel Containing Synthesized Hydrocarbons. In West Conshohocken, PA, 2011.
117. Sturm, B. S. M.; Peltier, E.; Smith, V.; deNoyelles, F., Controls of microalgal biomass and lipid production in municipal wastewater-fed bioreactors. *Environmental Progress & Sustainable Energy* **2012,** *31*, (1), 10-16.
118. Roberts, G. W.; Fortier, M.-O. P.; Sturm, B. S. M.; Stagg-Williams, S. M., Promising Pathway for Algal Biofuels through Wastewater Cultivation and Hydrothermal Conversion. *Energy & Fuels* **2013,** *27*, (2), 857-867.
119. Vasudevan, V.; Stratton, R. W.; Pearlson, M. N.; Jersey, G. R.; Beyene, A. G.; Weissman, J. C.; Rubino, M.; Hileman, J. I., Environmental Performance of Algal Biofuel Technology Options. *Environmental Science & Technology* **2012,** *46*, (4), 2451-2459.
120. Woertz, I.; Feffer, A.; Lundquist, T.; Nelson, Y., Algae Grown on Dairy and Municipal Wastewater for Simultaneous Nutrient Removal and Lipid Production for Biofuel Feedstock. *Journal of Environmental Engineering-Asce* **2009,** *135*, (11), 1115-1122.
121. Toor, S. S.; Rosendahl, L.; Rudolf, A., Hydrothermal liquefaction of biomass: A review of subcritical water technologies. *Energy* **2011,** *36*, (5), 2328-2342.
122. Akhtar, J.; Amin, N. A. S., A review on process conditions for optimum bio-oil yield in hydrothermal liquefaction of biomass. *Renewable and Sustainable Energy Reviews* **2011,** *15*, (3), 1615-1624.
123. Biller, P.; Ross, A. B., Potential yields and properties of oil from the hydrothermal liquefaction of microalgae with different biochemical content. *Bioresource Technology* **2011,** *102*, (1), 215-225.
124. Garcia Alba, L.; Torri, C.; Samorì, C.; van der Spek, J.; Fabbri, D.; Kersten, S. R. A.; Brilman, D. W. F., Hydrothermal Treatment (HTT) of Microalgae: Evaluation of the Process As Conversion Method in an Algae Biorefinery Concept. *Energy & Fuels* **2011**, 111201165948002.
125. Jena, U.; Das, K. C.; Kastner, J. R., Effect of operating conditions of thermochemical liquefaction on biocrude production from Spirulina platensis. *Bioresource Technology* **2011,** *102*, (10), 6221-6229.
126. Brown, T. M.; Duan, P.; Savage, P. E., Hydrothermal Liquefaction and Gasification of Nannochloropsis sp. *Energy & Fuels* **2010,** *24*, (6), 3639-3646.
127. Valdez, P. J.; Dickinson, J. G.; Savage, P. E., Characterization of Product Fractions from Hydrothermal Liquefaction ofNannochloropsissp. and the Influence of Solvents. *Energy & Fuels* **2011,** *25*, (7), 3235-3243.
128. Demirbas, M. F., Biofuels from algae for sustainable development. *Applied Energy* **2011,** *88*, (10), 3473-3480.
129. Anastasakis, K.; Ross, A. B., Hydrothermal liquefaction of the brown macro-alga Laminaria Saccharina: Effect of reaction conditions on product distribution and composition. *Bioresource Technology* **2011,** *102*, (7), 4876-4883.
130. Zhou, D.; Zhang, L.; Zhang, S.; Fu, H.; Chen, J., Hydrothermal Liquefaction of Macroalgae Enteromorpha prolifera to Bio-oil. *Energy & Fuels* **2010,** *24*, (7), 4054-4061.
131. Shuping, Z.; Yulong, W.; Mingde, Y.; Kaleem, I.; Chun, L.; Tong, J., Production and characterization of bio-oil from hydrothermal liquefaction of microalgae Dunaliella tertiolecta cake. *Energy* **2010,** *35*, (12), 5406-5411.
132. Ross, A. B.; Biller, P.; Kubacki, M. L.; Li, H.; Lea-Langton, A.; Jones, J. M., Hydrothermal processing of microalgae using alkali and organic acids. *Fuel* **2010,** *89*, (9), 2234-2243.

133. Minowa, T.; Yokoyama, S.-y.; Kishimoto, M.; Okakura, T., Oil production from algal cells of Dunaliella tertiolecta by direct thermochemical liquefaction. *Fuel* **1995,** *74*, (12), 1735-1738.
134. Biller, P.; Ross, A. B.; Skill, S. C.; Lea-Langton, A.; Balasundaram, B.; Hall, C.; Riley, R.; Llewellyn, C. A., Nutrient recycling of aqueous phase for microalgae cultivation from the hydrothermal liquefaction process. *Algal Research* **2012,** *1*, (1), 70-76.
135. Sills, D. L.; Paramita, V.; Franke, M. J.; Johnson, M. C.; Akabas, T. M.; Greene, C. H.; Tester, J. W., Quantitative Uncertainty Analysis of Life Cycle Assessment for Algal Biofuel Production. *Environmental Science & Technology* **2012,** *47*, (2), 687-694.
136. Baliga, R.; Powers, S. E., Sustainable Algae Biodiesel Production in Cold Climates. *International Journal of Chemical Engineering (1687806X)* **2010**, 1-13.
137. Chowdhury, R.; Viamajala, S.; Gerlach, R., Reduction of environmental and energy footprint of microalgal biodiesel production through material and energy integration. *Bioresource Technology* **2012,** *108*, (0), 102-111.
138. Grierson, S.; Strezov, V.; Bengtsson, J., Life cycle assessment of a microalgae biomass cultivation, bio-oil extraction and pyrolysis processing regime. *Algal Research* **2013,** *2*, (3), 299-311.
139. Liu, X.; Saydah, B.; Eranki, P.; Colosi, L. M.; Greg Mitchell, B.; Rhodes, J.; Clarens, A. F., Pilot-scale data provide enhanced estimates of the life cycle energy and emissions profile of algae biofuels produced via hydrothermal liquefaction. *Bioresource Technology* **2013,** *148*, (0), 163-171.
140. Hileman, J. I.; Stratton, R. W.; Donohoo, P. E., Energy content and alternative jet fuel viability. *Journal of Propulsion and Power* **2010,** *26*, (Compendex), 1184-1195.
141. Bare, J., TRACI 2.0: the tool for the reduction and assessment of chemical and other environmental impacts 2.0. *Clean Techn Environ Policy* **2011,** *13*, (5), 687-696.
142. Skone, T. J.; Gerdes, K. *Development of Baseline Data and Analysis of Life Cycle Greenhouse Gas Emissions of Petroleum-Based Fuels*; National Energy Technology Laboratory, Department of Energy: 2008.
143. Duan, P.; Savage, P. E., Hydrothermal Liquefaction of a Microalga with Heterogeneous Catalysts. *Industrial & Engineering Chemistry Research* **2010,** *50*, (1), 52-61.
144. Matar, S.; Hatch, L. F., *Chemistry of petrochemical processes*. Gulf Professional Publishing: 2001.
145. United States Energy Information Administration *Refinery Capacity Report 2011*; Washington, DC, 2011.
146. Jena, U.; Das, K. C., Comparative Evaluation of Thermochemical Liquefaction and Pyrolysis for Bio-Oil Production from Microalgae. *Energy & Fuels* **2011,** *25*, (11), 5472-5482.
147. Vardon, D. R.; Sharma, B. K.; Scott, J.; Yu, G.; Wang, Z. C.; Schideman, L.; Zhang, Y. H.; Strathmann, T. J., Chemical properties of biocrude oil from the hydrothermal liquefaction of Spirulina algae, swine manure, and digested anaerobic sludge. *Bioresource Technology* **2011,** *102*, (17), 8295-8303.
148. Matsui, T.-o.; Nishihara, A.; Ueda, C.; Ohtsuki, M.; Ikenaga, N.-o.; Suzuki, T., Liquefaction of micro-algae with iron catalyst. *Fuel* **1997,** *76*, (11), 1043-1048.
149. Valdez, P. J.; Dickinson, J. G.; Savage, P. E., Characterization of Product Fractions from Hydrothermal Liquefaction of Nannochloropsis sp and the Influence of Solvents. *Energy & Fuels* **2011,** *25*, (7), 3235-3243.
150. Toor, S. S.; Reddy, H.; Deng, S.; Hoffmann, J.; Spangsmark, D.; Madsen, L. B.; Holm-Nielsen, J. B.; Rosendahl, L. A., Hydrothermal liquefaction of Spirulina and Nannochloropsis

salina under subcritical and supercritical water conditions. *Bioresource Technology* **2013,** *131*, (0), 413-419.
151. Williams, P. J. l. B.; Laurens, L. M. L., Microalgae as biodiesel & biomass feedstocks: Review & analysis of the biochemistry, energetics & economics. *Energy & Environmental Science* **2010,** *3*, (5), 554-590.
152. Dote, Y.; Sawayama, S.; Inoue, S.; Minowa, T.; Yokoyama, S.-y., Recovery of liquid fuel from hydrocarbon-rich microalgae by thermochemical liquefaction. *Fuel* **1994,** *73*, (12), 1855-1857.
153. Yang, Y. F.; Feng, C. P.; Inamori, Y.; Maekawa, T., Analysis of energy conversion characteristics in liquefaction of algae. *Resources Conservation and Recycling* **2004,** *43*, (1), 21-33.
154. United States Department of Transportation (US DOT); Research and Innovative Technology Administration (RITA) National Transportation Atlas Database: Public-Use Airports. http://apps.bts.gov/publications/national_transportation_atlas_database/2011/
155. Gary, J. H.; Handwerk, G. E., *Petroleum Refining: Technology and Economics*. 4th ed.; Marcel Dekker: New York, NY, 2001.
156. Kadam, K. L., Environmental implications of power generation via coal-microalgae cofiring. *Energy* **2002,** *27*, (10), 905-922.
157. Stratton, R. W.; Wong, H. M.; Hileman, J. I. *Life Cycle Greenhouse Gas Emissions from Alternative Jet Fuels*; Massachusetts Institute of Technology: Cambridge, MA, 2010.
158. Spath, P. L.; Mann, M. K. *Life Cycle Assessment of Hydrogen Production via Natural Gas Steam Reforming*; National Renewable Energy Laboratory,: Golden, CO, 2001.
159. Cetinkaya, E.; Dincer, I.; Naterer, G. F., Life cycle assessment of various hydrogen production methods. *International Journal of Hydrogen Energy* **2012,** *37*, (3), 2071-2080.
160. Koroneos, C.; Dompros, A.; Roumbas, G., Hydrogen production via biomass gasification—A life cycle assessment approach. *Chemical Engineering and Processing: Process Intensification* **2008,** *47*, (8), 1261-1268.
161. Ozbilen, A.; Dincer, I.; Rosen, M. A., A comparative life cycle analysis of hydrogen production via thermochemical water splitting using a Cu–Cl cycle. *International Journal of Hydrogen Energy* **2011,** *36*, (17), 11321-11327.
162. Frank, E.; Elgowainy, A.; Han, J.; Wang, Z., Life cycle comparison of hydrothermal liquefaction and lipid extraction pathways to renewable diesel from algae. *Mitigation and Adaptation Strategies for Global Change* **2012**, 1-22.
163. Stratton, R. W.; Wong, H. M.; Hileman, J. I., Quantifying Variability in Life Cycle Greenhouse Gas Inventories of Alternative Middle Distillate Transportation Fuels. *Environmental Science & Technology* **2011,** *45*, (10), 4637-4644.
164. Agusdinata, D. B.; Zhao, F.; Ileleji, K.; DeLaurentis, D., Life Cycle Assessment of Potential Biojet Fuel Production in the United States. *Environmental Science & Technology* **2011,** *45*, (21), 9133-9143.
165. Handler, R. M.; Canter, C. E.; Kalnes, T. N.; Lupton, F. S.; Kholiqov, O.; Shonnard, D. R.; Blowers, P., Evaluation of environmental impacts from microalgae cultivation in open-air raceway ponds: Analysis of the prior literature and investigation of wide variance in predicted impacts. *Algal Research* **2012,** *1*, (1), 83-92.
166. Liu, X.; Clarens, A. F.; Colosi, L. M., Algae biodiesel has potential despite inconclusive results to date. *Bioresource Technology* **2012,** *104*, (0), 803-806.
167. Shonnard, D. R.; Williams, L.; Kalnes, T. N., Camelina-derived jet fuel and diesel: Sustainable advanced biofuels. *Environmental Progress & Sustainable Energy* **2010,** *29*, (3), 382-392.

168. Bailis, R. E.; Baka, J. E., Greenhouse gas emissions and land use change from Jatropha curcas -based jet fuel in brazil. *Environmental Science and Technology* **2010,** *44*, (Compendex), 8684-8691.
169. Passell, H.; Dhaliwal, H.; Reno, M.; Wu, B.; Ben Amotz, A.; Ivry, E.; Gay, M.; Czartoski, T.; Laurin, L.; Ayer, N., Algae biodiesel life cycle assessment using current commercial data. *Journal of Environmental Management* **2013,** *129*, (0), 103-111.
170. Davis, R.; Fishman, D. B.; Frank, E. D.; Johnson, M. C.; Jones, S. B.; Kinchin, C. M.; Skaggs, R. L.; Venteris, E. R.; Wigmosta, M. S., Integrated Evaluation of Cost, Emissions, and Resource Potential for Algal Biofuels at the National Scale. *Environmental Science & Technology* **2014**.
171. Geyer, R.; Stoms, D.; Kallaos, J., Spatially-Explicit Life Cycle Assessment of Sun-to-Wheels Transportation Pathways in the U.S. *Environmental Science & Technology* **2012,** *47*, (2), 1170-1176.
172. Delucchi, M. A., Impacts of biofuels on climate change, water use, and land use. *Annals of the New York Academy of Sciences* **2010,** *1195*, (1), 28-45.
173. Elliott, J.; Sharma, B.; Best, N.; Glotter, M.; Dunn, J. B.; Foster, I.; Miguez, F.; Mueller, S.; Wang, M., A Spatial Modeling Framework to Evaluate Domestic Biofuel-Induced Potential Land Use Changes and Emissions. *Environmental Science & Technology* **2014,** *48*, (4), 2488-2496.
174. Börjesson, P.; Tufvesson, L. M., Agricultural crop-based biofuels – resource efficiency and environmental performance including direct land use changes. *Journal of Cleaner Production* **2011,** *19*, (2–3), 108-120.
175. Fargione, J.; Hill, J.; Tilman, D.; Polasky, S.; Hawthorne, P., Land Clearing and the Biofuel Carbon Debt. *Science* **2008,** *319*, (5867), 1235-1238.
176. Lindeijer, E., Review of land use impact methodologies. *Journal of Cleaner Production* **2000,** *8*, (4), 273-281.
177. Mila i Canals, L.; Bauer, C.; Depestele, J.; Dubreuil, A.; Knuchel, R. F.; Gaillard, G.; Michelsen, O.; Müller-Wenk, R.; Rydgren, B., Key elements in a framework for land use impact assessment within LCA. *International Journal of Life Cycle Assessment* **2007,** *12*, (1), 5-15.
178. Hoefnagels, R.; Smeets, E.; Faaij, A., Greenhouse gas footprints of different biofuel production systems. *Renewable and Sustainable Energy Reviews* **2010,** *14*, (7), 1661-1694.
179. Caiazzo, F.; Malina, R.; Staples, M. D.; Wolfe, P. J.; Yim, S. H. L.; Barrett, S. R. H., Quantifying the climate impacts of albedo changes due to biofuel production: a comparison with biogeochemical effects. *Environmental Research Letters* **2014,** *9*, (2), 024015.
180. Houghton, R. A.; Lawrence, K. T.; Hackler, J. L.; Brown, S., The spatial distribution of forest biomass in the Brazilian Amazon: a comparison of estimates. *Global Change Biology* **2001,** *7*, (7), 731-746.
181. Malhi, Y.; Wood, D.; Baker, T. R.; Wright, J.; Phillips, O. L.; Cochrane, T.; Meir, P.; Chave, J.; Almeida, S.; Arroyo, L.; Higuchi, N.; Killeen, T. J.; Laurance, S. G.; Laurance, W. F.; Lewis, S. L.; Monteagudo, A.; Neill, D. A.; Vargas, P. N.; Pitman, N. C. A.; Quesada, C. A.; SalomÃO, R.; Silva, J. N. M.; Lezama, A. T.; Terborgh, J.; MartÍNez, R. V.; Vinceti, B., The regional variation of aboveground live biomass in old-growth Amazonian forests. *Global Change Biology* **2006,** *12*, (7), 1107-1138.
182. Dunn, J. B.; Mueller, S.; Kwon, H.-Y.; Wander, M.; Wang, M., Carbon Calculator for Land Use Change from Biofuels Production (CCLUB) Users' Manual and Technical Documentation. In Argonne National Laboratory; U.S. Department of Energy, Eds. Oak Ridge, TN, 2013.

183. Fortier, M.-O. P.; Roberts, G. W.; Stagg-Williams, S. M.; Sturm, B. S. M., Life cycle assessment of bio-jet fuel from hydrothermal liquefaction of microalgae. *Applied Energy* **2014,** *122*, (0), 73-82.
184. Roberts, G. W.; Sturm, B. S. M.; Hamdeh, U.; Stanton, G. E.; Rocha, A.; Kinsella, T. L.; Fortier, M.-O. P.; Sazdar, S.; Detamore, M. S.; Stagg-Williams, S. M., Promoting catalysis and high-value product streams by in situ hydroxyapatite crystallization during hydrothermal liquefaction of microalgae cultivated with reclaimed nutrients. *Green Chemistry* **2015,** *17*, (4), 2560-2569.
185. Connelly, E.; Colosi, L. M.; Clarens, A. F.; Lambert, J. H., Life cycle assessment of biofuels from algae hydrothermal liquefaction: The upstream and downstream factors affecting regulatory compliance. *Energy & Fuels* **2015**.
186. Huesemann, M. H.; Hausmann, T. S.; Bartha, R.; Aksoy, M.; Weissman, J. C.; Benemann, J. R., Biomass productivities in wild type and pigment mutant of Cyclotella sp.(Diatom). *Appl Biochem Biotechnol* **2009,** *157*, (3), 507-526.
187. Kellndorfer, J.; Walker, W.; Kirsch, K.; Fiske, G.; Bishop, J.; LaPoint, L.; Hoppus, M.; Westfall, J., NACP Aboveground Biomass and Carbon Baseline Data, V. 2 (NBCD 2000). In 2 ed.; ORNL DAAC, Ed. Oak Ridge, Tennessee, USA, 2013.
188. Muñoz, I.; Campra, P.; Fernández-Alba, A., Including CO2-emission equivalence of changes in land surface albedo in life cycle assessment. Methodology and case study on greenhouse agriculture. *The International Journal of Life Cycle Assessment* **2010,** *15*, (7), 672-681.
189. Müller-Wenk, R.; Brandão, M., Climatic impact of land use in LCA—carbon transfers between vegetation/soil and air. *The International Journal of Life Cycle Assessment* **2010,** *15*, (2), 172-182.
190. West, T. O.; Brandt, C. C.; Baskaran, L. M.; Hellwinckel, C. M.; Mueller, R.; Bernacchi, C. J.; Bandaru, V.; Yang, B.; Wilson, B. S.; Marland, G.; Nelson, R. G.; Ugarte, D. G. D. L. T.; Post, W. M., Cropland carbon fluxes in the United States: increasing geospatial resolution of inventory-based carbon accounting. *Ecological Applications* **2010,** *20*, (4), 1074-1086.
191. Peckham, S. D.; Gower, S. T., Simulating the effects of harvest and biofuel production on the forest system carbon balance of the Midwest, USA. *GCB Bioenergy* **2013,** *5*, (4), 431-444.
192. Cherubini, F.; Bright, R. M.; Strømman, A. H., Site-specific global warming potentials of biogenic CO 2 for bioenergy: contributions from carbon fluxes and albedo dynamics. *Environmental Research Letters* **2012,** *7*, (4), 045902.
193. Watson, R. T.; Noble, I. R.; Bolin, B.; Ravindranath, N.; Verardo, D. J.; Dokken, D. J., *Land use, land-use change and forestry: a special report of the Intergovernmental Panel on Climate Change*. Cambridge University Press: 2000.
194. The University of Montana Numerical Terradynamic Simulation Group, MODIS Gross/Net Primary Production (GPP/NPP) (MOD17), version 55. In Missoula, MT, 2008-2010.
195. Bright, R. M.; Cherubini, F.; Strømman, A. H., Climate impacts of bioenergy: Inclusion of carbon cycle and albedo dynamics in life cycle impact assessment. *Environmental Impact Assessment Review* **2012,** *37*, (0), 2-11.
196. Schwaiger, H. P.; Bird, D. N., Integration of albedo effects caused by land use change into the climate balance: Should we still account in greenhouse gas units? *For. Ecol. Manage.* **2010,** *260*, (3), 278-286.
197. IPCC, *Climate change 2007: The physical science basis: Working group I contribution to the fourth assessment report of the Intergovernmental Panel on Climate Change*. Cambridge University Press: Cambridge, UK and New York, NY, USA, 2007; Vol. 4.

198. Betts, R. A., Offset of the potential carbon sink from boreal forestation by decreases in surface albedo. *Nature* **2000,** *408*, (6809), 187-190.
199. Myhre, G.; Highwood, E. J.; Shine, K. P.; Stordal, F., New estimates of radiative forcing due to well mixed greenhouse gases. *Geophysical research letters* **1998,** *25*, (14), 2715-2718.
200. Susca, T., Enhancement of life cycle assessment (LCA) methodology to include the effect of surface albedo on climate change: Comparing black and white roofs. *Environmental Pollution* **2012,** *163*, (0), 48-54.
201. Bird, D. N.; Kunda, M.; Mayer, A.; Schlamadinger, B.; Canella, L.; Johnston, M., Incorporating changes in albedo in estimating the climate mitigation benefits of land use change projects. *Biogeosciences Discuss.* **2008,** *5*, (2), 1511-1543.
202. Yu, B.; Lu, Q., Estimation of albedo effect in pavement life cycle assessment. *Journal of Cleaner Production* **2014,** *64*, (0), 306-309.
203. de Wit, H. A.; Bryn, A.; Hofgaard, A.; Karstensen, J.; Kvalevåg, M. M.; Peters, G. P., Climate warming feedback from mountain birch forest expansion: reduced albedo dominates carbon uptake. *Global Change Biology* **2014**, n/a-n/a.
204. Lutz, D.; Howarth, R., Valuing albedo as an ecosystem service: implications for forest management. *Climatic Change* **2014**, 1-11.
205. Ward, D. S.; Mahowald, N. M.; Kloster, S., Potential climate forcing of land use and land cover change. *Atmos. Chem. Phys. Discuss.* **2014,** *14*, (8), 12167-12234.
206. Payne, R. E., Albedo of the sea surface. *Journal of the Atmospheric Sciences* **1972,** *29*, (5), 959-970.
207. Maritorena, S. M. A. G. B., Diffuse reflectance of oceanic shallow waters: influence of water depth and bottom albedo. **1994**.
208. Land Processes Distributed Active Archive Center (LP DAAC), MCD43A3 Albedo 16-Day L3 Global 500m, version 5. In NASA EOSDIS Land Processes DAAC, USGS Earth Resources Observation and Science (EROS) Center; Sioux Falls, SD, 2008-2015.
209. Dvoracek, M. J.; Hannabas, B., Prediction of albedo for use in evapotranspiration and irrigation scheduling. In *Visions of the future: proceedings of the Third National Irrigation Symposium held in conjunction with the 11th Annual International Irrigation Exposition*, Engineers, A. S. o. A., Ed. Phoenix, AZ, 1990; pp 692-699.
210. Sumner, M. E., *Handbook of Soil Science*. Taylor & Francis: 1999.
211. Duffie, J. A.; Beckman, W. A., *Solar Engineering of Thermal Processes*. Wiley: 2013.
212. Holtsmark, B., A comparison of the global warming effects of wood fuels and fossil fuels taking albedo into account. *GCB Bioenergy* **2014**, n/a-n/a.
213. NASA LaRC POWER Project NASA Surface meteorology and Solar Energy: Interannual Variability. https://eosweb.larc.nasa.gov/cgi-bin/sse/interann.cgi (September 22),
214. Campbell, G. S.; Norman, J. M., *An Introduction to Environmental Biophysics*. Springer New York: 2012.
215. Taha, H., Urban climates and heat islands: albedo, evapotranspiration, and anthropogenic heat. *Energy and Buildings* **1997,** *25*, (2), 99-103.
216. Campra, P.; Garcia, M.; Canton, Y.; Palacios-Orueta, A., Surface temperature cooling trends and negative radiative forcing due to land use change toward greenhouse farming in southeastern Spain. *Journal of Geophysical Research: Atmospheres (1984–2012)* **2008,** *113*, (D18).
217. Quenzel, H.; Kaestner, M., Optical properties of the atmosphere: calculated variability and application to satellite remote sensing of phytoplankton. *Appl. Opt.* **1980,** *19*, (8), 1338-1344.

218. Reichardt, T. A.; Collins, A. M.; Garcia, O. F.; Ruffing, A. M.; Jones, H. D. T.; Timlin, J. A., Spectroradiometric Monitoring of Nannochloropsis salina Growth. *Algal Research* **2012,** *1*, (1), 22-31.
219. Morel, A., Optical modeling of the upper ocean in relation to its biogenous matter content (case I waters). *Journal of Geophysical Research: Oceans* **1988,** *93*, (C9), 10749-10768.
220. Babin, M.; Morel, A.; Fournier-Sicre, V.; Fell, F.; Stramski, D., Light Scattering Properties of Marine Particles in Coastal and Open Ocean Waters as Related to the Particle Mass Concentration. *Limnology and Oceanography* **2003,** *48*, (2), 843-859.
221. Morel, A.; Gentili, B., Diffuse reflectance of oceanic waters: its dependence on Sun angle as influenced by the molecular scattering contribution. *Appl. Opt.* **1991,** *30*, (30), 4427-4438.
222. Raciti, S. M.; Hutyra, L. R.; Finzi, A. C., Depleted soil carbon and nitrogen pools beneath impervious surfaces. *Environmental Pollution* **2012,** *164*, (0), 248-251.
223. Pouyat, R.; Groffman, P.; Yesilonis, I.; Hernandez, L., Soil carbon pools and fluxes in urban ecosystems. *Environmental Pollution* **2002,** *116, Supplement 1*, (0), S107-S118.
224. Quinn, J.; de Winter, L.; Bradley, T., Microalgae bulk growth model with application to industrial scale systems. *Bioresource Technology* **2011,** *102*, (8), 5083-5092.
225. Allred, B. W.; Smith, W. K.; Twidwell, D.; Haggerty, J. H.; Running, S. W.; Naugle, D. E.; Fuhlendorf, S. D., Ecosystem services lost to oil and gas in North America. *Science* **2015,** *348*, (6233), 401-402.
226. Benemann, J.; Goebel, R.; Weissman, J.; Augenstein, D. *Microalgae as a source of liquid fuels. Final technical report*; US Department of Energy, Office of Research: 1982.
227. US Geological Survey, G. A. P. G., Protected Areas Database of the United States (PAD-US), version 1.3 Combined Feature Class. In November 2012.
228. Homer, C. G., Dewitz, J.A., Yang, L., Jin, S., Danielson, P., Xian, G., Coulston, J., Herold, N.D., Wickham, J.D., and Megown, K., National Land Cover Database 2011 (NLCD 2011). In Survey, U. S. G., Ed. 2015.
229. Wilcox, S., National Solar Radiation Database 1991-2010. In Laboratory, N. R. E., Ed. Golden, CO, 2012.
230. Daly, C.; Halbleib, M.; Smith, J. I.; Gibson, W. P.; Doggett, M. K.; Taylor, G. H.; Curtis, J.; Pasteris, P. P., Physiographically sensitive mapping of climatological temperature and precipitation across the conterminous United States. *International Journal of Climatology* **2008,** *28*, (15), 2031-2064.

Appendix A: Supporting Information for "Geographic Analysis of the Feasibility of Collocating Algal Biomass Production with Wastewater Treatment Plants"[1]

Wastewater Treatment Plant (WWTP) Statistics

Table A1: Number of Kansas municipal wastewater treatment plants analyzed by radial extent

Radial extent (miles)	Number of WWTPs included in analysis
0.25	387
0.50	385
0.75	382
1.0	376
1.5	373

Table A2: Wastewater treatment plants excluded from the analysis due to radial extent crossing the Kansas state boundary

NPDES Permit Number	WWTP Name	Minimum radial extent for exclusion from analysis (miles)
KS0038563	KCK WWTP #1	0.50
KS0080683	Arcadia WWTP	0.50
KS0026158	Wathena WWTP	0.75
KS0036366	Leavenworth WWTP	0.75
KS0081698	Treece WWTP	0.75
KS0048526	Elwood WWTP	1.0
KS0039128	Atchison WWTP	1.0
KS0085600	KCK WWTP #3	1.0
KS0092738	Johnson County Blue River WWTP	1.0
KS0027481	Caney WWTP	1.0
KS0081086	Hardtner WWTP	1.0
KS0055484	Johnson Co. Tomahawk Creek WWTP	1.5
KS0087467	Mulberry WWTP	1.5
KS0025500	Summerfield WWTP	1.5

Table A3: Kansas municipal WWTPs for which available areas become merged due to close proximity. Starred plants become merged with an additional plant as the radial extent increases.

Minimum radial extent at which merging is observed (miles)	WWTP Names
0.75	Havana WWTP Montgomery County Sewer District #4 Havana Lake
0.75	*Leavenworth County Sewer District #3 *Leavenworth County Sewer District #5
1.0	Perry WWTP Lecompton WWTP
1.0	Pottawatomie County Blue Township Sewer District Manhattan WWTP
1.5	Johnson County Mill Creek Regional WWTP Bonner Springs WWTP
1.5	Haysville WWTP Wichita WWTP #1 and #2
1.5	Maize WWTP Wichita WWTP #3
1.5	Cottonwood Falls WWTP Strong City WWTP
1.5	Hillsdale WWTP Mitchell County Sewer District Walnut Creek WWTP
1.5	Lakewood Hills Jefferson County WWTP #2 Jefferson County WWTP #6 Jefferson County WWTP #7
1.5	*Leavenworth County Sewer District #3 *Leavenworth County Sewer District #5 Basehor WWTP

Table A4: Statistics on urban, near-urban, and rural WWTPs in Kansas.

	Urban	Near-urban	Rural
Number of plants	26	63	298
Minimum flow rate (MGD)	0.025	0.009	0.006
Maximum flow rate (MGD)	40.6	5.42	0.450
Average flow rate ± standard deviation (MGD)	5.72 ± 8.76	0.989 ± 1.35	0.073 ± 0.074
Average net evaporation rate ± std dev. (in/yr)	11.3 ± 8.14	13.7 ± 10.4	15.6 ± 10.7

Potential production under wastewater limitation

First, the average TN and average TP in mg/L of available data from urban, near-urban, or rural WWTPs from 2000-2011 was determined by month of production. The average N:P ratio was then calculated. Example N:P ratio calculation for production in April for urban WWTPs:

$$\frac{13.7\ mg\ N}{L} \times \frac{1\ mmol\ N}{14.01\ mg\ N} \times \frac{L}{3.09\ mg\ P} \times \frac{30.97\ mg\ P}{1\ mmol\ P} \approx 9.80$$

For an N:P ratio lower than 16, which indicates that the wastewater effluent is nitrogen-limited for algal growth, the algal biofuel production calculations were based on the nitrogen concentration. Conversely, for an N:P ratio higher than 16, the following calculations were based on the phosphorus concentration instead.

Example calculation for production in April for urban WWTPs under the BAP scenario:

$$\frac{15.86\ mg\ dry\ algae}{mg\ N} \times \frac{13.7\ mg\ N}{L} \times \frac{1000\ L}{m^3} \times \frac{1\ m^3}{264.17\ gal} \times \frac{148.8\ \times\ 10^6\ gal}{day}$$

$$\times \frac{0.1\ mg\ lipids}{mg\ dry\ algae} \times \frac{1\ kg\ lipids}{10^6\ mg\ lipids} \times \frac{1\ m^3}{918\ kg} \times \frac{264.17\ gal}{1\ m^3} \times \frac{1\ barrel}{42\ gal}$$

$$\times \frac{30\ days}{month} \times 0.75 \approx 1887\ barrels/month$$

These steps were repeated for the months of the April-October growing season, as well as for near-urban and rural WWTPs, and summed to obtain the potential production for all KS WWTPs under wastewater limitation in barrels/year for each the BAP scenario and the HAP scenario.

Potential production under land limitation

Example calculation for production under land limitation, at a radial extent of 0.25 miles and for the BAP scenario:

$$40{,}208.55\ acres\ \times 0.85 \times \frac{4046.86\ m^2}{1\ acre} \times \frac{12\ g\ dry\ algae}{m^2 \cdot day} \times \frac{214\ days}{1\ year} \times \frac{0.1\ g\ lipids}{g\ dry\ algae}$$

$$\times \frac{1\ kg}{1000\ g} \times \frac{1\ m^3}{918\ kg} \times \frac{264.17\ gal}{1\ m^3} \times \frac{1\ barrel}{42\ gal} \times 0.75 \approx 1.83\ \times\ 10^5\ barrels/year$$

Land area needed to meet 100% of the Kansas liquid fuel demand

Example calculation for production under the HAP scenario:

$$\frac{62.44\ \times\ 10^6\ barrels}{year} \times \frac{42\ gal}{1\ barrel} \times \frac{1\ m^3}{264.17\ gal} \times \frac{918\ kg}{1\ m^3} \times \frac{1000\ g}{1\ kg} \times \frac{1}{0.75} \times \frac{1\ g\ algae}{0.3\ g\ lipids}$$

$$\times \frac{m^2 \cdot day}{25\ g\ algae} \times \frac{1\ year}{214\ days} \times \frac{1\ acre}{4046.86\ m^2} \times \frac{1}{0.85} \approx 2.20\ \times\ 10^6\ acres$$

Land area on which wastewater flow can meet the evaporative demand

Example calculation using the Andover WWTP, which has a wastewater flow rate of 0.96 MGD and a net evaporation rate of 17 in/year:

$$\frac{0.96\ \times\ 10^6\ gal}{day} \times \frac{365\ days}{year} \times \frac{1\ m^3}{264.17\ gal} \times \frac{1\ year}{17\ in} \times \frac{1\ in}{0.0254\ m} \times \frac{1\ acre}{4046.86\ m^2} \approx 759\ acres$$

This area was compared to the land available for algal ponds at each RE, and if the available land exceeded the land area on which wastewater flow can meet the evaporative demand, the WWTP was deemed water-limited at that RE. If the opposite was found to be the case, the WWTP was labeled land-limited.

Detailed results

Figure A1: Average total nitrogen and total phosphorus concentration by month from reporting Kansas municipal WWTPs categorized as urban, near-urban, and rural WWTPs. Error bars represent one standard deviation.

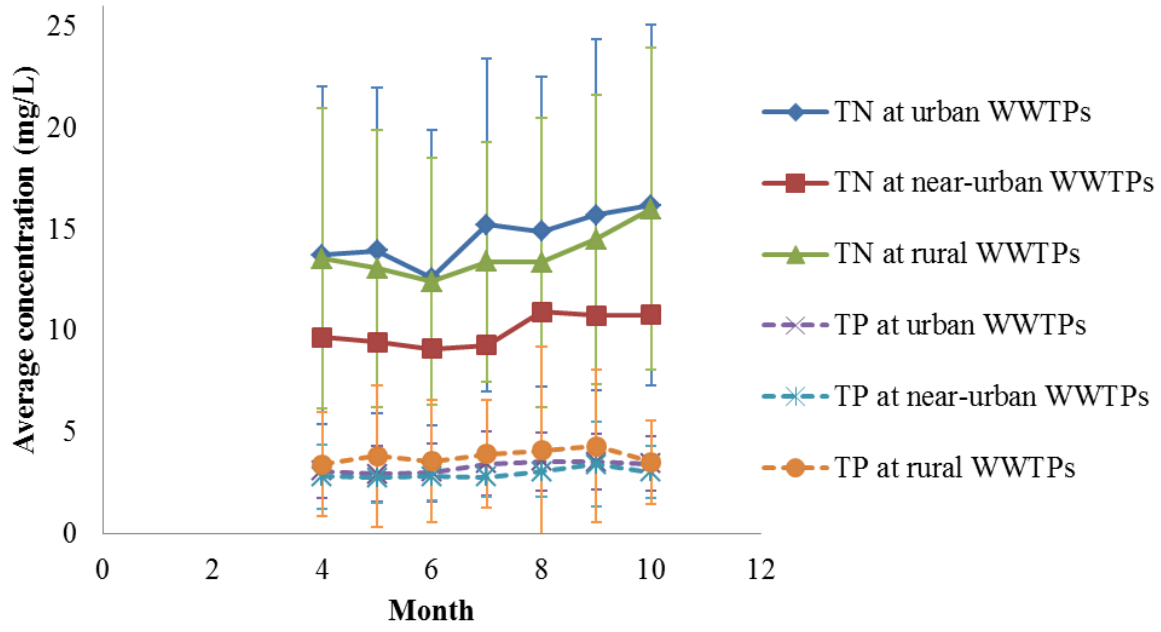

Figure A2: Cumulative potential annual algal biodiesel production under wastewater limitation by WWTP category (urban, near-urban, or rural).

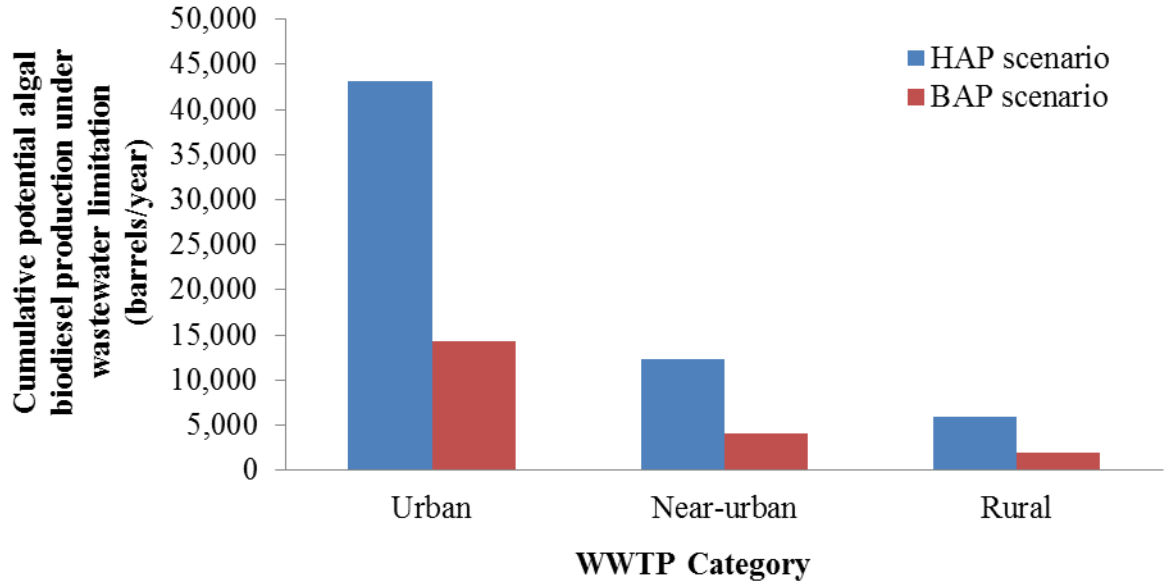

Table A5: Percent of land within each radial extent (RE) that is potentially available for algal production, calculated by wastewater treatment plant. Averages are shown with the standard deviation.

	Radial extent of implementation (miles)				
	0.25	*0.50*	*0.75*	*1.0*	*1.5*
Urban WWTPs					
Minimum	7.29	5.78	9.57	12.7	14.7
Average	50.9 ± 20.2	51.6 ± 17.0	51.5 ± 17.4	51.4 ± 18.5	54.6 ± 19.2
Maximum	81.8	83.2	79.7	82.3	83.5
Near-urban WWTPs					
Minimum	25.1	27.2	39.6	46.0	47.3
Average	75.3 ± 17.3	79.5 ± 14.4	79.2 ± 13.6	79.1 ± 12.6	78.6 ± 11.6
Maximum	98.6	98.7	98.9	98.0	95.8
Rural WWTPs					
Minimum	41.0	45.5	48.8	42.9	52.8
Average	87.1 ± 10.3	87.0 ± 9.1	86.5 ± 8.5	87.2 ± 8.5	89.5 ± 7.6
Maximum	100	99.7	99.8	99.6	99.3

Discussion of nutrients quantities in dairy and slaughterhouse wastewaters in Kansas

The quantities and nutrient concentrations of agricultural wastewaters indicate their potential as supplemental sources for algal production at municipal WWTPs. For example, dairies produce 0.7 to 1.7 m^3 of wastewater per metric ton of milk.[2] In 2010, the total amount of milk produced in Kansas was 2.499 billion pounds,[3] which corresponds to approximately 1.36 million cubic meters of dairy wastewater. A study measured an average total phosphorus concentration of 71 mg L^{-1} and an average total Kjeldahl nitrogen concentration of 91.4 mg L^{-1} across fifteen dairy facilities.[4] At these concentrations, there are a total of 96.6 thousand kilograms of phosphorus and 124 thousand kilograms of nitrogen in the dairy wastewater produced annually in Kansas.

Slaughterhouses may also be able to provide a supply of nutrients necessary for algal growth. Slaughterhouses produce 3 to 8 m^3 of wastewater per metric ton of meat products.[2] In 2010, the total amount of red meat produced in Kansas was 5.38 billion pounds.[5] The total nitrogen and total phosphorus concentrations in slaughterhouse wastewater can range from 150 to 10,000 mg L^{-1}, and from 22 to 217 mg L^{-1}, respectively.[6] Therefore, the amount of nitrogen available annually from wastewater from Kansas cattle slaughterhouses is between 1.10 and 195 million kilograms. The amount of phosphorus available is between 161 thousand kilograms and 4.24 million kilograms per year. These calculations exclude the nutrients that could be obtained from poultry, swine, and other slaughterhouses. These quantities of nutrients suggest that algal growth in wastewater effluent could be supplemented significantly with other waste sources of nutrients, thus avoiding a demand for commercial fertilizers.

References:

1. Fortier, M.-O. P.; Sturm, B. S. M., Geographic Analysis of the Feasibility of Collocating Algal Biomass Production with Wastewater Treatment Plants. *Environmental Science & Technology* **2012,** *46*, (20), 11426-11434.
2. Henze, M.; Harremoes, P.; la Cour Jansen, J.; Arvin, E., *Wastewater treatment: biological and chemical processes*. 3rd ed.; Springer: Berlin, 2002.
3. United States Department of Agriculture (USDA); National Agricultural Statistics Service (NASS) *Milk Production, Disposition, and Income: 2010 Summary*; 2011.
4. Danalewich, J. R.; Papagiannis, T. G.; Belyea, R. L.; Tumbleson, M. E.; Raskin, L., Characterization of dairy waste streams, current treatment practices, and potential for biological nutrient removal. *Water Res.* **1998,** *32*, (12), 3555-3568.
5. United States Department of Agriculture (USDA); National Agricultural Statistics Service (NASS) *Livestock Slaughter: 2010 Summary*; 2011.
6. Li, J.; Healy, M.; Zhan, X.; Norton, D.; Rodgers, M., Effect of Aeration Rate on Nutrient Removal from Slaughterhouse Wastewater in Intermittently Aerated Sequencing Batch Reactors. *Water, Air, & Soil Pollution* **2008,** *192*, (1), 251-261.

Appendix B: Supporting Information for "Life Cycle Assessment of Bio-Jet Fuel from Hydrothermal Liquefaction of Microalgae" [1]

List of variables

Input variables	Units	Description
Distance_Airport	miles	Distance from the refinery to the airport
Distance_Refinery	miles	Distance from the WWTP to the refinery
Lipid_content	%	Lipid content of the algae on a dry weight basis
Eff_settling	-	Efficiency of settling algal cells based on average results from experiments in 2012 at the Lawrence WWTP pilot project (unpublished)
Energy_natural_gas	GJ/1000 m^3	Energy density of natural gas
Heat_recycle	-	Fraction of heat from HTL that is recycled
Uncertainty_biocrude_yield	-	Uncertainty factor for the result of the equation from Frank et al. (2012) for biocrude yield based on algal lipid content [2]
Ash_fraction	-	Fraction of ash in algal biomass
Carbon_fraction_ash	-	Fraction of carbon in ash from algal biomass
Concentration_additives	mg L^{-1}	Concentration of phenols added to the fuel as per ASTM D7566-11 standards
Algae_solids_fraction	-	Solids fraction in algal biomass on a mass basis before HTL
Temp_HTL	˚C	Temperature at which HTL is conducted
Natural_gas_type	%	Gradient for natural gas types used: 0=100% from biogenic from anaerobic digestion or landfill gas, 1=100% from conventional fossil-derived natural gas
Fraction_ACP_recycle	-	Fraction of aqueous coproduct added to wastewater in algal pond reactors
WW_P_conc	mg L^{-1}	Municipal wastewater phosphorus concentration
WW_N_conc	mg L^{-1}	Municipal wastewater nitrogen concentration
ACP_N_conc	mg L^{-1}	Nitrogen concentration in ACP from HTL
ACP_P_conc	mg L^{-1}	Phosphorus concentration in ACP from HTL
Algae_nutrient_uptake	-	Fraction of the limiting nutrient that algae fixes from the ponds into biomass
Fuel_production_emissions	kg CO_{2eq}/ MMBtu	Emissions of carbon dioxide equivalents for the liquid fuel production stage of an LCA on 1 MMBtu of kerosene-based jet fuel produced based on Skone (2008) [3]
Refining_fuel_yield	-	Fraction of hydrocarbons entering refining processes that is converted into usable fuel
Elm_NP	-	Molar ratio of algal composition of N to P
Hydrogen_demand	g H_2/kg feed	Amount of additional hydrogen (compared to petroleum crude) needed in upgrading biocrude

		from HTL of algae
Hydrogen_GHGs	kg CO_{2eq}/ kg H_2	Life cycle greenhouse gas emissions from the production of H_2 gas
Calculated variables	**Units**	**Description**
Mass_biofuel	kg	Mass of algal biofuel produced
Volume_biofuel	L	Volume of algal biofuel produced
Mass_fuel	kg	Mass of fuel corresponding to the functional unit
HTL_amount_heat	J	Amount of heat generated for HTL based on temperature, mass of wet algae, and heat recycling capacity of the system
Mass_dry_algae	kg	Mass of dry algae entering HTL based on efficiency of upgrading and biocrude yield
Biocrude_yield_percent	%	Biocrude yield as a percent of original dry algae biomass, using an equation from Frank et al. (2012) based on averaged data from published HTL experiments that correlates algal lipid content to HTL oil yields [2]
Carbon_fraction_sequestered	-	Fraction of the carbon in the total dry algal biomass that is sequestered by being fixed in ash
Mass_carbon_sequestered	kg	Mass of carbon sequestered based on the entering dry algal biomass
Mass_additives_biofuel	mg	Mass of phenol additives added to biofuel
Mass_hydrocarbon_biofuel	kg	Mass of hydrocarbons before phenol addition
Mass_wet_algae	kg	Mass of algae entering HTL on a wet basis
Pond_N_conc	mg L^{-1}	Nitrogen concentration in algal pond influent
Pond_P_conc	mg L^{-1}	Concentration of phosphorus in the influent to the algal ponds
Molar_N_pond_conc	mmol L^{-1}	Molar nitrogen concentration in the influent to the algal ponds
Molar_P_pond_conc	mmol L^{-1}	Molar phosphorus concentration in the influent to the algal ponds
N_P_ratio	-	N:P molar ratio for algal pond conditions
Alg_pond_conc	mg L^{-1}	Concentration of dry algal biomass in the ponds based on an uptake or fixing rate and on the limiting nutrient concentration
Pond_water_vol	L	Volume of water in the algal ponds needed to produce the functional unit
Skimmer_energy	J	Energy needed to process the pond water volume using a skimmer described in Sturm and Lamer (2011) based on the functional unit [4]
Water_pump_energy	J	Energy needed to pump water into the ponds at 25ft of head and out of the ponds at 2m of head with 70% efficient centrifugal pumps
Centrifuge_energy	kWh	Energy needed to dewater algae using an Evodos 25 field centrifuge

Refining_stage_emissions	kg CO_{2eq}	Life cycle CO_2-equivalent emissions from the liquid fuel production stage of kerosene-based jet fuel production based on the functional unit
AlgN	g dry algae/ g N	Mass of dry algae produced per mass of N fixed
AlgP	g dry algae/ g P	Mass of dry algae produced per mass of P fixed
Cyclone_electricity	kWh	Electricity needed to separate biocrude, ACP, and biochar after HTL, based on an Alfa Laval X20 centrifuge (Alfa Laval, Lund, Sweden)
Extra_hydrogen	kg H_2	Mass of additional hydrogen needed for upgrading algal biocrude compared to petroleum crude due to the higher heteroatom content
Mass_biocrude	kg	Mass of biocrude before heteroatom removal and hydrogen addition through hydrotreatment
GHG_hydrogen	kg CO_{2eq}	Total greenhouse gas emissions for providing sufficient H_2 for production of the functional unit
Mass_ACP	kg	Mass of liquid ACP produced from HTL, assuming a 10% loss in water (to the solids)
Mass_water_preHTL	kg	Mass of water entering HTL

1. Extended Methods

The methods for the algal bio-jet fuel production pathways modeled in this LCA are described further below by process step with calculations in subsections.

1.1. Relating the functional unit to algae and fuel mass

The functional unit of 1 GJ of algal bio jet-fuel was converted to mass and volume units using an average energy density (44.1 MJ/kg) and specific energy (0.757 kg/L) for synthetic paraffinic kerosene [5].

$$Mass\_biofuel\ [kg] = (1\ GJ) * \left(\frac{1000\ MJ}{1\ GJ}\right) * \frac{1\ kg}{44.1\ MJ}$$

$$Volume\_biofuel\ [L] = Mass\_biofuel\ [kg] * \left(\frac{1\ L}{0.757\ kg}\right)$$

The mass of antioxidant additives needed was calculated based on 20 mg/L as stipulated in the ASTM D7566-11 guidelines. The difference between the final bio jet-fuel volume and the mass of additives was the mass of upgraded hydrocarbons generated from algal biomass.

$$Mass\_additives\_biofuel\ [mg] = \left(Concentration\_additives\left[\frac{mg}{L}\right]\right) * (Volume\_biofuel\ [L])$$

$$Mass\_hydrocarbon\_biofuel\ [kg] = Mass\_biofuel\ [kg] - \frac{Mass\_additives\_biofuel\ [mg]}{Refining\_fuel\_yield * \left(\frac{10^6\ mg}{kg}\right)}$$

The biocrude mass was calculated using the nitrogen, sulfur, and oxygen concentrations (4.4%, 0.5%, and 5.5% respectively on a weight basis) of the biocrude generated in the hydrothermal liquefaction reactions of wastewater-fed microalgae and the mass of hydrocarbons after upgrading. It was calculated that replacement of heteroatoms with hydrogen would decrease the biocrude mass by 9.22% as it is converted to hydrocarbon chains.

$$Mass\_biocrude\ [kg] = \frac{Mass\_hydrocarbon\_biofuel\ [kg]}{0.9078}$$

The mass of algae on a dry weight basis that corresponds to the mass of biocrude, and the mass of wet algae immediately prior to HTL were calculated as shown below. A range of inputs were used for “Biocrude_yield_percent” and “Algae_solids_fraction” in the Monte Carlo analysis, in order to calculate a valid probability of outcomes using these parameters that may vary.

$$Mass\_dry\_algae\ [kg] = \frac{100\% * Mass\_biocrude\ [kg]}{Biocrude\_yield\_percent\ [\%]}$$

$$Mass\_wet\_algae\ [kg] = \frac{Mass\_dry\_algae\ [kg]}{Algae\_solids\_fraction}$$

1.2. Algae production in wastewater effluent

Microalgae production was modeled according to our wastewater effluent-fed algal pond pilot system at the Lawrence Wastewater Treatment Plant (WWTP) in Lawrence, KS. These open ponds were not provided with additional CO_2 gas, and no added CO_2 was modeled in this LCA. The effluent from the secondary clarifier was pumped at a head of 7.62 m (25 ft) by pumps with 70% efficiency into open pond reactors. A solar-powered mixer was modeled for the ponds (SolarBee, Medora Corporation, Dickinson, ND). The effluent was pumped into a gravity sedimentation basin at a head of 2 m for harvesting the algae. The electricity needed for pumping the influent and effluent to the pond reactors was included in this process step.

Direct nitrous oxide (N_2O) emissions from open algal ponds were not included because they have been shown to be negligible in the overall algal bio-jet fuel LCA results. A study by Fagerstone et al. (2011) determined that the direct N_2O-N emissions produced from N in the media in bench-scale experiments simulating well-mixed open algal ponds with diurnal light-dark cycling were 0.002% ± 0.002% (n = 9), resulting in net GHG emissions of 58.4 mg CO_{2eq} over a 5-day growth cycle [6]. Moreover, with thorough mixing, these N_2O emissions can be virtually eliminated.

The mixed culture microalgae cultivated in the wastewater effluent-fed open pond reactors at the Lawrence WWTP was on average 14% lipids and 29% ash on a dry weight basis [7]. A possible range of 7.0% to 30% lipids and 5.0% to 50% ash was modeled.

The wastewater effluent total phosphorus (TP) and total nitrogen (TN) concentrations were the average concentrations for the 2012 growing season at the Lawrence WWTP pilot system. The range of possible concentrations was bound by one standard deviation from these average values. An algae nutrient uptake fraction was included in this LCA to represent the proportion of TN and TP that is both bioavailable and ultimately fixed in algal biomass. For the base case, 90% of the limiting nutrient concentration was modeled to be fixed into algal biomass. The range of algae nutrient uptake fractions was determined from our experimental data. The measured algae nutrient uptake fraction was 0.614 at start-up of open pond reactor operation to 0.989 during stable operation [4].

The elemental composition of microalgae affects which nutrient is limiting in its growth media and the mass of algae that can be cultivated in continuous flow reactors with a known nutrient composition and residence time. To account for various published results for the molar N:P of an algal cell, a range of values was modeled. The base case utilized the N:P determined for microalgae grown in wastewater effluent at the Lawrence WWTP pilot system, 6.0 [7]. This value also served as the minimum N:P modeled. The maximum algal cell N:P modeled was 27, which is the N:P determined for low-lipid algae by Williams and Laurens (2010) [8]. This range

encompassed the Redfield ratio N:P of 16 for marine algae and the Williams and Laurens (2010) medium-lipid algal cell N:P of 21 [8, 9]. The algal cell N:P was used to determine whether nitrogen or phosphorus would be limiting in the mixed wastewater effluent and ACP from hydrothermal liquefaction. The limiting nutrient concentration and the algae nutrient uptake fraction were subsequently used to relate the functional unit to microalgal mass, concentration of algae in the ponds, and the amount of water to be pumped.

1.2.1. Algae production in wastewater effluent and nutrient recycling calculations

The mass of dry algae produced per mass of N or P fixed into biomass was calculated based on the elemental algal N:P ratio and the ash fraction of algae using relationships developed from the literature on low-lipid, medium-lipid, and wastewater microalgae (Figure S1) [8, 10].

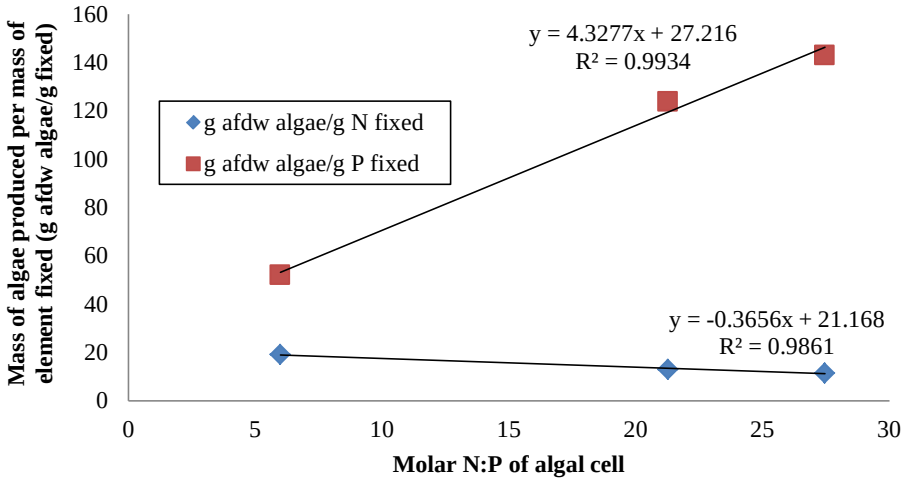

Figure S1: Relationship between algal cell N:P and algal mass produced per mass of nutrient fixed based on low-lipid and medium-lipid algae data from Williams & Laurens (2010) and wastewater microalgae data from Sturm et al. (2012) [8, 10].

$$AlgN\ [g\ dry\ algae/g\ N] = \frac{-0.3656 * Elm\_NP + 21.168}{1 - Ash\_fraction}$$

$$AlgP\ [g\ dry\ algae/g\ P] = \frac{4.3277 * Elm\_NP + 27.216}{1 - Ash\_fraction}$$

The N and P concentration of the algal ponds was calculated based on the volumetric fraction of ACP in the ponds versus municipal wastewater effluent, and the concentrations of these two sources of growth media.

$$Pond\_N\_conc\left[\frac{mg}{L}\right] = (Fraction\_ACP\_recycle) * \left(ACP\_N\_conc\left[\frac{mg}{L}\right]\right) + (1 - Fraction\_ACP\_recycle) * \left(WW\_N\_conc\left[\frac{mg}{L}\right]\right)$$

$$Pond\_P\_conc\left[\frac{mg}{L}\right] = (Fraction\_ACP\_recycle) * \left(ACP\_P\_conc\left[\frac{mg}{L}\right]\right) + (1 - Fraction\_ACP\_recycle) * \left(WW\_P\_conc\left[\frac{mg}{L}\right]\right)$$

These concentrations were converted to molar concentrations of N and P in the algal ponds using the atomic weight of these elements in order to calculate the molar N:P ratio of the ponds.

$$Molar\_N\_pond\_conc\left[\frac{mmol}{L}\right] = \frac{Pond\_N\_conc\left[\frac{mg}{L}\right]}{14.01\ mg/mmol}$$

$$Molar\_P\_pond\_conc\left[\frac{mmol}{L}\right] = \frac{Pond\_P\_conc\left[\frac{mg}{L}\right]}{30.97\ mg/mmol}$$

$$N\_P\_ratio = \frac{Molar\_N\_pond\_conc\left[\frac{mmol}{L}\right]}{Molar\_P\_pond\_conc\left[\frac{mmol}{L}\right]}$$

If the N:P ratio was less than the algal cell N:P ratio (N_P_ratio < Elm_NP), then nitrogen was the limiting nutrient and the algae concentration in the ponds depended on the nitrogen concentration of the pond. If the N:P ratio was greater than the algal cell N:P ratio, (N_P_ratio>Elm_NP), then the limiting nutrient was phosphorus and the algae concentration in the pond depended on the phosphorus concentration of the pond.

If N_P_ratio < Elm_NP:

$$Alg\_pond\_conc\ [mg/L] = AlgN * \left(Pond\_N\_conc\left[\frac{mg}{L}\right]\right) * (Algae\_nutrient\_uptake)$$

If N_P_ratio > Elm_NP:

$$Alg\_pond\_conc\ [mg/L] = AlgP * \left(Pond\_P\_conc\left[\frac{mg}{L}\right]\right) * (Algae\_nutrient\_uptake)$$

The volume of water required to grow the algal biomass corresponding to the functional unit was calculated based on the algae concentration in the ponds, the settling efficiency of the algae, and the mass of dry algae needed to produce the functional unit of bio-jet fuel.

$$Pond\_water\_vol\ [L] = \frac{\left(\frac{10^6\ mg}{kg}\right) * Mass\_dry\_algae\ [kg]}{(Alg\_pond\_conc\ [mg/L]) * (Eff\_settling)}$$

The energy required to pump this volume of water with pumps of 70% efficiency into the ponds at a head of 7.62 m (25 ft) and out of the ponds to the sedimentation tanks at a head of 2 m was calculated as shown below.

$$Water\_pump\_energy\ [J] = (Pond\_water\_vol\ [L]) * \left(\frac{1\ m^3}{1000\ L}\right) * \left(\frac{1000\ kg}{1\ m^3}\right)$$

$$* (9.81\ m/s^2) * 0.70 * (7.62\ m + 2\ m)$$

1.3. Algae harvesting

The microalgae was harvested by gravity sedimentation without added flocculants. This process step was tested at the pilot system at the Lawrence WWTP using four separate gravity sedimentation tanks. Each clarifier has a surface area of 1.56 ft^2 and an operating volume of 42.9 gal. A series of experiments at different flow rates yielded average settling efficiencies between 48% and 99%. This defined the possible range of settling efficiencies for this LCA process step. For the base case, a nominal value of 90% was chosen as a reasonable achievement for settling efficiency. Additionally, the electricity needed for a 1 HP/2500 gpm skimmer with 70% efficiency (FRC Systems International, Cumming, GA) to collect settled algae was calculated for this process [4].

1.3.1. Algae harvesting calculations

The energy required to use a skimmer that operates at 1 HP at a rate of 2500 gallons per minute for the volume of pond water required for production of the functional unit was calculated as shown below.

$$Skimmer\_energy\ [J] = \left(\frac{1\ HP \cdot min}{2500\ gal}\right) * \left(\frac{745.70\ W}{HP}\right) * \left(\frac{1\ J}{1\ W \cdot s}\right) * \left(\frac{60\ s}{1\ min}\right) * \left(\frac{264.172\ gal}{1\ m^3}\right) * \left(\frac{1\ m^3}{1000\ L}\right) * (Pond\_water\_vol\ [L])$$

1.4. Algae dewatering

Two processes were modeled as algal dewatering options following algae harvesting by gravity sedimentation: solar drying and centrifugation. Solar drying would be performed with manual labor and no fossil energy requirements. The centrifugation process was modeled based on the power requirements of an Evodos type 25 centrifuge (Evodos B.V., Breda, The Netherlands) which was designed for microalgae concentration. The base case utilized algae dewatered through solar drying to 5.7% solids, which was equivalent to the solids content used in the lab-scale HTL reactions of 3 g of wastewater effluent-fed microalgae in 50 mL of water [7]. A case that involves centrifugation to 10% solids was modeled as well. The possible range of solids content for dewatered algae modeled in this LCA reflected the range of algal solids contents tested in published HTL experiments, 5.0% to 30% solids [7, 11-27].

1.4.1. Algae dewatering calculations

The energy required to centrifuge the algae was based on the energy requirements of an Evodos type 25 centrifuge (Evodos B.V., Breda, The Netherlands). It was assumed that the algae would be concentrated to 1.5% solids through sedimentation prior to entering the centrifuge.

$$Centrifuge\_energy\ [kWh] = \left(\frac{1.20\ kWh}{1\ m^3}\right) * \left(\frac{1\ m^3}{1000\ kg}\right) * \left(\frac{Mass\_dry\_algae\ [kg]}{0.015}\right)$$

1.5. Transport to a refinery

This process step occurred prior to hydrothermal liquefaction and involved the transportation of dewatered algae in the HTL at the refinery pathway. In the HTL at the WWTP pathway, this process step occurred after hydrothermal liquefaction and phase separation, and only the biocrude was transported to a refinery.

Municipal wastewater treatment plants (n = 12,720) and all petroleum refineries (n = 141) in the continental United States were geocoded in ArcMap GIS software [28, 29]. The linear distances from each WWTP to the nearest petroleum refinery were assessed. The average distance and standard deviation were then calculated. Due to the average distance between WWTPs and petroleum refineries (104 miles or 167 km) and the rate at which algal biomass would be produced at each WWTP site, transportation by truck was selected as the most likely mode of transportation that would be utilized. In order to determine the greenhouse gas emissions for this process step, transportation of dewatered algae or produced biocrude by single-unit truck for the average distance between a wastewater treatment plant and the nearest refinery was modeled for the base cases. The range of possible distances was defined by one standard deviation (~74 miles or 119 km) from the average.

1.6. Hydrothermal liquefaction

The amount of heat needed for hydrothermal liquefaction (HTL) was determined using thermodynamic calculations, the mass of dewatered algae corresponding to the functional unit, the HTL reaction temperature, and the percent of heat generated that would be recycled. The thermodynamic calculations were based on no phase change occurring in the reactor under pressure and heat capacities of 4.22 J g^{-1} °C^{-1} for water at temperatures under 150°C and 4.86 J g^{-1} °C^{-1} for subcritical water at temperatures over 150°C [30]. The temperature modeled for the HTL reaction is 300°C for the base case with a range from 250 to 350°C which represents a central subset of the range of temperatures used in published HTL experiments on algal biomass [7, 11-27].

The heat was provided by a mixture of natural gas and biogenic methane, e.g. from the anaerobic digestion of wastewater sludge or from collected landfill gas. For the base cases, 85% of the heat was generated from the use of fossil natural gas. Additionally, a fraction of the heat used in HTL reactions can be recycled in commercial-scale systems using a heat exchanger. It was assumed that 80% of the heat generated for hydrothermal liquefaction could be recycled and reused. The fraction of heat recycled ranged from 0 to 90% as modeled in this LCA.

The biocrude yield was related to the original algal biomass through an equation by Frank et al. (2012) which correlates the average lipid content of algae with the biocrude yield using values reported by numerous published HTL reactions of algal biomass [2]. An uncertainty factor ranging from 0.75 to 1.25 (with 1.0 as the nominal value) was applied to the calculated biocrude yield from this equation.

Subsequent separation of the biocrude from the aqueous coproduct (ACP) and the biochar was modeled with an Alfa Laval X20 disc bowl centrifuge (Alfa Laval, Lund, Sweden). The biochar, or the ash that remains after HTL, contained a fraction of the original carbon from algal biomass. This carbon was modeled as sequestered carbon because unlike the carbon contained in the biocrude, it would not ultimately be released to the atmosphere in the form of a greenhouse gas. The biochar was determined to contain 20% carbon on a dry weight basis in the laboratory-scale HTL experiments [7]. This carbon content of the ash fraction was the nominal value modeled in this LCA. A biochar carbon content range from 5.0% to 30% was modeled.

The ACP from hydrothermal liquefaction contains a portion of the nitrogen and phosphorus that had been previously fixed in algal biomass. In our experience, the total nitrogen (TN) and total phosphorus (TP) concentrations in the ACP can vary greatly between HTL reactions. A nominal TN concentration of 2000 mg/L and a nominal TP concentration of 15 mg/L were chosen as representative of the concentrations measured in the ACP from different HTL reactions at the University of Kansas. The range of TN concentrations modeled for the ACP was 1600 to 2400 mg/L and the range of TP concentrations was 3.0 to 30 mg/L. These nutrients were recycled to generate new algal growth by dilution of ACP with wastewater effluent. However, due to inhibitory effects observed on algal growth at high ACP concentrations in growth media [31-33], the range of ACP concentration by volume in wastewater effluent was 0% to 10%, with 5.0% as the nominal value.

1.6.1. Hydrothermal liquefaction calculations

The volume of fossil natural gas needed for hydrothermal liquefaction was based on the energy density of natural gas (Energy_natural_gas), the amount of heat needed for HTL (HTL_amount_heat), and the percent of this heat that would be sourced from fossil versus biogenic methane (Natural_gas_type).

Assuming that the starting temperature of the wet algal biomass was 25°C, the following equation incorporating the heat capacities of normal water below 150°C and subcritical water above 150°C was used to determine the amount of heat in Joules needed for hydrothermal liquefaction [30].

$$HTL\_amount\_heat\ [J] = \left(\frac{4.22\ J}{g \cdot ℃} * (150℃ - 25℃) + \frac{4.86\ J}{g \cdot ℃} * (Temp\_HTL\ [℃] - 150℃)\right) * (Mass\_wet\_algae\ [kg]) * \frac{1000\ g}{kg} * (1 - Heat\_recycle)$$

Biocrude yield as a percent of original dry algae biomass was determined using an equation from Frank et al. (2012) that correlates algal lipid content to HTL oil yields using averaged data from published HTL experiments [2]. A variable uncertainty factor was applied.

$$Biocrude\_yield\_percent\ [\%] = (0.5638 * Lipid\_content\ [\%] + 21.006) * Uncertainty\_biocrude\_yield$$

The mass of carbon sequestered through the ash was calculated using the ash fraction and the fraction of the ash which was composed of carbon.

$$Carbon\_fraction\_sequestered = (Ash\_fraction) * (Carbon\_fraction\_ash)$$

$$Mass\_carbon\_sequestered\ [kg] = (Mass\_dry\_algae\ [kg]) * (Carbon\_fraction\_sequestered)$$

The electricity required to separate the biocrude, ACP, and biochar (together equal to the entering mass, the mass of wet algae) by cyclone was calculated based on an Alfa Laval X20 disc bowl centrifuge (Alfa Laval, Lund, Sweden).

$$Cyclone\_electricity = \frac{(130\ kW) * Mass\_wet\_algae}{\left(\frac{190\ m^3}{h}\right) * \left(\frac{1000\ kg}{m^3}\right)}$$

1.7. Transport of ACP to WWTP

The pumping of ACP from the cyclone to the ponds for the HTL at the WWTP pathway was assumed to be a negligible impact on the overall LCA. However, in the HTL at the refinery pathway, the ACP produced at the refinery must be returned to the WWTP for nutrients to be recycled towards algal growth. For this pathway, transportation by truck of the ACP volume corresponding to the functional unit was modeled for the same distance as the transport to the refinery process step.

1.7.1. Transport of ACP to WWTP calculations

The mass of ACP that would be collected and require transport back to the WWTP in the HTL at the refinery pathway was calculated based on an assumed loss of 10% of the water to the biochar upon separation.

$$Mass\_water\_preHTL\ [kg] = (Mass\_wet\_algae\ [kg]) - (Mass\_dry\_algae\ [kg])$$

$$Mass\_ACP\ [kg] = 0.90 * (Mass\_water\_preHTL\ [kg])$$

1.8. Upgrading processes

The biocrude obtained from the hydrothermal liquefaction of wastewater-fed microalgae resembles petroleum crude in its H/C atomic ratio, O/C atomic ratio, and higher heating value (HHV) [7]. Its quality suggests that biocrude could be a drop-in replacement for petroleum crude at a petroleum refinery, and thus the GHG emissions associated with refining processes for jet fuel production were modeled for this bio-jet fuel pathway [3]. However, the biocrude has a higher oxygen and nitrogen content and a lower sulfur content compared to petroleum crude (Table 1 in the manuscript). Due to the higher heteroatom (N, O) content of the biocrude compared to petroleum crude, the hydrogen demand for upgrading at a refinery is increased. The hydrogen needs for removing the N, O, and S concentrations in both algal biocrude and petroleum crude were calculated using hydrotreatment guidelines specific to the heteroatom content [34]. The additional hydrogen required to upgrade algal biocrude was the difference between these hydrotreatment needs. The maximum and minimum hydrogen demands were determined from the range of heteroatom concentrations for petroleum crude (Table 1 in the manuscript). The average hydrogen demand of 31.7 g H_2/kg biocrude feed was modeled as the nominal value. The range modeled was more conservative than the normal distribution of hydrogen demands with a mode of 15 g H_2/kg biocrude feed and a standard deviation of 2.5 g H_2/kg biocrude feed modeled in the algal biofuel LCA study by Sills et al. (2013) [35].

The life cycle greenhouse gas emissions of hydrogen gas differ significantly depending on the production methods used. Hydrogen can be extracted from fossil fuels through steam reforming of natural gas, gasification of coal, partial oxidation, catalytic decomposition, thermal cracking, and other means [36-38]. Hydrogen can also be extracted from water through direct electrolysis or through thermochemical cycles, which can be coupled with nuclear energy production or wind

or solar power generation [36, 39-44]. Additionally, biomass can be processed to produce hydrogen gas [42]. Examples of LCA results for hydrogen production by various methods (excluding impacts from infrastructure materials, construction, and facility dismantling to be consistent with the methodology of this LCA) are shown in Table 5 in the manuscript. Their range denoted the maximum and minimum values for the life cycle greenhouse gas emissions associated with hydrogen gas production in this LCA of algal bio-jet fuel production. The nominal value modeled was the SimaPro 7.3 Industry Data 2.0 LC-GHG emissions for hydrogen gas production by steam reforming.

To account for potential losses of hydrocarbons that do not result in useful coproducts in the refining process, a refining fuel yield factor was applied. It was assumed that 90% of the hydrocarbons would be converted to bio-jet fuel for the base case. The possible range of refining fuel yields chosen was 75 to 98%.

Before leaving the refinery, the upgraded hydrocarbons were blended with antioxidants to meet the ASTM D7566-11 standards [45]. For this LCA, the addition of 20 mg/L phenols was modeled as a proxy to 20 mg/L of 2,6-di-*tert*-butylphenol. At this stage, the upgraded hydrocarbons with additives were considered to be algal bio-jet fuel.

1.8.1. Upgrading processes calculations

The GHG emissions for the refining stage of the life cycle of algal bio-jet fuel were based on the refining stage for petroleum crude to conventional jet fuel, as shown below. These emissions were added to the GHG emissions associated with the production of the additional hydrogen gas needed for algal bio-jet fuel hydrotreatment to determine the complete upgrading processes' GHG emissions scaled to the functional unit.

$$Refining\_stage\_emissions\ [kg\ CO_{2eq}] = Fuel\_production\_emissions\ [kg\ CO_{2eq}/MMBtu] * \frac{1\ MMBtu}{1.0546\ GJ}$$

The additional hydrogen needed to upgrade the biocrude was calculated as shown below:

$$Extra\_hydrogen\ [kg\ H_2] = Mass\_biocrude\ [kg] * Hydrogen\_demand\ [g\ H_2/kg\ feed] * \frac{1\ kg}{1000\ g}$$

The greenhouse gas emissions from the production of the additional hydrogen needed to upgrade the biocrude were calculated based on the additional hydrogen demand and the life cycle greenhouse gas emissions per mass unit of hydrogen gas produced.

$$GHG\_hydrogen\ [kg\ CO_{2eq}] = (Extra\_hydrogen\ [kg\ H_2]) * (Hydrogen\_GHGs\ [kg\ CO_{2eq}/kg\ H_2])$$

1.9. Transport to an airport

The public-use airports (n = 19,729) in the continental United States, including heliports and small airports, were geocoded in ArcMap GIS software [46]. The linear distances from each airport to the nearest petroleum refinery were calculated. The transportation of algal bio-jet fuel by truck for the average distance (110 miles or 177 km) between a petroleum refinery and an airport as the nominal value was modeled. The range of possible distances was defined by one standard deviation (~84 miles or 135 km) from the mean.

1.10. Combustion in a jet engine

The emissions from combustion of JP-8 fuel in a PT6A-68 engine at maximum continuous operation were adjusted for the density difference between bio-jet fuel and conventional jet fuel and modeled for this process step [47]. The sulfur dioxide and carbon dioxide emissions were calculated separately. The sulfur dioxide emissions were determined stoichiometrically using an average bio-jet fuel sulfur content of 0.6 mg/kg [48]. The carbon dioxide emissions were obtained based on average emissions of combusted synthetic paraffinic kerosene [5]. For algal bio-jet fuel, these CO_2 emissions are biogenic (atmospheric CO_2 recently fixed in biomass) and are not counted as new greenhouse gas emissions.

References

[1] Fortier M-OP, Roberts GW, Stagg-Williams SM, Sturm BSM. Life cycle assessment of bio-jet fuel from hydrothermal liquefaction of microalgae. Applied Energy. 2014;122:73-82.
[2] Frank E, Elgowainy A, Han J, Wang Z. Life cycle comparison of hydrothermal liquefaction and lipid extraction pathways to renewable diesel from algae. Mitigation and Adaptation Strategies for Global Change. 2012:1-22.
[3] Skone TJ, Gerdes K. Development of Baseline Data and Analysis of Life Cycle Greenhouse Gas Emissions of Petroleum-Based Fuels. National Energy Technology Laboratory, Department of Energy; 2008.
[4] Sturm BSM, Lamer SL. An energy evaluation of coupling nutrient removal from wastewater with algal biomass production. Applied Energy. 2011;88:3499-506.
[5] Hileman JI, Stratton RW, Donohoo PE. Energy content and alternative jet fuel viability. Journal of Propulsion and Power. 2010;26:1184-95.
[6] Fagerstone KD, Quinn JC, Bradley TH, De Long SK, Marchese AJ. Quantitative Measurement of Direct Nitrous Oxide Emissions from Microalgae Cultivation. Environmental Science & Technology. 2011;45:9449-56.
[7] Roberts GW, Fortier M-OP, Sturm BSM, Stagg-Williams SM. Promising Pathway for Algal Biofuels through Wastewater Cultivation and Hydrothermal Conversion. Energy & Fuels. 2013;27:857-67.
[8] Williams PJlB, Laurens LML. Microalgae as biodiesel & biomass feedstocks: Review & analysis of the biochemistry, energetics & economics. Energy & Environmental Science. 2010;3:554-90.
[9] Stumm W, Morgan J, Dreyer J. Aquatic Chemistry. 3rd ed. New York: Wiley; 1996.
[10] Sturm BSM, Peltier E, Smith V, deNoyelles F. Controls of microalgal biomass and lipid production in municipal wastewater-fed bioreactors. Environmental Progress & Sustainable Energy. 2012;31:10-6.
[11] Alba LG, Torri C, Samori C, van der Spek J, Fabbri D, Kersten SRA, et al. Hydrothermal Treatment (HIT) of Microalgae: Evaluation of the Process As Conversion Method in an Algae Biorefinery Concept. Energy & Fuels. 2012;26:642-57.
[12] Anastasakis K, Ross AB. Hydrothermal liquefaction of the brown macro-alga Laminaria Saccharina: Effect of reaction conditions on product distribution and composition. Bioresource Technology. 2011;102:4876-83.
[13] Biller P, Ross AB. Potential yields and properties of oil from the hydrothermal liquefaction of microalgae with different biochemical content. Bioresource Technology. 2011;102:215-25.
[14] Brown TM, Duan P, Savage PE. Hydrothermal Liquefaction and Gasification of Nannochloropsis sp. Energy & Fuels. 2010;24:3639-46.
[15] Dote Y, Sawayama S, Inoue S, Minowa T, Yokoyama S-y. Recovery of liquid fuel from hydrocarbon-rich microalgae by thermochemical liquefaction. Fuel. 1994;73:1855-7.
[16] Duan P, Savage PE. Hydrothermal Liquefaction of a Microalga with Heterogeneous Catalysts. Industrial & Engineering Chemistry Research. 2010;50:52-61.
[17] Jena U, Das KC. Comparative Evaluation of Thermochemical Liquefaction and Pyrolysis for Bio-Oil Production from Microalgae. Energy & Fuels. 2011;25:5472-82.
[18] Jena U, Das KC, Kastner JR. Effect of operating conditions of thermochemical liquefaction on biocrude production from Spirulina platensis. Bioresource Technology. 2011;102:6221-9.
[19] Matsui T-o, Nishihara A, Ueda C, Ohtsuki M, Ikenaga N-o, Suzuki T. Liquefaction of micro-algae with iron catalyst. Fuel. 1997;76:1043-8.

[20] Minowa T, Yokoyama S-y, Kishimoto M, Okakura T. Oil production from algal cells of Dunaliella tertiolecta by direct thermochemical liquefaction. Fuel. 1995;74:1735-8.
[21] Ross AB, Biller P, Kubacki ML, Li H, Lea-Langton A, Jones JM. Hydrothermal processing of microalgae using alkali and organic acids. Fuel. 2010;89:2234-43.
[22] Shuping Z, Yulong W, Mingde Y, Kaleem I, Chun L, Tong J. Production and characterization of bio-oil from hydrothermal liquefaction of microalgae Dunaliella tertiolecta cake. Energy. 2010;35:5406-11.
[23] Valdez PJ, Dickinson JG, Savage PE. Characterization of Product Fractions from Hydrothermal Liquefaction of Nannochloropsis sp and the Influence of Solvents. Energy & Fuels. 2011;25:3235-43.
[24] Vardon DR, Sharma BK, Scott J, Yu G, Wang ZC, Schideman L, et al. Chemical properties of biocrude oil from the hydrothermal liquefaction of Spirulina algae, swine manure, and digested anaerobic sludge. Bioresource Technology. 2011;102:8295-303.
[25] Yu G, Zhang YH, Schideman L, Funk T, Wang ZC. Distributions of carbon and nitrogen in the products from hydrothermal liquefaction of low-lipid microalgae. Energy & Environmental Science. 2011;4:4587-95.
[26] Zhou D, Zhang L, Zhang S, Fu H, Chen J. Hydrothermal Liquefaction of Macroalgae Enteromorpha prolifera to Bio-oil. Energy & Fuels. 2010;24:4054-61.
[27] Toor SS, Reddy H, Deng S, Hoffmann J, Spangsmark D, Madsen LB, et al. Hydrothermal liquefaction of Spirulina and Nannochloropsis salina under subcritical and supercritical water conditions. Bioresource Technology. 2013;131:413-9.
[28] United States Environmental Protection Agency (US EPA). Clean Watersheds Needs Survey 2008 Report to Congress. Washington, D.C.: US EPA, Office of Water Management; 2008.
[29] United States Energy Information Administration. Refinery Capacity Report 2011. Washington, DC2011.
[30] Krammer P, Vogel H. Hydrolysis of esters in subcritical and supercritical water. The Journal of Supercritical Fluids. 2000;16:189-206.
[31] Jena U, Vaidyanathan N, Chinnasamy S, Das KC. Evaluation of microalgae cultivation using recovered aqueous co-product from thermochemical liquefaction of algal biomass. Bioresource Technology. 2011;102:3380-7.
[32] Biller P, Ross AB, Skill SC, Lea-Langton A, Balasundaram B, Hall C, et al. Nutrient recycling of aqueous phase for microalgae cultivation from the hydrothermal liquefaction process. Algal Research. 2012;1:70-6.
[33] Zhou Y, Schideman L, Zhang Y, Yu G, Wang Z, Pham M. Resolving bottlenecks in current algal wastewater treatment paradigms: a synergistic combination of low-lipid algal wastewater treatment and hydrothermal liquefaction for large-scale biofuel production. Energy and Water. Chicago, Illinois: Water Environment Federation; 2011. p. 347-61.
[34] Gary JH, Handwerk GE. Petroleum Refining: Technology and Economics. 4th ed. New York, NY: Marcel Dekker; 2001.
[35] Sills DL, Paramita V, Franke MJ, Johnson MC, Akabas TM, Greene CH, et al. Quantitative Uncertainty Analysis of Life Cycle Assessment for Algal Biofuel Production. Environmental Science & Technology. 2012;47:687-94.
[36] Utgikar V, Thiesen T. Life cycle assessment of high temperature electrolysis for hydrogen production via nuclear energy. International Journal of Hydrogen Energy. 2006;31:939-44.

[37] Dufour J, Serrano DP, Gálvez JL, Moreno J, García C. Life cycle assessment of processes for hydrogen production. Environmental feasibility and reduction of greenhouse gases emissions. International Journal of Hydrogen Energy. 2009;34:1370-6.
[38] Spath PL, Mann MK. Life Cycle Assessment of Hydrogen Production via Natural Gas Steam Reforming. Golden, CO: National Renewable Energy Laboratory,; 2001.
[39] Cetinkaya E, Dincer I, Naterer GF. Life cycle assessment of various hydrogen production methods. International Journal of Hydrogen Energy. 2012;37:2071-80.
[40] Spath PL, Mann MK. Life Cycle Assessment of Renewable Hydrogen Production via Wind/Electrolysis. Golden, CO: National Renewable Energy Laboratory,; 2004.
[41] Kalinci Y, Hepbasli A, Dincer I. Life cycle assessment of hydrogen production from biomass gasification systems. International Journal of Hydrogen Energy. 2012;37:14026-39.
[42] Koroneos C, Dompros A, Roumbas G. Hydrogen production via biomass gasification—A life cycle assessment approach. Chemical Engineering and Processing: Process Intensification. 2008;47:1261-8.
[43] Lubis LL, Dincer I, Rosen MA. Life Cycle Assessment of Hydrogen Production Using Nuclear Energy: An Application Based on Thermochemical Water Splitting. Anglais. 2010;132:021004-1 to -6.
[44] Ozbilen A, Dincer I, Rosen MA. A comparative life cycle analysis of hydrogen production via thermochemical water splitting using a Cu–Cl cycle. International Journal of Hydrogen Energy. 2011;36:11321-7.
[45] ASTM. ASTM Standard D7566: Specification for Aviation Turbine Fuel Containing Synthesized Hydrocarbons. West Conshohocken, PA2011.
[46] United States Department of Transportation (US DOT), Research and Innovative Technology Administration (RITA). National Transportation Atlas Database: Public-Use Airports. Washington, DC2011.
[47] Gerstle T, Wade MD. PT6A-68 Emissions Measurement Program Summary. U.S. Air Force Insitute for Environment, Safety and Occupational Health Risk Analysis,; 2002.
[48] Moses CA. Comparative Evaluation of Semi-Synthetic Jet Fuels: Addendum: Further Analysis of Hydrocarbons and Trace Materials to Support Dxxxx. New Braunfels, TX2009.

Appendix C: Ecoregion-specific LCA Input Parameters

Table C1: (Ecoregion 1) LCA model input parameters

Input parameter	Minimum value	Baseline value	Maximum value	Units
Temperature (January)	-13.77	-6.27	-1.21	°C
Temperature (February)	-11.68	-4.75	0.26	°C
Temperature (March)	-5.54	-0.02	4.75	°C
Temperature (April)	2.76	6.93	10.98	°C
Temperature (May)	9.82	12.94	16.42	°C
Temperature (June)	15.21	17.90	21.55	°C
Temperature (July)	17.91	20.33	24.09	°C
Temperature (August)	16.94	19.49	23.33	°C
Temperature (September)	12.26	15.27	18.97	°C
Temperature (October)	5.64	8.85	12.65	°C
Temperature (November)	-0.76	3.29	7.40	°C
Temperature (December)	-8.57	-3.05	1.52	°C
Solar radiation (January)	1.889	3.032	4.099	kWh m^{-2} day^{-1}
Solar radiation (February)	2.272	3.376	4.183	kWh m^{-2} day^{-1}
Solar radiation (March)	2.954	3.855	4.544	kWh m^{-2} day^{-1}
Solar radiation (April)	3.956	4.562	5.419	kWh m^{-2} day^{-1}
Solar radiation (May)	3.959	4.351	5.073	kWh m^{-2} day^{-1}
Solar radiation (June)	3.708	4.252	5.120	kWh m^{-2} day^{-1}
Solar radiation (July)	3.951	4.479	5.297	kWh m^{-2} day^{-1}
Solar radiation (August)	3.714	4.318	5.038	kWh m^{-2} day^{-1}
Solar radiation (September)	3.483	4.081	4.815	kWh m^{-2} day^{-1}
Solar radiation (October)	2.494	2.990	3.660	kWh m^{-2} day^{-1}
Solar radiation (November)	1.762	2.379	2.940	kWh m^{-2} day^{-1}
Solar radiation (December)	1.749	2.580	3.368	kWh m^{-2} day^{-1}
Atmospheric transmittance, Kt (January)	0.350	0.444	0.510	-
Atmospheric transmittance, Kt (February)	0.410	0.480	0.550	-

Input parameter (continued)	Minimum value	Baseline value	Maximum value	Units
Atmospheric transmittance, Kt (March)	0.400	0.464	0.520	-
Atmospheric transmittance, Kt (April)	0.370	0.443	0.520	-
Atmospheric transmittance, Kt (May)	0.340	0.455	0.530	-
Atmospheric transmittance, Kt (June)	0.380	0.470	0.540	-
Atmospheric transmittance, Kt (July)	0.410	0.493	0.550	-
Atmospheric transmittance, Kt (August)	0.420	0.491	0.560	-
Atmospheric transmittance, Kt (September)	0.370	0.482	0.570	-
Atmospheric transmittance, Kt (October)	0.370	0.452	0.540	-
Atmospheric transmittance, Kt (November)	0.290	0.399	0.450	-
Atmospheric transmittance, Kt (December)	0.330	0.415	0.470	-
Albedo of original land conditions (January)	0.1407	0.2740	0.3834	-
Albedo of original land conditions (February)	0.1486	0.2973	0.3899	-
Albedo of original land conditions (March)	0.1350	0.1940	0.2535	-
Albedo of original land conditions (April)	0.1233	0.1300	0.1429	-
Albedo of original land conditions (May)	0.1300	0.1318	0.1339	-
Albedo of original land conditions (June)	0.1409	0.1428	0.1459	-
Albedo of original land conditions (July)	0.1411	0.1430	0.1466	-
Albedo of original land conditions (August)	0.1383	0.1393	0.1424	-
Albedo of original land conditions (September)	0.1330	0.1342	0.1362	-
Albedo of original land conditions (October)	0.1248	0.1276	0.1316	-
Albedo of original land conditions (November)	0.1208	0.1225	0.1258	-
Albedo of original land conditions (December)	0.1280	0.1535	0.1868	-
Original net primary productivity (NPP)	0.000440	0.002820	0.009871	kg C m^{-2} day^{-1}
Latitude	40.331	42.787	47.240	°
Amount of original biomass on land	0	2.909	13.988	kg m^{-2}
Distance to refinery	3.74	249	864	km

Table C2: Central USA Plains (Ecoregion 2) LCA model input parameters

Input parameter	Minimum value	Baseline value	Maximum value	Units
Temperature (January)	-8.07	-4.13	1.28	°C
Temperature (February)	-6.18	-2.22	3.42	°C
Temperature (March)	-0.93	3.19	8.29	°C
Temperature (April)	5.63	9.80	13.97	°C
Temperature (May)	10.98	15.58	19.04	°C
Temperature (June)	16.52	20.89	23.72	°C
Temperature (July)	19.79	22.91	25.67	°C
Temperature (August)	19.45	22.01	25.19	°C
Temperature (September)	15.25	17.97	21.22	°C
Temperature (October)	8.63	11.39	14.86	°C
Temperature (November)	1.62	5.00	8.98	°C
Temperature (December)	-5.67	-1.83	2.94	°C
Solar radiation (January)	0.985	2.266	3.257	kWh m^{-2} day^{-1}
Solar radiation (February)	1.746	3.030	4.178	kWh m^{-2} day^{-1}
Solar radiation (March)	3.092	3.913	4.738	kWh m^{-2} day^{-1}
Solar radiation (April)	3.957	4.385	5.493	kWh m^{-2} day^{-1}
Solar radiation (May)	3.974	4.322	5.196	kWh m^{-2} day^{-1}
Solar radiation (June)	4.485	4.925	5.629	kWh m^{-2} day^{-1}
Solar radiation (July)	4.503	5.157	6.045	kWh m^{-2} day^{-1}
Solar radiation (August)	4.228	4.686	5.344	kWh m^{-2} day^{-1}
Solar radiation (September)	4.008	4.543	5.417	kWh m^{-2} day^{-1}
Solar radiation (October)	2.405	3.312	4.089	kWh m^{-2} day^{-1}
Solar radiation (November)	1.533	2.501	3.222	kWh m^{-2} day^{-1}
Solar radiation (December)	1.180	2.151	3.027	kWh m^{-2} day^{-1}
Atmospheric transmittance, Kt (January)	0.330	0.416	0.480	-
Atmospheric transmittance, Kt (February)	0.370	0.440	0.490	-
Atmospheric transmittance, Kt (March)	0.390	0.463	0.560	-
Atmospheric transmittance, Kt (April)	0.350	0.471	0.560	-

Input parameter (continued)	Minimum value	Baseline value	Maximum value	Units
Atmospheric transmittance, Kt (May)	0.390	0.488	0.610	-
Atmospheric transmittance, Kt (June)	0.470	0.516	0.600	-
Atmospheric transmittance, Kt (July)	0.400	0.539	0.590	-
Atmospheric transmittance, Kt (August)	0.460	0.519	0.580	-
Atmospheric transmittance, Kt (September)	0.420	0.527	0.640	-
Atmospheric transmittance, Kt (October)	0.380	0.486	0.540	-
Atmospheric transmittance, Kt (November)	0.280	0.409	0.510	-
Atmospheric transmittance, Kt (December)	0.270	0.396	0.490	-
Albedo of original land conditions (January)	0.1739	0.3750	0.5251	-
Albedo of original land conditions (February)	0.1594	0.3900	0.5244	-
Albedo of original land conditions (March)	0.1506	0.2128	0.3029	-
Albedo of original land conditions (April)	0.1489	0.1523	0.1553	-
Albedo of original land conditions (May)	0.1495	0.1540	0.1585	-
Albedo of original land conditions (June)	0.1529	0.1547	0.1562	-
Albedo of original land conditions (July)	0.1543	0.1588	0.1611	-
Albedo of original land conditions (August)	0.1516	0.1607	0.1652	-
Albedo of original land conditions (September)	0.1494	0.1554	0.1590	-
Albedo of original land conditions (October)	0.1494	0.1544	0.1645	-
Albedo of original land conditions (November)	0.1501	0.1586	0.1704	-
Albedo of original land conditions (December)	0.1506	0.2818	0.4186	-
Original net primary productivity (NPP)	0.001524	0.002739	0.011188	kg C m^{-2} day^{-1}
Latitude	38.286	41.215	44.556	°
Amount of original biomass on land	0	0.714	6.14	kg m^{-2}
Distance to refinery	0.654	114	322	km

Table C3: Cold Deserts (Ecoregion 3) LCA model input parameters

Input parameter	Minimum value	Baseline value	Maximum value	Units
Temperature (January)	-7.98	-1.79	4.43	°C
Temperature (February)	-6.32	0.57	6.46	°C
Temperature (March)	-1.19	5.22	10.11	°C
Temperature (April)	3.73	9.17	14.19	°C
Temperature (May)	8.79	13.76	19.29	°C
Temperature (June)	13.19	18.11	24.51	°C
Temperature (July)	17.26	22.12	28.16	°C
Temperature (August)	16.38	21.50	26.90	°C
Temperature (September)	12.02	16.59	22.65	°C
Temperature (October)	5.68	10.09	16.36	°C
Temperature (November)	-1.66	3.29	8.97	°C
Temperature (December)	-7.34	-1.87	4.12	°C
Solar radiation (January)	1.039	3.146	7.004	kWh m^{-2} day^{-1}
Solar radiation (February)	1.849	4.078	7.275	kWh m^{-2} day^{-1}
Solar radiation (March)	2.91	5.252	7.94	kWh m^{-2} day^{-1}
Solar radiation (April)	4.707	6.208	8.812	kWh m^{-2} day^{-1}
Solar radiation (May)	5.214	7.066	9.504	kWh m^{-2} day^{-1}
Solar radiation (June)	5.583	8.064	10.009	kWh m^{-2} day^{-1}
Solar radiation (July)	6.595	8.511	9.962	kWh m^{-2} day^{-1}
Solar radiation (August)	5.747	7.661	9.447	kWh m^{-2} day^{-1}
Solar radiation (September)	5.487	7.034	8.769	kWh m^{-2} day^{-1}
Solar radiation (October)	3.392	5.603	7.872	kWh m^{-2} day^{-1}
Solar radiation (November)	1.671	3.826	7.391	kWh m^{-2} day^{-1}
Solar radiation (December)	1.198	2.992	6.64	kWh m^{-2} day^{-1}
Atmospheric transmittance, Kt (January)	0.400	0.510	0.580	-
Atmospheric transmittance, Kt (February)	0.460	0.535	0.610	-
Atmospheric transmittance, Kt (March)	0.510	0.564	0.620	-
Atmospheric transmittance, Kt (April)	0.470	0.572	0.650	-

Input parameter (continued)	Minimum value	Baseline value	Maximum value	Units
Atmospheric transmittance, Kt (May)	0.510	0.575	0.620	-
Atmospheric transmittance, Kt (June)	0.540	0.608	0.670	-
Atmospheric transmittance, Kt (July)	0.540	0.609	0.650	-
Atmospheric transmittance, Kt (August)	0.500	0.592	0.640	-
Atmospheric transmittance, Kt (September)	0.530	0.598	0.660	-
Atmospheric transmittance, Kt (October)	0.480	0.572	0.650	-
Atmospheric transmittance, Kt (November)	0.450	0.522	0.610	-
Atmospheric transmittance, Kt (December)	0.400	0.518	0.600	-
Albedo of original land conditions (January)	0.2980	0.4355	0.5728	-
Albedo of original land conditions (February)	0.2708	0.3803	0.5115	-
Albedo of original land conditions (March)	0.1912	0.2368	0.2822	-
Albedo of original land conditions (April)	0.1632	0.1706	0.1866	-
Albedo of original land conditions (May)	0.1592	0.1623	0.1649	-
Albedo of original land conditions (June)	0.1585	0.1617	0.1663	-
Albedo of original land conditions (July)	0.1639	0.1661	0.1698	-
Albedo of original land conditions (August)	0.1708	0.1725	0.1759	-
Albedo of original land conditions (September)	0.1751	0.1768	0.1806	-
Albedo of original land conditions (October)	0.1736	0.1774	0.1819	-
Albedo of original land conditions (November)	0.1787	0.1984	0.2439	-
Albedo of original land conditions (December)	0.3002	0.3577	0.3931	-
Original net primary productivity (NPP)	0.000134	0.002044	0.011016	kg C m^{-2} day^{-1}
Latitude	34.591	41.206	48.925	°
Amount of original biomass on land	0	0.089	1.444	kg m^{-2}
Distance to refinery	1.65	249	532	km

Table C4: Everglades (Ecoregion 4) LCA model input parameters

Input parameter	Minimum value	Baseline value	Maximum value	Units
Temperature (January)	17.14	18.81	19.94	°C
Temperature (February)	18.51	19.91	20.90	°C
Temperature (March)	20.19	21.27	22.00	°C
Temperature (April)	22.21	23.15	23.82	°C
Temperature (May)	25.04	25.56	26.06	°C
Temperature (June)	27.03	27.46	27.71	°C
Temperature (July)	27.83	28.23	28.61	°C
Temperature (August)	27.97	28.37	28.59	°C
Temperature (September)	27.24	27.79	28.00	°C
Temperature (October)	24.72	25.83	26.35	°C
Temperature (November)	21.41	22.76	23.65	°C
Temperature (December)	18.39	20.08	21.15	°C
Solar radiation (January)	4.743	5.203	5.839	kWh m^{-2} day^{-1}
Solar radiation (February)	4.914	5.315	6.102	kWh m^{-2} day^{-1}
Solar radiation (March)	4.948	5.577	6.421	kWh m^{-2} day^{-1}
Solar radiation (April)	5.499	5.994	6.730	kWh m^{-2} day^{-1}
Solar radiation (May)	5.026	5.422	5.951	kWh m^{-2} day^{-1}
Solar radiation (June)	3.924	4.280	4.814	kWh m^{-2} day^{-1}
Solar radiation (July)	3.871	4.457	5.148	kWh m^{-2} day^{-1}
Solar radiation (August)	3.913	4.322	4.987	kWh m^{-2} day^{-1}
Solar radiation (September)	3.624	3.959	4.504	kWh m^{-2} day^{-1}
Solar radiation (October)	3.956	4.486	5.082	kWh m^{-2} day^{-1}
Solar radiation (November)	4.008	4.663	5.304	kWh m^{-2} day^{-1}
Solar radiation (December)	3.816	4.328	4.995	kWh m^{-2} day^{-1}
Atmospheric transmittance, Kt (January)	0.430	0.540	0.600	-
Atmospheric transmittance, Kt (February)	0.500	0.553	0.620	-
Atmospheric transmittance, Kt (March)	0.480	0.556	0.630	-
Atmospheric transmittance, Kt (April)	0.500	0.571	0.650	-
Atmospheric transmittance, Kt (May)	0.490	0.551	0.590	-

Input parameter (continued)	Minimum value	Baseline value	Maximum value	Units
Atmospheric transmittance, Kt (June)	0.380	0.477	0.570	-
Atmospheric transmittance, Kt (July)	0.430	0.485	0.560	-
Atmospheric transmittance, Kt (August)	0.430	0.486	0.520	-
Atmospheric transmittance, Kt (September)	0.410	0.483	0.530	-
Atmospheric transmittance, Kt (October)	0.470	0.531	0.590	-
Atmospheric transmittance, Kt (November)	0.440	0.540	0.590	-
Atmospheric transmittance, Kt (December)	0.470	0.540	0.590	-
Albedo of original land conditions (January)	0.1398	0.1421	0.1446	-
Albedo of original land conditions (February)	0.1374	0.1409	0.1444	-
Albedo of original land conditions (March)	0.1401	0.1427	0.1468	-
Albedo of original land conditions (April)	0.1414	0.1438	0.1498	-
Albedo of original land conditions (May)	0.1444	0.1467	0.1503	-
Albedo of original land conditions (June)	0.1330	0.1387	0.1442	-
Albedo of original land conditions (July)	0.1346	0.1388	0.1444	-
Albedo of original land conditions (August)	0.1260	0.1339	0.1384	-
Albedo of original land conditions (September)	0.1298	0.1357	0.1402	-
Albedo of original land conditions (October)	0.1349	0.1389	0.1409	-
Albedo of original land conditions (November)	0.1393	0.1409	0.1431	-
Albedo of original land conditions (December)	0.1385	0.1420	0.1445	-
Original net primary productivity (NPP)	0.00108	0.00874	0.01795	kg C m^{-2} day^{-1}
Latitude	25.853	26.237	26.742	°
Amount of original biomass on land	0.000	2.646	9.667	kg m^{-2}
Distance to refinery	597	656	692	km

Table C5: Marine West Coast Forest (Ecoregion 5) LCA model input parameters

Input parameter	Minimum value	Baseline value	Maximum value	Units
Temperature (January)	3.58	5.92	10.83	°C
Temperature (February)	4.65	6.66	11.55	°C
Temperature (March)	6.61	8.28	11.79	°C
Temperature (April)	8.28	9.99	13.14	°C
Temperature (May)	10.55	12.71	15.54	°C
Temperature (June)	11.84	15.13	18.06	°C
Temperature (July)	12.31	17.43	21.12	°C
Temperature (August)	12.89	17.72	21.19	°C
Temperature (September)	12.69	15.68	19.34	°C
Temperature (October)	9.91	11.79	16.95	°C
Temperature (November)	5.80	8.02	13.41	°C
Temperature (December)	2.90	5.32	10.98	°C
Solar radiation (January)	1.152	1.687	3.632	kWh m^{-2} day^{-1}
Solar radiation (February)	2.142	2.529	3.637	kWh m^{-2} day^{-1}
Solar radiation (March)	1.728	2.723	5.311	kWh m^{-2} day^{-1}
Solar radiation (April)	2.766	3.815	6.347	kWh m^{-2} day^{-1}
Solar radiation (May)	2.834	4.193	7.260	kWh m^{-2} day^{-1}
Solar radiation (June)	3.163	4.697	7.968	kWh m^{-2} day^{-1}
Solar radiation (July)	3.740	5.953	8.784	kWh m^{-2} day^{-1}
Solar radiation (August)	3.344	5.474	8.170	kWh m^{-2} day^{-1}
Solar radiation (September)	3.531	4.995	7.369	kWh m^{-2} day^{-1}
Solar radiation (October)	2.043	2.979	5.689	kWh m^{-2} day^{-1}
Solar radiation (November)	1.174	1.793	4.484	kWh m^{-2} day^{-1}
Solar radiation (December)	1.061	1.558	3.679	kWh m^{-2} day^{-1}
Atmospheric transmittance, Kt (January)	0.310	0.375	0.490	-
Atmospheric transmittance, Kt (February)	0.320	0.433	0.560	-
Atmospheric transmittance, Kt (March)	0.330	0.439	0.570	-
Atmospheric transmittance, Kt (April)	0.360	0.450	0.560	-

Input parameter (continued)	Minimum value	Baseline value	Maximum value	Units
Atmospheric transmittance, Kt (May)	0.370	0.466	0.610	-
Atmospheric transmittance, Kt (June)	0.410	0.497	0.590	-
Atmospheric transmittance, Kt (July)	0.400	0.557	0.650	-
Atmospheric transmittance, Kt (August)	0.490	0.569	0.620	-
Atmospheric transmittance, Kt (September)	0.430	0.552	0.650	-
Atmospheric transmittance, Kt (October)	0.340	0.460	0.570	-
Atmospheric transmittance, Kt (November)	0.310	0.370	0.470	-
Atmospheric transmittance, Kt (December)	0.320	0.366	0.500	-
Albedo of original land conditions (January)	0.1300	0.1322	0.1388	-
Albedo of original land conditions (February)	0.1284	0.1324	0.1369	-
Albedo of original land conditions (March)	0.1309	0.1324	0.1347	-
Albedo of original land conditions (April)	0.1301	0.1338	0.1368	-
Albedo of original land conditions (May)	0.1353	0.1401	0.1433	-
Albedo of original land conditions (June)	0.1397	0.1424	0.1449	-
Albedo of original land conditions (July)	0.1409	0.1458	0.1518	-
Albedo of original land conditions (August)	0.1473	0.1485	0.1503	-
Albedo of original land conditions (September)	0.1344	0.1395	0.1471	-
Albedo of original land conditions (October)	0.1296	0.1320	0.1368	-
Albedo of original land conditions (November)	0.1228	0.1278	0.1325	-
Albedo of original land conditions (December)	0.1249	0.1359	0.1651	-
Original net primary productivity (NPP)	0.000325	0.003317	0.011748	kg C m^{-2} day^{-1}
Latitude	37.040	45.605	48.977	°
Amount of original biomass on land	0	0.951	8.636	kg m^{-2}
Distance to refinery	2.16	180	529	km

Table C6: Mediterranean California (Ecoregion 6) LCA model input parameters

Input parameter	Minimum value	Baseline value	Maximum value	Units
Temperature (January)	6.47	10.25	14.33	°C
Temperature (February)	6.84	11.61	14.80	°C
Temperature (March)	8.70	13.03	15.75	°C
Temperature (April)	10.67	14.75	18.23	°C
Temperature (May)	11.71	17.34	20.34	°C
Temperature (June)	13.35	19.92	24.17	°C
Temperature (July)	14.19	22.01	27.61	°C
Temperature (August)	15.02	22.04	26.69	°C
Temperature (September)	14.90	20.90	24.59	°C
Temperature (October)	14.43	17.79	21.25	°C
Temperature (November)	9.95	13.41	17.00	°C
Temperature (December)	6.26	10.19	14.10	°C
Solar radiation (January)	2.206	3.513	5.599	kWh m^{-2} day^{-1}
Solar radiation (February)	3.054	3.839	5.114	kWh m^{-2} day^{-1}
Solar radiation (March)	4.896	5.437	6.506	kWh m^{-2} day^{-1}
Solar radiation (April)	5.581	6.348	7.125	kWh m^{-2} day^{-1}
Solar radiation (May)	4.771	7.099	8.643	kWh m^{-2} day^{-1}
Solar radiation (June)	4.654	7.795	10.114	kWh m^{-2} day^{-1}
Solar radiation (July)	4.267	8.079	9.913	kWh m^{-2} day^{-1}
Solar radiation (August)	4.506	7.698	9.397	kWh m^{-2} day^{-1}
Solar radiation (September)	4.39	6.841	8.597	kWh m^{-2} day^{-1}
Solar radiation (October)	4.647	5.549	6.909	kWh m^{-2} day^{-1}
Solar radiation (November)	3.338	4.325	6.168	kWh m^{-2} day^{-1}
Solar radiation (December)	2.308	3.518	5.495	kWh m^{-2} day^{-1}
Atmospheric transmittance, Kt (January)	0.390	0.535	0.630	-
Atmospheric transmittance, Kt (February)	0.410	0.555	0.680	-
Atmospheric transmittance, Kt (March)	0.520	0.606	0.710	-
Atmospheric transmittance, Kt (April)	0.560	0.645	0.700	-

Input parameter (continued)	Minimum value	Baseline value	Maximum value	Units
Atmospheric transmittance, Kt (May)	0.560	0.694	0.760	-
Atmospheric transmittance, Kt (June)	0.600	0.705	0.780	-
Atmospheric transmittance, Kt (July)	0.640	0.686	0.780	-
Atmospheric transmittance, Kt (August)	0.630	0.669	0.730	-
Atmospheric transmittance, Kt (September)	0.590	0.659	0.710	-
Atmospheric transmittance, Kt (October)	0.560	0.634	0.680	-
Atmospheric transmittance, Kt (November)	0.480	0.583	0.690	-
Atmospheric transmittance, Kt (December)	0.460	0.527	0.660	-
Albedo of original land conditions (January)	0.1408	0.1459	0.1511	-
Albedo of original land conditions (February)	0.1461	0.1478	0.1494	-
Albedo of original land conditions (March)	0.1455	0.1508	0.1551	-
Albedo of original land conditions (April)	0.1441	0.1501	0.1552	-
Albedo of original land conditions (May)	0.1465	0.1503	0.1589	-
Albedo of original land conditions (June)	0.1428	0.1536	0.1628	-
Albedo of original land conditions (July)	0.1492	0.1605	0.1689	-
Albedo of original land conditions (August)	0.1557	0.1640	0.1689	-
Albedo of original land conditions (September)	0.1586	0.1660	0.1719	-
Albedo of original land conditions (October)	0.1485	0.1603	0.1700	-
Albedo of original land conditions (November)	0.1424	0.1491	0.1536	-
Albedo of original land conditions (December)	0.1368	0.1443	0.1506	-
Original net primary productivity (NPP)	0.000463	0.004113	0.016094	kg C m^{-2} day^{-1}
Latitude	32.544	36.658	40.686	°
Amount of original biomass on land	0	0.395	4.739	kg m^{-2}
Distance to refinery	2.43	74.2	292	km

Table C7: Mississippi Alluvial & Southeast USA (Ecoregion 7) LCA model input parameters

Input parameter	Minimum value	Baseline value	Maximum value	Units
Temperature (January)	-1.54	6.40	18.11	°C
Temperature (February)	-0.43	8.23	19.14	°C
Temperature (March)	2.87	12.10	20.61	°C
Temperature (April)	7.79	16.62	22.73	°C
Temperature (May)	12.62	21.24	25.70	°C
Temperature (June)	17.71	25.25	27.75	°C
Temperature (July)	21.28	26.94	28.57	°C
Temperature (August)	21.06	26.48	28.52	°C
Temperature (September)	17.30	23.43	27.79	°C
Temperature (October)	11.59	18.03	25.43	°C
Temperature (November)	6.82	12.86	22.17	°C
Temperature (December)	1.58	7.98	19.50	°C
Solar radiation (January)	2.444	3.784	5.751	kWh m^{-2} day^{-1}
Solar radiation (February)	3.273	4.171	6.062	kWh m^{-2} day^{-1}
Solar radiation (March)	3.707	4.657	6.381	kWh m^{-2} day^{-1}
Solar radiation (April)	3.985	5.099	6.899	kWh m^{-2} day^{-1}
Solar radiation (May)	4.058	4.998	6.612	kWh m^{-2} day^{-1}
Solar radiation (June)	4.155	4.996	5.692	kWh m^{-2} day^{-1}
Solar radiation (July)	3.902	4.904	5.846	kWh m^{-2} day^{-1}
Solar radiation (August)	3.96	4.862	5.912	kWh m^{-2} day^{-1}
Solar radiation (September)	3.507	4.291	4.935	kWh m^{-2} day^{-1}
Solar radiation (October)	3.282	4.302	5.299	kWh m^{-2} day^{-1}
Solar radiation (November)	2.637	3.953	5.544	kWh m^{-2} day^{-1}
Solar radiation (December)	2.546	3.527	5.015	kWh m^{-2} day^{-1}
Atmospheric transmittance, Kt (January)	0.360	0.458	0.550	-
Atmospheric transmittance, Kt (February)	0.380	0.457	0.570	-
Atmospheric transmittance, Kt (March)	0.400	0.490	0.580	-

Input parameter (continued)	Minimum value	Baseline value	Maximum value	Units
Atmospheric transmittance, Kt (April)	0.400	0.509	0.570	-
Atmospheric transmittance, Kt (May)	0.400	0.503	0.560	-
Atmospheric transmittance, Kt (June)	0.410	0.496	0.570	-
Atmospheric transmittance, Kt (July)	0.450	0.504	0.600	-
Atmospheric transmittance, Kt (August)	0.440	0.495	0.590	-
Atmospheric transmittance, Kt (September)	0.430	0.519	0.600	-
Atmospheric transmittance, Kt (October)	0.420	0.546	0.660	-
Atmospheric transmittance, Kt (November)	0.360	0.490	0.620	-
Atmospheric transmittance, Kt (December)	0.390	0.465	0.530	-
Albedo of original land conditions (January)	0.1340	0.1388	0.1471	-
Albedo of original land conditions (February)	0.1331	0.1428	0.1732	-
Albedo of original land conditions (March)	0.1324	0.1345	0.1384	-
Albedo of original land conditions (April)	0.1333	0.1355	0.1378	-
Albedo of original land conditions (May)	0.1368	0.1377	0.1389	-
Albedo of original land conditions (June)	0.1375	0.1390	0.1411	-
Albedo of original land conditions (July)	0.1379	0.1393	0.1416	-
Albedo of original land conditions (August)	0.1354	0.1385	0.1410	-
Albedo of original land conditions (September)	0.1321	0.1335	0.1356	-
Albedo of original land conditions (October)	0.1291	0.1332	0.1362	-
Albedo of original land conditions (November)	0.1310	0.1348	0.1375	-
Albedo of original land conditions (December)	0.1323	0.1345	0.1382	-
Original net primary productivity (NPP)	0.000213	0.004863	0.016697	kg C m^{-2} day^{-1}
Latitude	26.151	34.374	41.964	°
Amount of original biomass on land	0	2.826	11.456	kg m^{-2}
Distance to refinery	1.07	133	662	km

Table C8: Mixed Wood Plains (Ecoregion 8) LCA model input parameters

Input parameter	Minimum value	Baseline value	Maximum value	Units
Temperature (January)	-13.61	-5.57	0.38	°C
Temperature (February)	-11.56	-3.90	1.74	°C
Temperature (March)	-5.49	1.10	5.59	°C
Temperature (April)	2.77	8.05	11.47	°C
Temperature (May)	9.66	13.94	16.90	°C
Temperature (June)	14.20	19.13	22.31	°C
Temperature (July)	16.83	21.58	25.17	°C
Temperature (August)	16.93	20.73	24.54	°C
Temperature (September)	12.29	16.48	20.58	°C
Temperature (October)	5.67	10.00	14.31	°C
Temperature (November)	-2.17	3.87	9.00	°C
Temperature (December)	-10.26	-2.67	3.41	°C
Solar radiation (January)	0.913	2.438	4.114	kWh m^{-2} day^{-1}
Solar radiation (February)	1.628	2.972	4.378	kWh m^{-2} day^{-1}
Solar radiation (March)	2.446	3.830	4.831	kWh m^{-2} day^{-1}
Solar radiation (April)	3.889	4.711	6.019	kWh m^{-2} day^{-1}
Solar radiation (May)	3.907	4.550	5.726	kWh m^{-2} day^{-1}
Solar radiation (June)	3.708	4.715	5.906	kWh m^{-2} day^{-1}
Solar radiation (July)	4.112	5.096	6.439	kWh m^{-2} day^{-1}
Solar radiation (August)	3.815	4.658	5.714	kWh m^{-2} day^{-1}
Solar radiation (September)	3.516	4.351	5.085	kWh m^{-2} day^{-1}
Solar radiation (October)	2.274	3.030	3.690	kWh m^{-2} day^{-1}
Solar radiation (November)	1.362	2.353	3.075	kWh m^{-2} day^{-1}
Solar radiation (December)	0.928	2.301	3.463	kWh m^{-2} day^{-1}
Atmospheric transmittance, Kt (January)	0.420	0.460	0.530	-
Atmospheric transmittance, Kt (February)	0.410	0.493	0.530	-
Atmospheric transmittance, Kt (March)	0.370	0.470	0.550	-

Input parameter (continued)	Minimum value	Baseline value	Maximum value	Units
Atmospheric transmittance, Kt (April)	0.380	0.457	0.540	-
Atmospheric transmittance, Kt (May)	0.400	0.477	0.550	-
Atmospheric transmittance, Kt (June)	0.420	0.510	0.580	-
Atmospheric transmittance, Kt (July)	0.430	0.525	0.590	-
Atmospheric transmittance, Kt (August)	0.450	0.503	0.570	-
Atmospheric transmittance, Kt (September)	0.370	0.503	0.610	-
Atmospheric transmittance, Kt (October)	0.350	0.448	0.530	-
Atmospheric transmittance, Kt (November)	0.290	0.375	0.430	-
Atmospheric transmittance, Kt (December)	0.330	0.412	0.490	-
Albedo of original land conditions (January)	0.2017	0.4142	0.4790	-
Albedo of original land conditions (February)	0.1706	0.3990	0.4753	-
Albedo of original land conditions (March)	0.1458	0.2428	0.3433	-
Albedo of original land conditions (April)	0.1390	0.1436	0.1512	-
Albedo of original land conditions (May)	0.1396	0.1436	0.1457	-
Albedo of original land conditions (June)	0.1475	0.1490	0.1498	-
Albedo of original land conditions (July)	0.1482	0.1503	0.1520	-
Albedo of original land conditions (August)	0.1469	0.1502	0.1526	-
Albedo of original land conditions (September)	0.1452	0.1466	0.1479	-
Albedo of original land conditions (October)	0.1417	0.1437	0.1451	-
Albedo of original land conditions (November)	0.1392	0.1480	0.1676	-
Albedo of original land conditions (December)	0.1619	0.2887	0.3934	-
Original net primary productivity (NPP)	0.000169	0.002795	0.010954	kg C m^{-2} day^{-1}
Latitude	39.690	43.050	47.354	°
Amount of original biomass on land	0	1.463	9.378	kg m^{-2}
Distance to refinery	4.19	201	889	km

Table C9: Mixed Wood Shield (Ecoregion 9) LCA model input parameters

Input parameter	Minimum value	Baseline value	Maximum value	Units
Temperature (January)	-15.40	-10.42	-5.29	°C
Temperature (February)	-12.23	-8.44	-4.03	°C
Temperature (March)	-5.09	-2.75	0.82	°C
Temperature (April)	3.20	4.87	8.07	°C
Temperature (May)	8.00	11.42	14.05	°C
Temperature (June)	12.08	16.61	19.29	°C
Temperature (July)	15.99	19.30	21.62	°C
Temperature (August)	16.83	18.49	20.60	°C
Temperature (September)	11.98	13.81	16.26	°C
Temperature (October)	4.93	7.06	9.79	°C
Temperature (November)	-3.49	-0.25	3.61	°C
Temperature (December)	-12.12	-7.46	-2.32	°C
Solar radiation (January)	1.158	2.588	3.539	kWh m^{-2} day^{-1}
Solar radiation (February)	1.853	3.012	4.422	kWh m^{-2} day^{-1}
Solar radiation (March)	2.623	3.859	4.875	kWh m^{-2} day^{-1}
Solar radiation (April)	4.462	5.103	5.999	kWh m^{-2} day^{-1}
Solar radiation (May)	4.248	4.962	5.917	kWh m^{-2} day^{-1}
Solar radiation (June)	4.555	5.107	6.098	kWh m^{-2} day^{-1}
Solar radiation (July)	5.098	5.687	6.450	kWh m^{-2} day^{-1}
Solar radiation (August)	4.505	5.025	5.911	kWh m^{-2} day^{-1}
Solar radiation (September)	3.702	4.248	4.699	kWh m^{-2} day^{-1}
Solar radiation (October)	2.132	2.788	3.194	kWh m^{-2} day^{-1}
Solar radiation (November)	1.255	2.285	2.919	kWh m^{-2} day^{-1}
Solar radiation (December)	0.837	2.479	3.196	kWh m^{-2} day^{-1}
Atmospheric transmittance, Kt (January)	0.410	0.456	0.500	-
Atmospheric transmittance, Kt (February)	0.440	0.507	0.560	-
Atmospheric transmittance, Kt (March)	0.420	0.500	0.570	-

Input parameter (continued)	Minimum value	Baseline value	Maximum value	Units
Atmospheric transmittance, Kt (April)	0.420	0.492	0.590	-
Atmospheric transmittance, Kt (May)	0.430	0.509	0.620	-
Atmospheric transmittance, Kt (June)	0.450	0.508	0.570	-
Atmospheric transmittance, Kt (July)	0.430	0.526	0.620	-
Atmospheric transmittance, Kt (August)	0.450	0.517	0.620	-
Atmospheric transmittance, Kt (September)	0.400	0.477	0.550	-
Atmospheric transmittance, Kt (October)	0.340	0.440	0.510	-
Atmospheric transmittance, Kt (November)	0.340	0.408	0.500	-
Atmospheric transmittance, Kt (December)	0.370	0.433	0.500	-
Albedo of original land conditions (January)	0.2370	0.4163	0.4755	-
Albedo of original land conditions (February)	0.3320	0.4341	0.4755	-
Albedo of original land conditions (March)	0.2114	0.3107	0.4138	-
Albedo of original land conditions (April)	0.1277	0.1539	0.2129	-
Albedo of original land conditions (May)	0.1279	0.1313	0.1349	-
Albedo of original land conditions (June)	0.1397	0.1401	0.1408	-
Albedo of original land conditions (July)	0.1399	0.1425	0.1456	-
Albedo of original land conditions (August)	0.1383	0.1414	0.1442	-
Albedo of original land conditions (September)	0.1368	0.1392	0.1409	-
Albedo of original land conditions (October)	0.1352	0.1361	0.1372	-
Albedo of original land conditions (November)	0.1307	0.1531	0.2199	-
Albedo of original land conditions (December)	0.1717	0.3230	0.4369	-
Original net primary productivity (NPP)	0.000172	0.002300	0.009151	kg C m^{-2} day^{-1}
Latitude	43.170	46.149	48.901	°
Amount of original biomass on land	0	1.364	7.042	kg m^{-2}
Distance to refinery	21.8	216	490	km

Table C10: Ozark/ Ouachita-Appalachian Forests (Ecoregion 10) LCA model input parameters

Input parameter	Minimum value	Baseline value	Maximum value	Units
Temperature (January)	-5.29	-0.04	6.51	°C
Temperature (February)	-3.92	1.78	8.70	°C
Temperature (March)	0.13	6.28	12.82	°C
Temperature (April)	5.86	11.97	16.79	°C
Temperature (May)	11.23	16.92	21.39	°C
Temperature (June)	15.63	21.58	25.58	°C
Temperature (July)	17.57	23.77	28.06	°C
Temperature (August)	17.28	23.22	27.84	°C
Temperature (September)	13.79	19.18	23.67	°C
Temperature (October)	7.89	12.97	17.66	°C
Temperature (November)	2.34	7.39	12.39	°C
Temperature (December)	-3.33	1.76	7.88	°C
Solar radiation (January)	2.009	3.26	4.602	kWh m^{-2} day^{-1}
Solar radiation (February)	2.576	3.602	4.963	kWh m^{-2} day^{-1}
Solar radiation (March)	3.206	4.097	5.139	kWh m^{-2} day^{-1}
Solar radiation (April)	3.818	4.463	5.188	kWh m^{-2} day^{-1}
Solar radiation (May)	3.646	4.424	5.114	kWh m^{-2} day^{-1}
Solar radiation (June)	3.73	4.713	5.696	kWh m^{-2} day^{-1}
Solar radiation (July)	3.068	4.675	6.734	kWh m^{-2} day^{-1}
Solar radiation (August)	3.512	4.679	6.156	kWh m^{-2} day^{-1}
Solar radiation (September)	3.482	4.382	5.382	kWh m^{-2} day^{-1}
Solar radiation (October)	2.669	3.829	4.673	kWh m^{-2} day^{-1}
Solar radiation (November)	2.103	3.259	4.362	kWh m^{-2} day^{-1}
Solar radiation (December)	2.04	3.024	4.243	kWh m^{-2} day^{-1}
Atmospheric transmittance, Kt (January)	0.320	0.409	0.470	-
Atmospheric transmittance, Kt (February)	0.310	0.425	0.490	-
Atmospheric transmittance, Kt (March)	0.350	0.449	0.540	-

Input parameter (continued)	Minimum value	Baseline value	Maximum value	Units
Atmospheric transmittance, Kt (April)	0.380	0.476	0.550	-
Atmospheric transmittance, Kt (May)	0.360	0.457	0.560	-
Atmospheric transmittance, Kt (June)	0.420	0.503	0.590	-
Atmospheric transmittance, Kt (July)	0.450	0.503	0.560	-
Atmospheric transmittance, Kt (August)	0.450	0.498	0.570	-
Atmospheric transmittance, Kt (September)	0.440	0.533	0.610	-
Atmospheric transmittance, Kt (October)	0.370	0.511	0.610	-
Atmospheric transmittance, Kt (November)	0.270	0.440	0.580	-
Atmospheric transmittance, Kt (December)	0.340	0.403	0.510	-
Albedo of original land conditions (January)	0.1529	0.1797	0.2128	-
Albedo of original land conditions (February)	0.1498	0.1845	0.2266	-
Albedo of original land conditions (March)	0.1482	0.1524	0.1570	-
Albedo of original land conditions (April)	0.1454	0.1482	0.1523	-
Albedo of original land conditions (May)	0.1483	0.1506	0.1534	-
Albedo of original land conditions (June)	0.1495	0.1510	0.1524	-
Albedo of original land conditions (July)	0.1492	0.1508	0.1523	-
Albedo of original land conditions (August)	0.1463	0.1488	0.1523	-
Albedo of original land conditions (September)	0.1425	0.1457	0.1480	-
Albedo of original land conditions (October)	0.1450	0.1478	0.1494	-
Albedo of original land conditions (November)	0.1489	0.1547	0.1601	-
Albedo of original land conditions (December)	0.1480	0.1619	0.1731	-
Original net primary productivity (NPP)	0.000025	0.002109	0.006987	kg C m^{-2} day^{-1}
Latitude	33.094	38.487	41.847	°
Amount of original biomass on land	0	0.527	5.186	kg m^{-2}
Distance to refinery	1.92	141	313	km

Table C11: South Central Semi-Arid Prairies (Ecoregion 11) LCA model input parameters

Input parameter	Minimum value	Baseline value	Maximum value	Units
Temperature (January)	-5.16	2.65	12.07	°C
Temperature (February)	-2.91	4.83	13.91	°C
Temperature (March)	1.79	9.49	17.36	°C
Temperature (April)	5.68	14.50	21.16	°C
Temperature (May)	10.95	19.59	25.32	°C
Temperature (June)	16.01	24.25	28.23	°C
Temperature (July)	19.31	26.88	29.92	°C
Temperature (August)	18.14	26.47	30.11	°C
Temperature (September)	13.69	22.01	26.76	°C
Temperature (October)	7.98	15.72	22.34	°C
Temperature (November)	1.46	9.08	17.37	°C
Temperature (December)	-4.18	3.33	12.89	°C
Solar radiation (January)	3.088	4.327	6.913	$kWh\ m^{-2}\ day^{-1}$
Solar radiation (February)	3.540	4.602	7.336	$kWh\ m^{-2}\ day^{-1}$
Solar radiation (March)	3.767	4.819	7.509	$kWh\ m^{-2}\ day^{-1}$
Solar radiation (April)	4.210	5.451	7.941	$kWh\ m^{-2}\ day^{-1}$
Solar radiation (May)	4.388	5.528	8.192	$kWh\ m^{-2}\ day^{-1}$
Solar radiation (June)	4.960	6.201	8.593	$kWh\ m^{-2}\ day^{-1}$
Solar radiation (July)	5.121	6.722	8.502	$kWh\ m^{-2}\ day^{-1}$
Solar radiation (August)	4.951	6.176	7.763	$kWh\ m^{-2}\ day^{-1}$
Solar radiation (September)	4.608	5.708	7.508	$kWh\ m^{-2}\ day^{-1}$
Solar radiation (October)	4.028	4.872	7.302	$kWh\ m^{-2}\ day^{-1}$
Solar radiation (November)	3.496	4.470	7.216	$kWh\ m^{-2}\ day^{-1}$
Solar radiation (December)	2.949	4.140	6.538	$kWh\ m^{-2}\ day^{-1}$
Atmospheric transmittance, Kt (January)	0.410	0.531	0.650	-
Atmospheric transmittance, Kt (February)	0.410	0.519	0.640	-
Atmospheric transmittance, Kt (March)	0.460	0.535	0.650	-

Input parameter (continued)	Minimum value	Baseline value	Maximum value	Units
Atmospheric transmittance, Kt (April)	0.470	0.552	0.630	-
Atmospheric transmittance, Kt (May)	0.440	0.550	0.640	-
Atmospheric transmittance, Kt (June)	0.480	0.562	0.640	-
Atmospheric transmittance, Kt (July)	0.550	0.607	0.660	-
Atmospheric transmittance, Kt (August)	0.490	0.563	0.630	-
Atmospheric transmittance, Kt (September)	0.490	0.565	0.640	-
Atmospheric transmittance, Kt (October)	0.410	0.550	0.650	-
Atmospheric transmittance, Kt (November)	0.380	0.541	0.660	-
Atmospheric transmittance, Kt (December)	0.380	0.520	0.610	-
Albedo of original land conditions (January)	0.1714	0.1980	0.2262	-
Albedo of original land conditions (February)	0.1750	0.1834	0.1972	-
Albedo of original land conditions (March)	0.1556	0.1649	0.1724	-
Albedo of original land conditions (April)	0.1553	0.1595	0.1619	-
Albedo of original land conditions (May)	0.1514	0.1545	0.1574	-
Albedo of original land conditions (June)	0.1519	0.1563	0.1623	-
Albedo of original land conditions (July)	0.1509	0.1591	0.1694	-
Albedo of original land conditions (August)	0.1537	0.1604	0.1750	-
Albedo of original land conditions (September)	0.1522	0.1587	0.1762	-
Albedo of original land conditions (October)	0.1499	0.1597	0.1692	-
Albedo of original land conditions (November)	0.1576	0.1698	0.1746	-
Albedo of original land conditions (December)	0.1849	0.1922	0.2016	-
Original net primary productivity (NPP)	0	0.001338	0.005877	kg C m^{-2} day^{-1}
Latitude	28.972	36.086	42.805	°
Amount of original biomass on land	0	0.130	1.774	kg m^{-2}
Distance to refinery	2.16	135	404	km

Table C12: Southeastern USA Plains (Ecoregion 12) LCA model input parameters

Input parameter	Minimum value	Baseline value	Maximum value	Units
Temperature (January)	-5.76	3.53	12.85	°C
Temperature (February)	-3.44	5.56	14.61	°C
Temperature (March)	3.03	10.02	17.97	°C
Temperature (April)	9.49	15.03	21.64	°C
Temperature (May)	15.44	19.85	25.91	°C
Temperature (June)	19.93	24.20	28.74	°C
Temperature (July)	22.63	26.08	29.55	°C
Temperature (August)	21.76	25.57	29.92	°C
Temperature (September)	17.77	21.92	27.10	°C
Temperature (October)	11.17	15.92	22.97	°C
Temperature (November)	4.10	10.39	18.11	°C
Temperature (December)	-3.50	5.00	13.57	°C
Solar radiation (January)	2.032	3.527	4.587	kWh m^{-2} day^{-1}
Solar radiation (February)	3.017	4.001	4.993	kWh m^{-2} day^{-1}
Solar radiation (March)	3.571	4.385	5.377	kWh m^{-2} day^{-1}
Solar radiation (April)	3.947	4.815	5.652	kWh m^{-2} day^{-1}
Solar radiation (May)	4.035	4.781	5.715	kWh m^{-2} day^{-1}
Solar radiation (June)	4.158	5.056	5.818	kWh m^{-2} day^{-1}
Solar radiation (July)	4.078	4.981	6.591	kWh m^{-2} day^{-1}
Solar radiation (August)	4.066	4.931	6.165	kWh m^{-2} day^{-1}
Solar radiation (September)	3.781	4.497	5.423	kWh m^{-2} day^{-1}
Solar radiation (October)	3.152	4.218	5.025	kWh m^{-2} day^{-1}
Solar radiation (November)	2.452	3.724	4.638	kWh m^{-2} day^{-1}
Solar radiation (December)	2.008	3.307	4.317	kWh m^{-2} day^{-1}
Atmospheric transmittance, Kt (January)	0.360	0.441	0.560	-
Atmospheric transmittance, Kt (February)	0.340	0.452	0.540	-
Atmospheric transmittance, Kt (March)	0.380	0.482	0.610	-

Input parameter (continued)	Minimum value	Baseline value	Maximum value	Units
Atmospheric transmittance, Kt (April)	0.410	0.497	0.550	-
Atmospheric transmittance, Kt (May)	0.420	0.496	0.590	-
Atmospheric transmittance, Kt (June)	0.400	0.502	0.600	-
Atmospheric transmittance, Kt (July)	0.440	0.512	0.590	-
Atmospheric transmittance, Kt (August)	0.440	0.510	0.580	-
Atmospheric transmittance, Kt (September)	0.440	0.537	0.610	-
Atmospheric transmittance, Kt (October)	0.380	0.533	0.640	-
Atmospheric transmittance, Kt (November)	0.350	0.483	0.580	-
Atmospheric transmittance, Kt (December)	0.370	0.447	0.550	-
Albedo of original land conditions (January)	0.1400	0.1544	0.1619	-
Albedo of original land conditions (February)	0.1396	0.1582	0.1744	-
Albedo of original land conditions (March)	0.1403	0.1412	0.1423	-
Albedo of original land conditions (April)	0.1403	0.1428	0.1453	-
Albedo of original land conditions (May)	0.1437	0.1448	0.1459	-
Albedo of original land conditions (June)	0.1437	0.1451	0.1476	-
Albedo of original land conditions (July)	0.1430	0.1450	0.1457	-
Albedo of original land conditions (August)	0.1400	0.1439	0.1468	-
Albedo of original land conditions (September)	0.1371	0.1408	0.1442	-
Albedo of original land conditions (October)	0.1349	0.1413	0.1464	-
Albedo of original land conditions (November)	0.1390	0.1449	0.1480	-
Albedo of original land conditions (December)	0.1398	0.1471	0.1540	-
Original net primary productivity (NPP)	0	0.002604	0.009461	kg C m^{-2} day^{-1}
Latitude	28.386	35.889	41.857	°
Amount of original biomass on land	0	1.53	8.618	kg m^{-2}
Distance to refinery	1.91	136	371	km

Table C13: Tamaulipas-Texas Semi-Arid Plain (Ecoregion 13) LCA model input parameters

Input parameter	Minimum value	Baseline value	Maximum value	Units
Temperature (January)	10.93	12.60	15.39	°C
Temperature (February)	12.95	14.75	17.56	°C
Temperature (March)	16.64	18.53	20.92	°C
Temperature (April)	20.53	22.45	24.63	°C
Temperature (May)	24.76	26.35	27.93	°C
Temperature (June)	27.69	29.01	30.53	°C
Temperature (July)	28.79	29.86	30.92	°C
Temperature (August)	29.06	30.14	31.30	°C
Temperature (September)	26.21	27.38	28.55	°C
Temperature (October)	21.63	23.03	24.76	°C
Temperature (November)	16.15	17.73	20.24	°C
Temperature (December)	11.27	13.00	15.97	°C
Solar radiation (January)	3.335	4.034	4.687	kWh m^{-2} day^{-1}
Solar radiation (February)	3.726	4.424	5.234	kWh m^{-2} day^{-1}
Solar radiation (March)	3.768	4.394	5.209	kWh m^{-2} day^{-1}
Solar radiation (April)	4.110	4.714	5.172	kWh m^{-2} day^{-1}
Solar radiation (May)	4.502	5.073	5.603	kWh m^{-2} day^{-1}
Solar radiation (June)	5.359	5.989	6.663	kWh m^{-2} day^{-1}
Solar radiation (July)	5.499	6.089	6.705	kWh m^{-2} day^{-1}
Solar radiation (August)	5.333	6.083	6.671	kWh m^{-2} day^{-1}
Solar radiation (September)	4.577	5.292	5.745	kWh m^{-2} day^{-1}
Solar radiation (October)	4.519	4.800	5.545	kWh m^{-2} day^{-1}
Solar radiation (November)	3.816	4.292	4.759	kWh m^{-2} day^{-1}
Solar radiation (December)	3.391	3.974	4.882	kWh m^{-2} day^{-1}
Atmospheric transmittance, Kt (January)	0.400	0.493	0.630	-
Atmospheric transmittance, Kt (February)	0.340	0.498	0.620	-
Atmospheric transmittance, Kt (March)	0.410	0.530	0.660	-
Atmospheric transmittance, Kt (April)	0.410	0.530	0.660	-
Atmospheric transmittance, Kt (May)	0.470	0.529	0.610	-

Input parameter (continued)	Minimum value	Baseline value	Maximum value	Units
Atmospheric transmittance, Kt (June)	0.500	0.567	0.660	-
Atmospheric transmittance, Kt (July)	0.520	0.599	0.670	-
Atmospheric transmittance, Kt (August)	0.490	0.580	0.630	-
Atmospheric transmittance, Kt (September)	0.470	0.556	0.640	-
Atmospheric transmittance, Kt (October)	0.390	0.532	0.620	-
Atmospheric transmittance, Kt (November)	0.410	0.520	0.640	-
Atmospheric transmittance, Kt (December)	0.360	0.501	0.610	-
Albedo of original land conditions (January)	0.1464	0.1525	0.1585	-
Albedo of original land conditions (February)	0.1460	0.1513	0.1563	-
Albedo of original land conditions (March)	0.1486	0.1512	0.1537	-
Albedo of original land conditions (April)	0.1477	0.1520	0.1561	-
Albedo of original land conditions (May)	0.1442	0.1515	0.1590	-
Albedo of original land conditions (June)	0.1469	0.1576	0.1643	-
Albedo of original land conditions (July)	0.1447	0.1573	0.1674	-
Albedo of original land conditions (August)	0.1470	0.1601	0.1739	-
Albedo of original land conditions (September)	0.1441	0.1566	0.1728	-
Albedo of original land conditions (October)	0.1521	0.1578	0.1699	-
Albedo of original land conditions (November)	0.1585	0.1633	0.1708	-
Albedo of original land conditions (December)	0.1510	0.1597	0.1675	-
Original net primary productivity (NPP)	0.000322	0.001163	0.004563	kg C m^{-2} day^{-1}
Latitude	26.214	28.363	29.344	°
Amount of original biomass on land	0.000	0.353	2.330	kg m^{-2}
Distance to refinery	11.8	125	239	km

Table C14: Temperate Prairies (Ecoregion 14) LCA model input parameters

Input parameter	Minimum value	Baseline value	Maximum value	Units
Temperature (January)	-15.73	-5.19	3.90	°C
Temperature (February)	-12.86	-2.65	6.27	°C
Temperature (March)	-6.01	3.52	10.99	°C
Temperature (April)	3.84	10.37	15.95	°C
Temperature (May)	10.99	16.34	20.69	°C
Temperature (June)	16.20	21.58	25.03	°C
Temperature (July)	18.75	23.98	27.81	°C
Temperature (August)	18.14	23.01	27.70	°C
Temperature (September)	12.36	18.27	23.02	°C
Temperature (October)	4.59	11.50	16.97	°C
Temperature (November)	-4.82	3.85	10.80	°C
Temperature (December)	-13.07	-3.40	4.94	°C
Solar radiation (January)	1.233	2.801	4.154	kWh m^{-2} day^{-1}
Solar radiation (February)	1.961	3.497	4.403	kWh m^{-2} day^{-1}
Solar radiation (March)	2.854	4.244	4.850	kWh m^{-2} day^{-1}
Solar radiation (April)	4.218	5.048	6.304	kWh m^{-2} day^{-1}
Solar radiation (May)	4.210	4.972	5.772	kWh m^{-2} day^{-1}
Solar radiation (June)	4.798	5.356	5.985	kWh m^{-2} day^{-1}
Solar radiation (July)	5.210	6.049	7.066	kWh m^{-2} day^{-1}
Solar radiation (August)	4.608	5.405	6.237	kWh m^{-2} day^{-1}
Solar radiation (September)	4.238	5.077	5.612	kWh m^{-2} day^{-1}
Solar radiation (October)	2.875	3.890	4.533	kWh m^{-2} day^{-1}
Solar radiation (November)	2.359	3.251	4.180	kWh m^{-2} day^{-1}
Solar radiation (December)	1.560	2.751	4.025	kWh m^{-2} day^{-1}
Atmospheric transmittance, Kt (January)	0.410	0.472	0.540	-
Atmospheric transmittance, Kt (February)	0.330	0.469	0.550	-
Atmospheric transmittance, Kt (March)	0.360	0.484	0.580	-

Input parameter (continued)	Minimum value	Baseline value	Maximum value	Units
Atmospheric transmittance, Kt (April)	0.380	0.476	0.560	-
Atmospheric transmittance, Kt (May)	0.350	0.493	0.580	-
Atmospheric transmittance, Kt (June)	0.440	0.530	0.620	-
Atmospheric transmittance, Kt (July)	0.410	0.549	0.610	-
Atmospheric transmittance, Kt (August)	0.430	0.536	0.590	-
Atmospheric transmittance, Kt (September)	0.410	0.547	0.620	-
Atmospheric transmittance, Kt (October)	0.390	0.515	0.630	-
Atmospheric transmittance, Kt (November)	0.310	0.468	0.590	-
Atmospheric transmittance, Kt (December)	0.380	0.462	0.560	-
Albedo of original land conditions (January)	0.2083	0.3944	0.5382	-
Albedo of original land conditions (February)	0.2220	0.3654	0.4888	-
Albedo of original land conditions (March)	0.1712	0.2158	0.2529	-
Albedo of original land conditions (April)	0.1512	0.1542	0.1622	-
Albedo of original land conditions (May)	0.1462	0.1503	0.1553	-
Albedo of original land conditions (June)	0.1500	0.1512	0.1553	-
Albedo of original land conditions (July)	0.1578	0.1592	0.1619	-
Albedo of original land conditions (August)	0.1587	0.1616	0.1655	-
Albedo of original land conditions (September)	0.1556	0.1594	0.1620	-
Albedo of original land conditions (October)	0.1562	0.1650	0.1727	-
Albedo of original land conditions (November)	0.1637	0.1733	0.1819	-
Albedo of original land conditions (December)	0.1870	0.3041	0.3920	-
Original net primary productivity (NPP)	0.000005	0.001434	0.004206	kg C m^{-2} day^{-1}
Latitude	35.366	41.308	48.759	°
Amount of original biomass on land	0	0.105	1.91	kg m^{-2}
Distance to refinery	3.45	256	457	km

Table C15: Texas-Louisiana Coastal Plain (Ecoregion 15) LCA model input parameters

Input parameter	Minimum value	Baseline value	Maximum value	Units
Temperature (January)	9.95	12.01	15.96	°C
Temperature (February)	11.90	13.76	17.65	°C
Temperature (March)	15.61	17.17	20.83	°C
Temperature (April)	19.56	20.84	24.23	°C
Temperature (May)	23.76	24.81	27.35	°C
Temperature (June)	26.76	27.66	29.61	°C
Temperature (July)	27.76	28.63	30.15	°C
Temperature (August)	27.78	28.87	30.47	°C
Temperature (September)	25.30	26.49	28.29	°C
Temperature (October)	20.21	22.09	25.10	°C
Temperature (November)	15.37	17.22	21.49	°C
Temperature (December)	11.15	12.85	17.09	°C
Solar radiation (January)	3.121	3.538	4.071	kWh m^{-2} day^{-1}
Solar radiation (February)	3.364	3.723	4.382	kWh m^{-2} day^{-1}
Solar radiation (March)	3.685	4.107	4.914	kWh m^{-2} day^{-1}
Solar radiation (April)	3.986	4.494	5.154	kWh m^{-2} day^{-1}
Solar radiation (May)	4.298	4.796	5.418	kWh m^{-2} day^{-1}
Solar radiation (June)	4.599	5.216	6.401	kWh m^{-2} day^{-1}
Solar radiation (July)	4.254	5.127	6.246	kWh m^{-2} day^{-1}
Solar radiation (August)	4.358	5.034	6.110	kWh m^{-2} day^{-1}
Solar radiation (September)	4.052	4.583	5.321	kWh m^{-2} day^{-1}
Solar radiation (October)	4.183	4.575	5.099	kWh m^{-2} day^{-1}
Solar radiation (November)	3.603	3.977	4.477	kWh m^{-2} day^{-1}
Solar radiation (December)	2.955	3.432	3.935	kWh m^{-2} day^{-1}
Atmospheric transmittance, Kt (January)	0.360	0.457	0.550	-
Atmospheric transmittance, Kt (February)	0.350	0.443	0.540	-
Atmospheric transmittance, Kt (March)	0.400	0.480	0.610	-

Input parameter (continued)	Minimum value	Baseline value	Maximum value	Units
Atmospheric transmittance, Kt (April)	0.420	0.492	0.620	-
Atmospheric transmittance, Kt (May)	0.450	0.506	0.560	-
Atmospheric transmittance, Kt (June)	0.430	0.511	0.580	-
Atmospheric transmittance, Kt (July)	0.480	0.532	0.600	-
Atmospheric transmittance, Kt (August)	0.450	0.520	0.590	-
Atmospheric transmittance, Kt (September)	0.460	0.531	0.600	-
Atmospheric transmittance, Kt (October)	0.370	0.517	0.610	-
Atmospheric transmittance, Kt (November)	0.340	0.494	0.630	-
Atmospheric transmittance, Kt (December)	0.350	0.469	0.580	-
Albedo of original land conditions (January)	0.1488	0.1514	0.1548	-
Albedo of original land conditions (February)	0.1450	0.1481	0.1551	-
Albedo of original land conditions (March)	0.1473	0.1479	0.1488	-
Albedo of original land conditions (April)	0.1460	0.1489	0.1505	-
Albedo of original land conditions (May)	0.1493	0.1505	0.1514	-
Albedo of original land conditions (June)	0.1496	0.1517	0.1534	-
Albedo of original land conditions (July)	0.1441	0.1483	0.1496	-
Albedo of original land conditions (August)	0.1464	0.1474	0.1495	-
Albedo of original land conditions (September)	0.1452	0.1482	0.1523	-
Albedo of original land conditions (October)	0.1476	0.1516	0.1540	-
Albedo of original land conditions (November)	0.1515	0.1545	0.1570	-
Albedo of original land conditions (December)	0.1444	0.1533	0.1596	-
Original net primary productivity (NPP)	0.000133	0.003598	0.014121	kg C m^{-2} day^{-1}
Latitude	25.897	29.384	30.716	°
Amount of original biomass on land	0	0.534	4.234	kg m^{-2}
Distance to refinery	0.782	43.1	210	km

Table C16: Upper Gila Mountains (Ecoregion 16) LCA model input parameters

Input parameter	Minimum value	Baseline value	Maximum value	Units
Temperature (January)	-0.95	2.30	7.73	°C
Temperature (February)	0.41	3.67	9.45	°C
Temperature (March)	2.74	6.27	12.26	°C
Temperature (April)	6.14	9.96	16.21	°C
Temperature (May)	10.52	14.61	20.96	°C
Temperature (June)	15.01	19.29	25.96	°C
Temperature (July)	16.25	21.60	28.42	°C
Temperature (August)	15.12	20.58	27.35	°C
Temperature (September)	13.18	17.53	24.44	°C
Temperature (October)	8.10	11.96	18.48	°C
Temperature (November)	3.20	6.31	12.00	°C
Temperature (December)	-0.83	2.22	7.41	°C
Solar radiation (January)	6.095	6.698	7.090	$kWh\ m^{-2}\ day^{-1}$
Solar radiation (February)	6.098	6.776	7.474	$kWh\ m^{-2}\ day^{-1}$
Solar radiation (March)	7.290	7.623	7.930	$kWh\ m^{-2}\ day^{-1}$
Solar radiation (April)	8.045	8.579	8.903	$kWh\ m^{-2}\ day^{-1}$
Solar radiation (May)	8.048	9.102	9.560	$kWh\ m^{-2}\ day^{-1}$
Solar radiation (June)	7.531	9.292	10.371	$kWh\ m^{-2}\ day^{-1}$
Solar radiation (July)	5.463	6.496	7.361	$kWh\ m^{-2}\ day^{-1}$
Solar radiation (August)	5.156	6.065	6.883	$kWh\ m^{-2}\ day^{-1}$
Solar radiation (September)	6.449	7.204	7.724	$kWh\ m^{-2}\ day^{-1}$
Solar radiation (October)	6.937	7.472	7.856	$kWh\ m^{-2}\ day^{-1}$
Solar radiation (November)	6.728	7.158	7.384	$kWh\ m^{-2}\ day^{-1}$
Solar radiation (December)	6.038	6.522	6.850	$kWh\ m^{-2}\ day^{-1}$
Atmospheric transmittance, Kt (January)	0.480	0.598	0.670	-
Atmospheric transmittance, Kt (February)	0.510	0.608	0.700	-
Atmospheric transmittance, Kt (March)	0.590	0.641	0.720	-
Atmospheric transmittance, Kt (April)	0.610	0.668	0.740	-

Input parameter (continued)	Minimum value	Baseline value	Maximum value	Units
Atmospheric transmittance, Kt (May)	0.510	0.674	0.750	-
Atmospheric transmittance, Kt (June)	0.570	0.656	0.740	-
Atmospheric transmittance, Kt (July)	0.490	0.555	0.630	-
Atmospheric transmittance, Kt (August)	0.470	0.535	0.580	-
Atmospheric transmittance, Kt (September)	0.520	0.615	0.690	-
Atmospheric transmittance, Kt (October)	0.530	0.625	0.750	-
Atmospheric transmittance, Kt (November)	0.550	0.627	0.720	-
Atmospheric transmittance, Kt (December)	0.510	0.598	0.710	-
Albedo of original land conditions (January)	0.1577	0.2394	0.3051	-
Albedo of original land conditions (February)	0.1336	0.2130	0.3020	-
Albedo of original land conditions (March)	0.1304	0.1497	0.2007	-
Albedo of original land conditions (April)	0.1260	0.1299	0.1335	-
Albedo of original land conditions (May)	0.1280	0.1315	0.1340	-
Albedo of original land conditions (June)	0.1276	0.1325	0.1352	-
Albedo of original land conditions (July)	0.1270	0.1301	0.1322	-
Albedo of original land conditions (August)	0.1229	0.1250	0.1270	-
Albedo of original land conditions (September)	0.1253	0.1270	0.1289	-
Albedo of original land conditions (October)	0.1327	0.1358	0.1379	-
Albedo of original land conditions (November)	0.1366	0.1422	0.1455	-
Albedo of original land conditions (December)	0.1848	0.2173	0.2546	-
Original net primary productivity (NPP)	0.000290	0.004520	0.017955	kg C m^{-2} day^{-1}
Latitude	32.959	34.106	35.226	°
Amount of original biomass on land	0	0.896	5.686	kg m^{-2}
Distance to refinery	137	239	338	km

Table C17: Warm Deserts (Ecoregion 17) LCA model input parameters

Input parameter	Minimum value	Baseline value	Maximum value	Units
Temperature (January)	3.36	9.95	13.65	°C
Temperature (February)	5.78	12.02	15.49	°C
Temperature (March)	8.58	15.19	18.69	°C
Temperature (April)	12.28	19.04	22.15	°C
Temperature (May)	17.27	23.94	27.25	°C
Temperature (June)	22.10	28.42	32.00	°C
Temperature (July)	23.72	30.70	35.21	°C
Temperature (August)	22.52	30.11	34.75	°C
Temperature (September)	19.68	26.97	31.00	°C
Temperature (October)	14.15	20.85	24.32	°C
Temperature (November)	8.03	14.20	17.75	°C
Temperature (December)	3.11	9.56	13.13	°C
Solar radiation (January)	5.577	6.463	7.332	kWh m^{-2} day^{-1}
Solar radiation (February)	5.417	6.627	7.668	kWh m^{-2} day^{-1}
Solar radiation (March)	6.322	7.561	8.178	kWh m^{-2} day^{-1}
Solar radiation (April)	7.133	8.179	9.075	kWh m^{-2} day^{-1}
Solar radiation (May)	7.260	8.632	9.563	kWh m^{-2} day^{-1}
Solar radiation (June)	7.293	9.029	10.465	kWh m^{-2} day^{-1}
Solar radiation (July)	6.149	7.749	9.734	kWh m^{-2} day^{-1}
Solar radiation (August)	5.807	7.277	9.180	kWh m^{-2} day^{-1}
Solar radiation (September)	6.178	7.560	8.910	kWh m^{-2} day^{-1}
Solar radiation (October)	6.214	7.175	7.869	kWh m^{-2} day^{-1}
Solar radiation (November)	5.770	6.803	7.469	kWh m^{-2} day^{-1}
Solar radiation (December)	5.240	6.252	7.103	kWh m^{-2} day^{-1}
Atmospheric transmittance, Kt (January)	0.510	0.604	0.680	-
Atmospheric transmittance, Kt (February)	0.520	0.608	0.700	-
Atmospheric transmittance, Kt (March)	0.550	0.649	0.730	-
Atmospheric transmittance, Kt (April)	0.620	0.694	0.760	-

Input parameter (continued)	Minimum value	Baseline value	Maximum value	Units
Atmospheric transmittance, Kt (May)	0.590	0.695	0.760	-
Atmospheric transmittance, Kt (June)	0.610	0.679	0.750	-
Atmospheric transmittance, Kt (July)	0.570	0.621	0.690	-
Atmospheric transmittance, Kt (August)	0.550	0.597	0.670	-
Atmospheric transmittance, Kt (September)	0.580	0.646	0.720	-
Atmospheric transmittance, Kt (October)	0.570	0.638	0.730	-
Atmospheric transmittance, Kt (November)	0.580	0.636	0.700	-
Atmospheric transmittance, Kt (December)	0.520	0.607	0.660	-
Albedo of original land conditions (January)	0.1988	0.2063	0.2122	-
Albedo of original land conditions (February)	0.1969	0.2066	0.2126	-
Albedo of original land conditions (March)	0.1971	0.2055	0.2096	-
Albedo of original land conditions (April)	0.1977	0.2046	0.2066	-
Albedo of original land conditions (May)	0.2016	0.2065	0.2095	-
Albedo of original land conditions (June)	0.2031	0.2072	0.2110	-
Albedo of original land conditions (July)	0.1983	0.2023	0.2066	-
Albedo of original land conditions (August)	0.1961	0.2007	0.2065	-
Albedo of original land conditions (September)	0.1965	0.2011	0.2065	-
Albedo of original land conditions (October)	0.1994	0.2059	0.2119	-
Albedo of original land conditions (November)	0.2091	0.2115	0.2144	-
Albedo of original land conditions (December)	0.2038	0.2075	0.2101	-
Original net primary productivity (NPP)	0.000034	0.002502	0.013366	kg C m^{-2} day^{-1}
Latitude	30.399	33.102	37.105	°
Amount of original biomass on land	0	0.040	0.972	kg m^{-2}
Distance to refinery	0.917	253	474	km

Table C18: West-Central Semi-Arid Prairies (Ecoregion 18) LCA model input parameters

Input parameter	Minimum value	Baseline value	Maximum value	Units
Temperature (January)	-11.10	-6.38	-2.24	°C
Temperature (February)	-8.06	-4.18	-1.00	°C
Temperature (March)	-1.79	1.09	3.47	°C
Temperature (April)	5.21	7.60	9.92	°C
Temperature (May)	9.84	13.45	16.16	°C
Temperature (June)	14.37	18.66	21.38	°C
Temperature (July)	18.18	22.45	24.45	°C
Temperature (August)	17.72	21.76	23.88	°C
Temperature (September)	12.31	16.03	18.61	°C
Temperature (October)	6.25	8.79	11.13	°C
Temperature (November)	-2.04	0.75	2.47	°C
Temperature (December)	-9.36	-5.52	-2.72	°C
Solar radiation (January)	1.823	2.979	4.228	$kWh\ m^{-2}\ day^{-1}$
Solar radiation (February)	2.404	3.678	4.801	$kWh\ m^{-2}\ day^{-1}$
Solar radiation (March)	3.507	4.488	5.231	$kWh\ m^{-2}\ day^{-1}$
Solar radiation (April)	4.064	5.399	6.080	$kWh\ m^{-2}\ day^{-1}$
Solar radiation (May)	4.926	5.847	6.640	$kWh\ m^{-2}\ day^{-1}$
Solar radiation (June)	5.608	6.260	7.328	$kWh\ m^{-2}\ day^{-1}$
Solar radiation (July)	6.620	7.410	8.408	$kWh\ m^{-2}\ day^{-1}$
Solar radiation (August)	5.731	6.531	7.399	$kWh\ m^{-2}\ day^{-1}$
Solar radiation (September)	5.046	5.692	6.604	$kWh\ m^{-2}\ day^{-1}$
Solar radiation (October)	3.545	4.263	5.211	$kWh\ m^{-2}\ day^{-1}$
Solar radiation (November)	2.459	3.271	4.212	$kWh\ m^{-2}\ day^{-1}$
Solar radiation (December)	1.950	2.807	3.954	$kWh\ m^{-2}\ day^{-1}$
Atmospheric transmittance, Kt (January)	0.430	0.491	0.550	-
Atmospheric transmittance, Kt (February)	0.380	0.516	0.590	-
Atmospheric transmittance, Kt (March)	0.410	0.500	0.570	-
Atmospheric transmittance, Kt (April)	0.430	0.520	0.630	-

Input parameter (continued)	Minimum value	Baseline value	Maximum value	Units
Atmospheric transmittance, Kt (May)	0.380	0.540	0.600	-
Atmospheric transmittance, Kt (June)	0.500	0.565	0.640	-
Atmospheric transmittance, Kt (July)	0.490	0.597	0.650	-
Atmospheric transmittance, Kt (August)	0.530	0.588	0.640	-
Atmospheric transmittance, Kt (September)	0.440	0.566	0.620	-
Atmospheric transmittance, Kt (October)	0.460	0.529	0.590	-
Atmospheric transmittance, Kt (November)	0.400	0.490	0.580	-
Atmospheric transmittance, Kt (December)	0.350	0.485	0.590	-
Albedo of original land conditions (January)	0.2774	0.5008	0.6839	-
Albedo of original land conditions (February)	0.2970	0.4564	0.6553	-
Albedo of original land conditions (March)	0.1824	0.2932	0.3932	-
Albedo of original land conditions (April)	0.1556	0.1767	0.2215	-
Albedo of original land conditions (May)	0.1482	0.1552	0.1613	-
Albedo of original land conditions (June)	0.1465	0.1510	0.1567	-
Albedo of original land conditions (July)	0.1520	0.1553	0.1617	-
Albedo of original land conditions (August)	0.1563	0.1602	0.1633	-
Albedo of original land conditions (September)	0.1606	0.1683	0.1827	-
Albedo of original land conditions (October)	0.1651	0.1765	0.1971	-
Albedo of original land conditions (November)	0.1804	0.2084	0.2353	-
Albedo of original land conditions (December)	0.2486	0.4475	0.5382	-
Original net primary productivity (NPP)	0.000392	0.001166	0.003152	kg C m^{-2} day^{-1}
Latitude	41.539	45.148	48.647	°
Amount of original biomass on land	0	0.044	1.038	kg m^{-2}
Distance to refinery	2.53	237	467	km

Table C19: Western Cordillera (Ecoregion 19) LCA model input parameters

Input parameter	Minimum value	Baseline value	Maximum value	Units
Temperature (January)	-10.43	-1.98	6.91	°C
Temperature (February)	-8.38	-0.45	8.04	°C
Temperature (March)	-4.25	3.14	9.91	°C
Temperature (April)	0.00	6.73	12.02	°C
Temperature (May)	5.43	11.13	15.65	°C
Temperature (June)	10.20	15.24	20.28	°C
Temperature (July)	13.23	18.97	24.12	°C
Temperature (August)	12.13	18.48	23.10	°C
Temperature (September)	8.50	14.20	20.98	°C
Temperature (October)	3.17	8.32	16.08	°C
Temperature (November)	-3.73	2.14	9.82	°C
Temperature (December)	-10.31	-2.28	6.58	°C
Solar radiation (January)	1.433	3.147	6.903	$kWh\ m^{-2}\ day^{-1}$
Solar radiation (February)	1.892	3.776	7.267	$kWh\ m^{-2}\ day^{-1}$
Solar radiation (March)	2.104	4.509	7.496	$kWh\ m^{-2}\ day^{-1}$
Solar radiation (April)	3.097	5.437	7.981	$kWh\ m^{-2}\ day^{-1}$
Solar radiation (May)	3.087	6.143	8.758	$kWh\ m^{-2}\ day^{-1}$
Solar radiation (June)	3.554	7.131	9.791	$kWh\ m^{-2}\ day^{-1}$
Solar radiation (July)	5.275	7.972	10.470	$kWh\ m^{-2}\ day^{-1}$
Solar radiation (August)	4.737	7.122	9.912	$kWh\ m^{-2}\ day^{-1}$
Solar radiation (September)	4.156	6.496	8.841	$kWh\ m^{-2}\ day^{-1}$
Solar radiation (October)	2.211	4.967	7.457	$kWh\ m^{-2}\ day^{-1}$
Solar radiation (November)	1.310	3.457	7.333	$kWh\ m^{-2}\ day^{-1}$
Solar radiation (December)	1.249	3.040	6.643	$kWh\ m^{-2}\ day^{-1}$
Atmospheric transmittance, Kt (January)	0.410	0.504	0.600	-
Atmospheric transmittance, Kt (February)	0.420	0.539	0.610	-
Atmospheric transmittance, Kt (March)	0.480	0.547	0.600	-
Atmospheric transmittance, Kt (April)	0.480	0.545	0.630	-

Input parameter (continued)	Minimum value	Baseline value	Maximum value	Units
Atmospheric transmittance, Kt (May)	0.470	0.545	0.650	-
Atmospheric transmittance, Kt (June)	0.490	0.599	0.710	-
Atmospheric transmittance, Kt (July)	0.590	0.662	0.720	-
Atmospheric transmittance, Kt (August)	0.590	0.657	0.720	-
Atmospheric transmittance, Kt (September)	0.470	0.627	0.720	-
Atmospheric transmittance, Kt (October)	0.490	0.570	0.690	-
Atmospheric transmittance, Kt (November)	0.380	0.480	0.590	-
Atmospheric transmittance, Kt (December)	0.420	0.503	0.570	-
Albedo of original land conditions (January)	0.2552	0.3872	0.4654	-
Albedo of original land conditions (February)	0.3080	0.3533	0.4329	-
Albedo of original land conditions (March)	0.2119	0.2534	0.2868	-
Albedo of original land conditions (April)	0.1489	0.1651	0.1891	-
Albedo of original land conditions (May)	0.1442	0.1454	0.1471	-
Albedo of original land conditions (June)	0.1398	0.1427	0.1454	-
Albedo of original land conditions (July)	0.1446	0.1470	0.1503	-
Albedo of original land conditions (August)	0.1484	0.1519	0.1550	-
Albedo of original land conditions (September)	0.1529	0.1584	0.1624	-
Albedo of original land conditions (October)	0.1555	0.1608	0.1674	-
Albedo of original land conditions (November)	0.1608	0.2016	0.2534	-
Albedo of original land conditions (December)	0.2451	0.3406	0.4270	-
Original net primary productivity (NPP)	0.000219	0.001697	0.007358	kg C m^{-2} day^{-1}
Latitude	35.567	44.268	48.864	°
Amount of original biomass on land	0	0.334	4.141	kg m^{-2}
Distance to refinery	22.2	256	509	km

Table C20: Western Sierra Madre Piedmont (Ecoregion 20) LCA model input parameters

Input parameter	Minimum value	Baseline value	Maximum value	Units
Temperature (January)	8.11	8.24	8.46	°C
Temperature (February)	9.26	9.58	9.74	°C
Temperature (March)	11.92	12.12	12.39	°C
Temperature (April)	15.34	15.71	16.22	°C
Temperature (May)	20.03	20.57	20.92	°C
Temperature (June)	24.81	25.38	25.89	°C
Temperature (July)	26.26	26.60	26.99	°C
Temperature (August)	25.15	25.41	25.68	°C
Temperature (September)	23.13	23.41	23.80	°C
Temperature (October)	17.92	18.08	18.37	°C
Temperature (November)	12.26	12.34	12.45	°C
Temperature (December)	7.95	8.09	8.29	°C
Solar radiation (January)	6.840	7.096	7.303	kWh m^{-2} day^{-1}
Solar radiation (February)	6.582	7.023	7.284	kWh m^{-2} day^{-1}
Solar radiation (March)	7.733	8.036	8.223	kWh m^{-2} day^{-1}
Solar radiation (April)	8.930	9.072	9.339	kWh m^{-2} day^{-1}
Solar radiation (May)	9.031	9.385	9.579	kWh m^{-2} day^{-1}
Solar radiation (June)	8.740	9.233	9.777	kWh m^{-2} day^{-1}
Solar radiation (July)	5.970	6.360	7.083	kWh m^{-2} day^{-1}
Solar radiation (August)	5.925	6.260	6.652	kWh m^{-2} day^{-1}
Solar radiation (September)	7.105	7.333	7.642	kWh m^{-2} day^{-1}
Solar radiation (October)	7.589	7.728	7.845	kWh m^{-2} day^{-1}
Solar radiation (November)	7.181	7.430	7.588	kWh m^{-2} day^{-1}
Solar radiation (December)	6.686	6.878	7.050	kWh m^{-2} day^{-1}
Atmospheric transmittance, Kt (January)	0.510	0.620	0.730	-
Atmospheric transmittance, Kt (February)	0.530	0.623	0.700	-
Atmospheric transmittance, Kt (March)	0.630	0.684	0.740	-
Atmospheric transmittance, Kt (April)	0.650	0.710	0.760	-

Input parameter (continued)	Minimum value	Baseline value	Maximum value	Units
Atmospheric transmittance, Kt (May)	0.580	0.710	0.790	-
Atmospheric transmittance, Kt (June)	0.600	0.678	0.750	-
Atmospheric transmittance, Kt (July)	0.500	0.559	0.610	-
Atmospheric transmittance, Kt (August)	0.490	0.553	0.610	-
Atmospheric transmittance, Kt (September)	0.520	0.613	0.670	-
Atmospheric transmittance, Kt (October)	0.560	0.635	0.710	-
Atmospheric transmittance, Kt (November)	0.580	0.651	0.720	-
Atmospheric transmittance, Kt (December)	0.540	0.624	0.690	-
Albedo of original land conditions (January)	0.1565	0.1602	0.1631	-
Albedo of original land conditions (February)	0.1539	0.1593	0.1658	-
Albedo of original land conditions (March)	0.1560	0.1604	0.1660	-
Albedo of original land conditions (April)	0.1562	0.1611	0.1661	-
Albedo of original land conditions (May)	0.1567	0.1618	0.1675	-
Albedo of original land conditions (June)	0.1537	0.1620	0.1682	-
Albedo of original land conditions (July)	0.1510	0.1558	0.1605	-
Albedo of original land conditions (August)	0.1480	0.1506	0.1530	-
Albedo of original land conditions (September)	0.1483	0.1504	0.1525	-
Albedo of original land conditions (October)	0.1542	0.1587	0.1609	-
Albedo of original land conditions (November)	0.1622	0.1653	0.1704	-
Albedo of original land conditions (December)	0.1557	0.1607	0.1636	-
Original net primary productivity (NPP)	0.000187	0.000273	0.000387	kg C m^{-2} day^{-1}
Latitude	31.516	31.964	32.615	°
Amount of original biomass on land	0	0.185	1.983	kg m^{-2}
Distance to refinery	343	377	412	km